

Stony Brook University



OFFICIAL COPY

The official electronic file of this thesis or dissertation is maintained by the University Libraries on behalf of The Graduate School at Stony Brook University.

© All Rights Reserved by Author.

Synthesis of Carbon-11 Labeled Organic Molecules for PET Studies

A Dissertation Presented

by

So Jeong Lee

to

The Graduate School

in Partial Fulfillment of the

Requirements

for the Degree of

Doctor of Philosophy

in

Chemistry

Stony Brook University

August 2015

Stony Brook University
The Graduate School

So Jeong Lee

We, the dissertation committee for the above candidate for the
Doctor of Philosophy degree, hereby recommend
acceptance of this dissertation.

Joanna S. Fowler – Dissertation Advisor
Professor, Department of Chemistry

Iwao Ojima – Chairperson of Dissertation Committee
Distinguished Professor, Department of Chemistry

Isaac Carrico – Third Member of Dissertation Committee
Professor, Department of Chemistry

Paul Vaska – External Member of Dissertation Committee
Professor, Biomedical Engineering Department

This dissertation is accepted by the Graduate School

Charles Taber
Dean of the Graduate School

Synthesis of Carbon-11 Labeled Organic Molecules for PET Studies

by

So Jeong Lee

Doctor of Philosophy

in

Chemistry

Stony Brook University

2015

PET has played a key role in the field of molecular imaging and nuclear medicine over the past decades. PET represents a non-invasive molecular imaging technique to study and visualize human physiology by detecting positron-emitting radiopharmaceuticals labeled with short half-life radioisotopes (i.e., ^{11}C , ^{13}N , ^{15}O , and ^{18}F) that visualize in vivo biochemical processes and metabolic pathways (i.e., glycolysis and protein/DNA synthesis). PET is also an emerging method for measuring body function and tailoring disease treatment in living human by detecting biochemical changes preceding anatomical changes occurring a disease. The capability of imaging quantitatively and with high sensitivity without limitation in tissue penetration has facilitated development of PET imaging probes. Therefore normal biological processes and their malfunctions are the targets of PET.

Blood-brain barrier (BBB) permeability is one of the most important criteria for PET radiotracers targeting different cellular elements in the brain as well as for the development of drugs for treating brain diseases. However, there is no quantitative prediction tool for in vivo pharmacokinetic properties of radiotracer such as rate constants of plasma-to-brain transfer (K_1)

and brain-to-plasma transfer (k_2). Instead of relying on trial-and-error based strategy, we designed a set of model compounds based on the benzamide structure, which is a widely used structural element in drugs and radiotracers (e.g., histone deacetylase (HDAC) inhibitors, [^{11}C]raclopride), to build up the quantitative structure-property relationship (QSPR) as a prediction tool for dynamic modeling of BBB permeability. Parallel synthesis was performed to provide seven benzamides and the corresponding precursor molecules for high yield C-11 labelling using [^{11}C]methyl iodide and [^{11}C]methyl triflate. PET imaging studies in the female baboon along with collecting blood samples over a scan time of 60 min revealed high brain uptake and rapid washout. Kinetic modeling enabled the calculation of pharmacokinetic properties of this series of benzamides and their relationship to physicochemical properties and to BBB penetration. .

PET imaging is also a very useful method to develop and use radiotracers as scientific tools to understand signaling pathways controlling plant growth and development by imaging the biosynthesis and movement of plant hormones in the whole plant in vivo. Plant oriented PET studies are meaningful to gain new knowledge on whole plant physiology for basic research and for developing better biofuel plants.

Auxins are important plant hormones that play an essential role in plant growth and development. Indole-3-acetic acid (IAA) is the most common and potent among naturally occurring auxins. Although IAA was structurally characterized in the 1930s, its translocation in the whole plant in response to growth and environmental stimuli is still not completely understood. The development and application of PET radiotracers to probe the auxin biosynthesis pathway, to study sites of auxin biosynthesis, and auxin distribution and metabolism builds on our recent development of tetraethylene glycol promoted two-step, one-pot rapid

synthesis of [^{11}C]IAA from [^{11}C]cyanide and its use in studies of root herbivory. Based on this study, routine production of [^{11}C]IAA has become reliable and can be accomplished within 45 – 50 min in high radiochemical yield and high specific activity for plant studies.

Labeling indole, the first substrate in auxin synthesis, with carbon-11 builds on a new method to incorporate C-11 into ring positions including indole. It can be assumed that the ring label will be present in all intermediates in auxin biosynthesis, since indole is a key intermediate in auxin biosynthesis. Accordingly radiolabeling indole allows tracer studies of auxin biosynthesis *in vivo* in plants. Therefore, we developed a radiosynthesis of [2- ^{11}C]indole via rapid [^{11}C]cyanation followed by reductive cyclization. Our approach involved the reaction of 2-nitrobenzyl bromide with no-carrier-added [^{11}C]cyanide to form [^{11}C]2-nitrophenylacetonitrile followed by reductive cyclization with Raney nickel and hydrazinium monoformate to form [^{11}C]indole. Each step for the synthesis of [2- ^{11}C]indole was fully controlled and systematically optimized to give a high radiochemical yield and high specific activity of [2- ^{11}C]indole in 45 minutes. This new radiosynthetic method feeds into studies of signaling molecule biosynthesis and movement in whole plants.

There is evidence that asparagine, similar to glutamine, plays an important role as a nitrogen source in plants. Our objective was to develop a stereospecific synthesis of ^{11}C -labeled L-asparagine, using a five-membered ring sulfamidate precursor and nucleophilic ring-opening with carbon-11 labeled hydrogen cyanide ([^{11}C]HCN) as a radioprecursor. For that, efficient preparation of the cyclic sulfamidate and model reaction without radioisotope (cold chemistry) has been developed. The synthesis of (S)-di-*tert*-butyl 1,2,3-oxathiazolidine-3,4-dicarboxylate 2,2-dioxide started from commercially available Boc-*O*-benzyl-L-serine was accomplished in four steps. Based on the success of model reactions in cold chemistry, selective radiosynthesis

of L[4-¹¹C]asparagine was accomplished via [¹¹C]cyanation of the sulfamidate followed by hydrolysis with strong acid (TFA/H₂SO₄) through selective deprotection. Further biological studies via PET imaging are in progress.

Table of Contents

Abstract of the Dissertation	iii
Table of Contents	vii
List of Figures	xii
List of Tables	xvi
List of Abbreviations	xvii
Acknowledgement	xx
List of Publications	xxi
CHAPTER 1. Positron Emission Tomography	1
1. Background	1
1.1. Principle of PET	2
1.2. Positron emitting radioisotopes and PET imaging	4
1.2.1. Cyclotron produced positron-emitters via nuclear reactions	4
1.2.2. Decay of radioisotope by positron emission and annihilation in vivo..	5
1.2.3. Radionuclides in use for PET: standard vs. non-standard PET radioisotopes	7
2. Radioprecursors labeled with short half-lived positron emitters and radiotracer synthesis	9
2.1. Selecting priority for radiosynthesis	10
2.1.1. In vivo interactions of radiotracers	11
2.1.2. Biodistribution	11
2.1.3. Position of labeling	12
2.2. Radiotracer synthesis	12
2.2.1. Typical strategies for the radiosynthesis	12
2.2.2. Specific activity	13
2.2.3. Stoichiometry and the reaction scale	14
2.2.4. Purification and quality control	15
3. Radiolabeling with fluorine-18	15
3.1. Nucleophilic [¹⁸ F]fluorination	16
3.1.1. Labeling with aryl [¹⁸ F]fluorides	16

3.1.2. Labeling with aliphatic [¹⁸ F]fluorides	17
3.2. Electrophilic [¹⁸ F]chlorination	19
4. Radiolabeling with carbon-11	20
4.1. Primary radioprecursors for 11C-labeling	21
4.2. ¹¹ C-labeling with radiocompound derived from [¹¹ C]CO ₂ and [¹¹ C]CH ₄	23
4.2.1. Nucleophilic methylation with [¹¹ C]CH ₃ I	24
4.2.2. Application of [¹¹ C]CH ₃ OTf	28
4.2.3. Displacement and addition reactions with [¹¹ C]cyanide and [¹¹ C]phosgene	28
5. Development of PET radiotracers with [¹¹ C]HCN	30
5.1. Development of methodology for the production of [¹¹ C]HCN	30
5.2. Radiochemistry with [¹¹ C]HCN	32
5.2.1. Nucleophilic [¹¹ C]cyanation reactions	32
5.2.2. Development of novel PET radiotracers and radioligands via nucleophilic [¹¹ C]cyanation	35
6. References	39
CHAPTER 2. Synthesis and PET Studies of C-11 Labeled Benzamides for the Prediction of Blood-Brain Barrier Penetration	45
1. Abstract	45
2. Introduction	46
3. Experimental details	50
3.1. Cold synthesis of benzamide derivatives	52
3.1.1. General procedure of N-methylation of amide on benzamide derivatives	54
3.1.2. General procedure of formation of amide to prepare benzamide derivatives	55
3.1.3. General procedure of Suzuki coupling to prepare benzamide derivatives	61
3.2. Rapid radiolabeling and purification of the nor-precursors with C-11 ...	63
3.2.1. General procedure of radiosynthesis of label benzamides with C-11 ..	64

3.2.2. General procedure of quality control for [¹¹ C]benzamide derivative analysis	64
4. PET study in baboon	70
5. Result and discussion.....	71
5.1. In vivo PET imaging in the female baboon brain	71
5.2. Application to kinetic modeling	74
6. Conclusion	74
7. Appendix	75
7.1. Plasma-protein binding (PPB) assay	75
7.2. Determination of log D value of seven [¹¹ C]benzamides	76
7.3. In vivo metabolite study with baboon plasma	76
7.4. Using quantitative structure-property relationship (QSPR) as a prediction tool for dynamic modeling of blood-brain barrier permeability	77
7.4.1. PET studies and data analysis	78
7.4.2. Blood glows	80
7.4.3. QSPR mode	81
7.4.4. Results and discussion	81
8. References	87
Supplementary Information for CHAPTER 2.	89
CHAPTER 3. Tetraethylene Glycol Promoted Two-Step, One-Pot Rapid Synthesis of Indole-3-[1-¹¹C]Acetic Acid	144
1. Abstract	144
2. Introduction	144
3. Experimental details	147
3.1. General	147
3.2. Production of [¹¹ C]CO ₂ and [¹¹ C]HCN	148
3.3. General procedures for optimizing the [¹¹ C]cyanation and hydrolysis ...	149
3.4. Radiosynthesis of [¹¹ C] indole-3-acetic acid via two-step, one-pot method based on the optimized reaction conditions	151
3.5. Formulation of [¹¹ C]indole-3-acetic acid ([¹¹ C]IAA)	153
3.6. Quality control and specific activity determination	153

4. Results and discussion	155
5. Conclusion	161
6. References	163
CHAPTER 4. Radiosynthesis of [2-¹¹C]Indole via Rapid Nucleophilic [¹¹C]Cyanation Followed by Reductive Cyclization	165
1. Abstract	165
2. Introduction	165
3. Experimental details	170
3.1. General	170
3.2. Controlled production system for anhydrous [¹¹ C]HCN	171
3.2.1. Production of [¹¹ C]CO ₂ and [¹¹ C]HCN	171
3.2.2. Purification of [¹¹ C]HCN	172
3.3. Nucleophilic [¹¹ C]cyanation for [¹¹ C]benzyl nitrile intermediate	172
3.3.1. General procedure for analysis of [¹¹ C]cyanation	172
3.3.2. Optimized radiosynthesis of [¹¹ C]2-nitrophenylacetonitrile from 2- nitrobenzyl bromide	173
3.4. Reductive cyclization of [¹¹ C]nitrile to [2- ¹¹ C]indole	174
3.5. Formulation of [2- ¹¹ C]indole for plant studies	174
3.6. Quality control and specific activity determination	175
3.7. Cold chemistry	175
3.7.1. Preparation of 2,3-bis(2-nitrophenyl) malonitrile (dimer)	175
3.7.2. Preparation of indole from the benzyl nitrile without the benzyl bromide	176
3.7.3. Reductive cyclization of the nitrile in presence of the benzyl bromide	176
4. Results and discussion	177
5. Conclusion.....	193
6. References	195
Supplementary Information for CHAPTER 4.	198
CHAPTER 5. Stereoselective Radiosynthesis of L-[4-¹¹C]-Asparagine from Cyclic Sulfamidate Precursor	207
1. Abstract	207

2. Introduction	208
3. Experimental details	211
3.1. General	211
3.2. Cold chemistry	212
3.2.1. Synthesis of the five-membered ring sulfamidate	213
3.2.2. Synthesis of asparagine from the prepared sulfamidate	216
3.3. Radiochemistry	217
3.3.1. Production of [¹¹ C]CO ₂ and [¹¹ C]HCN	218
3.3.2. Purification of [¹¹ C]HCN	218
3.3.3. Radiosynthesis of [¹¹ C]asparagine	218
3.3.4. General procedure of [¹¹ C]Asn quality control	220
3.3.5. General procedure for obtaining Fmoc-[¹¹ C]Asn specific activity	220
3.3.6. Further hydrolysis to [¹¹ C]Asn and confirmation fo L/D ratio	221
4. Results and discussion	221
5. Conclusion	224
6. References	226
Supplementary Information for CHAPTER 5.	228

List of Figures and Schemes

CHAPTER 1.

Figure 1. Production of radioisotopes via proton induced nuclear reaction....	4
Figure 2. Decay of an ^{11}C isotope and formation of ^{11}B atom, a positron (β^+), and a neutrino (ν)	6
Figure 3. The positron decay and annihilation which results in two 511 keV gamma quanta detected by PET scanner	6
Figure 4. Common nuclear reactions and targets for C-11 and F-18 production	10
Figure 5. Radioprecursors derived from $\text{H}[^{18}\text{F}]$	16
Figure 6. Radioprecursors derived from $[^{18}\text{F}]\text{F}_2$	16
Figure 7. F-18 chemistry via nucleophilic substitution of $[^{18}\text{F}]\text{fluoride}$	18
Figure 8. F-18 chemistry via electrophilic substitution of $[^{18}\text{F}]\text{fluorine}$	19
Figure 9. The map of production of radiolabeled precursors for labeling with ^{11}C derived from the target and on-line conversion to further radioprecursors	21
Figure 10. Synthesis of typical ^{11}C -labeled radiotracers from $[^{11}\text{C}]\text{CO}_2$	22
Figure 11. Radioprecursors derived from $[^{11}\text{C}]\text{CO}_2$	24
Figure 12. Radioprecursors derived from $[^{11}\text{C}]\text{CH}_4$	24
Figure 13. Selected examples of radiosynthesis by nucleophilic $[^{11}\text{C}]\text{methylation}$ with $[^{11}\text{C}]\text{CH}_3\text{I}$ to hetero atoms	27
Figure 14. $[^{11}\text{C}]\text{methylation}$ involving protection and deprotection	27
Figure 15. Synthesis of N- $[^{11}\text{C}$ -methyl]-6-OH-BTA-1($[^{11}\text{C}]\text{PiB}$) with $[^{11}\text{C}]\text{CH}_3\text{OTf}$	28
Figure 16. Displacement with $[^{11}\text{C}]\text{cyanation}$ for synthesis of radiotracer, $[^{11}\text{C}]\text{spiroperidol}$	29
Figure 17. Preparation of a ring-labeled monoamine oxidase inhibitor ($[^{11}\text{C}]\text{MAO}$) with $[^{11}\text{C}]\text{COCl}_2$	30
Figure 18. Selected $[^{11}\text{C}]\text{cyanation}$ reactions and further transformation for aromatic $[^{11}\text{C}]\text{nitriles}$	33

Figure 19. Summary of the preparation of aliphatic [¹¹ C]nitrile	34
Figure 20. Selected examples of nucleophilic [¹¹ C]cyanation followed by transformation of the [¹¹ C]nitrile functions on aliphatic substrates	35
Figure 21. The structures of pharmaceutically and biologically important small radioligand and complex drug-based radiotracers containing cyano group	36
Figure 22. Syntheses of C-11 labeled drugs via [¹¹ C]cyanation using biaryl phosphine Pd(0) complexes	37
Figure 23. Synthesis of [¹¹ C]indole-3-acetic acid ([¹¹ C]IAA) via [¹¹ C]cyanation and alkaline hydrolysis	38
CHAPTER 2.	
Figure 1. Parallel synthesis of precursors and reference compounds of seven benzamides (through nor 1 to nor 7 ; through 1 to 7)	52
Figure 2. Strategic radiosynthesis of seven benzamides with [¹¹ C]CH ₃ I and [¹¹ C]CH ₃ OTf	63
Figure 3. Baboon study with [¹¹ C] 1	72
Figure 4. Brain time-activity curve of seven [¹¹ C]benzamides through [¹¹ C] 1 to [¹¹ C] 7	73
Figure 5. Blood time-activity curve of seven [¹¹ C]benzamides through [¹¹ C] 1 to [¹¹ C] 7	73
Figure 6. Structures of the 15 benzamide compounds besides 7 benzamides ([¹¹ C] 1 – [¹¹ C] 7 shown on Table 1) contained in Table 3	79
Figure 7. The correlation between clogBB and apparent uptake value K ₁	82
Figure 8. The relation between clogBB and efflux rate k ₂	82
Figure 9. The comparison between apparent uptake value K ₁ and calculated logD	83
Figure 10. QSAR result for K ₁ apparent	85
Figure 11. Correlation between in house calculated k ₂ values and experimental k ₂ values	86
CHAPTER 3.	
Figure 1. Previously reported radiosynthesis process of [¹¹ C]IAA	147

Figure 2. A typical analytical HPLC profile of [¹¹ C]cyanation of gramine to [¹¹ C]IAN	150
Figure 3. A typical semi-preparative HPLC purification profile of [¹¹ C]IAA..	152
Figure 4. A typical analytical HPLC for quality control of [¹¹ C]IAA.	154
Figure 5. Scheme of designed two-step, one-pot method	156
Figure 6. Reaction parameters of the optimized two-step, one-pot method ...	161

CHAPTER 4.

Scheme 1. Three reports of synthesis of deuterium or ¹⁴ C labeled indole derivatives	167
Scheme 2. Previous reports for synthesis of ¹¹ C-labeled indole	168
Scheme 3. Our design of synthesis [2- ¹¹ C]indole using H ¹¹ CN as radiolabeling precursor	169
Scheme 4. Reaction of nitrobenzyl bromide with NaCN to form 2-nitrobenzyl cyanide (<i>nitrile</i>) and side-product (<i>dimer</i>) under basic conditions	169
Scheme 5. Reference reports for the synthesis nitrile	178
Scheme 6. Results for the synthesis of nitrile and carrier added [¹¹ C] nitrile	178
Scheme 7. Preliminary results for the radiosynthesis of [¹¹ C] nitrile	179
Scheme 8. Optimized L-[5- ¹¹ C]-glutamine synthesis method	180
Figure 1. Procedure of total radiosynthesis of [2- ¹¹ C]indole	185
Scheme 9. Reductive cyclization inhibition test	188
Figure 2. The amount of residual bromide after purification of “cold” cyanation reaction mixture by SPE method	188
Figure 3. Analytical radio-HPLC profiles of two reaction samples from the reaction of 0.1 mg and 0.2 mg of bromide with [¹¹ C]cyanide in DMA solution for 0.6 min at 40 °C	190
Scheme 10. Further exploration of hydrogenation with reduced starting amount of bromide	193

CHAPTER 5.

Figure 1. Preparation of sulfamidate precursor for the synthesis of asparagine	212
--	-----

Figure 2. Cold reaction for asparagine via nucleophilic cyanation of sulfamidate followed by acidic hydrolysis	213
Figure 3. Radiosynthesis of [¹¹ C]asparagine via [¹¹ C]cyanation followed by alkaline hydrolysis from sulfamidate precursor	217

List of Tables

CHAPTER 1.

Table 1. Characteristics of the important radionuclides for PET	5
Table 2. Primary radiolabeled precursor with ^{11}C , ^{13}N , ^{15}O , and ^{18}F	10

CHAPTER 2.

Table 1. Structures of unlabelled and labelled benzamide derivatives containing different number of hydrogen bonds	51
Table 2. In vivo metabolite study with baboon plasma by analytical HPLC...	77
Table 3. To do QSPR K_1 and k_2 prediction modeling study, the interesting/high-correlated descriptors are molecular volume and topological polar surface area (TPSA)	78
Table 4. Summary of baboon PET studies	80

CHAPTER 3.

Table 1. Screen of better reaction conditions	157
Table 2. Further optimization of hydrolysis reaction of $[^{11}\text{C}]\text{IAN}$ to $[^{11}\text{C}]\text{IAA}$	159

CHAPTER 4.

Table 1. Exploratory results of $[^{11}\text{C}]$ cyanation based upon recent update of the synthesis of L-[5- ^{11}C]-glutamine	183
Table 2. Exploration of reductive cyclization method to convert $[^{11}\text{C}]\text{nitrile}$ to $[2\text{-}^{11}\text{C}]\text{indole}$ catalyzed by Raney Ni with hydrazinium monoformate as hydrogen donor	185
Table 3. Further exploration of the $[^{11}\text{C}]$ cyanation reaction with reduced amount of bromide	190
Table 4. Further exploration of hydrogenation with reduced starting amount of bromide	192

CHAPTER 5.

Table 1. Optimization of $[^{11}\text{C}]$ cyanation reaction	222
Table 2. Optimization of acidic hydrolysis and deprotection to L-[4- ^{11}C]asparagine	223

List of Abbreviations

%ID/cc	% of injected dose per cubic centimeter
1-TCM	1-Tissue compartment model
Asn	Asparagine
Asp	Aspartic acid
Aq.	Aqueous
A_{unbound}	The amount of radioactivity that passed through the membrane
BBB	Blood-brain barrier
Boc	Ter-butyloxycarbonyl
CA	Carrier added
calcd	Calculated
ClogD	Calculated logarithm of distribution coefficient
CNS	Central nervous system
Compd	Compound
CT	Computerized tomography
DMA	N,N-Dimethylacetamide
DMF	N,N-Dimethylformamide
DMSO	Dimethyl sulfoxide
dppf	1,1'-Bis(diphenylphosphino)
EG	Ethylene glycol
EOB	End of bombardment
EOS	End of synthesis
ESI	Electrospray ionization
FDA	Food and Drug Administration
$[^{18}\text{F}]\text{FDG}$	2- $[^{18}\text{F}]$ -Fluorodeoxy-D-glucose

[¹⁸ F]FDOPA	6-[¹⁸ F]fluoro-L-3,4-dihydroxyphenylalanin
Fmoc	Fluorenylmethyloxycarbonyl chloride
GC	Gas chromatography
HBD	Hydrogen-bond donor/acceptor
HE	Hexane
HPLC	High-performance liquid chromatography
IAA	Indole-3-acetic acid
IAM	Indole-3-acetamide
IAN	Indole-3-acetonitrile
LAH	Lithium aluminum hydride
LFER	Linear free-energy relationship
LogBB	Steady-state blood to brain concentration ratio ($\log C_{\text{brain}}/C_{\text{blood}}$)
LogD	Logarithm of distribution coefficient between n-octanol and water Concentration
LogBP	$\log C_{\text{brain}}/C_{\text{plasma}}$
MAO	Monoamine oxidase
mGluR5	Metabotropic glutamate receptor 5
MRI	Magnetic resonance imaging
MS	Mass spectrometry
MV	Molecular volume
MW	Molecular weight
NCA	No-carrier added
NIH	National Institution of Health
NMR	Nuclear magnetic resonance
ORCY	Overall radiochemical yield from multiple steps of radiosynthesis
PET	Positron Emission Tomography
Phe	Phenylalanine
PHNO	(+)-4-propyl-3,4,4a,5,6,10b-hexahydro-2H-naphtho[1,2-b][1,4]oxazin-9-ol

[¹¹ C]PiB	β -amyloid plaque tracer N-[¹¹ C-methyl]-6-OH-BTA-1
PIN	P-type/intrinsic/n-type
PPB	Plasma protein binding
PS	Permeability-surface area
PTC	Phase transfer catalyst
QSPR	Quantitative structure-property relationship
QSAR	Quantitative structure-activity relationship
RCY	Radiochemical yield (decay-corrected)
R&D	Research and development
R.t	Room temperature
SAR	Structure-activity relationship
SPECT	Single-photon Emission Computed Tomography
SPE	Solid phase extraction
TAC	Time-activity curve
TBTA	<i>tert</i> -Butyl 2,2,2-trichloroacetimidate
TEG	Tetraethylene glycol
THF	Tetrahydrofuran
TLC	Thin-layer chromatography
TPSA	Topological polar surface area
Tyr	Tyrosine
UHPLC	Ultra-high performance liquid chromatography
US	Ultrasound

Acknowledgments

I would like express my deepest gratitude to my advisor, Prof. Joanna S. Fowler, for her tremendous support and encouragement that makes me keep moving forward. Her support and advice has not been only for my research but also for my personal life. Thanks to her clear view and guidance, I have been led to overcome most challenging obstacles. Without her, it would not been possible to finish up this journey for Ph.D.

I would also like to thank Prof. Iwao Ojima, the chairperson of my dissertation committee, for his support, thoughtful criticism and valuable suggestions. I am grateful to Prof. Isaac Carrico, the third member of my dissertation committee, for teaching organometallic chemistry course and supporting my qualifications. It is my great pleasure to thank Prof. Paul Vaska, the outside member of my committee, for his intelligent advice and kind help. I own sincere and earnest thankfulness to Dr. Wenchao Qu for his hands on mentorship and inspiration. I also specially thank to Dr. Sung Won Kim for his kind concern and support. I would like to thank my friends and colleagues in BNL PET Group who shared unforgettable memories with me. I will cherish those moments in my whole life. Finally, and the most importantly, I would like to thank my parents and sister in Korea for supporting me and embracing me through my life. I am proud of being your daughter and your sister.

List of publications

1. **Lee SJ**, Alexoff D, Shea C, Kim D, Schueller M, Fowler JS, Qu W*. Tetraethylene Glycol Promoted Two-Step, One-Pot Rapid Synthesis of Indole-3-[1-¹¹C]Acetic Acid. *Tetrahedron Letters*, **2015**, 56, 517-20.
2. **Lee SJ**, Fowler JS, Alexoff D, Kim D, Schueller M, Kim SW, Hooker J, Ma L, Nauth A, Weber C, Qu W*. An efficient and Practical Synthesis of [2-¹¹C]Indole via Superfast Nucleophilic [¹¹C]Cyanation and Raney Nickel Catalyzed Reductive Cyclization. Manuscript in preparation.

CHAPTER 1.

Positron Emission Tomography (PET)

1. Background

Non-invasive imaging and monitoring molecular events in vivo and in real time has significantly contributed to understand fundamental biochemical and physiological process in living organism. Molecular imaging technologies use molecular probes or interactions with molecule, thereby is an essential tool for the development of novel approaches for early prognosis of diseases and for the design of new drugs and treatment. Consequently there are continuous needs to develop and improve imaging techniques with better sensitivity, spatial resolution, selectivity and tissue specificity¹.

Many different technologies have been developed to image the structure and function of systems with unique applications, as well as advantages and limitations. For instance, electron microscopy, autoradiography, optical imaging are capable to generate clear structural image with high resolution for preclinical study. Magnetic resonance imaging (MRI), X-ray diffraction, ultrasound (US), or computerized tomography (CT) mainly provides valuable anatomical information by generating detailed structural images^{1a, 2}. However these imaging methods are able to give only limited or no information on metabolic or molecular events in living subjects, thereby in vivo detection of diseases via these imaging methods can be restricted to disorders causing structural abnormalities^{1a, 3}. While other molecular imaging techniques such as single-photon emission computed tomography (SPECT) and positron emission tomography (PET)

enable to prognose and diagnose malfunctions at molecular level and to monitor metabolic processes in living humans^{2,3}. These methods require exogenous radioactive imaging probes (gamma- and positron-emitters) that provide detectable signals to visualize their body distribution by scanners². These radioactive tracers can be designed for targeting specific tissue or receptor/enzyme to provide detailed images of the targeted area of interest or information about morphofunctional process and biochemical mechanism in living tissues⁴.

1.1. Principle of PET

Traditionally, the application of tracer methods for molecular imaging to study of biochemical processes has continued to heavily rely on the use of negatron-emitters, ^{14}C and ^3H , since these nuclides can be introduced for stable carbon and hydrogen in organic molecules without influence in biological properties of the molecules. Relatively long half-lives, short range of negatron, and ubiquitous availability of ^{14}C and ^3H suit them to trace various complex biochemical and metabolic pathways in the tissue or cell for preclinical study and in vitro study via autoradiography. The means of extending some of these methods in order to directly apply to human studies has been developed via PET with suitable positron emitters^{1b, 5}.

PET has played a key role in the field of molecular imaging and nuclear medicine over the past decades. PET represents a non-invasive molecular imaging technique to study and visualize human physiology by detecting positron-emitting radiopharmaceuticals that label in vivo biochemical process and metabolic pathways (i.e., glycolysis and protein/DNA synthesis)³⁻⁴. Since some of positron-emitting radionuclides (i.e., ^{11}C , ^{13}N , and ^{15}O) are low atomic mass elements commonly and naturally found in biomolecules it is also ideal to directly label target molecules or species rather than interfering with their biological activity for probing human

physiology and biochemistry^{1a}. This is very unique and strong advantage of PET technique for human study comparing with other molecular imaging techniques using a relatively large imaging agent attached to the target species that modify its biological activity⁶. For instance, gamma-emitting radiopharmaceuticals visualized by SPECT scanner are able to indirectly enter in a specific metabolic function (i.e., ²⁰¹thallium, a cardiac perfusion radiotracer, labels the Na⁺/K⁺ ion exchange pump and it is transported into myocytes)^{2b, 3, 7}.

PET is also an emerging method in terms of measuring body function and tailoring disease treatment in living human by detecting trivial chemical changes caused before macroscopic anatomical sign of a disease. The capability of imaging quantification and high sensitivity without limitation in tissue penetration has facilitated development of PET imaging probes. Therefore normal biological processes and their malfunctions are the targets of PET^{1a}.

Many different technologies for molecular imaging have been continued and developed with unique applications as well as advantages and limitations. In order to complement each method, imaging technology has been improved to integrate two different methods in one device. The combined PET/CT technique allows the matching of functional information on the PET scan to the detailed anatomical images from the CT scan⁸. Other integrated systems such as PET/MRI, SPECT/CT and SPECT/MRI also have been used for in-line multi-modality preclinical and clinical study⁹.

1.2. Positron-emitting radioisotopes and PET imaging

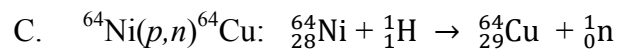
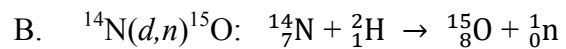
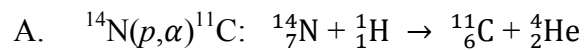
1.2.1. Cyclotron produced positron-emitters via nuclear reactions

Positron-emitting radioisotopes are produced on cyclotrons or generators. Cyclotrons have been in regular use for medical radioisotope production since about 1950 and several hundreds of cyclotrons in operation in U.S.

Cyclotron, a cyclic accelerator of charged particles, can be considered as devices providing a source of reactants such as proton, deuterons, ^3He , and ^4He that can give the nuclear reactions leading to the desired radionuclides¹⁰. At small-sized cyclotrons, the nuclear reactions such as (p,n), (d,n), (p, α) and (d, α) shown on Figure 1 are involved¹¹. The thresholds for the nuclear reactions involved are 5 to 6 MeV (Table 1). Medical cyclotrons that exclusively devoted for the production of positron-emitting radionuclides generate low maximum proton energy (10 – 20 MeV) and the maximum proton beam current is 10 – 500 μA ^{1a, 11a}. Due to the nature of the proton-induced nuclear reactions, there is a change in element:

$$Z \rightarrow Z + 1 \text{ or } Z \rightarrow Z - 1 \quad (Z: \text{atomic number})$$

Figure 1. Production of radioisotopes via proton induced nuclear reaction.



p : proton (^1_1H); α : alpha particle (^4_2He); d : deuterium (^2_1H); n : neutron (^1_0n)

Table 1. Characteristics of the important radionuclides for PET.

Isotope	Half-life	Nuclear reaction	E_{\max}^a (MeV)	β^+ branching ratio ^b	Target	S.A. ^b (Ci/mmol)	Product
¹¹ C	20.4 min	¹⁴ N(<i>p,α</i>) ¹¹ C	0.959	1.0	N ₂ (+O ₂)	9.22 × 10 ⁶	¹¹ CO ₂
¹³ N	9.96 min	¹⁶ N(<i>p,α</i>) ¹³ N	1.197	1.0	H ₂ O+EtOH	1.89 × 10 ⁷	¹³ NO ₂ , ¹³ NO ₃ , ¹³ NH ₃
¹⁵ O	2.04 min	¹⁴ N(<i>d,n</i>) ¹⁵ O ¹⁵ N(<i>p,n</i>) ¹⁵ O	1.738	1.0	N ₂ (+O ₂) ¹⁵ N ₂ (+O ₂)	9.08 × 10 ⁷	¹⁵ O ₂
¹⁸ F	109.8 min	¹⁸ O(<i>p,n</i>) ¹⁸ F ²⁰ Ne(<i>d,α</i>) ¹⁸ F	0.633	0.97	H ₂ ¹⁸ O ¹⁸ O ₂ (+F ₂) Ne(+F ₂)	1.71 × 10 ⁶	¹⁸ F- ¹⁸ F ₂
⁶⁴ Cu	12.7 h	⁶⁴ Ni(<i>p,n</i>) ⁶⁴ Cu ⁶⁴ Ni(<i>d,2n</i>) ⁶⁴ Cu	0.66	0.17	Enriched ⁶⁴ Ni (99.6%)	2.45 × 10 ⁵	⁶⁴ CuCl ₂
⁶⁸ Ga	68 min	⁶⁸ Ge/ ⁶⁸ Ga generator	1.898	0.89	Ga ₂ O	2.75 × 10 ⁶	⁶⁸ Ga ³⁺
⁸⁹ Zr	78.5 h	⁸⁹ Y(<i>p,n</i>) ⁸⁹ Zr	0.40	0.23	Natural Y metal foil	4.00 × 10 ⁴	⁸⁹ Zr ⁴⁺
¹²⁴ I	4.2 d	¹²⁴ Te(<i>p,n</i>) ¹²⁴ I	2.15	0.23	¹²⁴ TeO	3.11 × 10 ⁴	¹²⁴ I ⁻
⁸² Rb	1.27 min	⁸² Sr/ ⁸² Rb generator	3.15	0.95	Rb (natural)	1.50 × 10 ⁸	⁸² RbCl

^a Maximum energy of positron (β^+); ^b the fraction of atom that decay by β^+ emission

^b Theoretical maximum specific activity

1.2.2. Decay of radioisotope by positron emission and annihilation in vivo

Inhalation or intravenous injection is required to administer the PET probe to the living subject (plant, animal and human). The PET radionuclides decay in the body by positron emission (Figure 2). The emitted positron (β^+) is not detected directly, but travels a short distance (0.5 – 2.0 cm, depending on its characteristic kinetic energy) and collides with an electron in the surrounding tissue^{1a, 12}. This collision of particle (positron) and antiparticle (electron) results in an annihilation event that produces two gamma ray photon (γ) of 511 keV

that travel at 180° to each other which are measured in coincident (Figure 3)^{1a}. The PET scanner simultaneously detects these two coincident gamma rays that travel out through the body and get annihilated, thereby the approximate location of the PET probe in the body is indicated¹².

The subject is situated in the circular ring type of PET scanner consists of a series of gamma ray detectors. Each detector is connected in a coincidence circuit with another detector located on the opposite side of the ring. Millions of individual annihilation events are required in order to produce enough data for PET image reconstruction¹³. PET technology generates quantitative physiological and biochemical information in the real time by monitoring the biodistribution and concentration of the radiolabeled probe in the body over time.

Figure 2. Decay of an ¹¹C isotope and formation of ¹¹B atom, a positron (β^+), and a neutrino (ν).

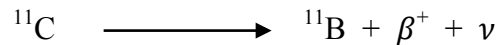
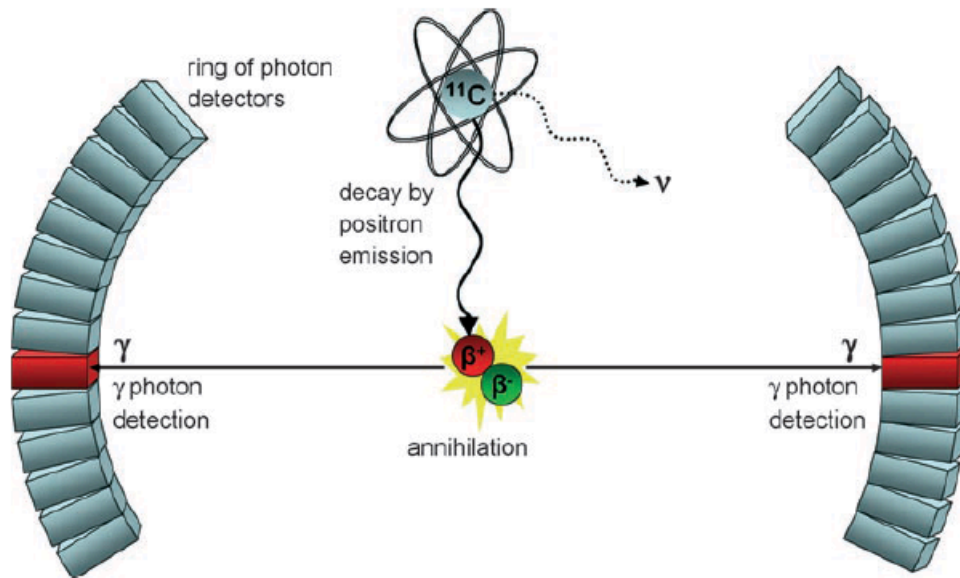


Figure 3. The positron decay and annihilation which results in two 511 keV gamma quanta detected by PET scanner^{1a}.



1.2.3. Radionuclides in use for PET: standard vs. non-standard PET radioisotopes

According to the principle of PET, PET isotopes ideally suited for probing physiology and biochemistry of living subjects, especially human should have 1) low positron energy; 2) high positron branch ratio; 3) practically long half-life that matches with the biological half-life of the labeled molecule or the biological events and enables total synthesis of PET radiopharmaceuticals within three half-lives of the isotope; 4) but also not too long half-life to minimize radiation dose to the subject; and 5) the labeling procedure that minimally alter the properties of the molecule of interest^{1b}.

Essential radionuclides used in PET are typically labeled with short-lived radionuclides categorized as “standard radionuclides” such as carbon-11 ($T_{1/2} = 20$ min), nitrogen-13 ($T_{1/2} = 10$ min), oxygen-15 ($T_{1/2} = 2$ min), and fluorine-18 ($T_{1/2} = 109$ min). F-18 labeled 2-deoxyglucose ($[^{18}\text{F}]\text{FDG}$) is the most commonly used radiotracer for PET imaging for therapeutic or research purpose¹⁴. There are high uptakes with this radiolabeled glucose analog particularly in high-glucose using cells such as brain, kidney and cancer cells. $[^{18}\text{F}]\text{FDG}$ is used in essentially all scans for oncology and most scans in neurology, and thus composes the large majority of all of the radiotracer (> 95%) used in PET and PET-CT scan^{2b, 7a}.

Due to extremely short half-life, however, the high cost of on-site cyclotron operation and specially adapted apparatus for on-site chemical synthesis of the radiopharmaceutical production after radioisotope preparation is required. Only fluorine-18 radiolabeled compounds with relatively long half-life (about 2 hours) are available to be transported from the place where they were produced so they are commercially available. Because of the restriction by short half-life, it would decrease availability and flexibility for labeling with these radionuclides. Nevertheless it is noteworthy that the four standard positron emitters (^{11}C , ^{13}N , ^{15}O , and ^{18}F) provide a range

of half-lives ranging from 2 min to nearly 2 hour, thereby providing potential flexibility in tailoring radiotracer half-life to different needs.

The use of non-standard PET nuclides such as ^{64}Cu , ^{68}Ga , ^{89}Zr , and ^{124}I for preclinical and clinical studies has been growing in the past decade. For instance, Cu-64-labeled diacetylbis(N4-methylthiosemicarabane) (^{64}Cu -ATSM) has been shown to be selective for hypoxia in tumor imaging¹⁵. Despite the mechanisms of ^{64}Cu -ATSM are not fully verified, PET imaging of hypoxia in the brain, heart and cancer has been explored since human trial was commenced on 2006 with the United State Food and Drug Administration (U.S. FDA) approval.

Although most of them are not superior than the four standard PET nuclides based on the criteria for the “ideal PET isotope”, the non-standard PET nuclides have suggested novel approaches for design and synthesis of a wider range of PET probes for targeted imaging and therapy in various subjects. Using non-standard nuclides for radiolabeling is also beneficial in respect with a wider spectrum of half-lives ranging from seconds to days. However, non-standard radionuclides are not particularly ideal for PET imaging due to high energy positron emitted, extended positron range and to the numerous cascade gamma ray emissions¹⁶. Thus the radionuclide should be judiciously chosen for specific applications and the positron range and cascade gamma rays are given proper consideration for high image quality and quantification accuracy.

2. Radioprecursors labeled with short half-lived positron-emitters and radiotracer synthesis

The majority in the field of nuclear medicine and radiopharmaceutics have carried out PET technology with the short half-lived positron emitters to establish and developed their medical research and therapy for human, since 1960s. However using short-half lived radioisotopes for PET studies has specific challenges.

One of the main challenges of radiochemistry for PET with these radioisotopes is the development of methodology for introducing relatively short-lived positron-emitting isotopes into target molecules.

It is infeasible that organic radiotracers containing a positron emitter are synthesized first and then the radioisotope prepared within them, because bombardment with proton beam from the cyclotron for nuclear reaction in order to produce a radioisotope destroys any organic carrier molecules. Thus the isotope should be prepared first and then afterward, chemistry to obtain any organic tracer accomplished rapidly.

The radiolabeled molecules have to be synthesized, purified, analyzed and formulated roughly within three isotopes half-lives in order to obtain enough radiolabeled material to administer to a subject undergoing the PET scan. The short half-lives of isotopes require that the synthesis of labeled compounds should be prepared where the isotopes are produced and the labeled compounds have to be immediately used after their synthesis. Therefore, precursor yield always needs to be maximized, because subsequent steps in a radiotracer synthesis and the time consumed cause a significant decrease in radiochemical yield¹⁷.

The chemical form of radionuclides is controlled by the bombardment followed by nuclear reaction with a certain target. Although number factors are considered for target chemistry, the

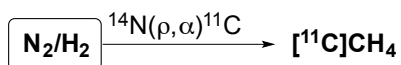
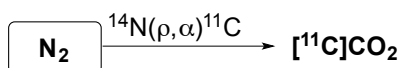
most critical factor is the thermal stability of the target and its contents. The radiolytic and chemical stability of the contents is also highly important⁶. The primary radioprecursors labeled with ¹¹C, ¹³N, ¹⁵O, and ¹⁸F that produced directly from different targets are presented in Table 2¹⁸. Common nuclear reactions and target materials for C-11 and F-18 production is described in Figure 4^{1b}.

Table 2. Primary radiolabeled precursor with ¹¹C, ¹³N, ¹⁵O, and ¹⁸F.

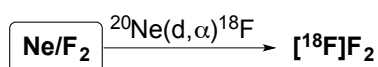
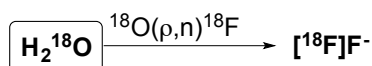
Carbon-11	Nitrogen-13	Oxygen-15	Fluorine-18
[¹¹ C]O ₂ , [¹¹ C]O, [¹¹ C]H ₄	[¹³ N]H ₃ , [¹³ N]O ₃ ⁻ , [¹³ N]O ₂ ⁻ , [¹³ N]O	¹⁵ O ₂ , C[¹⁵ O], C[¹⁵ O]O ₂ , N ₂ [¹⁵ O], H ₂ [¹⁵ O]	[¹⁸ F]F ₂ , H[¹⁸ F]

Figure 4. Common nuclear reactions and targets for C-11 and F-18 production.

Carbon-11 Production



Fluorine-18 Production



2.1. Selecting priority compounds for radiosynthesis

It is essential to set the priority compound for synthesis of radiotracer in order to sort out appropriate molecular structures for probing a particular physiological process or imaging specific species of interest. The various chemical interactions of radiotracer with living systems (i.e., tissue biochemistry, molecular requirements for tissue uptake, and intracellular pH, etc.) are critical factors for selecting the priority. Thus, comprehension of structure-activity correlations

as well as prediction of possible metabolites and biodistribution patterns of the molecules in the body helps to select a proper structure to be synthesized for a PET radiotracer.

2.1.1. In vivo interactions of radiotracers

PET is a scientific tool measuring the rates of biochemical reactions in the living human by using positron-emitting radiotracers involving the in vivo reactions. Since PET only visualizes in vivo information by detecting emitted positron (radioactivity) it does not demonstrate that the chemical form of radioactivity responsible for proving the PET image accords with that of the tracer injected. After injection, the original radiotracer undergoes metabolism and results in its labeled/unlabeled metabolic products. Therefore before proceeding actual preclinical and clinical studies with a new tracer for PET, it must be required to clarify any chemical and biochemical reactions associated with the designed tracer in order to identify the actual chemical form of the tracer contributing PET imaging¹⁹. In animal studies, the chemical forms of radioactivity providing the PET images used to be determined by in vitro assay of tissue samples from blood of the animals.

2.1.2. Biodistribution

It is important to define the chemical identification of the radioactive source in the area of interest when selecting priorities for synthesis. The determination of structure-activity relationship allows predicting the biodistribution patterns of molecules in the body. There are limitations for amount of radioactivity that can be administrated for reasons of radiation safety and minimizing radioation dose so detection of in vivo radioactivity is restricted. Therefore the design of a tracer which has the high uptake in the area of interest is especially important to provide sufficient count rate for PET imaging. For example, although domperidone is highly selective dopamine antagonist, it would be useless to label dopamine receptors in the brain

because the blood-brain barrier permeability of this pharmaceutical is poor²⁰. In this regard, not only the selective and specific delivery or targeting of radiotracer is important but also its behavior in the tissue of interest and its transport must be considered for sufficient uptake for PET study.

2.1.3. Position of labeling

The choice for labeling position is usually dictated by the structure of the molecule and the limited number of possible strategies for introducing the radionuclides. The half-life of nuclides should be long enough compared with the turnover rates of the physiological process of interest but also not too long to increase unnecessarily radiation dose. Also if labeled metabolites which is in organic molecule formula and if there is high uptake of the labeled metabolites, it results in high background noise for PET scan and interrupts desire image obtained with original tracer uptake. Thus if a foreign radioisotope is used to label the molecule, the resulting radiotracer has to have the desired characteristics of the parent molecule and less potential to produce unlabeled metabolites. As an example, in the extension of the [¹⁴C]leucine method²¹ to PET using a radiotracer labeled with C-11, it is required that the C-11 be contained in the carboxyl group of the leucine so that decarboxylated metabolites are not detected in the PET scan, thereby simplifying the measurement of regional protein synthesis.

2.2. Radiotracer synthesis

2.2.1. Typical strategies for the radiosynthesis

A readily accessible labeled precursor molecule is obtained directly from the target (i.e, [¹¹C]CO₂) or synthesized from the labeled species produced in the target. The synthetic sequence is organized with consideration of the reaction mechanism as well as the specific

activity of the product and stoichiometry of each step of the synthesis. In general, the reaction including and subsequent to the introduction of radioactivity is in the terminal or near-terminal step of total synthesis of a radiotracer.

2.2.2. Specific activity

Specific activity is the amount of radioactivity per mass (or per mole) of a labeled compound. The term “no-carrier-added (NCA)” means that no “cold” material (carrier) of the same chemical identity is intentionally added during preparation of radiopharmaceutical²². The maximum specific activity (carrier-free state) for a radionuclide is obtained when there is no dilution by other isotopes of the same element but it is very difficult to achieve because of natural contamination from the environment. The theoretical maximum of specific activity is related to the number of nuclides:

$$A = (\ln 2/t_{1/2})N$$

A : radioactive decay rate; $t_{1/2}$: half-life; N : the number of atoms of the radioactive elements.

The short-lived positron emitting isotopes results in very low masses per becquerel in carrier-free state so specific activity is also very low, while higher masses results from the longer-lived isotope so specific activity of long-lived isotope is higher. It is obviously explained by comparison of the maximum specific activity of ^{11}C (349 TBq/ μmol) with that of ^{14}C (2.3×10^{-9} TBq/ μmol) and the difference in their half-lives, 20.4 min vs. 5730 yrs.

In reality, small amounts of unlabeled (cold) material is introduced unintentionally. Although it can be very near carrier-free status with special precautions to keep the dilution factors low, specific activity never gets reached to maxima. For instance, $[^{11}\text{C}]\text{CO}_2$ and $[^{11}\text{C}]\text{HCN}$ are diluted with $[^{12}\text{C}]\text{CO}_2$ and $[^{12}\text{C}]\text{HCN}$, respectively so $[^{11}\text{C}]\text{HCN}$ is available in even higher specific activity than $[^{11}\text{C}]\text{CO}_2$. It is possible to increase specific activity of

$[^{11}\text{C}]\text{HCN}$ via the removal of the only source of carrier ($[^{12}\text{C}]\text{CH}_4$) from the target but difficult. While, in the case of $[^{11}\text{C}]\text{CO}_2$, it enables to convert to other forms of radioprecursor such as $[^{11}\text{C}]\text{HCHO}$ or $[^{11}\text{C}]\text{CH}_3\text{I}^{23}$ and a number of sources of $[^{12}\text{C}]\text{CO}_2$ have been identified in the process of converting and affect the specific activity of derived radioprecursor.

This factor is concerned seriously to prepare C-11 labeled tracers for clinical studies that only allows mass of compound that will not result in any toxic or physiological effect. For the reason, radiopharmaceutical with high specific activity is essential in most cases for human studies.

2.2.3. Stoichiometry and the reaction scale

The requirement for radiotracer with respect to high specific activity for human study gives rise to more extra limitations on the radiosynthesis. The concept of NCA (or CA) is also highly related to the scale of reaction and the stoichiometry in the synthesis. For example, in $[^{11}\text{C}]\text{cyanation}$ with $[^{11}\text{C}]\text{NaCN}$ (specific activity is $74 \text{ GBq}/\mu\text{mol}$), the mass of NaCN in use for reaction is only 50 nmol if one starts with 3.7 GBq. With such trace amount of radioprecursor, all other substrates or reactants used in the synthesis are necessarily in huge excess and this extremely unbalanced stoichiometry presents difficulties to drive labeling reaction properly.

Thus the substrate that supposed to react with the radioprecursor must be sufficient to react both with the labeled precursor and other competing reactant in the reaction mixture because in case relatively higher concentrations of less reactive species is more favorable to give side reaction by consuming all of the substrate before the desired labeling reaction carried out. Also because this reaction for labeling tracer in high specific activity is ultramicroscale organic synthesis, it is advantageous in respect of short reaction time; handling small quantities of reagents and solvents; ease with purification.

2.2.4. Purification and quality control

The final radiotracer purification is usually carried out by preparative high performance liquid chromatography (HPLC). In the purification, excessive substrate as well as chemical and radiochemical impurities was separated. To deliver the desire tracer to human subject, it does not only require that the radiotracer must be chemically and radiochemically pure but also sterile and pyrogen free. The final quality of the desire tracer is confirmed by HPLC, thin-layer liquid chromatography (TLC), gas chromatography (GC) or mass spectroscopy (MS) and all the procedure for satisfying strict standard must be accomplished within a limited time scale.

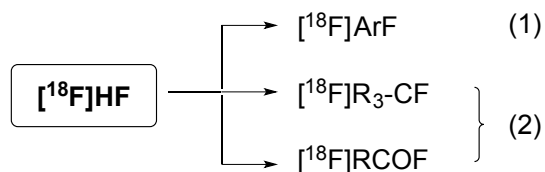
3. Radiolabeling with fluorine-18

Fluorine-18 is an exceedingly useful nuclide for PET. Use of F-18 labeling resulting in low-energy positron – average range is 0.6 mm – is advantageous with respect to the improved resolution of PET image. The longest half-life of F-18 (109 min) among the four standard radionuclides allows relative flexibility regarding the restriction in time for production and delivery process. The similar van der Waal's radius of the fluorine atom is also favorable to give substitution for hydrogen with little steric perturbation so a facile radioprecursor, $\text{H}[^{18}\text{F}]$ is used in common for F-18 labeling. In addition, due to the great electronegativity resulting in high C-F bond energy, rapid fluorination in small-scale reactions for radiolabeling is feasible with highly reactive precursors such as ^{18}F -labeled F_2 , CF_3OF , ClO_3F , and HF (Figure 5). Even though organofluorine compounds are rarely in nature, a number of synthetic approaches for efficient ^{18}F fluorination for labeling PET tracers via C-F bond formation has been developed.

The chemistry with nucleophilic ^{18}F fluoride (Figure 6) is frequently used for ^{18}F -labeling not only because of the ease of preparation and use of precursor but the high specific activity

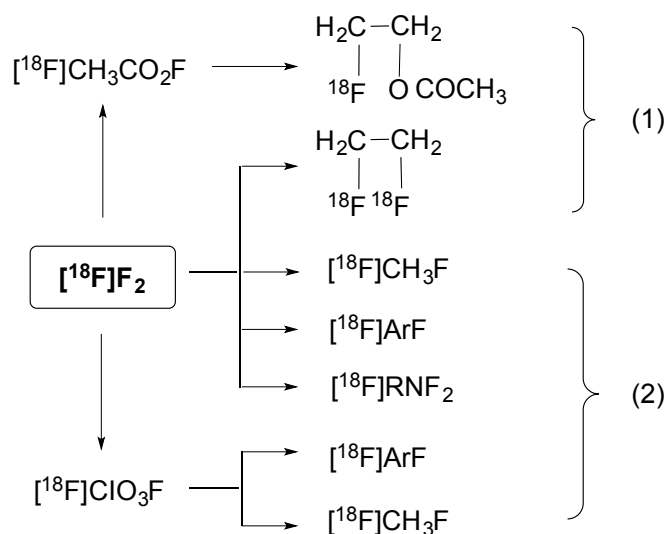
resulted from the fluorination. Substitution reactions with electrophilic [^{18}F]fluorine are rarely used.

Figure 5. Radioprecursors derived from $\text{H}[^{18}\text{F}]$



(1) Schiemann reaction, triazene decomposition, nucleophilic substitution; (2) nucleophilic substitution.

Figure 6. Radioprecursors derived from $[^{18}\text{F}]\text{F}_2$



(1) Electrophilic addition; (2) electrophilic substitution.

3.1. Nucleophilic [^{18}F]fluorination

3.1.1. Labeling with aryl [^{18}F]fluorides

The [^{18}F]fluoride can be introduced into the desire position on aromatic ring by displacement of an aryl amino group via either Balz-Schiemann reaction (Figure 7-a) or Wallach reaction

(Figure 7-b)²⁴. Radiochemical yield of both reactions is low (less than 15%) because of the decomposition of substrates in the presence of fluoride and specific activity is also usually low for Balz-Schiemann reaction due to exchange with ¹⁹F-fluoride²⁴.

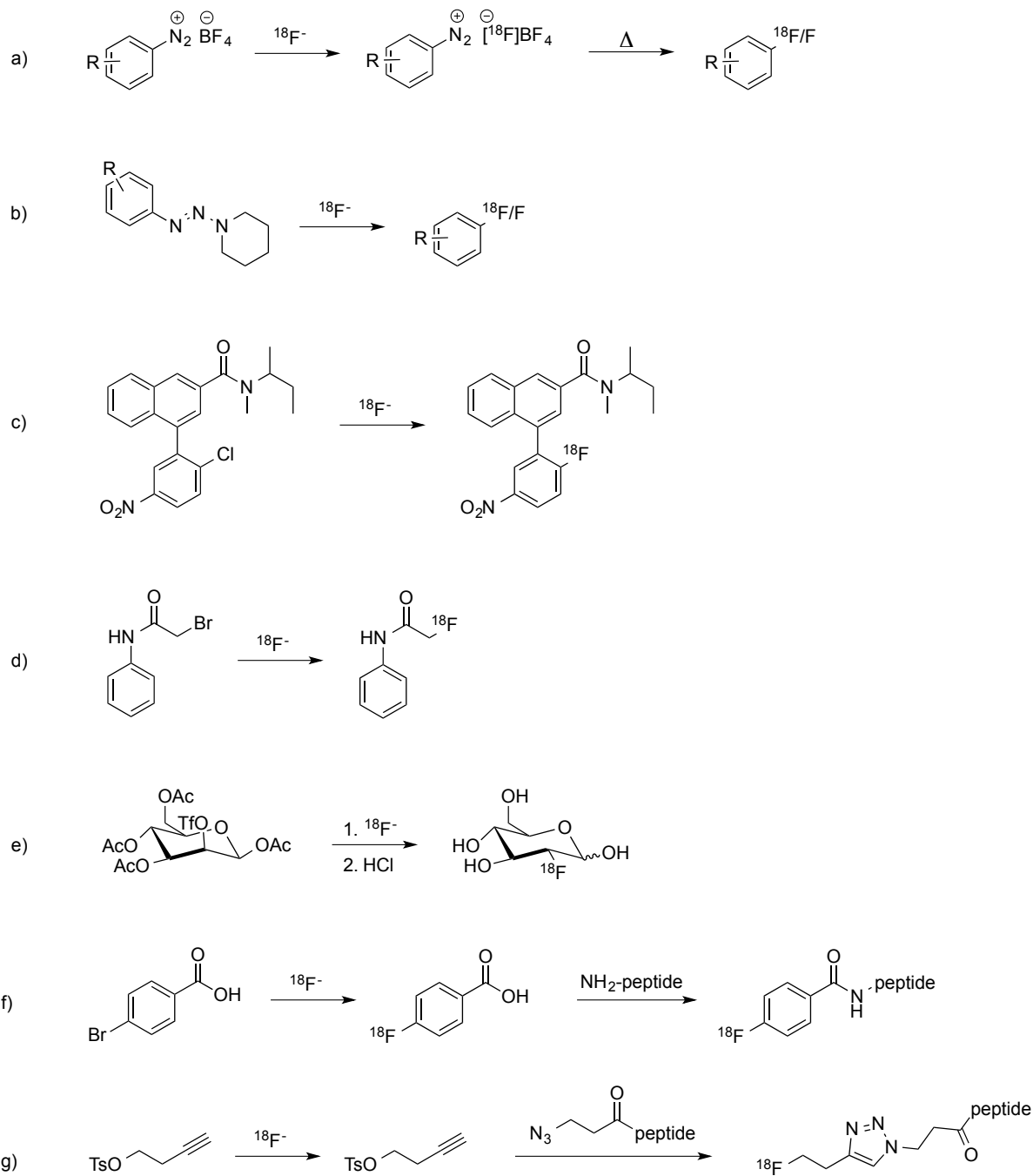
Nucleophilic aromatic substitution driven by an activating electron-withdrawing group on the ortho or para position and an good leaving group (i.e., halogens, nitro groups, and trimethylammonium salts) is the most successful method for incorporation of [¹⁸F]fluoride onto an aryl position (Figure 7-c). However it usually requires high reaction temperature (>100 °C) in the presence of cryptand or base²⁴.

3.1.2. Labeling with aliphatic [¹⁸F]fluorides

Aliphatic nucleophilic substitution is very efficient and common method to introduce F-18 into organic molecules. Basically aliphatic nucleophilic fluorination requires a good leaving group such as a halogen or a sulfonate and prefers formation of primary carbon and fluoride bond. Direct substitution with [¹⁸F]fluoride to an aliphatic target molecule gives rise to very high radiochemical yield (Figure 7-d)^{24,25}. A nucleophilic substitution with [¹⁸F]fluoride to 2-deoxy-2- [¹⁸F]fluoro-D-glucose ([¹⁸F]FDG) is also a representative example for efficiency of this type of nucleophilic [¹⁸F]fluorination (Figure 7-e)^{14c}.

In case direct fluorination is not feasible, for example, labeling macromolecules or electron-rich arene, fluorination in multi-step is inevitable. Thereby the functionalized aliphatic chain labeled with F-18 is obtained first, then afterward, introduced into the target molecule (Figure 6-f)²⁶. Recently, incorporation of ¹⁸F-labeled synthons to the target via “Click” chemistry has recently intrigued radiochemists (Figure 7-g)^{24,26-27}. It is particularly useful for peptide and protein labeling²⁷.

Figure 7. F-18 chemistry via nucleophilic substitution of [¹⁸F]fluoride

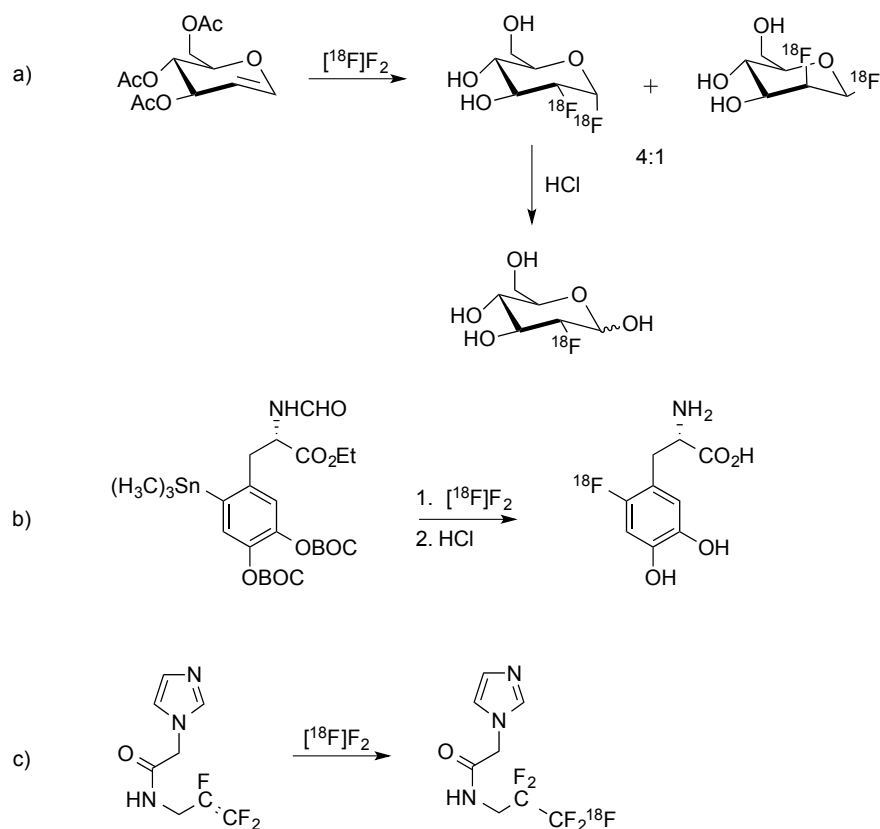


a) Balz-Schiemann reaction; b) Wallach reaction; c) Nucleophilic aromatic substitution; d) Direct fluorination in one-step; e) Nucleophilic route to [¹⁸F]FDG; f) Nucleophilic fluorination in multiple steps; g) Nucleophilic fluorination via “click” chemistry

3.2. Electrophilic [¹⁸F]fluorination

The C-F bond formation with electrophilic fluorine resulting in poor specific activity and radiochemical purity is less favorable but it was the original way to obtain many key radiopharmaceuticals such as [¹⁸F]FDG (Figure 8-a)^{14b} and 6-[¹⁸F]fluoro-L-3,4-dihydroxyphenylalanine ([¹⁸F]fluoro-L-DOPA, [¹⁸F]FDOPA) (Figure 8-b)²⁸. For the reaction, F-18 labeled electrophiles (i.e., CF₃OF, F₂, ClO₃F, XeF₂ or CH₃CO₂F) and electron-rich substrate such as unsaturated molecule and a carbanion are involved (Figure 8-c)^{1a, 29}.

Figure 8. F-18 chemistry via electrophilic substitution of [¹⁸F]fluorine



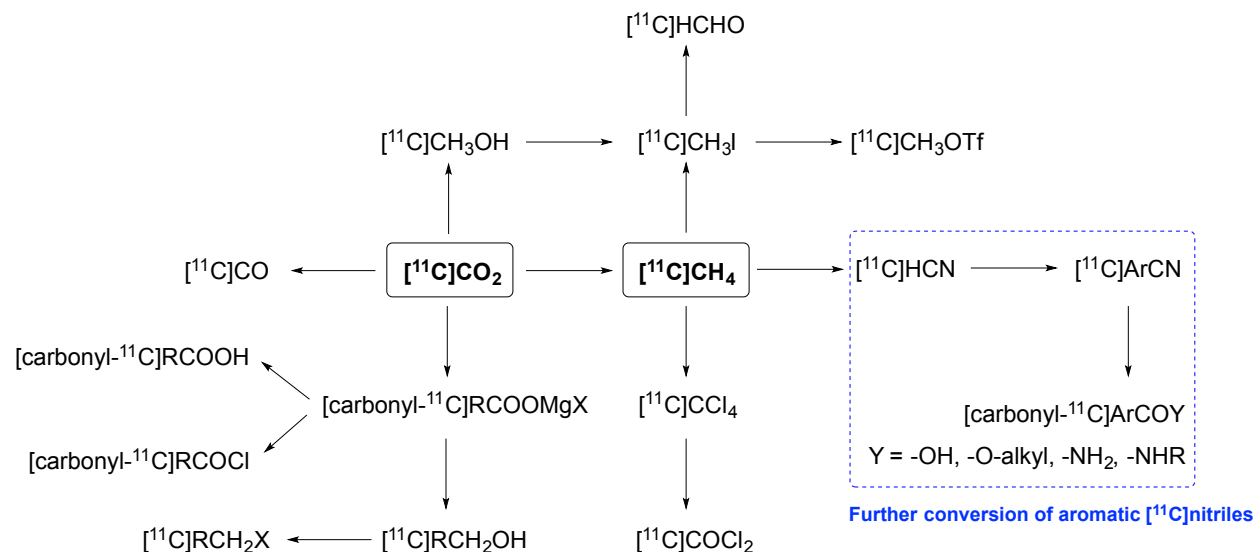
a) Electrophilic route to [¹⁸F]FDG; b) electrophilic method for [¹⁸F]FDOPA; c) electrophilic substitution with [¹⁸F]F₂ to electron rich substrate.

4. Radiolabeling with carbon-11

Carbon and hydrogen are the most ubiquitous elements contained in the biomolecules in the living species and also exist in stable and radioactive forms. Only carbon, however, has positron-emitting radionuclides that provide body-penetrating radiation for imaging dynamic physiological process in the living animal and humans. Carbon has a number of different forms of isotopes such as ^{14}C emitting long-lived β , and ^{13}C commonly used in nuclear magnetic resonance (NMR) spectroscopy besides radioactive forms including ^9C ($t_{1/2} = 0.13$ sec), ^{10}C ($t_{1/2} = 19.4$ sec) and ^{11}C ($t_{1/2} = 20.4$ min). Among many different form of isotopes only ^{11}C , which is the short-lived positron-emitter with small electron capture component and decays to stable ^{11}B , has used significantly in biochemical and medical research. Its short-half life (20.4 min) is particularly appreciated in serial studies of the ^{11}C -labeled radiotracers in a single human or animal subject at short time intervals based on a multiple runs per day.

A wide spectrum of compounds has been prepared from cyclotron-produced ^{11}C -labeled radioprecursors in order to synthesize and develop novel ^{11}C -labeled radiopharmaceuticals (Figure 9)^{1a, 30}. The syntheses of various classes of compounds are not always simple and straightforward like carboxylation of ^{11}C -labeled Grignard reagent but sometimes much more complicated.

Figure 9. The map of production of radiolabeled precursors for labeling with ^{11}C derived from the target and on-line conversion to further radioprecursors.



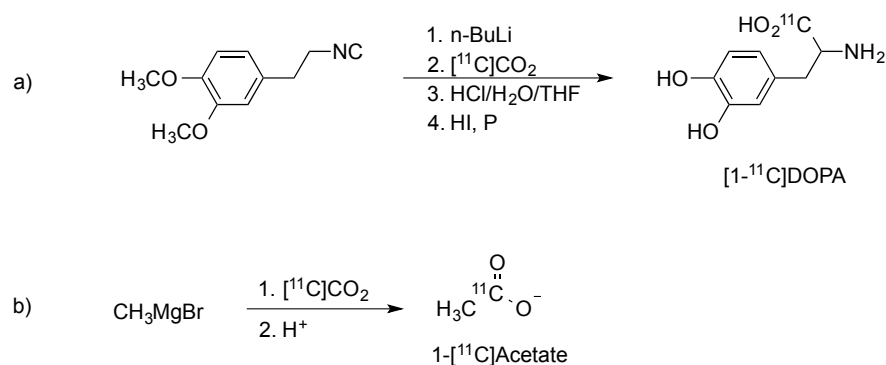
4.1. Primary radioprecursors for ^{11}C -labeling

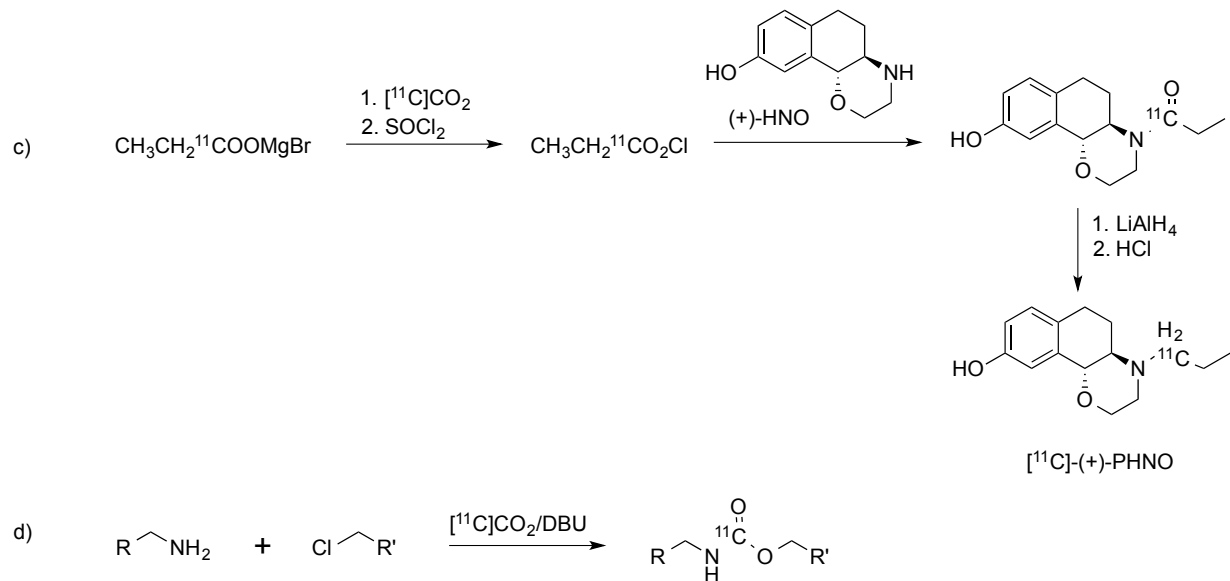
Both $[^{11}\text{C}]\text{CO}_2$ and $[^{11}\text{C}]\text{CH}_4$ are available at the end of cyclotron bombardment. These two primary radioprecursors enable to be converted to many different classes of radiocompounds or directly used in organic synthesis for preparing radiopharmaceuticals (Figure 8). In general, ^{11}C -chemistry has involved formation of C-C bond and C-Y bond, where Y is heteroatom with one or more lone pairs such as N, O, or S via alkylation and carboxylation from $[^{11}\text{C}]\text{CO}_2$ as well as displacement or addition reactions with $[^{11}\text{C}]\text{HCN}$ derived from $[^{11}\text{C}]\text{CH}_4$.

There are typical examples of PET tracers labeled by using $[^{11}\text{C}]\text{CO}_2$ directly. Labeled carbon dioxide was used for the early synthesis of ^{11}C labeled DOPA on 1970s for the investigation of dopaminergic process in the human brain. A reaction between collected $[^{11}\text{C}]\text{CO}_2$ and the lithium salt of β -(3,4-dimethoxyphenyl)-ethyl isocyanide followed by hydrolysis affords $[1\text{-}^{11}\text{C}]\beta$ -(3,4-dimethoxyphenyl)-D,L- α -alanine. Subsequent purification of

the intermediate and hydrolysis gives rise to [carboxyl- ^{11}C]DOPA (Figure 10-a)³¹. [^{11}C]Acetate is a useful PET tracer for monitoring the recurrence of prostate cancer. This tracer is synthesized with [^{11}C]CO₂ via Grignard reaction (Figure 10-b)³². Non-radioactive (+)-4-propyl-3,4,4a,5,6,10b-hexahydro-2H-naphtho[1,2-b][1,4]oxazin-9-ol (PHNO) was synthesized as a potent D2 subunit of dopamine receptor. [^{11}C]PHNO has been developed as a new dopamine agonist radiotracer for PET imaging of the dopamine D3 high-affinity state by specific binding to dopamine D3 receptor. [^{11}C]propionyl chloride is prepared via Grignard reaction with [^{11}C]CO₂ followed by chlorination to react secondary amine precursor. The desired [^{11}C]PHNO is obtained by reduction of the [^{11}C]carbonyl (Figure 10-c)³³. Recently, an operationally simple and mild reaction based on the direct fixation of [^{11}C]CO₂ with 1,8-diazabicyclo[5.4.0]undec-7-ene (DBU) has been developed for the synthesis of [^{11}C]carbamates in high radiochemical yields (>70%) (Figure 10-d)³⁴. This strategy should be useful for the development of new radiotracers for PET and other applications.

Figure 10. Synthesis of typical ^{11}C -labeled radiotracers from [^{11}C]CO₂





It is not practical to directly use $[^{11}\text{C}]\text{CH}_4$ in order for introduction of ^{11}C into organic molecules not only because it is hard to be trapped in the organic solvents but the carbon atom in methane, which is neither electron deficient nor rich, is not being able to be a site for electrophile or nucleophile for substitution reactions. Thus $[^{11}\text{C}]\text{CH}_4$ is converted to a wide variety of reactive forms of radiocompounds involved in efficient $[^{11}\text{C}]$ carboxylation and $[^{11}\text{C}]$ alkylation and $[^{11}\text{C}]$ cyanation for synthesis of ^{11}C -radiopharmaceuticals.

4.2. ^{11}C -labeling with radiocompounds derived from $[^{11}\text{C}]\text{CO}_2$ and $[^{11}\text{C}]\text{CH}_4$

A number of other simple one-carbon compounds are synthesized from labeled carbon dioxide (Figure 11) or methane (Figure 12) via one step or multiple steps of synthetic manipulation during or after cyclotron bombardment (Figure 9). Their use in particular synthetic applications take into account differences in their specific activity.

Figure 11. Radioprecursors derived from $[^{11}\text{C}]\text{CO}_2$

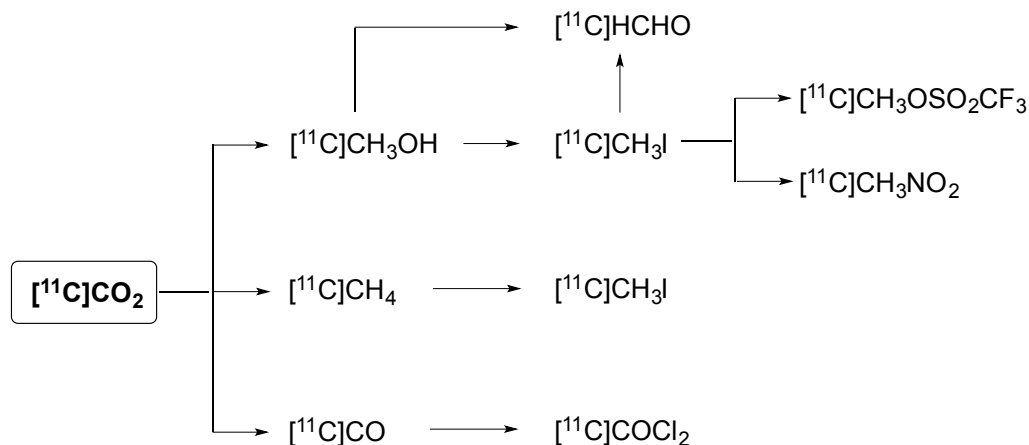
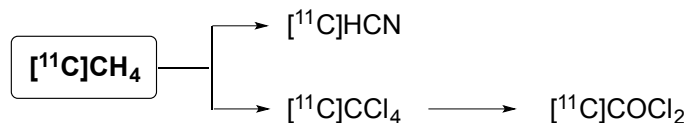


Figure 12. Radioprecursors derived from $[^{11}\text{C}]\text{CH}_4$



4.2.1. Nucleophilic methylation with $[^{11}\text{C}]\text{CH}_3\text{I}$

Some of the earliest radiosyntheses with C-11 relied on labeled carbon dioxide and cyanide. While alkylation with methyl iodide is the most widely used method for ^{11}C -involved organic synthesis of today.

In fact, the vast majority of PET tracers utilized routinely for clinical purposes have been produced by ^{11}C methylation at heteroatoms, i.e. N, O or S. The reasons for this fact can be found from the ready availability of a precursor through *des*-alkyl, e.g. *des*-methyl, versions of a well-known model compound. In addition, according to the evaluation of substructure analyses on the frequencies of functional groups of drugs, tertiary aliphatic amines are the most frequent functional group in drug molecules, with carboxamides as the second most frequently occurring

functional group. Esters and aromatic ethers are also common existing in drugs and natural products. This emphasizes the selection of *des*-methyl form of the corresponding model compounds or their amine/alcohol/thiol-containing derivatives for use as precursors.

Furthermore, [^{11}C]methylation of heteroatoms is generally beneficial with respect to the metabolic fate of a radiotracer. Radioactive metabolites may result in an undesired background signal in the organ under study during the PET scan that decreases the signal to noise ratio. The metabolites may also have affinity for the target and cause difficulties in the quantification of binding. Controlling the metabolic fate of a radiotracer is especially crucial in the determination of the best labeling position for imaging of targets in the central nervous system (CNS).

The brain is separated from the circulatory system by the blood-brain-barrier (BBB) which is a membrane constituted of capillary endothelial cells. Under normal physiological conditions, diffusion of polar molecules across the BBB is restricted. PET radiotracers for studying the CNS brain biochemistry are thus frequently labeled at metabolically labile position in the molecule (i.e. N-, O-, S- ^{11}C methyl group) to produce hydrophilic radiolabeled metabolites staying in the peripheral organs and keep out of an intact parent radiotracer signal within the brain tissue. Heteroatom-methylated tracers are mostly metabolized by demethylation that gives rise to the formation of polar radiometabolites in small-molecular weight possessing poor BBB permeability³⁵.

Particularly [^{11}C]methylation of primary and secondary alcohols and amines as well as thiols with methyl iodide (or with even reactive [^{11}C]CH₃OTf) is the most common strategy for a facile ^{11}C -labeling via nucleophilic substitution in the last stage for the synthesis of radiopharmaceuticals. This nucleophilic [^{11}C]methylation occurs in high yield within a short time frame compatible with the half-life of ^{11}C (20.4 min).

$[^{11}\text{C}]\text{CH}_3\text{I}$ is currently produced by two different methods: wet-chemistry and dry-chemistry methods. One method is based on trapping the cyclotron produced $[^{11}\text{C}]\text{CO}_2$ in a solution of the reduction agent lithium aluminium hydride (LAH) in tetrahydrofuran (THF) or diethyl ether followed by treatment of the $[^{11}\text{C}]\text{CH}_3\text{OH}$ with iodide sources such as HI^{36} , $\text{P}_2\text{I}_4^{37}$ or $\text{PPh}_3\text{I}_2^{38}$. After removal of the solvent, $[^{11}\text{C}]\text{CH}_3\text{I}$ is distilled in a stream of inert gas and lead through a $\text{NaOH}/\text{P}_2\text{O}_5$ trap before being delivered into the solution of the precursor of the $[^{11}\text{C}]\text{methylation}$. Although this wet-chemistry method gives $[^{11}\text{C}]\text{CH}_3\text{I}$ in high radiochemical yield, final specific activity is low. It is because the use of LAH, which is the primary source of cold CO_2 , limits the specific activity of the $[^{11}\text{C}]\text{methylation}$ agent. Thus only limited amount of LAH (5 – 7 μmol) is used for a good trapping efficiency of $[^{11}\text{C}]\text{CO}_2$ with a good specific activity of the tracer³⁹.

An alternative method that developed in the 1990s was Ni-catalyzed reduction of $[^{11}\text{C}]\text{CO}_2$ with H_2 to yield $[^{11}\text{C}]\text{CH}_4$ followed by gas-phase ($\sim 700\text{ }^\circ\text{C}$) free radical iodination of the latter to yield $[^{11}\text{C}]\text{H}_3\text{I}^{40}$. More recently, $[^{11}\text{C}]\text{CH}_4$ can be produced directly in the target chamber via the $^{14}\text{N}(\text{p},\alpha)^{11}\text{C}$ nuclear reaction using a 5% or 10% H_2/N_2 target mix⁴¹.

A single passage of $[^{11}\text{C}]\text{CH}_4$ through the heated reaction containment results in a relatively low conversion. The radiochemical yield of $[^{11}\text{C}]\text{CH}_3\text{I}$ can be improved to > 60 % by utilizing a loop system in which the produced $[^{11}\text{C}]\text{CH}_3\text{I}$ is trapped while the remaining $[^{11}\text{C}]\text{CH}_4$ is recirculated. This dry-chemistry method, also referred to as the ‘gas phase’ method, is much more decent and less labor intensive than wet-chemistry method because multiple production runs are performed without the intermediate cleaning and drying of the production system⁴².

Nucleophilic $[^{11}\text{C}]\text{methylations}$ to heteroatoms, N, O, and S, are generally very straightforward. For the methylation, $[^{11}\text{C}]\text{CH}_3\text{I}$ is delivered in the solution of precursor treated

with base and it is widely applied as a key strategy in order to introduce ^{11}C into important PET tracers (e.g. $[^{11}\text{C}]$ methionine⁴³, $[^{11}\text{C}]$ choline⁴⁴, and $[^{11}\text{C}]$ PK11195⁴⁵) shown on Figure 13. Due to competing reactions with nucleophiles contained in the molecule, however, protection groups are frequently used for obtaining $[^{11}\text{C}]$ methylation at the desired position in the molecule. The protection groups can be rapidly removed afterward⁴⁶ (Figure 14).

Figure 13. Selected examples of radiosynthesis by nucleophilic $[^{11}\text{C}]$ methylation with $[^{11}\text{C}]\text{CH}_3\text{I}$ to hetero atoms

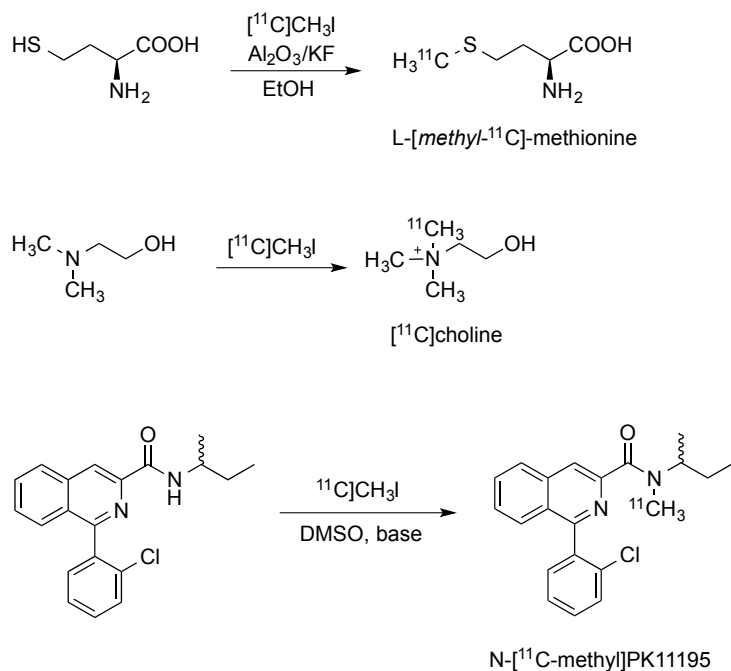
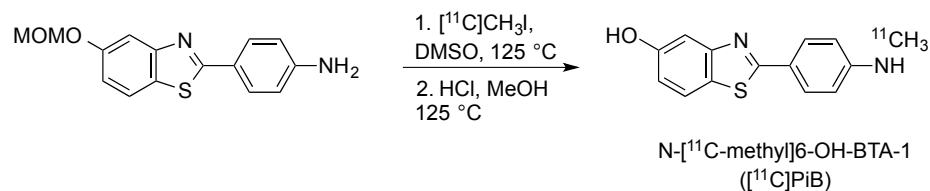


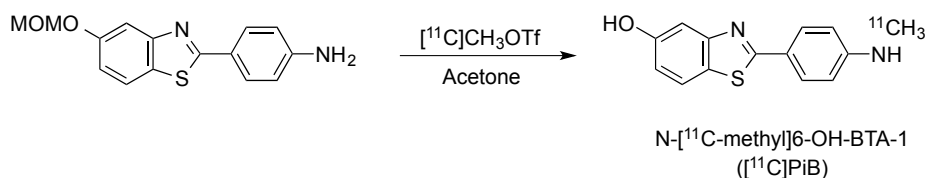
Figure 14. $[^{11}\text{C}]$ methylation involving protection and deprotection⁴⁶



4.2.2. Application of [^{11}C]CH $_3$ OTf

Production of [^{11}C]CH $_3$ OTf is achieved with [^{11}C]CH $_3$ I delivered by a stream of inert gas through a column of silver triflate kept at 180 °C (Figure 9). For [^{11}C]alkylation of nucleophile with a low activity, the use of more reactive counter electrophile such as [^{11}C]CH $_3$ OTf is required. Several cases of the use of [^{11}C]CH $_3$ OTf have reported higher radiochemical yields of the ^{11}C -methylated tracer in shorter reaction times, at lower temperatures, and with lower amounts of precursor compared to that of [^{11}C]CH $_3$ I. Also due to its higher reactivity, ^{11}C -methylation can be carried out under milder conditions using [^{11}C]CH $_3$ OTf, in the case of relatively unstable compounds. For example, the β -amyloid plaque tracer N-[^{11}C -methyl]-6-OH-BTA-1([^{11}C]PiB) was originally synthesized by reacting the 6-O-MOM protected precursor with [^{11}C]H $_3$ I in a polar aprotic solvent⁴⁶. While shifting the methylation agent to [^{11}C]CH $_3$ OTf and conducting the reaction in acetone provides chemoselective N-[^{11}C]methylation without protecting⁴⁷ (Figure 15).

Figure 15. Synthesis of N-[^{11}C -methyl]-6-OH-BTA-1([^{11}C]PiB) with [^{11}C]CH $_3$ OTf⁴⁷



4.2.3. Displacement and addition reactions with [^{11}C]cyanide and [^{11}C]phosgene

Even though [^{11}C]CH $_4$ is not able to directly involve for labeling organic molecules, labeled methane is very useful in radiosynthesis because it is available in large quantities and can be readily converted to [^{11}C]HCN by simply passing the target gas (N_2/H_2 in the presence of a small quantity of ammonia) over platinum quartz wool at 950 °C. [^{11}C]Cyanide can be used as a

nucleophile in the presence of base to replace a leaving group to $^{11}\text{C}\text{N}^-$. Subsequent transformations of ^{11}C -nitriles yield useful functional groups including carboxylic acids, amides⁴⁸ and amidines⁴⁹ and tetrazoles⁵⁰ so it has been widely used in the synthesis of ^{11}C -labeled compounds containing these functionalities. For instance, ^{11}C cyanation followed by Grignard reaction was performed for the synthesis of ^{11}C spiroperidol for early studies of the dopamine D2 receptor (Figure 16)⁵¹.

^{11}C -labeled methane has also been converted to ^{11}C phosgene (^{11}C COCl₂) which is a highly reactive bi-functional reagent and useful for introducing a ^{11}C -carbonyl group into a molecule. ^{11}C COCl₂ is preferably obtained by oxidation of ^{11}C CCl₄ which is obtained by chlorination of ^{11}C CH₄. ^{11}C phosgene reacts readily with nucleophiles such as amines and alcohols, yielding ^{11}C -labeled urea, carbamate, or amide derivatives. For example, the synthesis of a ring-labeled monoamine oxidase inhibitor is carried out with ^{11}C phosgene (Figure 17)⁵². Although ^{11}C phosgene has been used for past decades, the use of this extremely reactive compounds for radiolabeling is still impeded by low radiochemical yields and difficulties in the reproducibility of its preparation and side-reaction with nucleophiles in the radiosynthesis of complex tracers.

Figure 16. Displacement with ^{11}C cyanation for synthesis of radiotracer, ^{11}C spiroperidol⁵¹

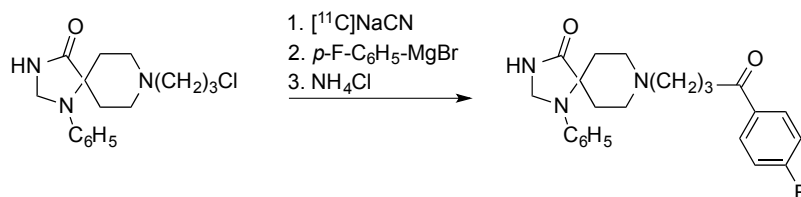
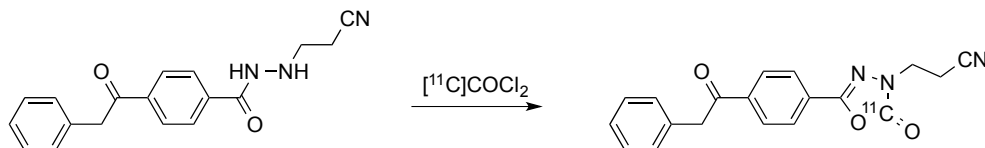


Figure 17. Preparation of a ring-labeled monoamine oxidase inhibitor ($[^{11}\text{C}]\text{MAO}$) with $[^{11}\text{C}]\text{COCl}_2$ ⁵²



5. Development of PET radiotracers with $[^{11}\text{C}]\text{HCN}$

5.1. Development of methodology for the production of $[^{11}\text{C}]\text{HCN}$

Practical methodology for the preparation of carbon-11 labeled cyanide by recoil synthesis has been actively developed since 1960s⁵³. According to recoil synthesis, produced radioisotope from the cyclotron was incorporated into the compound of interest directly. Thereby overall total synthesis of radiopharmaceuticals became simpler and faster. The target of this direct preparation of recoil $[^{11}\text{C}]\text{cyanide}$ was powdered NaCN wrapped in aluminum foil in order to be in a volume of uniform thickness as the beam area. The target was irradiated with proton beam (33 MeV) and the nuclear reactions operative in this process are $^{14}\text{N}(p, \alpha)^{11}\text{C}$ acting on the nitrogen in the cyanide and $^{12}\text{C}(p, pn)^{11}\text{C}$ acting on the carbon in the cyanide. Because, however, this method is not carrier free, maximum specific activity was directly influenced by the mass of the target⁵⁴.

Following method for the preparation of carrier-free $[^{11}\text{C}]\text{HCN}$ was inspired by the work of Wolf A. P. This method for direct recoil synthesis of large quantities of $[^{11}\text{C}]\text{cyanide}$ with high specific activity was improved by using two different target systems: one was a solid batch process (lithium amide target) and the other was a continuous flow gas target (nitrogen-hydrogen

gas target). Both targets are based on the $^{14}\text{N}(p, \alpha)^{11}\text{C}$ reaction via irradiation with proton beam (15 MeV)⁵⁵.

A system for the simple routine production of carrier-free, high-activity [^{11}C]HCN in an on-line process in the gas stream was originated from PET imaging group at Brookhaven National Laboratory for medical purpose⁵⁶. The primary radioprecursor [^{11}C]CH₄ produced from cyclotron target was quantitatively converted to [^{11}C]HCN in the presence of ammonia flow over heated Pt (1000 °C) in an on-line process. The target gas was N₂ (95 %) + H₂ (5 %) irradiated with 25 MeV proton beam and $^{14}\text{N}(p, \alpha)^{11}\text{C}$ reaction was involved. According to this method, highly reproducible and predictable production of [^{11}C]HCN was feasible and the yields from a given target were available in the gas phase within 10 – 12 min after the end of bombardment (EOB). In this way, ^{11}C -dopamine (specific activity ~ 40 mCi/mg at the time of delivery) was produced for use in animal studies by scale down the injection dose level by approximately a factor of 100⁵⁶.

A efficient technique for on-line production of [^{11}C]HCN from cyclotron produced [^{11}C]CO₂ was reported on 1987⁵⁷. This system was comprised of N₂ gas target irradiated by proton bombardment and reduction of CO₂ to CH₄ H₂ with Pt catalyst at 950 °C. This method was systematically invested by optimization and evaluation of affecting factors like beam current dependent in-target ammonia formation and product composition⁵⁸ and has been used until nowadays for routine production runs. Recently the yield of [^{11}C]HCN was maximized to 50 – 70 % by further investigation for optimizing the on-line process⁵⁹.

5.2. Radiochemistry with [^{11}C]HCN

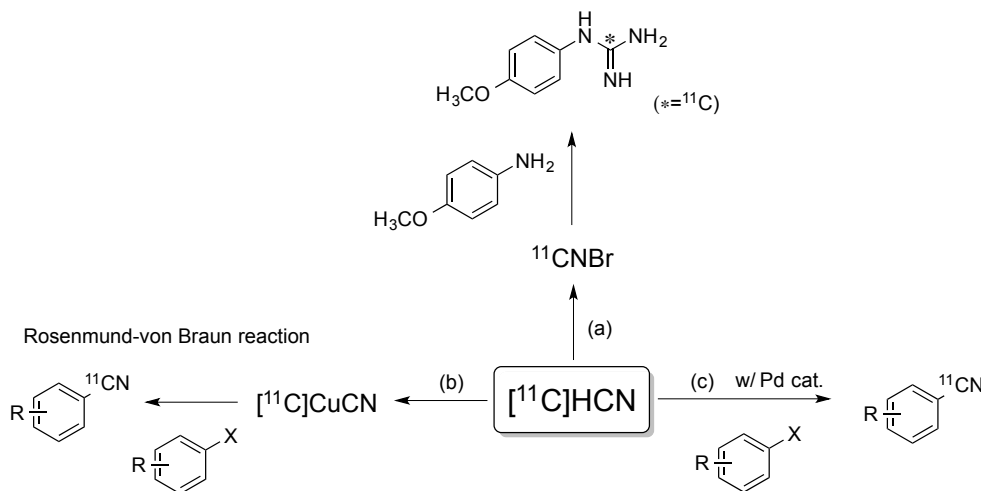
5.2.1. Nucleophilic [^{11}C]cyanation reactions

The nitrile group is frequently found in a large number of important drug molecules (e.g. vildagliptin (antidiabetic), letrozole (aromatase inhibitor), cyamemazine (antipsychotic), and rilpivirine (anti-HIV agent), etc.))⁶⁰. Those biologically important compounds naturally became target molecules for C-11 labeling reactions, thereby efficient nucleophilic [^{11}C]cyanation with [^{11}C]cyanide have been developed and accomplished for medical and pharmaceutical use.

Introduction of [^{11}C]cyanide to aromatic substrates and further transformations

[^{11}C]HCN can be used directly for introducing [^{11}C]CN group to aromatic substrate by carbon (SP²) – carbon (SP) coupling. [^{11}C]cyanogen bromide has been prepared for the synthesis of ^{11}C -labeled guanidines. Once amines were converted into [^{11}C]cyanamides by cyanation with [^{11}C]CNBr, subsequent conversion to the corresponding guanidines was accomplished with ammonia in the supercritical fluid synthesis system at high pressure and temperature (Figure 18-a)⁶¹. The incorporation of a [^{11}C]cyanide anion into an aryl ring works efficiently when mediated by copper (I) or palladium. Palladium-mediated [^{11}C]cyanation reactions may become a more favorable route for introducing [^{11}C]cyano group based on increased number of methodology development in respect of palladium-catalyzed cyanations⁶² (Figure 18-b)⁶². Additionally [^{11}C]HCN can be converted into [^{11}C]CuCN and reacted with aryl halides via Rosenmund – von Braun reaction (Figure 18-c)³⁵. Subsequent transformations of [^{11}C]nitriles yield useful functional groups such as carboxylic acids and derivatives and have been employed for the synthesis of C-11 labeled compounds containing these functionalities³⁵.

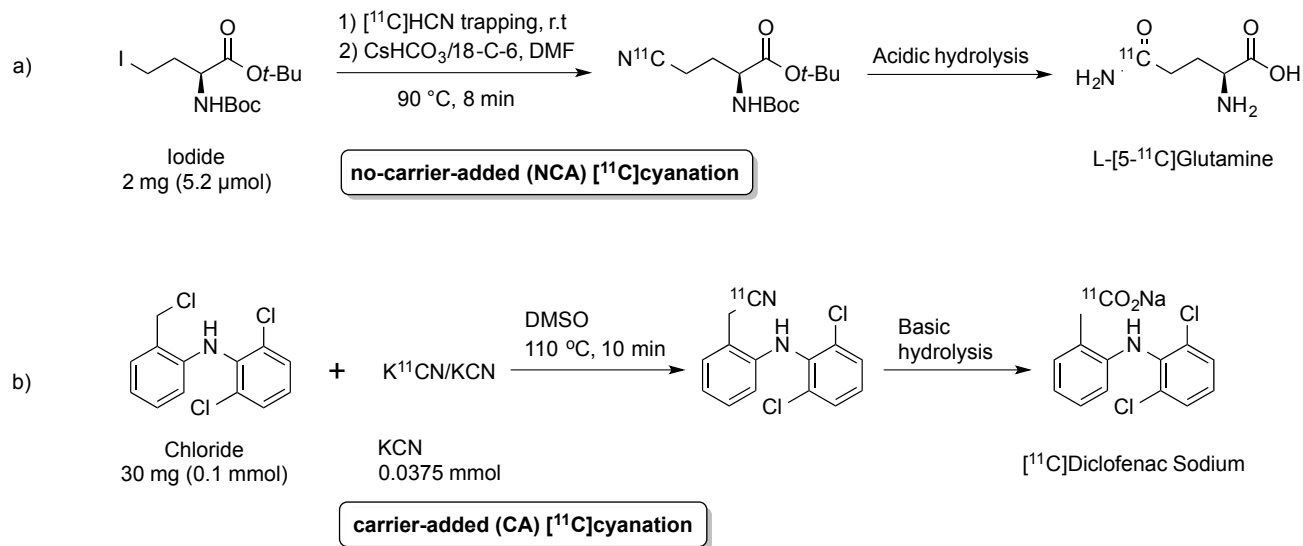
Figure 18. Selected [^{11}C]cyanation reactions and further transformation for aromatic [^{11}C]nitriles



Introduction of [^{11}C]cyanide to aliphatic substrates

Nucleophilic [^{11}C]cyanation with [^{11}C]HCN can be accomplished via carbon (SP³) – carbon (SP) coupling in carrier-added or no-carrier-added condition. This type of [^{11}C]cyanation reactions has been widely used for the preparation of C-11 labeled amino acids such as [^{11}C]aminobutyric acids⁶³, L-[5- ^{11}C]glutamine⁶⁴, L-[4- ^{11}C]asparagine⁶⁵, L-[5- ^{11}C]glutamate⁶⁶, [4- ^{11}C]aspartate⁶⁶, [^{11}C]5-hydroxy-L-tryptophan⁶⁷, [^{11}C] and [^{11}C]tyrosine⁶⁸. This strategy is also useful for other C-11 labeling of biologically active compounds. For example, L-[5- ^{11}C]glutamine can be prepared solid phase-supported reaction of [^{11}C]HCN with arabinose followed by hydrolysis (Figure 19-a)⁶⁴. Dichlofenac sodium which belongs to the family of non-steroidal anti-inflammatory drugs was labeled with C-11 via carrier-added [^{11}C]cyanation followed by hydrolysis (Figure 19-b)⁶⁹.

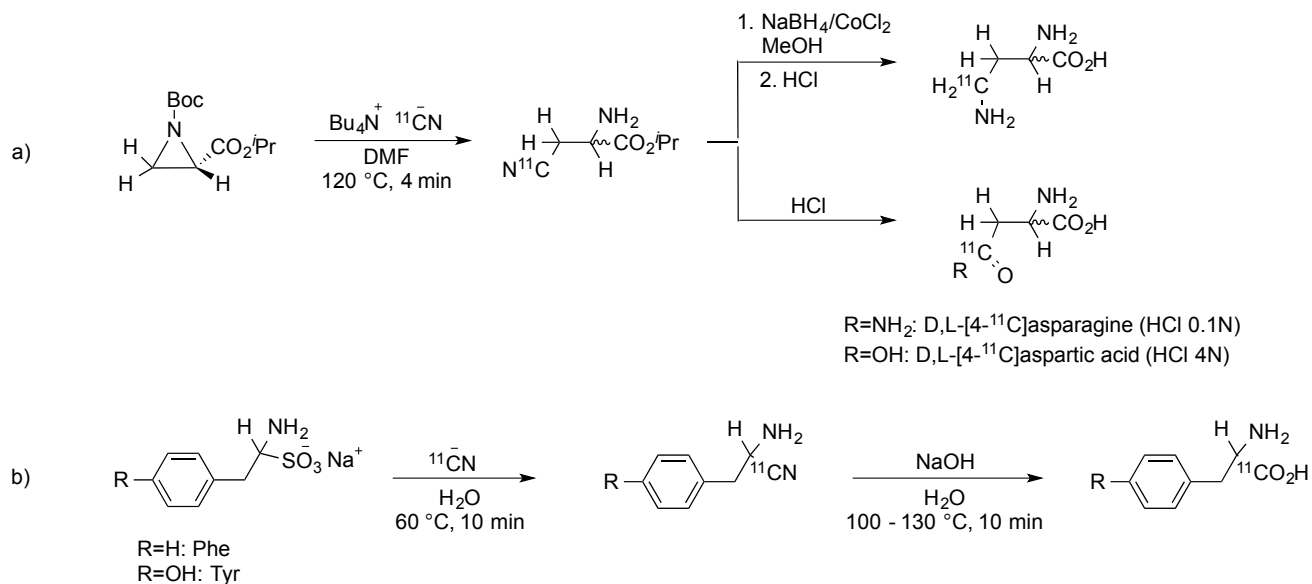
Figure 19. Summary of the preparation of aliphatic [^{11}C]nitrile



Further transformation of [^{11}C]cyano group on aliphatic substrates

The [^{11}C]cyano group introduced into a target molecule has potential to be converted into a wide range of other functional groups such as carboxylic acid, amides, amidines and tetrazoles⁷⁰. For instance, ring-opening of N-activated aziridine-2-carboxylates with [^{11}C]cyanide was useful for synthesis of amino acids (i.e. [4- ^{11}C]aspartic acid, [4- ^{11}C]asparagine, and 2,4-diamino[4- ^{11}C]butyric acid via formation of β -[^{11}C]cyano-alanine ester (Figure 20-a)³⁰. Only racemic amino acids products were obtained via this ring-opening method in high radiochemical yield (30 – 40%, decay-corrected, counted from [^{11}C]CN⁻). Beside this ring-opening methodology, the natural amino acids tyrosine (Tyr) and phenylalanine (Phe) were labelled with carbon- 11 via a modified Bucherer-Strecker synthesis (Figure 20-b)³⁰.

Figure 20. Selected examples of nucleophilic [^{11}C]cyanation followed by transformation of the [^{11}C]nitrile functions on aliphatic substrates.



5.2.2. Development of novel PET radiotracers and radioligands via nucleophilic [^{11}C]cyanation

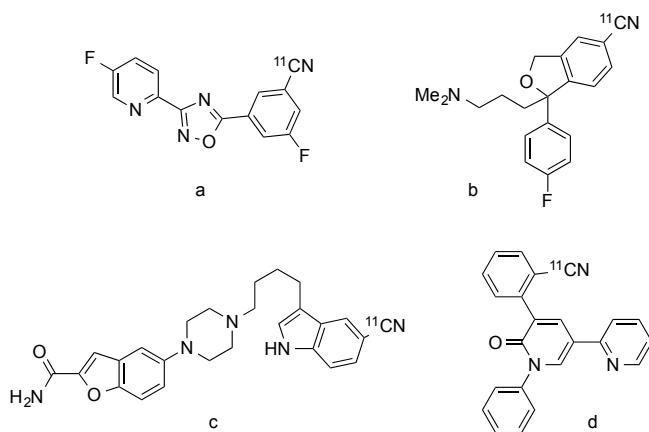
There are critical restrictions in the incorporation of short half-life carbon-11 ($t_{1/2} = 20.4$ min) into organic molecules for applications for PET: 1) limited time for reactions (in seconds/minutes) and purification; 2) biased stoichiometry between radionuclide and all other substrates in the reaction mixture (i.g. typically submicromolar concentration of cyclotron generated [^{11}C]HCN); 3) controlled reaction condition to be mild in order to minimize decomposition of radiotracers that formed. These challenges prevent the application of a number of high yielding catalytic and even stoichiometric reactions to be applied to the synthesis of radiolabeled compounds with C-11. Thus there are only a few promising reactions for introducing C-11 into organic molecules using [^{11}C]HCN as a radioprecursor.

Generally, nucleophilic [^{11}C]cyanation with [^{11}C]HCN is one of the most common strategies for C-11 labeling, along with [^{11}C]methylation with [^{11}C]CH $_3$ I. Although carrier-added manner for [^{11}C]cyanations is one way in order to favorably drive the cyanation reaction by balancing biased stoichiometry in the reaction mixture, only facile methods for no-carrier added nucleophilic [^{11}C]cyanation is considered in this section (5.2.2.).

Transition-metal mediated [^{11}C]cyanation

Traditionally, transition-metal (i.g. Cr(0), Pd(0), and Cu(I)) mediated cyanation reactions have been used for preparing C-11 derivatives of aryl rings which occur in biologically important organic molecules. Among them, the Pd-mediated cyanation of aryl (pseudo)halides is one of the most promising strategies for simple, rapid cyanation. For instance, [^{11}C]AZD9272 (Figure 21-a) that is a novel metabotropic glutamate receptor 5 (mGluR5) radioligand evaluated in the non-human primate brain, was prepared via Pd-mediated [^{11}C]cyanation with Pd(Ph $_3$) $_4$ in presence of KOH and Kryptofix 2.2.2^{62, 71}.

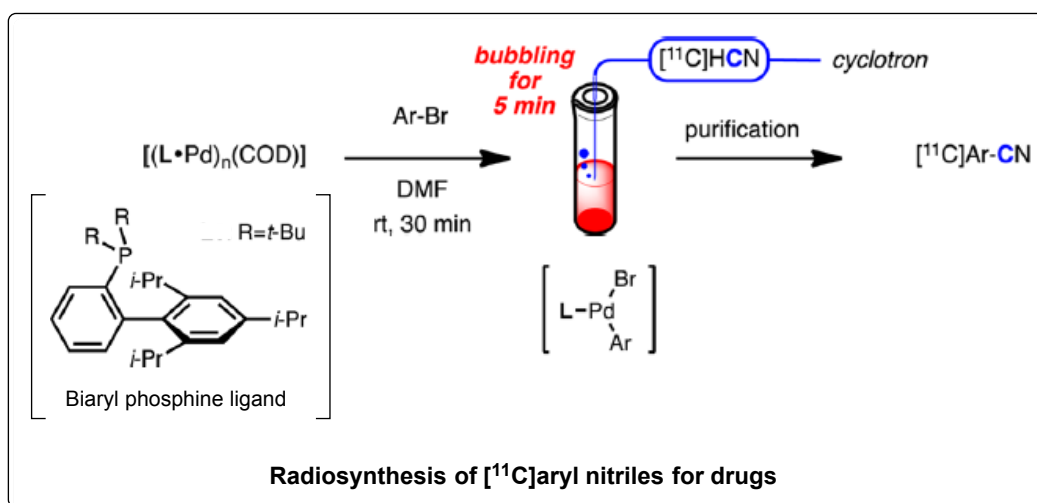
Figure 21. The structures of pharmaceutically and biologically important small radioligand and complex drug-based radiotracers containing cyano group.



a) [^{11}C]AZD9272 (mGluR5 radioligand); b) [^{11}C]citalopram (antidepressant); c) [^{11}C]vilazodone (antidepressant); d) [^{11}C]perampanel (antiepileptic).

In addition, the most recent discovery by usage of biarylphosphine ligands rather than traditional Pd ligands (e.g., Ph_3P or bis(diphenylphosphino)ferrocene (dppf)) requiring harsh reaction conditions (e.g., high temperature, long reaction time, and the use of base) contributed to facile stoichiometric transmetalation with cyanide and reductive elimination of aryl nitriles at room temperature in under 5 min^{70, 72} (Figure 22).

Figure 22. Syntheses of C-11 labeled drugs via [^{11}C]cyanation using biaryl phosphine Pd(0) complexes⁷⁰

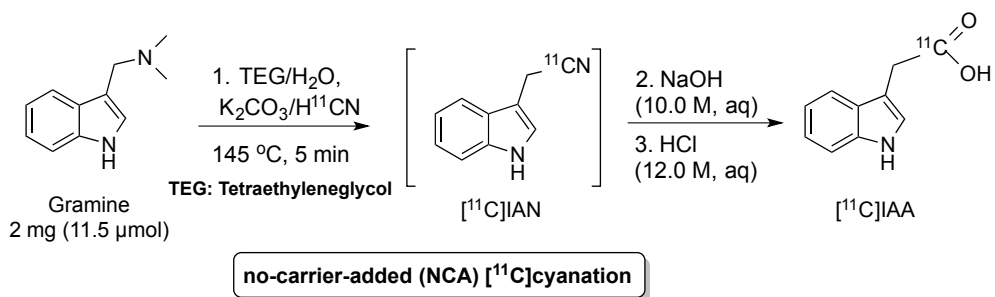


Nucleophilic [^{11}C]cyanation without metal catalysts

$\text{S}_{\text{N}}2$ cyanations without metal catalysts also have been widely used under various basic conditions. In 1973, [$1\text{-}^{11}\text{C}$]dopamine was synthesized via carrier-free [^{11}C]cyanation in presence of base (0.05 M NaOH) followed by hydrogenation and evaluated in mongrel dogs⁵⁶. Recently, useful radiotracers such as L-[5- ^{11}C]glutamine⁶⁴ (Figure 18-a) and [^{11}C]auxin ([^{11}C]IAA, plant hormone)⁷³ (Figure 23) for both animal and plant studies were developed via rapid [^{11}C]cyanation in presence of base and cyclic polyether (18-crown-6) without transition

metal mediation, thereby this type of [^{11}C]cyanation not requiring metal catalyst has attracted attention of radiochemists.

Figure 23. Synthesis of [^{11}C]indole-3-acetic acid ([^{11}C]IAA) via [^{11}C]cyanation and alkaline hydrolysis⁷³



6. Reference

1. (a) Miller, P. W.; Long, N. J.; Vilar, R.; Gee, A. D., Synthesis of ^{11}C , ^{18}F , ^{15}O , and ^{13}N radiolabels for positron emission tomography. *Angew. Chem., Int. Ed.* **2008**, *47* (47), 8998-9033; (b) Fowler, J. S.; Wolf, A. P., Working against Time: Rapid Radiotracer Synthesis and Imaging the Human Brain. *Acc. Chem. Res.* **1997**, *30* (4), 181-188.
2. (a) Galldiks, N.; Stoffels, G.; Ruge, M. I.; Rapp, M.; Sabel, M.; Reifenberger, G.; Erdem, Z.; Shah, N. J.; Fink, G. R.; Coenen, H. H.; Langen, K. J., Role of O-(2- ^{18}F -fluoroethyl)-L-tyrosine PET as a diagnostic tool for detection of malignant progression in patients with low-grade glioma. *Journal of nuclear medicine : official publication, Society of Nuclear Medicine* **2013**, *54* (12), 2046-54; (b) Palumbo, B., Brain tumour recurrence: brain single-photon emission computerized tomography, PET and proton magnetic resonance spectroscopy. *Nuclear medicine communications* **2008**, *29* (8), 730-5; (c) Kickingereder, P.; Dorn, F.; Blau, T.; Schmidt, M.; Kocher, M.; Galldiks, N.; Ruge, M. I., Differentiation of local tumor recurrence from radiation-induced changes after stereotactic radiosurgery for treatment of brain metastasis: case report and review of the literature. *Radiation oncology* **2013**, *8*, 52.
3. Palumbo, B.; Buresta, T.; Nuvoli, S.; Spanu, A.; Schillaci, O.; Fravolini, M. L.; Palumbo, I., SPECT and PET serve as molecular imaging techniques and in vivo biomarkers for brain metastases. *International journal of molecular sciences* **2014**, *15* (6), 9878-93.
4. Lucignani, G.; Bombardieri, E., Molecular imaging: seeing the invisible beyond the "hot spot". *The quarterly journal of nuclear medicine and molecular imaging : official publication of the Italian Association of Nuclear Medicine* **2004**, *48* (1), 1-3.
5. Biegon, A.; Dillon, K.; Volkow, N. D.; Hitzemann, R. J.; Fowler, J. S.; Wolf, A. P., Quantitative Autoradiography of Cocaine Binding-Sites in Human Brain Postmortem. *Synapse* **1992**, *10* (2), 126-130.
6. Wolf, A.; Fowler, J., Cyclotrons and Positron Emitting Radiopharmaceuticals. In *Physics and Engineering of Medical Imaging*, Guzzardi, R., Ed. Springer Netherlands: 1987; Vol. 119, pp 721-749.
7. (a) Benard, F.; Romsa, J.; Hustinx, R., Imaging gliomas with positron emission tomography and single-photon emission computed tomography. *Seminars in nuclear medicine* **2003**, *33* (2), 148-62; (b) Minn, H., PET and SPECT in low-grade glioma. *European journal of radiology* **2005**, *56* (2), 171-8.
8. (a) Townsend, D. W.; Cherry, S. R., Combining anatomy and function: the path to true image fusion. *European radiology* **2001**, *11* (10), 1968-74; (b) Townsend, D. W., A combined PET/CT scanner: the choices. *Journal of nuclear medicine : official publication, Society of Nuclear Medicine* **2001**, *42* (3), 533-4; (c) Beyer, T.; Townsend, D. W.; Brun, T.; Kinahan, P. E.; Charron, M.; Roddy, R.; Jerin, J.; Young, J.; Byars, L.; Nutt, R., A combined PET/CT scanner for clinical oncology. *Journal of nuclear medicine : official publication, Society of Nuclear Medicine* **2000**, *41* (8), 1369-79.
9. Blodgett, T. M.; Meltzer, C. C.; Townsend, D. W., PET/CT: form and function. *Radiology* **2007**, *242* (2), 360-85.
10. Brinkman, G. A., In-Beam Production of Labeled Compounds. *Int J Appl Radiat Is* **1982**, *33* (7), 525-532.

11. (a) Ferrieri, R. A.; Wolf, A. P., The Chemistry of Positron Emitting Nucleogenic (Hot) Atoms with Regard to Preparation of Labeled Compounds of Practical Utility. *Radiochim Acta* **1983**, *34* (1-2), 69-83; (b) Nickles, R. J., A shotgun approach to the chart of the nuclides. Radiotracer production with an 11 MeV proton cyclotron. *Acta radiologica. Supplementum* **1991**, *376*, 69-71.
12. Ziegler, S. I., Positron emission tomography: Principles, technology, and recent developments. *Nucl Phys A* **2005**, *752*, 679C-687C.
13. Xu, M.; Cutler, P. D.; Luk, W. K., Adaptive, segmented attenuation correction for whole-body PET imaging. *Ieee T Nucl Sci* **1996**, *43* (1), 331-336.
14. (a) Ido, T.; Wan, C. N.; Casella, V.; Fowler, J. S.; Wolf, A. P.; Reivich, M.; Kuhl, D. E., Labeled 2-Deoxy-D-Glucose Analogs - F-18-Labeled 2-Deoxy-2-Fluoro-D-Glucose, 2-Deoxy-2-Fluoro-D-Mannose and C-14-2-Deoxy-2-Fluoro-D-Glucose. *J Labelled Compd Rad* **1978**, *14* (2), 175-183; (b) Fowler, J. S.; Wolf, A. P., 2-Deoxy-2-[F-18]Fluoro-D-Glucose for Metabolic Studies - Current Status. *Appl Radiat Isotopes* **1986**, *37* (8), 663-668; (c) Hamacher, K.; Coenen, H. H.; Stocklin, G., Efficient stereospecific synthesis of no-carrier-added 2-[18F]-fluoro-2-deoxy-D-glucose using aminopolyether supported nucleophilic substitution. *Journal of nuclear medicine : official publication, Society of Nuclear Medicine* **1986**, *27* (2), 235-8.
15. (a) Fujibayashi, Y.; Taniuchi, H.; Yonekura, Y.; Ohtani, H.; Konishi, J.; Yokoyama, A., Copper-62-ATSM: A new hypoxia imaging agent with high membrane permeability and low redox potential. *Journal of Nuclear Medicine* **1997**, *38* (7), 1155-1160; (b) Fujibayashi, Y.; Cutler, C. S.; Anderson, C. J.; McCarthy, D. W.; Jones, L. A.; Sharp, T.; Yonekura, Y.; Welch, M. J., Comparative studies of Cu-64-ATSM and C-11-acetate in an acute myocardial infarction model: Ex vivo imaging of hypoxia in rats. *Nuclear Medicine and Biology* **1999**, *26* (1), 117-121; (c) Obata, A.; Yoshimoto, M.; Kasamatsu, S.; Naiki, H.; Takamatsu, S.; Kashikura, K.; Furukawa, T.; Lewis, J. S.; Welch, M. J.; Saji, H.; Yonekura, Y.; Fujibayashi, Y., Intra-tumoral distribution of (64)Cu-ATSM: a comparison study with FDG. *Nucl Med Biol* **2003**, *30* (5), 529-34.
16. (a) Laforest, R.; Liu, X., Image quality with non-standard nuclides in PET. *The quarterly journal of nuclear medicine and molecular imaging : official publication of the Italian Association of Nuclear Medicine* **2008**, *52* (2), 151-8; (b) Hao, G.; Singh, A. N.; Liu, W.; Sun, X., PET with non-standard nuclides. *Current topics in medicinal chemistry* **2010**, *10* (11), 1096-112.
17. Phelps, M. E.; Mazziotta, J. C.; Schelbert, H. R., *Positron emission tomography and autoradiography: principles and applications for the brain and heart*. Raven Press: 1986.
18. Fowler, J. S.; Wolf, A. P. *Synthesis of carbon-11, fluorine-18, and nitrogen-13 labeled radiotracers for biomedical applications*; BNL-31222; Other: ON: DE82013799; TRN: 82-013604 United States10.2172/5260761Other: ON: DE82013799; TRN: 82-013604Thu Aug 28 07:36:03 EDT 2008NTIS, PC A06/MF A01.BNL; ERA-07-047599; NTS-82-009821; EDB-82-128867English; 1981; p Medium: ED; Size: Pages: 124.
19. Ter-Pogossian, M. M.; Raichle, M. E.; Sobel, B. E., Positron-emission tomography. *Scientific American* **1980**, *243* (4), 170-81 inverted question mark.
20. (a) Schinkel, A. H.; Wagenaar, E.; Mol, C. A.; van Deemter, L., P-glycoprotein in the blood-brain barrier of mice influences the brain penetration and pharmacological activity of many drugs. *The Journal of clinical investigation* **1996**, *97* (11), 2517-24; (b) Schinkel, A. H., P-

Glycoprotein, a gatekeeper in the blood-brain barrier. *Advanced drug delivery reviews* **1999**, *36* (2-3), 179-194.

21. Smith, C. B.; Deibler, G. E.; Eng, N.; Schmidt, K.; Sokoloff, L., Measurement of local cerebral protein synthesis in vivo: influence of recycling of amino acids derived from protein degradation. *Proceedings of the National Academy of Sciences of the United States of America* **1988**, *85* (23), 9341-5.

22. Wolf, A. P., Synthesis of Organic-Compounds Labeled with Positron Emitters and the Carrier Problem. *J Labelled Compd Rad* **1981**, *18* (1-2), 1-2.

23. Hooker, J. M.; Schoenberger, M.; Schieferstein, H.; Fowler, J. S., A simple, rapid method for the preparation of [(11)C]formaldehyde. *Angew Chem Int Edit* **2008**, *47* (32), 5989-5992.

24. Cai, L. S.; Lu, S. Y.; Pike, V. W., Chemistry with [F-18]fluoride ion. *Eur J Org Chem* **2008**, (17), 2853-2873.

25. (a) Kim, D. W.; Ahn, D. S.; Oh, Y. H.; Lee, S.; Kil, H. S.; Oh, S. J.; Lee, S. J.; Kim, J. S.; Ryu, J. S.; Moon, D. H.; Chi, D. Y., A new class of S(N)2 reactions catalyzed by protic solvents: Facile fluorination for isotopic labeling of diagnostic molecules. *Journal of the American Chemical Society* **2006**, *128* (50), 16394-16397; (b) Vincent, M. A.; Hillier, I. H., The solvated fluoride anion can be a good nucleophile. *Chemical communications* **2005**, (47), 5902-3.

26. (a) Jelinski, M.; Hamacher, K.; Coenen, H. H., C-Terminal F-18-fluoroethylamidation exemplified on [Gly-OH9] oxytocin. *J Labelled Compd Rad* **2002**, *45* (3), 217-229; (b) Block, D.; Coenen, H. H.; Stocklin, G., Nca F-18-Fluoroacylation Via Fluorocarboxylic Acid-Esters. *J Labelled Compd Rad* **1988**, *25* (2), 185-200.

27. Kolb, H. C.; Finn, M. G.; Sharpless, K. B., Click chemistry: Diverse chemical function from a few good reactions. *Angew Chem Int Edit* **2001**, *40* (11), 2004-+.

28. Firnaeu, G.; Garnett, E. S.; Chirakal, R.; Sood, S.; Nahmias, C.; Schrobilgen, G., [18F]fluoro-L-dopa for the in vivo study of intracerebral dopamine. *International journal of radiation applications and instrumentation. Part A, Applied radiation and isotopes* **1986**, *37* (8), 669-75.

29. Ehrenkauf, R. E.; Potocki, J. F.; Jewett, D. M., Simple synthesis of F-18-labeled 2-fluoro-2-deoxy-D-glucose: concise communication. *Journal of nuclear medicine : official publication, Society of Nuclear Medicine* **1984**, *25* (3), 333-7.

30. Allard, M.; Fouquet, E.; James, D.; Szlosek-Pinaud, M., State of art in 11C labelled radiotracers synthesis. *Current medicinal chemistry* **2008**, *15* (3), 235-77.

31. Korf, J.; Reiffers, S.; Beerling-van der Molen, H. D.; Lakke, J. P.; Paans, A. M.; Vaalburg, W.; Woldring, M. G., Rapid decarboxylation of carbon-11 labelled DL-DOPA in the brain: a potential approach for external detection of nervous structures. *Brain research* **1978**, *145* (1), 59-67.

32. Soloviev, D.; Tamburella, C., Captive solvent [11C]acetate synthesis in GMP conditions. *Applied radiation and isotopes : including data, instrumentation and methods for use in agriculture, industry and medicine* **2006**, *64* (9), 995-1000.

33. Wilson, A. A.; McCormick, P.; Kapur, S.; Willeit, M.; Garcia, A.; Hussey, D.; Houle, S.; Seeman, P.; Ginovart, N., Radiosynthesis and evaluation of [11C]-(+)-4-propyl-3,4,4a,5,6,10b-hexahydro-2H-naphtho[1,2-b][1,4]oxazin-9-ol as a potential radiotracer for in vivo imaging of the dopamine D2 high-affinity state with positron emission tomography. *Journal of medicinal chemistry* **2005**, *48* (12), 4153-60.

34. Hooker, J. M.; Reibel, A. T.; Hill, S. M.; Schueller, M. J.; Fowler, J. S., One-Pot, Direct Incorporation of [C-11]CO₂ into Carbamates. *Angew Chem Int Edit* **2009**, *48* (19), 3482-3485.
35. Wester, H. J., *Pharmaceutical Radiochemistry: I*. Scintomics: 2010.
36. Langstrom, B.; Lundqvist, H., The preparation of carbon-11-labeled methyl iodide and its use in the synthesis of carbon-11-labeled methyl-L-methionine. *Int. J. Appl. Radiat. Isot.* **1976**, *27* (7), 357-63.
37. Oberdorfer, F.; Hanisch, M.; Helus, F.; Maier-Borst, W., A new procedure for the preparation of ¹¹C-labeled methyl iodide. *Int. J. Appl. Radiat. Isot.* **1985**, *36* (6), 435-8.
38. Holschbach, M.; Schuller, M.; Bender, D.; Roden, W.; Stocklin, G., A New and Simple Online Method for the Production of [C-11] Methyl-Iodide and [C-11] Methyl Triflate, and Examples of Efficient C-11 Labeling with [C-11] Methyl Triflate. *Journal of Nuclear Medicine* **1993**, *34* (5), P68-P68.
39. Matarrese, M.; Soloviev, D.; Todde, S.; Neutro, F.; Petta, P.; Carpinelli, A.; Brussermann, M.; Kienle, M. G.; Fazio, F., Preparation of [C-11] radioligands with high specific radioactivity on a commercial PET tracer synthesizer. *Nuclear Medicine and Biology* **2003**, *30* (1), 79-83.
40. (a) Larsen, P.; Ulin, J.; Dahlstrom, K.; Jensen, M., Synthesis of [C-11]iodomethane by iodination of [C-11]methane. *Appl Radiat Isotopes* **1997**, *48* (2), 153-157; (b) Link, J. M.; Krohn, K. A.; Clark, J. C., Production of [C-11]CH₃I by single pass reaction of [C-11]CH₄ with I-2. *Nuclear Medicine and Biology* **1997**, *24* (1), 93-97.
41. (a) Buckley, K. R.; Huser, J.; Jivan, S.; Chun, K. S.; Ruth, T. J., C-11-methane production in small volume, high pressure gas targets. *Radiochim Acta* **2000**, *88* (3-4), 201-205; (b) Buckley, K. R.; Jivan, S.; Ruth, T. J., Improved yields for the in situ production of [C-11]CH₄ using a niobium target chamber. *Nuclear Medicine and Biology* **2004**, *31* (6), 825-827.
42. Zhang, M. R.; Suzuki, K., Sources of carbon which decrease the specific activity of [¹¹C]CH₃I synthesized by the single pass I₂ method. *Applied radiation and isotopes : including data, instrumentation and methods for use in agriculture, industry and medicine* **2005**, *62* (3), 447-50.
43. Schmitz, F.; Plenevaux, A.; Delfiore, G.; Lemaire, C.; Comar, D.; Luxen, A., Fast Routine Production of L-[C-11-Methyl]Methionine with Al₂O₃/Kf. *Appl Radiat Isotopes* **1995**, *46* (9), 893-897.
44. Hara, T.; Kosaka, N.; Shinoura, N.; Kondo, T., PET imaging of brain tumor with [methyl-C-11]choline. *Journal of Nuclear Medicine* **1997**, *38* (6), 842-847.
45. (a) Hashimoto, K.; Inoue, O.; Suzuki, K.; Yamasaki, T.; Kojima, M., Synthesis and evaluation of ¹¹C-PK 11195 for in vivo study of peripheral-type benzodiazepine receptors using positron emission tomography. *Annals of nuclear medicine* **1989**, *3* (2), 63-71; (b) Shah, F.; Hume, S. P.; Pike, V. W.; Ashworth, S.; McDermott, J., Synthesis of the enantiomers of [N-methyl-¹¹C]PK 11195 and comparison of their behaviours as radioligands for PK binding sites in rats. *Nucl Med Biol* **1994**, *21* (4), 573-81; (c) Debruyne, J. C.; Versijpt, J.; Van Laere, K. J.; De Vos, F.; Keppens, J.; Strijckmans, K.; Achten, E.; Slegers, G.; Dierckx, R. A.; Korf, J.; De Reuck, J. L., PET visualization of microglia in multiple sclerosis patients using [¹¹C]PK11195. *European journal of neurology : the official journal of the European Federation of Neurological Societies* **2003**, *10* (3), 257-64.

46. Mathis, C. A.; Wang, Y.; Holt, D. P.; Huang, G. F.; Debnath, M. L.; Klunk, W. E., Synthesis and evaluation of ¹¹C-labeled 6-substituted 2-arylbenzothiazoles as amyloid imaging agents. *Journal of medicinal chemistry* **2003**, *46* (13), 2740-54.
47. (a) Wilson, A. A.; Garcia, A.; Chestakova, A.; Kung, H.; Houle, S., A rapid one-step radiosynthesis of the beta-amyloid imaging radiotracer N-methyl-[C-11]2-(4'-methylaminophenyl)-6-hydroxybenzothiazole ([C-11]-6-OH-BTA-1). *J Labelled Compd Rad* **2004**, *47* (10), 679-682; (b) Solbach, C.; Uebele, M.; Reischl, G.; Machulla, H. J., Efficient radiosynthesis of carbon-11 labelled uncharged Thioflavin T derivatives using [C-11]methyl triflate for beta-amyloid imaging in Alzheimer's disease with PET. *Appl Radiat Isotopes* **2005**, *62* (4), 591-595.
48. Andersson, Y.; Bergstrom, M.; Langstrom, B., Synthesis of C-11 Labeled Benzamide Compounds as Potential Tracers for Poly(Adp-Ribose) Synthetase. *Appl Radiat Isotopes* **1994**, *45* (6), 707-714.
49. Simeon, F.; Sobrio, F.; Gourand, F.; Barre, L., Total synthesis and radiolabelling of an efficient rt-PA inhibitor: [C-11] (Z,Z)-BABCH. A first route to [C-11] labelled amidines. *J Chem Soc Perk T I* **2001**, (7), 690-694.
50. Ponchant, M.; Hinnen, F.; Demphel, S.; Crouzel, C., [C-11]Copper(I) cyanide: A new radioactive precursor for C-11-cyanation and functionalization of haloarenes. *Appl Radiat Isotopes* **1997**, *48* (6), 755-762.
51. (a) Fowler, J. S.; Arnett, C. D.; Wolf, A. P.; MacGregor, R. R.; Norton, E. F.; Findley, A. M., [11C]spiroperidol: synthesis, specific activity determination, and biodistribution in mice. *Journal of nuclear medicine : official publication, Society of Nuclear Medicine* **1982**, *23* (5), 437-45; (b) Arnett, C. D.; Fowler, J. S.; Wolf, A. P.; Logan, J.; MacGregor, R. R., Mapping brain neuroleptic receptors in the live baboon. *Biological psychiatry* **1984**, *19* (10), 1365-75.
52. Bernard, S.; Fuseau, C.; Schmid, L.; Milcent, R.; Crouzel, C., Synthesis and in vivo studies of a specific monoamine oxidase B inhibitor: 5-[4-(benzyloxy)phenyl]-3-(2-cyanoethyl)-1,3,4-oxadiazol-[11C]-2(3H)-one. *European journal of nuclear medicine* **1996**, *23* (2), 150-6.
53. Wolf, A. P., Labeling of Organic Compounds by Recoil Methods. *Ann Rev Nucl Sci* **1960**, *10*, 259-290.
54. Finn, R. D.; Christman, D. R.; Ache, H. J.; Wolf, A. P., Preparation of Cyanide C-11 for Use in Synthesis of Organic Radiopharmaceuticals Ii. *Int J Appl Radiat Is* **1971**, *22* (12), 735-&.
55. Christman, D. R.; Finn, R. D.; Karlstrom, K. I.; Wolf, A. P., Production of carrier-free hydrogen cyanide (carbon-11) for medical use and radiopharmaceutical syntheses. IX. *J. Nucl. Med.* **1973**, *14* (11), 864-6.
56. Fowler, J. S.; Ansari, A. N.; Atkins, H. L.; Bradley-Moore, P. R.; MacGregor, R. R.; Wolf, A. P., Synthesis and preliminary evaluation in animals of carrier-free ¹¹C-1-dopamine hydrochloride: X. *Journal of nuclear medicine : official publication, Society of Nuclear Medicine* **1973**, *14* (11), 867-9.
57. Hara, T.; Iio, M., Online Synthesis of [C-11] Cyanide from Cyclotron-Produced [C-11] Carbon-Dioxide. *Appl Radiat Isotopes* **1987**, *38* (12), 1092-1093.
58. Meyer, G. J.; Osterholz, A.; Harms, T., A Systematic Investigation of [C-11] Hcn Production. *Radiochim Acta* **1990**, *50* (1-2), 43-47.
59. Kim, D.; Alexoff, D.; Kim, S. W.; Hooker, J.; Ferrieri, R. A. ¹¹C-Labeled cyanide production system. US20130045151A1, 2013.

60. Fleming, F. F.; Yao, L.; Ravikumar, P. C.; Funk, L.; Shook, B. C., Nitrile-Containing Pharmaceuticals: Efficacious Roles of the Nitrile Pharmacophore. *J. Med. Chem.* **2010**, *53* (22), 7902-7917.
61. Westerberg, G.; Karger, W.; Onoe, H.; Langstrom, B., [C-11] Cyanogen-Bromide in the Synthesis of 1,3-Di(2-Tolyl)-[C-11]Guanidine. *J Labelled Compd Rad* **1994**, *34* (8), 691-696.
62. Andersson, J. D.; Seneca, N.; Truong, P.; Wensbo, D.; Raboisson, P.; Farde, L.; Halldin, C., Palladium mediated ¹¹C-cyanation and characterization in the non-human primate brain of the novel mGluR5 radioligand [¹¹C]AZD9272. *Nucl Med Biol* **2013**, *40* (4), 547-53.
63. (a) Antoni, G.; Langstrom, B., Synthesis of Racemic [3-C-11]-Labeled Alanine, 2-Aminobutyric Acid, Norvaline, Norleucine, Leucine and Phenylalanine and Preparation of L-[3-C-11]Alanine and L-[3-C-11]Phenylalanine. *J Labelled Compd Rad* **1987**, *24* (2), 125-143; (b) Zhang, Z. R.; Ding, Y. S.; Studenov, A. R.; Gerasimov, M. R.; Ferrieri, R. A., Novel synthesis of 1-C-11]gamma-vinyl-gamma-aminobutyric acid ([1-C-11]GVG) for pharmacokinetic studies of addiction treatment. *J Labelled Compd Rad* **2002**, *45* (3), 199-211.
64. Gleede, T.; Riehl, B.; Shea, C.; Kersting, L.; Cankaya, A. S.; Alexoff, D.; Schueller, M.; Fowler, J. S.; Qu, W., Investigation of SN2 [¹¹C]cyanation for base-sensitive substrates: an improved radiosynthesis of L-[5-¹¹C]-glutamine. *Amino Acids* **2015**, *47* (3), 525-533.
65. Gillings, N. M.; Gee, A. D., Synthesis of [4-¹¹C]amino acids via ring-opening of aziridine-2-carboxylates. *J. Labelled Compd. Radiopharm.* **2001**, *44* (13), 909-920.
66. Antoni, G.; Omura, H.; Ikemoto, M.; Moulder, R.; Watanabe, Y.; Langstrom, B., Enzyme catalysed synthesis of L-[4-C-11]aspartate and L-[5-C-11]glutamate. *J Labelled Compd Rad* **2001**, *44* (4), 287-294.
67. Sundin, A.; Eriksson, B.; Bergstrom, M.; Bjurling, P.; Lindner, K. J.; Oberg, K.; Langstrom, B., Demonstration of [¹¹C] 5-hydroxy-L-tryptophan uptake and decarboxylation in carcinoid tumors by specific positioning labeling in positron emission tomography. *Nucl. Med. Biol.* **2000**, *27* (1), 33-41.
68. Studenov, A. R.; Szalda, D. E.; Ding, Y. S., Synthesis of no-carrier-added C-11 labeled D- and L-enantiomers of phenylalanine and tyrosine for comparative PET Studies. *Nucl Med Biol* **2003**, *30* (1), 39-44.
69. Petroni, D.; Menichetti, L.; Sorace, O.; Poli, M.; Vanasia, M.; Salvadori, P. A., [C-11]diclofenac sodium: synthesis and PET assessment of transdermal penetration. *Nuclear Medicine and Biology* **2011**, *38* (2), 181-189.
70. Lee, H. G.; Milner, P. J.; Placzek, M. S.; Buchwald, S. L.; Hooker, J. M., Virtually instantaneous, room-temperature [(11)C]-cyanation using biaryl phosphine Pd(0) complexes. *J Am Chem Soc* **2015**, *137* (2), 648-51.
71. Airaksinen, A. J.; Andersson, J.; Truong, P.; Karlsson, O.; Halldin, C., Radiosynthesis of [(11)C]ximelagatran via palladium catalyzed [(11)C]cyanation. *J Labelled Compd Rad* **2008**, *51* (1-2), 1-5.
72. Senecal, T. D.; Shu, W.; Buchwald, S. L., A General, Practical Palladium-Catalyzed Cyanation of (Hetero)Aryl Chlorides and Bromides. *Angew. Chem., Int. Ed.* **2013**, *52* (38), 10035-10039.
73. Lee, S.; Alexoff, D. L.; Shea, C.; Kim, D.; Schueller, M.; Fowler, J. S.; Qu, W., Tetraethylene glycol promoted two-step, one-pot rapid synthesis of indole-3-[1-¹¹C]acetic acid. *Tetrahedron Lett.* **2015**, *56* (3), 517-520.

CHAPTER 2.

Synthesis and PET Studies of C-11 Labeled Benzamides for the Prediction of Blood-Brain Barrier Penetration

1. Abstract

Blood-brain barrier (BBB) permeability is one of the most important criteria for the development of PET radiotracers as well as for the development of drugs targeting the central nervous system (CNS). However, there is no quantitative prediction tool for in vivo pharmacokinetic properties of new radiotracer such as rate constants of plasma-to-brain transfer (K_1 , which is related to BBB permeability) and brain-to-plasma transfer (k_2). Instead of relying on trial-and-error based strategy, we designed a set of model compounds based on benzamide structures which each have different numbers of hydrogen bonds and other physic-chemical descriptors to test the quantitative structure-property relationship (QSPR) as a prediction tool for BBB penetration which we could measure in vivo with PET imaging. Parallel synthesis was performed to provide seven benzamides and the corresponding nor-precursor molecules for labelling with carbon-11 (half life: 20.4 min) using [^{11}C]methyl iodide. C-11 labeled benzamides were purified via semi-prep HPLC and delivered for PET imaging studies in the baboon. The seven benzamide precursors and corresponding non-radioactive standard benzamides have been prepared in reasonable yield (> 44 %). Radiosynthesis for labelling of these seven benzamide compounds with [^{11}C]CH₃I or [^{11}C]CH₃OTf was done and gave similar radiochemical yields (~35 %). For PET studies in baboon, these seven C-11 labeled benzamide compounds were delivered and injected to female baboon along with collecting blood samples over the time of

scan (60 min). The concentration of radioactivity in brain (% injected dose/cc) vs time was measured and the concentration of radioactivity in arterial plasma (corrected from the presence of labeled metabolites) was measured. Brain uptake was high (0.027%ID/cc) and clearance was rapid for each member of the series. The calculation of K_1 and k_2 from these PET measures of time-activity-curves (TACs) in brain and plasma and the development and evaluation of a QPSR tool for predicting BBB penetration of new compounds is on-going at NIH.

2. Introduction

PET is a non-invasive *in vivo* molecular imaging tool to observe the organ uptake of radioligands that are designed bind into a specific molecular target in the central nervous system and other organs. Widely accepted criteria for a good radiotracer include the ability to be radiolabeled, low toxicity to human at tracer doses, a range of properties involving high selectivity for the target of interest, the ability to reach the target site, low nonspecific binding, and high binding affinity¹.

The development of new *in vivo* radiotracers targeting central nervous system (CNS) usually focuses on screening compounds based on lipophilicity, binding affinity, selectivity, target density, and labelling feasibility with carbon-11 (half life: 20.4 min) or other short lived positron emitting nuclides such as fluorine-18². Central nervous system (CNS) studies require the radiotracers or drugs to pass the Blood Brain Barrier (BBB), which selectively excludes most substances from entering the brain. The blood-brain barrier is the most important barrier between systemic circulation and the central nervous system (CNS) due to its considerably large surface area, and it shows a major challenge to therapeutic treatment for brain disorders because

it is hard to penetrate into brain due to this neuroprotective role¹⁻³. To avoid the high attrition of potential CNS targeted drug candidates for clinical treatment, investigation of prediction of BBB penetration for new compounds in early research is critically important. Thus the successful pharmacological treatment of diseases of the brain as well as the development of radiotracers for studying the brain depends on their ability to cross the BBB. For example, for addictive drugs, high blood brain barrier penetration and fast uptake are the most likely to result in addiction. Both cocaine and methamphetamine have these properties⁴.

Prediction of BBB penetration is important not only for CNS drug development but in also in the development of PET tracers. In general, blood-brain barrier (BBB) penetration is predicted through calculated lipophilicity ($2 < \text{clogP} < 4$), molecular weight ($\text{MW} < 450$), polar surface area ($\text{PSA} < 70$), number of hydrogen-bonds acceptors and donors ($\text{HBD} = 0 - 1$), and $\text{pKa} (\leq 0.8)$ each weighted from 0 to 1.0 (the desirable range was shown for each parameter rather than suggested limits)²⁻³. A number of trial and error studies for predicting BBB uptake have been performed but there are still no effective tools to predict whether a specific molecular structure will penetrate the BBB⁵. Also the failure of many CNS radiotracer candidates to show appropriate brain uptake, pharmacokinetics and specificity emphasizes the need to develop and validate tools with predictive value⁶.

Generally speaking, there are three different computational approaches to predict BBB uptake; (1) quantitative structure-activity relationship (QSAR)-based methods, studies concerning PSA; (2) number of nitrogen and oxygen atoms, clogP ; (3) statistical analysis of rat in vivo $\log\text{BP}$ ($\log[\text{brain}]/[\text{plasma}]$) data⁷. Traditionally, steady-state blood to brain concentration ratio ($\log\text{BB}=\log(C_{\text{brain}}/C_{\text{blood}})$) has been used as a quantitative measure of BBB penetration. The experimental $\log\text{BB}$ values can be generated in using animals as part of

standard pharmacokinetic profiling of compounds. However the actual experimental process is very complex and there is no uniform standard protocol at present. Furthermore, these experimental measurements are generally made over several hours, with several animals required per data point, so they are costly and labor intensive⁵. Thus computer assisted drug design methodologies (CADD), such as quantitative structure-property and/or structure-activity relationship studies (QSPR or QSAR, respectively) have been developed to predict clogBB (computed logBB) and commonly used as an important tool in the design and development of new drugs and novel leads⁶. QSAR/QSPR modeling, first developed by Hansch et al.,⁸ has been invaluable for understanding BBB permeability by predicting logBB. Also, QSAR/QSPR methods for the clogBB have been well reviewed by several research groups⁹.

In recent years, however, it has been observed that logBB may not reflect the BBB permeability in the brain since it is highly influenced by the steady state blood to brain concentrations¹⁰. In fact, BBB penetration is a relatively early event after the drug enters the bloodstream and is highly correlated with the dynamical passive diffusion process. Therefore, one suggestion to replace logBB is the permeability-surface area (PS) product, an estimate of the net influx clearance^{10a, 11}. For calculating the PS, there are still experimental limitations, similarly with logBB, and so computational prediction modeling has been developed¹². However some drawbacks still exist, for example, very small datasets generalized the data from different sources and the represented molecular sizes ranges were inconsistent (too wide/broad).

Permeability-surface area product (PS) is the major factor influencing the uptake/influx rate constant, K_1 , developed by Renkin and Crone¹³. K_1 might be the best parameter to show quantitative value of which a compound can transport from blood into brain dynamically. Since

K_1 is related to early time points of event and is very dynamic term, the research for developing and validating a predictive model has not been yet completed.

QSAR based model is correlated in vivo logBB (log [brain]/[blood]) with various diverse descriptors from the simple, logP or PSA which is related to the number of polar atoms, N, O, and H, in the molecule, to the linear free-energy relationship (LFER) descriptors¹. Our ultimate goal is to build up a reliable prediction method based on QSAR for BBB permeability, which can be used for PET radiotracer development. In this study, we considered a set of model compounds based on the benzamide structure, which is widely used in the drug and radiotracer R&D to introduce a novel prediction tools based on QSPR. We designed structurally well-defined benzamide derivatives with different numbers of hydrogen bonds but which are not known to bind to any cellular element. Lack of specific binding *for* this benzamide series is intentional to avoid introducing another variable into this complex system. In addition to lack of known specific binding, this series had the following characteristics: 1) molecular weight (MW) < 500; 2) no anionic charge in physiological pH; 3) limited lipophilicity ($0 < \log PS \leq 3$); 4) parallel synthesis available for precursor and reference compounds; 5) rapid radiosynthesis via N-or O-methylation using [¹¹C]MeI or [¹¹C]MeOTf in one-step

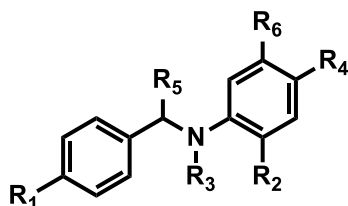
As an initial strategy for the development of a QSPR model for predicting BBB penetration of new compounds, we (1) designed a series of seven structurally well-defined benzamides having a range of physico-chemical descriptors; (2) synthesized their nor-precursors for labelling and the non-radioactive benzamides as authentic standards; (3) radiolabeled the nor-precursor with [¹¹C]methyl iodide or [¹¹C]methyl triflate and purified and formulated them for PET studies; (4) measured the brain uptake and clearance of each [¹¹C]benzamide with PET imaging over a 90 minute experimental period; (5) measured the plasma uptake and clearance and

correction for the presence of labelled metabolites for each baboon study. The calculation of K_1 and k_2 from these PET measures of time-activity-curves (TACs) in brain and plasma and the development and evaluation of a QPSR tool for predicting BBB penetration of new compounds is on-going at NIH.

3. Experimental details

All chemicals and solvents were purchased from Aldrich Chemical (Milwaukee, WI, USA). NMR spectra were recorded by using a Bruker Avance 400 MHz NMR spectrometer (Bruker Instruments, Billerica, MA, USA). [^{11}C]Methyl iodide was produced by PETtrace MeI Microlab (GE Medical Systems, Milwaukee, WI, USA) from [^{11}C]carbon dioxide, which was generated from a nitrogen/oxygen (1000 ppm) target [$^{14}\text{N}(p,\alpha)^{11}\text{C}$] using EBCO TR 19 cyclotron (Advanced Cyclotron Systems, Richmond, Canada). High-performance liquid chromatography (HPLC) purification was performed by a Knauer HPLC system (Sonntek, Woodcliff Lake, NJ, USA) with a model K-5000 pump, a Rheodyne 7125 injector, a model 87 variable wavelength monitor and NaI radioactivity detector. During the radiosynthesis, ^{11}C was measured by three p-type/intrinsic/n-type (PIN) diode detectors (3×3 mm Si diode, Carroll Ramsey Associates, Berkeley, CA) equipped with a triple-channel amplifier (model 101-HDC-3; Carroll Ramsey Associates, Berkeley, CA, USA) and NI USB- 6008 (National Instruments, Austin, TX, USA). Radioactivity of [^{11}C]benzamides was measured by a Capintec CRC-712MV radioisotope calibrator (Capintec, Ramsey, NJ, USA).

Table 1. Structures of unlabelled and labelled benzamide derivatives containing different number of hydrogen bonds.



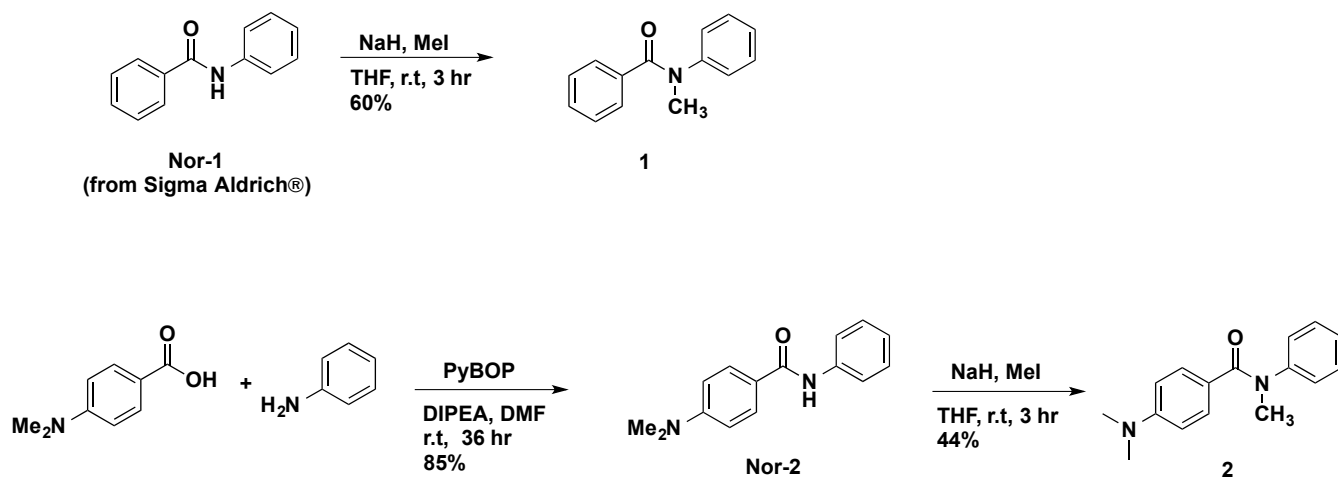
Compd	R ₁	R ₂	R ₃	R ₄	R ₅	R ₆	H-bonds*
Nor-1	-H	-H	-H	-H	Carbonyl	-H	N/A
Nor-2	-NMe ₂	-H	-H	-H	Carbonyl	-H	N/A
Nor-3	-H	-OH	-H	-H	Carbonyl	-H	N/A
Nor-4	-H	-OH	-CH ₃	-OCH ₃	Carbonyl	-H	N/A
Nor-5	-NH ₂	-OH	-CH ₃	-H	Carbonyl	-H	N/A
Nor-6	-H	-H	-H	-H	-H	-H	N/A
Nor-7	phenyl	-H	-H	-H	Carbonyl	<i>t</i> -Bu phenyl	N/A
1	-H	-H	-CH ₃	-H	Carbonyl	-H	2
2	-NMe ₂	-H	-CH ₃	-H	Carbonyl	-H	3
3	-H	-OCH ₃	-H	-H	Carbonyl	-H	4
4	-H	-OCH ₃	-CH ₃	-OCH ₃	Carbonyl	-H	5
5	-NH ₂	-OCH ₃	-CH ₃	-H	Carbonyl	-H	6
6	-H	-H	-CH ₃	-H	-H	-H	1
7	phenyl	-H	-CH ₃	-H	Carbonyl	<i>t</i> -Bu phenyl	2

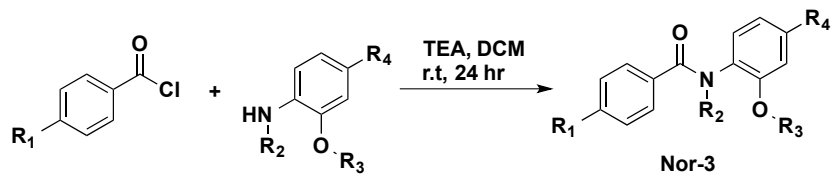
[¹¹ C]1	-H	-H	- ¹¹ CH ₃	-H	Carbonyl	-H	2
[¹¹ C]2	-NMe ₂	-H	- ¹¹ CH ₃	-H	Carbonyl	-H	3
[¹¹ C]3	-H	-O ¹¹ CH ₃	-H	-H	Carbonyl	-H	4
[¹¹ C]4	-H	-O ¹¹ C H ₃	-CH ₃	-OCH ₃	Carbonyl	-H	5
[¹¹ C]5	-NH ₂	-O ¹¹ C H ₃	-CH ₃	-H	Carbonyl	-H	6
[¹¹ C]6	-H	-H	- ¹¹ CH ₃	-H	-H	-H	1
[¹¹ C]7	phenyl	-H	- ¹¹ CH ₃	-H	Carbonyl	<i>t</i> -Bu phenyl	2

* Counts of hydrogen-bonds acceptors and donors (HBD) (e.g., O, N, and H); the counts of HBD was not applicable for nor-compounds.

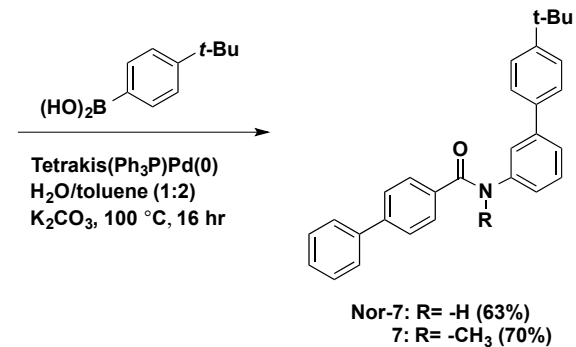
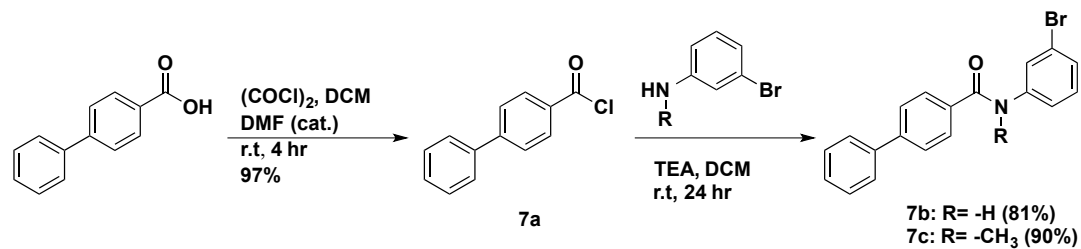
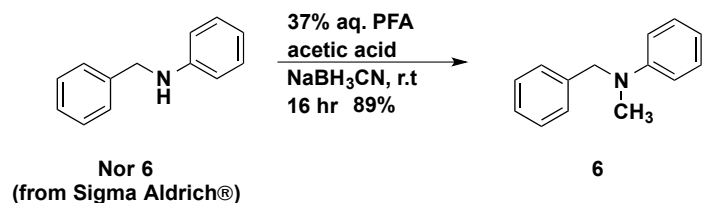
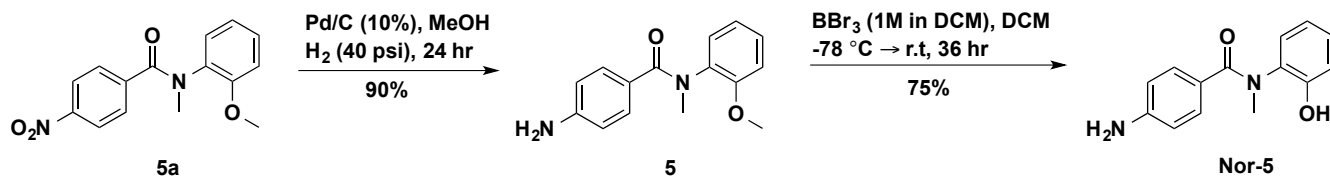
3.1. Cold synthesis of benzamide derivatives

Figure 1. Parallel synthesis of precursors and reference compounds of seven benzamides (through **nor 1** to **nor 7**; through **1** to **7**)





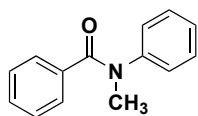
Nor-3 (83%): $\text{R}_1 = \text{H}, \text{R}_2 = \text{H}, \text{R}_3 = \text{H}, \text{R}_4 = \text{H}$
 3 (87%): $\text{R}_1 = \text{H}, \text{R}_2 = \text{H}, \text{R}_3 = \text{CH}_3, \text{R}_4 = \text{H}$
 Nor-4 (90%): $\text{R}_1 = \text{H}, \text{R}_2 = \text{H}, \text{R}_3 = \text{H}, \text{R}_4 = \text{OMe}$
 4 (84%): $\text{R}_1 = \text{H}, \text{R}_2 = \text{H}, \text{R}_3 = \text{CH}_3, \text{R}_4 = \text{OMe}$
 5a (88%): $\text{R}_1 = \text{NO}_2, \text{R}_2 = \text{CH}_3, \text{R}_3 = \text{CH}_3, \text{R}_4 = \text{H}$



3.1.1. General procedure of N-methylation of amide on benzamide derivatives [A]

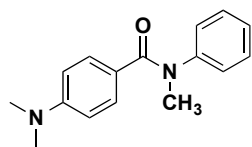
We modified the procedure of Chabaud et al¹⁴. To a suspension of NaH (95% in mineral oil, 3.04 mmol) in dry THF (13mL) at r.t, a solution of benzamide derivative (1.52 mmol) in dry THF (12 mL) was added dropwise. The solution was stirred for 15 min and MeI (0.66 ml, 10.65 mmol) was added. The reaction mixture was stirred for 3 h. After addition of distilled water, the aqueous layer was extracted with ethyl acetate. The combined organic layers were washed with brine (3 × 10mL) and dried over MgSO₄. The crude mixture was purified by flash chromatography on silica gel.

N-methyl-N-phenyl-benzamide, 1



Experiment was performed as described in [A]. Starting material (benzanilide, **nor-1**) was purchased from Sigma-Aldrich®. **1** was produced as 0.19 g of a yellow oil in 60% yield. ¹H NMR (400 MHz, CDCl₃): δ 7.28-7.30 (d, 6.8 Hz, 2H), 7.21-7.24 (m, 3H), 7.12-7.18 (q, 5.2 Hz, 3H), 7.03-7.05 (d, 8 Hz, 2H), 3.51 (s, 3H). ¹³C NMR (100 MHz, CDCl₃): δ 170.90, 145.14, 136.14, 129.79, 129.34, 128.92, 127.93, 127.13, 126.68, 38.61. MS (ESI): m/z [M+H⁺] calcd for C₁₄H₁₃NO 211.10 found 212.1.

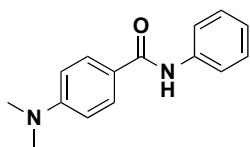
N-methyl-N-phenyl-4-dimethylaminobenzamide, 2



Experiment was performed as described in [A]. **2** was produced as 47 mg of a pale yellow solid in 44% yield. ¹H NMR (CDCl₃, 400MHz): δ 7.72-7.86 (d, 6.8 Hz, 2H), 7.6-7.69 (m, 2H),

7.11-7.18 (m, 1H), 7.06-7.08 (d, 8 Hz, 2H), 6.41-6.43 (d, 8 Hz, 2H), 3.48 (s, 3H), 2.91 (s, 6H).
¹³C NMR (100 MHz, CDCl₃): δ 170.92, 151.37, 146.37, 131.24, 129.31, 126.99, 126.06, 122.53, 110.61, 40.21, 38.99. MS (ESI): m/z [M+H⁺] calcd for C₁₄H₁₈N₂O 254.14 found 255.1.

N-phenyl-4-dimethylaminobenzamide, **nor-2**



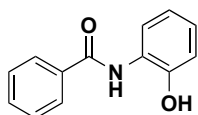
We modified the procedure of Baures et al¹⁵. 4-Dimethylamino benzoic acid (0.5 g, 0.61 mmol), diisopropyl ethyl amine (0.58 mL, 0.67 mmol), and aniline (0.42 g, 0.91 mmol) were dissolved in anhydrous DMF (10 mL) and stirred for 5 min. PyBOP (2.36 g, 0.91 mmol) was added and the mixture was stirred 36 h at r.t. A saturated solution of Na₂CO₃ was added and the product extracted with EtOAc (3 × 10mL). The organic layers were washed with 1M HCl (3 × 10mL) then extracted with EtOAc after adding a saturated solution of Na₂CO₃ again. The organics were dried over MgSO₄. The crude mixture was purified through silica gel (HE:EtOAc (3:1)) to afford 0.12 g of a white solid, **nor-2**, in reasonable yield (85%). ¹H NMR (CDCl₃, 400MHz): δ 7.72-7.86 (d, 6.8 Hz, 2H), 7.6-7.69 (m, 2H), 7.31-7.4 (m, 2H), 7.13-7.22 (m, 1H), 6.72-6.75 (q, 4.5 Hz, 2H), 3.06 (s, 6H). ¹³C NMR (100 MHz, CDCl₃): δ 165.86, 162.91, 138.67, 129.22, 128.80, 124.14, 121.51, 120.21, 111.37, 40.33. MS (ESI): m/z [M+H⁺] calcd for C₁₅H₁₆N₂O 240.13 found 241.1.

3.1.2. General procedure of formation of amide to prepare benzamide derivatives [B]

To a solution of o-aminophenol derivative (2.13 mmol) in dichloromethane (6 ml) were added triethylamine (0.43 mmol) and benzoyl chloride (2.13 mmol). The reaction mixture was stirred at room temperature overnight. After 24 hours later, the reaction was quenched with distilled water

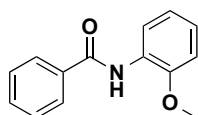
(10ml) then the mixture was extracted with dichloromethane. The organic layer was washed with 5% NaHCO₃ and 1M HCl and dried over CaSO₄. The solvent was evaporated under reduced pressure. The residue was purified by isorela (eluent: EtOAc/n-hexane = 1/3).

N-(2-hydroxyphenyl)benzamide, nor-3



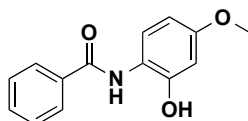
Experiment was performed as described in [B]. **Nor-3** was obtained in 83% chemical yield as white powder. ¹H NMR (CDCl₃, 400MHz): δ 8.60-8.63 (d, 12 Hz, 1H), 8.10-8.15 (d, 20 Hz, 1H), 7.90-7.92 (d, 8 Hz, 2H), 7.61-7.63 (m, 3H), 7.16-7.19 (m, 1H), 7.07-7.10 (d, 12 Hz, 1H), 6.91-6.95 (t, 16 Hz, 1H). MS (ESI): m/z [M+H⁺] calcd for C₁₃H₁₁NO₂ 213.24 found 214.1.

N-methyl-*N*-(2-methoxyphenyl)benzamide, 3



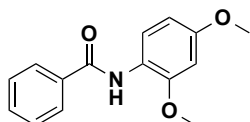
Experiment was performed as described in [B]. **3** was obtained in 87% chemical yield as pale yellow liquid. ¹H NMR (CDCl₃, 400MHz): δ 8.53-8.55 (d, 8 Hz, 1H), 7.86-7.91 (d, 20 Hz, 2H), 7.48-7.56 (m, 3H), 7.08-7.11 (t, 12 Hz, 1H), 7.03-7.07 (t, 16 Hz, 1H), 6.92-6.94 (d, 8 Hz, 1H), 3.93 (s, 3H). ¹³C NMR (100 MHz, CDCl₃): δ 165.50, 148.35, 135.55, 131.91, 128.97, 128.00, 127.27, 124.09, 121.44, 120.07, 110.14, 56.03.

N-(2-hydroxy-4-methoxyphenyl)benzamide, nor-4



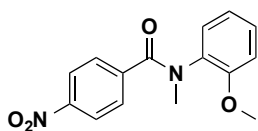
Experiment was performed as described in [B]. **Nor-4** was obtained in 90 % chemical yield as a white powder. ^1H NMR (CDCl_3 , 400MHz): δ 8.10-8.15 (d, 20 Hz, 1H), 7.89-7.91 (d, 8 Hz, 2H), 7.49-7.53 (m, 3H), 6.98-7.01 (d, 12 Hz, 1H), 6.87-6.88 (d, 4 Hz, 1H), 6.73-6.78 (d, 20 Hz, 1H), 3.87 (s, 3H), 3.75 (s, 3H). ^{13}C NMR (100 MHz, CDCl_3): δ 167.05, 153.85, 142.33, 132.64, 130.43, 129.13, 129.11, 129.08, 127.53, 127.11, 119.93, 112.64, 107.73, 56.04. MS (ESI): m/z $[\text{M}+\text{H}^+]$ calcd for $\text{C}_{14}\text{H}_{13}\text{NO}_3$ 243.09 found 244.1.

N-(2-methoxy-4-methoxyphenyl)benzamide, **4**



Experiment was performed as described in [B]. **4** was obtained in 84 % chemical yield as pale brown liquid. ^1H NMR (CDCl_3 , 400MHz): δ 8.60 (s, 1H), 7.86-7.91 (d, 20 Hz, 2H), 7.48-7.58 (m, 3H), 6.83-6.85 (d, 8 Hz, 1H), 6.61-6.63 (d, 8 Hz, 1H), 3.89 (s, 3H), 3.80 (s, 3H). ^{13}C NMR (100 MHz, CDCl_3): δ 165.45, 154.17, 142.56, 135.40, 131.99, 128.99, 127.23, 110.94, 109.13, 106.07, 56.54, 56.04. MS (ESI): m/z $[\text{M}+\text{H}^+]$ calcd for $\text{C}_{15}\text{H}_{15}\text{NO}_3$ 257.11 found 258.0.

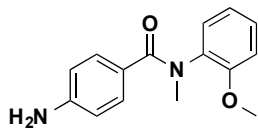
N-methyl-*N*-(2-methoxyphenyl)-4-nitrobenzamide, **5a**



Experiment was performed as described in [B]. *N*-methyl-*N*-(2-methoxyphenyl)-4-nitrobenzamide was produced in 88% chemical yield as yellow powder. ^1H NMR (CDCl_3 , 400MHz): δ 7.98-8.00 (d, 8Hz, 2H), 7.44-7.46 (d, 8Hz, 2H), 7.13-7.18 (t, 20Hz, 1H), 7.04-7.06 (d, 8Hz, 1H), 6.81-6.85 (t, 16Hz, 1H), 6.76-6.78 (d, 8Hz, 1H), 3.74 (s, 3H), 3.39 (s, 3H). ^{13}C NMR (100 MHz, CDCl_3): δ 154.26, 147.94, 142.64, 132.39, 129.52, 128.99, 128.70, 124.05,

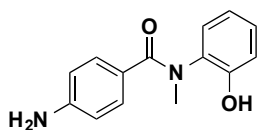
123.67, 122.74, 121.12, 111.89, 55.32, 37.05. MS (ESI): m/z $[M+H^+]$ calcd for $C_{15}H_{14}N_2O_4$ 286.10 found 287.0.

N*-methyl-*N*-(2-methoxyphenyl)-4-aminobenzamide, **5*



N-methyl-*N*-(2-methoxyphenyl)-4-nitrobenzamide (300 mg, 1.0 mmol) which is synthesized was dissolved in methanol (15 ml) and Pd/C 10% (100 mg) was added as catalyst to the reaction solution. Pressurized hydrogenation with H_2 (40 psi) was performed overnight. The crude product was filtered through celite and dried over $CaSO_4$. Purification was performed by isoleraTM (Biotage) (eluent: EtOAc/n-hexane = 1/1). The precursor of **5** was obtained in 90% chemical yield as a white powder. 1H NMR ($CDCl_3$, 400MHz): δ 7.13-7.15 (d, 8 Hz, 3H), 7.00-7.02 (d, 8 Hz, 1H), 6.80-6.82 (d, 8 Hz, 2H), 6.37-6.39 (d, 8 Hz, 2H), 3.75 (s, 3H), 3.32 (s, 3H). ^{13}C NMR (100 MHz, $CDCl_3$): δ 171.59, 154.38, 147.63, 134.41, 130.08, 129.13, 128.21, 126.07, 120.82, 113.44, 111.82. MS (ESI): m/z $[M+H^+]$ calcd for $C_{15}H_{16}N_2O_2$ 256.12 found 257.1.

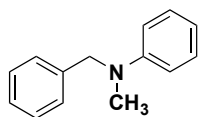
***N*-(2-methoxyphenyl)-4-aminobenzamide, *nor*-5**



Nor-5 (40 mg) was dissolved in anhydrous dichloromethane (4ml). BBr_3 1M solution in dichloromethane was slowly added for 5 min at $-78\text{ }^\circ\text{C}$ under Ar and stirred for 10 min at the same temperature. The reaction mixture was stirred for 1hr at $-10\text{ }^\circ\text{C}$. Reaction was warmed up to $0\text{ }^\circ\text{C}$ and stirred for 30 min then slowly warmed up to r.t and stirred for 36 hr. Reaction was quenched with brine (10 ml) and extracted with ethyl acetate. The organic layer was neutralized

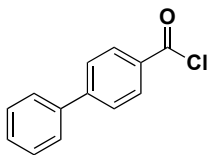
with saturated NaHCO₃ solution and washed with brine again then dried over CaSO₄. (LC-MS check: only starting material was detected in aqueous layer and major product with minor starting material were detected in organic layer (starting material MW 256.12 → MS peak at 257, product MW 242.11 → MA peak at 243). On TLC, R_f value of product (nor-5) was 0.23 and that of starting material (5) was 0.25 with eluent HE: EA=1:1 condition. A pale yellow oil type pure **nor-5** was separated from minor starting material by IsoleraTM with gradient eluent system. Chemical yield was 75%. HR-LCMS: m/z [M+H⁺] calcd for C₁₄H₁₄N₂O₂ 242.11 found 243.0.

N-methyl-N-benzylaniline, 6



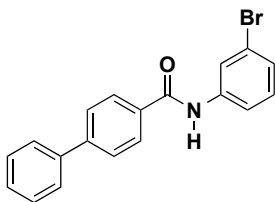
In a 5 mL vial, commercially available N-benzylaniline (Sigma-Aldrich®) and 37% aqueous paraformaldehyde (10 equiv) were dissolved in MeCN. Acetic acid (15 equiv) was added and the reaction mixture was stirred at rt for 10 min. Then, the reaction was cooled down to 0 °C and sodium cyanoborohydride (1.3 equiv) was added in two portions over 10 min. The reaction was allowed to stir from 0 °C to rt for 16 hr. The reaction was quenched with a saturated aqueous NaHCO₃ solution and then extracted with Et₂O. The combined organic layers were dried over NaSO₄. After filtration, the solvent was removed under reduced pressure. The crude **6** was purified with IsoleraTM under gradient elution with combination of hexane and ethyl acetate. The pure product was obtained as a clear oil (89 %). ¹H-NMR (CDCl₃, 400MHz): δ 7.29-7.33 (m, 3H), 7.19-7.24 (m, 2H), 6.73-6.76 (t, 12 Hz, 3H), 6.69-6.71 (d, 8 Hz, 2H), 4.54 (s, 2H), 3.02 (s, 3H). MS (ESI): m/z [M+H⁺] calcd for C₁₄H₁₅N 197.28 found 198.1.

4-Phenylbenzoyl chloride, 7a



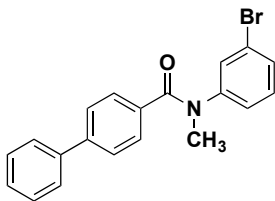
4-biphenylcarboxylic acid (1.7 g, 8.56 mmol) was suspended in dry dichloromethane (10 ml) and 3.67 ml of oxalyl chloride (42.78 mmol) was added dropwise over 10 min. Dimethylformamide (DMF, 0.1 mL) was added and the solution was stirred at r.t for 4 hrs under Ar. The excess oxalyl chloride was evaporated under vacuum to provide a quantitative yield of 4-biphenylcarbonyl chloride as a pale yellow solid. 7a was used for Suzuki coupling with 7b and 7c without purification. Proton NMR was taken with crude product after workup. ^1H NMR (CDCl_3 , 400MHz): δ 8.19-8.21 (d, 12 Hz, 2H), 7.72-7.75 (d, 12 Hz, 2H), 7.63-7.66 (d, 12 Hz, 2H), 7.42-7.52 (m, 3H).

N-(3-Bromophenyl)-4-phenylbenzamide, 7b



Experiment was performed as described in [B]. N-(3-Bromophenyl)-4-phenylbenzamide was obtained in 90% chemical yield as a white powder. ^1H NMR (CDCl_3 , 400MHz): δ 7.92-7.94 (d, 8 Hz, 2H), 7.87 (s, 1H), 7.72-7.74 (d, 8 Hz, 2H), 7.65-7.67 (d, 8 Hz, 1H), 7.44-7.48 (t, 16 Hz, 2H), 7.41-7.43 (d, 8Hz, 1H), 7.17-7.30 (m, 1H). ^{13}C NMR (100 MHz, CDCl_3): δ 145.21, 139.96, 139.42, 133.29, 130.92, 130.60, 129.21, 128.43, 127.78, 127.74, 127.45, 127.39, 123.30, 122.97, 118.81. MS (ESI): m/z $[\text{M}+\text{H}^+]$ calcd for $\text{C}_{19}\text{H}_{14}\text{BrNO}$ 351.03 found 352.0.

N-methyl-*N*-(3-bromophenyl)-4-phenylbenzamide, **7c**



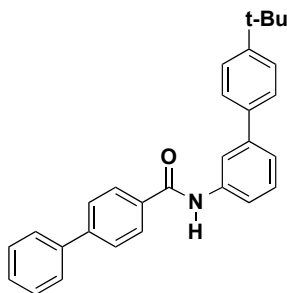
Experiment was performed as described in [B]. *N*-methyl-*N*-(3-bromophenyl)-4-phenylbenzamide was obtained in 88 % chemical yield as a white powder. ¹H NMR (CDCl₃, 400MHz): δ 7.53-7.55 (d, 8 Hz, 2H), 7.43-7.46 (t, 16 Hz, 3H), 7.37-7.39 (d, 8 Hz, 2H), 7.35-7.37 (d, 8 Hz, 1H), 7.31-7.33 (d, 8 Hz, 2H), 7.29-7.31 (d, 8 Hz, 1H), 7.06-7.10 (t, 16 Hz, 1H), 6.94-6.96 (d, 8 Hz, 1H), 3.51 (s, 3H). ¹³C NMR (100 MHz, CDCl₃): δ 170.47, 146.47, 142.86, 140.18, 134.28, 130.55, 129.81, 129.79, 129.49, 129.01, 128.00, 127.28, 126.76, 126.02, 122.71. MS (ESI): m/z [M+H⁺] calcd for C₂₀H₁₆BrNO 365.04 found 366.0.

3.1.3. General procedure of Suzuki coupling to prepare benzamide derivatives [C]

In 5 mL vial, distilled water (1 mL) was flushed with Ar for 5 min and then 2 mL of toluene was added by flushing with Ar. The solvent mixture was flushed with Ar for additional 5 min. 4-*t*-butyl phenyl boronic acid (0.22 mmol), *N*-(3-bromophenyl)-4-phenylbenzamide/ *N*-methyl-*N*-(bromophenyl)-4-phenylbenzamide (0.17 mmol), K₂CO₃ (0.68 mmol), and tetrakis(triphenylphosphine)palladium(0) (0.071 mmol) were added into the solvent mixture. The reaction vessel was capped tightly and stirred at 100°C for 10 min with monitoring of the color change. The color of the mixture was turned from orange to dark brown. The mixture was stirred at 100°C for additional 16 hr and then cooled down to r.t. The biphasic solution was diluted with saturated aqueous NH₄Cl and dichloromethane and separated. The aqueous phase was extracted with ethyl acetate and the combined organic phases were washed by saturated aqueous NaHCO₃.

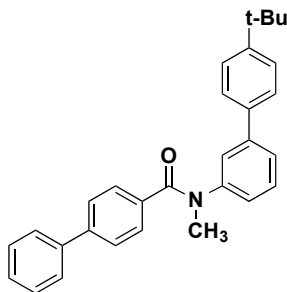
The organic phase was dried over Na₂SO₄ and filtered. Purification of the crude material was performed by Isolera with gradient elution.

***N*-(3-*tert*Butylphenyl)phenyl-(4-phenyl)benzamide, nor-7**



Experiment was performed as described in [C]. **Nor-7** was obtained in 63 % chemical yield as a white powder. ¹H-NMR (CDCl₃, 400MHz): δ 7.97-7.99 (d, 8 Hz, 2H), 7.88-7.90 (d, 8 Hz, 2H), 7.73-7.75 (d, 8 Hz, 2H), 7.64-7.66 (d, 8 Hz, 3H), 7.55-7.57 (d, 8 Hz, 2H), 7.51-53 (d, 8 Hz, 2H), 7.49-7.51 (d, 8 Hz, 2H), 7.47-7.49 (d, 8 Hz, 1H), 7.45-7.47 (d, 8 Hz, 1H), 7.41-7.43 (d, 8 Hz, 1H), 7.39-7.41 (d, 8 Hz, 1H), 1.37 (s, 9H). ¹³C NMR (100 MHz, CDCl₃): δ 165.66, 150.82, 144.95, 142.32, 140.09, 138.53, 137.91, 133.80, 129.68, 129.19, 128.35, 127.80, 127.69, 127.46, 127.05, 125.95, 123.49, 119.05, 119.00, 34.77, 31.57. MS (ESI): m/z [M+H⁺] calcd for C₂₉H₂₇NO 405.21 found 406.2.

***N*-methyl-*N*-(3-*tert*butylphenyl)phenyl-(4-phenyl)benzamide, 7**

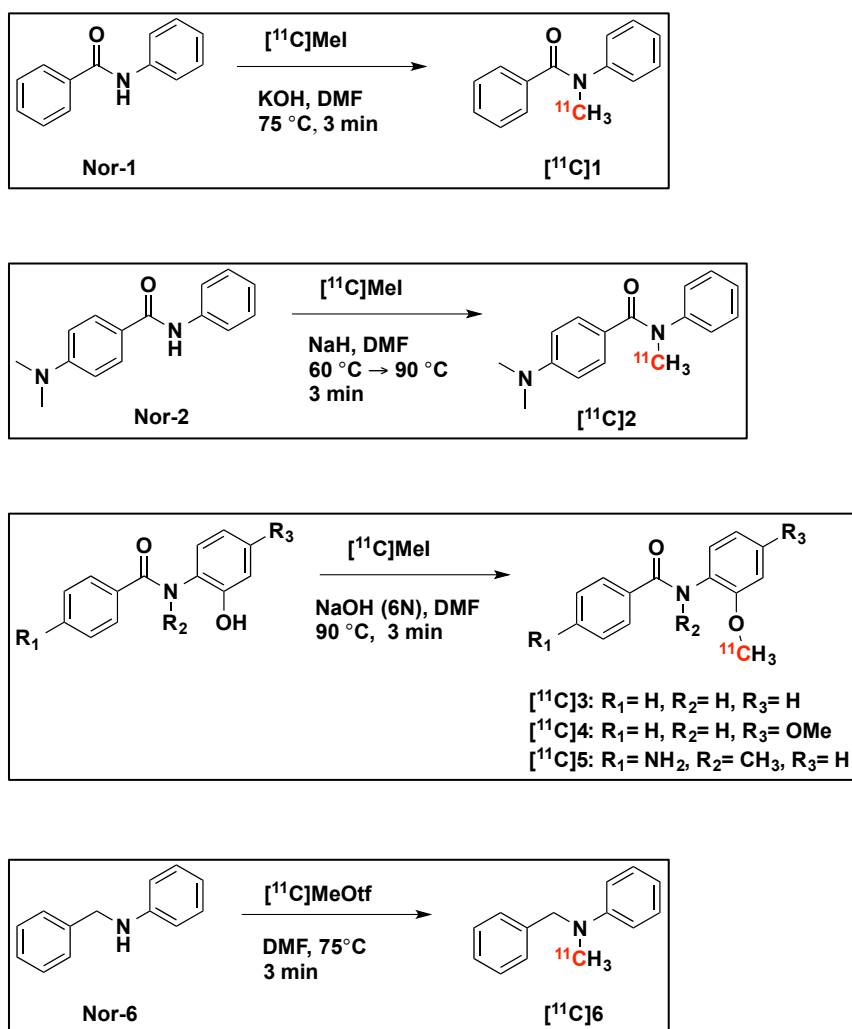


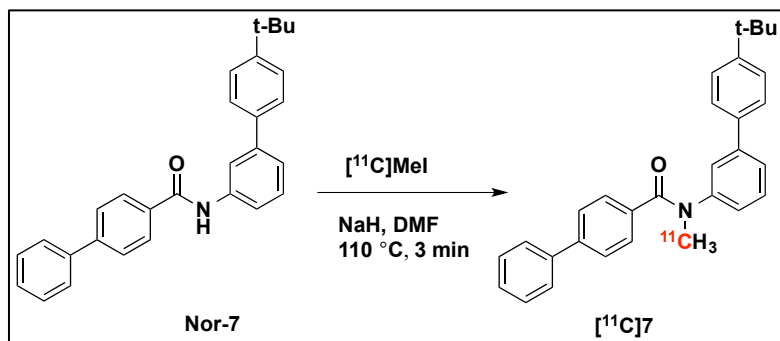
Experiment was performed as described in [C]. *N*-methyl-*N*-(3-bromophenyl)-4-phenylbenzamide (0.164 mmol, 19 mg), **7**, was obtained in 70% chemical yield as a white

powder. $^1\text{H-NMR}$ (CDCl_3 , 400MHz): δ 7.97-7.99 (d, 8 Hz, 2H), 7.88-7.90 (d, 8 Hz, 2H), 7.73-7.75 (d, 8 Hz, 2H), 7.64-7.66 (d, 8 Hz, 3H), 7.55-7.57 (d, 8 Hz, 2H), 7.51-53 (d, 8 Hz, 2H), 7.49-7.51 (d, 8 Hz, 2H), 7.47-7.49 (d, 8 Hz, 1H), 7.45-7.47 (d, 8 Hz, 1H), 7.41-7.43 (d, 8 Hz, 1H), 7.39-7.41 (d, 8 Hz, 1H), 3.58 (s, 3H) 1.37 (s, 9H).

3.2. Rapid radiolabeling and purification of the nor-precursors with carbon-11

Figure 2. Strategic adiosynthesis of seven benzamides with $[^{11}\text{C}]\text{CH}_3\text{I}$ and $[^{11}\text{C}]\text{CH}_3\text{OTf}$





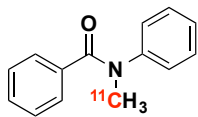
3.2.1. General procedure of radiosynthesis to label benzamides with C-11 [D]

NaOH (6N, 5 μ l) was added to a V-shaped reaction vessel and the benzamide derivative precursor (1 mg) in DMF (300 μ l) was also added in to the vessel. After mixing by vortex for a few seconds, the reaction mixture was warmed to 90 $^\circ$ C for 1 min and switched to ice bath. [^{11}C]methyl iodide was purged into the solution at 0 $^\circ$ C and peak trapping was observed by a pin-diode detector. After the reaction mixture was heated to 90 $^\circ$ C for 3 min, cooled and diluted with high-performance liquid chromatography (HPLC) isocratic eluent (1.0 ml). C-11 labeled product was purified at flow rate 1 ml/min on Luna PFP(2) column (250 \times 10 mm, 5 μ m particles). After separating the labeled product via HPLC, the solvent was removed by using rotary evaporation. The addition of 10 ml of sterile water 3 times every 2 min was needed to avoid volatilization of the product for; [^{11}C]3, [^{11}C]4, [^{11}C]6.

3.2.2. General procedure of quality control for [^{11}C]benzamide derivative analysis [E]

For quality control, analytical TLC and HPLC were performed. [^{11}C]N-methyl-N-phenylbenzamide and C-11 labeled benzamide compounds were cospotted with non-radioactive standard and non-labeled benzamide compound and analyzed by radio TLC. Analytical HPLC was fulfilled by using Phenomenex Luna PFP column (250 \times 4.6 mm, 5 μ m particles) using isocratic elution at flow rate of 1.0 ml/min over 20 min.

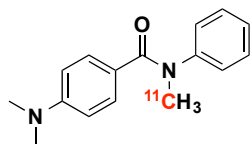
[¹¹C]N-methyl-N-phenyl-benzamide, [¹¹C]1



KOH (5 M, 1 μ l) was added to benzanilide (1 mg) which was purchased from Sigma-Aldrich® in DMF (300 μ l). After mixing by vortex for a few seconds, the reaction mixture was transferred into a V-shaped reaction vessel. The reaction solution was warmed to 60 °C for 1 min and switched to ice bath. [¹¹C]methyl iodide was purged into the solution at 0°C and peak trapping was observed by pin-diode detector. After the reaction mixture was heated to 90°C for 3 min, it was cooled and diluted with high-performance liquid chromatography (HPLC) isocratic eluent (1.0 ml) (acetonitrile: 0.1 M (aq) ammonium formate (40:60)). [¹¹C]N-Methyl-N-phenyl-benzamide was purified at flow rate 1 ml/min on Luna PFP(2) column (250 \times 4.6 mm, 5 μ m particles). [¹¹C]N-Methyl-N-phenyl-benzamide, [¹¹C]1, was eluted (retention time 15.7–18.5 min) and the solvent was removed by using rotary evaporator by adding 10 ml of sterile water 3 times in every 2min to avoid volatilization of [¹¹C]1.

For quality control, general procedure [E] was performed. Radio TLC: (HE:EtOAc (4:1), R_f = 0.28). Isocratic elution for analytical HPLC: (acetonitrile: 0.1 M (aq) ammonium formate (60:40)). Based on this analysis, [¹¹C]1 eluted at 18.9 min. Radiochemical yield was 90 % (decay-corrected) and synthesis time was 20 – 25 min (from radioactivity trapping, 40 – 45 min from EOB). log D 2.36. PPB 90 %

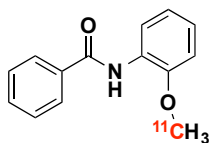
[¹¹C]N-methyl-N-phenyl-4-dimethylaminobenzamide, [¹¹C]2



N-Phenyl-4-dimethylaminobenzamide (1 mg) was dissolved in DMF (300 μ l) and transferred into a V-shaped reaction vessel. After adding NaH (5 mg) to the solution, the reaction solution was mixed by vortex for a few seconds. The reaction vessel was warmed to 60°C for 1 min and switched to ice bath. [^{11}C] methyl iodide was purged into the solution at 0°C and peak trapping was observed by pin-diode detector. After the reaction mixture was heated to 90°C for 3 min, cooled and diluted with HPLC isocratic eluent (1.0 ml) (acetonitrile: 0.1M (aq) ammonium formate (50:50)). [^{11}C]N-methyl-N-phenyl-4-dimethylaminobenzamide, [^{11}C]2, was purified at flow rate 1 ml/min on Luna PFP(2) column (250 \times 4.6 mm, 5 μ m particles). [^{11}C]N-methyl-N-phenyl-4-dimethylaminobenzamide, [^{11}C]2, was eluted (retention time 10.2–12.8 min) and the solvent was removed by rotary evaporation.

For quality control, general procedure [E] was performed. Radio TLC: ((HE:EtOAc (4:1), R_f = 0.28). Isocratic elution for analytical HPLC: (acetonitrile: 0.1 M (aq) ammonium formate (60:40)). Based on this analysis, [^{11}C]N-methyl-N-phenyl-benzamide eluted at 11 min. Radiochemical yield was 86 % (decay-corrected) and synthesis time was 20 – 25 min (from radioactivity trapping, 40 – 45 min from end of bombardment (EOB)). log D 2.68.

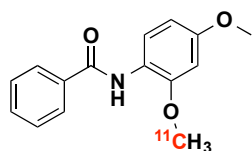
[^{11}C]N-methyl-N-(2-methoxyphenyl)benzamide, [^{11}C]3



Radiosynthesis was performed by the general procedure [D]. High-performance liquid chromatography (HPLC) isocratic eluent: (acetonitrile: 0.1 M (aq) ammonium formate (50:50)). [^{11}C]3 was eluted (retention time 11.2 min) and the solvent was removed by rotary evaporation by adding 10 ml of sterile water 3 times in every 2min to avoid volatilization of [^{11}C]3.

For quality control, general procedure **[E]** was followed. Radio TLC: ((HE:EtOAc (1:1), $R_f=$ 0.81). Isocratic elution for analytical HPLC: ((acetonitrile: 0.1 M (aq) ammonium formate (50:50)): acetonitrile (50:50)). Based on this analysis, [^{11}C]**3** eluted at 8.4 min. Radiochemical yield was 59 % (decay-corrected) and synthesis time was 30 – 35 min (from trapping radioactivity, 50 – 55 min from EOB). log D 2.47. PPB 97%.

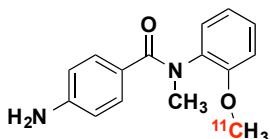
[^{11}C]N-(2-methoxy-4-methoxyphenyl)benzamide, [^{11}C]**4**



Radiosynthesis was performed by following procedure **[D]**. High-performance liquid chromatography (HPLC) isocratic eluent: (acetonitrile: 0.1 M (aq) ammonium formate (50:50)). [^{11}C]**4** was eluted (retention time 13.9 min) and the solvent was removed by rotary evaporation by adding 10 ml of sterile water 3 times every 2 min to avoid volatilization of [^{11}C]**4**.

For quality control, general procedure **[E]** was followed. Radio TLC: ((HE:EtOAc (1:1), $R_f=$ 0.81). Isocratic elution for analytical HPLC: ((acetonitrile: 0.1 M (aq) ammonium formate (50:50)): acetonitrile (50:50)). Based on this analysis, [^{11}C]**4** eluted at 8.5 min. The highest radiochemical yield of [^{11}C]**4** in practice run was 72 % (decay-corrected) and synthesis time was 30 min (from trapping radioactivity, 50 – 55 min from EOB). log D 2.85. PPB 97 %

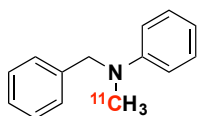
[^{11}C]N-methyl-N-(2-methoxyphenyl)-4-aminobenzamide, [^{11}C]**5**



Radiosynthesis was performed by following procedure **[D]**. High-performance liquid chromatography (HPLC) isocratic eluent: (acetonitrile: 0.1 M (aq) ammonium formate (35:65)). [¹¹C]**5** was eluted (retention time 9.8 min) and the solvent was removed by using rotary evaporation under reduced pressure.

For quality control, general procedure **[E]** was followed. Radio TLC: ((HE:EtOAc (1:1), R_f= 0.35). Isocratic elution for analytical HPLC: ((acetonitrile: 0.1 M (aq) ammonium formate (60:40)): acetonitrile = 40:60). Based on this analysis, pure [¹¹C]**5** eluted at 5.3 min. Radiochemical yield was 67 % (decay-corrected) and synthesis time was 30 – 35 min (from trapping radioactivity, 50 – 55 min from EOB). log D 2.17. PPB 28 %

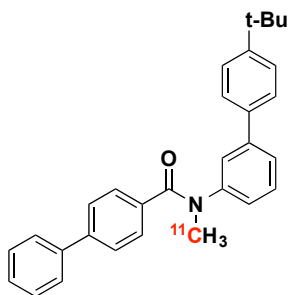
*[¹¹C]N-methyl-N-benzylaniline, [¹¹C]**6***



Commercially available N-benzylaniline (**nor-6**) from Sigma-Aldrich (1 mg) in 2-butanone (300 μl) was added to a V-shaped reaction vessel. After mixing by vortex for a few seconds, the reaction mixture was cooled down with ice bath for trapping C-11 methyl-triflate. [¹¹C]methyl triflate was purged into the solution at -10°C and peak trapping was observed by pin-diode detector. After the reaction mixture was heated to 75°C for 3 min, cooled and diluted with high-performance liquid chromatography (HPLC) eluent (1.0 ml) (acetonitrile: 0.1 M (aq) ammonium formate (60:40)). After injection of the hot crude product, the resulting mixture was purified with gradient HPLC system at flow rate 1 ml/min on Luna PFP(2) column (250 × 10 mm, 5 μm particles) and the whole prep HPLC procedure was monitored. [¹¹C]**6** was eluted (retention time 24.3 min). 0.1 mL of 1M aqueous solution was added to the collected product and the solvent was removed by using rotary evaporation under reduced pressure.

For quality control, general procedure [E] was followed. Radio TLC: ((HE:EtOAc (10:1), R_f = 0.8). Isocratic elution for analytical HPLC: ((acetonitrile: 0.1 M (aq) ammonium formate (60:40)): acetonitrile = 40:60). Based on this analysis, pure [^{11}C]6 eluted at 5.3 min. Radiochemical yield was 87 % and synthesis time was 30 – 35 min (from trapping radioactivity, 50 – 55 min from EOB). log D 2.61. PPB 60 %.

[^{11}C]N-methyl-N-(3-tertbutylphenyl)phenyl-(4-phenyl)benzamide, [^{11}C]7



NaH in a V-shaped reaction vessel was decanted with hexane and dried over argon. To the reaction vessel **nor-7** (1 mg) dissolved in DMF (300 μl) was added. After mixing by vortex for a few seconds, the reaction mixture was warmed to 110°C for 1 min and switched to an ice bath. [^{11}C]Methyl iodide was purged into the solution at 0°C and peak trapping was observed by pin-diode detector. After the reaction mixture was heated to 110°C for 3 min, it was cooled and diluted with high-performance liquid chromatography (HPLC) eluent (1.0 ml) (acetonitrile: 0.1 M (aq) ammonium formate (40:60)). [^{11}C]SJ-8 was purified with gradient system at flow rate 1 ml/min on Luna PFP(2) column (250 \times 10 mm, 5 μm particles). [^{11}C]7 was eluted (retention time 18 min) and the solvent was removed by using rotary evaporator under reduced pressure.

For quality control, general procedure [E] was followed. Radio TLC: ((HE:EtOAc (4:1), R_f =0.3). Isocratic elution for analytical HPLC: ((acetonitrile: 0.1 M (aq) ammonium formate (50:50)): acetonitrile (50:50)). Based on this analysis, [^{11}C]7 eluted at 7.6 min. Radiochemical

yield was 85 % and synthesis time was 25 – 30 min (from trapping radioactivity, 45 – 50 min from EOB). log D 3.75. PPB 84 %.

4. PET study in baboon

All animal studies were reviewed and approved by the Brookhaven Institutional Animal Use and Care committee. A baboon was anesthetized with ketamine (10 mg/kg) and then intubated and ventilated with a mixture of isoflurane (Forane, 1–4%) and nitrous oxide (1500 ml/min) and oxygen (800 ml/min). The baboon was transported to and from the PET facility in a temperature controlled transfer cage and a member of the staff attended them while the animal recovered from anesthesia. Catheters were inserted in a popliteal artery and radial arm vein for arterial sampling a radiotracer injection respectively. Dynamic PET imaging was carried out on a Siemen's HR+high resolution, whole body PET scanner (4.5×4.5×4.8 mm at center of field of view) in 3D acquisition mode, 63 planes. A transmission scan was obtained with a ⁶⁸Ge rotating rod source before the emission scan to correct for attenuation before each radiotracer injection. During the PET scan, the baboon was monitored for heart rate, respiration rate, PO₂ and temperature. The baboon was allowed 4 weeks between studies to recover from anesthesia and blood sampling.

The radiosynthesis was performed by above **3.2. Rapid radiolabeling and purification of the nor-precursors with carbon-11**. Seven [¹¹C]labeled benzamide compounds were obtained in water/acetonitrile solvent (15 – 20 mL) from semi-preparative HPLC purification. The [¹¹C]labeled benzamide compounds were concentrated via evaporation of the HPLC solvent by rotary evaporator under reduced pressure. After concentration 5 – 10 mCi of the [¹¹C]labeled

benzamides were dissolved in sterile water (5 cc) and filtered through a Millipore filter and then delivered for baboon PET studies. PET images are integral images over 60 min. In order to obtain quantitative result by analyzing PET data, corresponding time-activity curves for C-11 labeled compounds were given. The curve shows the concentration of radioactivity (% of injected dose/cc of brain tissue) vs time.

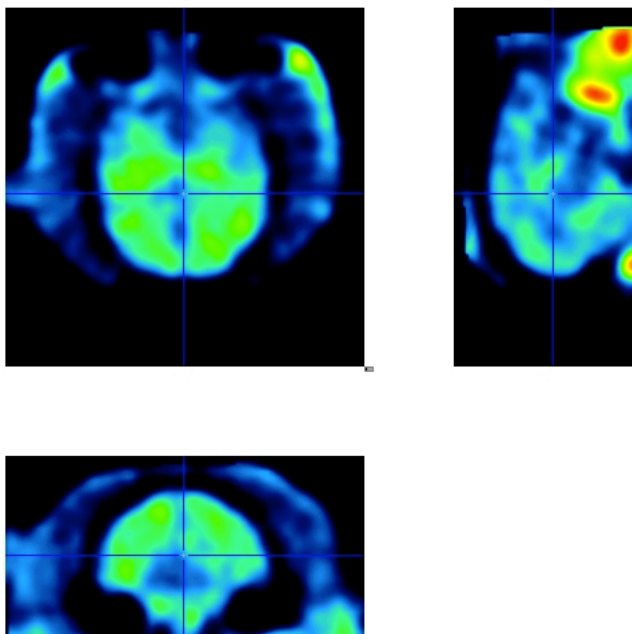
5. Result and discussion

5.1. In vivo PET imaging in female baboon brain (baboon study performed by Pauline Carter and Payton King; PET image analysis by S. W. Kim)

[¹¹C]1 which has two of hydrogen bonding atoms was used to test BBB permeability in baboon on Oct 10th, 2011. In order to obtain quantitative result by analyzing PET data, corresponding time-activity curves (TAC) for C-11 labeled compounds were obtained.

Even though [¹¹C]1 showed volatility resulting in some product loss during labeling, the hot product was successfully delivered to PET laboratory for a baboon study (Figure 3) and time-activity data from baboon brain and blood samples was obtained over a 60 minute scanning period.. Summed frames over 60 minutes provide the images with [¹¹C]1 in female baboon brain shown in Figure 3.

Figure 3. Baboon study with [^{11}C]1: [^{11}C]1 PET images in female baboon brain mark transaxial, sagittal and coronal planes



Baboon studies were carried out with other six benzamide compounds ([^{11}C]2 – [^{11}C]7) labeled with C-11 as well and the brain (Figure 4) and blood time-activity curves (Figure 5) of total seven [^{11}C]benzamides were obtained over 60 min PET scan. Brain time-activity curves (Figure 4) quantitatively show high initial brain uptake and rapid washout and the shape of curve is acceptable as this series of benzamides was intended to penetrate the brain but not bind to any specific molecular target.

Figure 4. Brain time-activity curve of seven [^{11}C]benzamides through [^{11}C]1 to [^{11}C]7

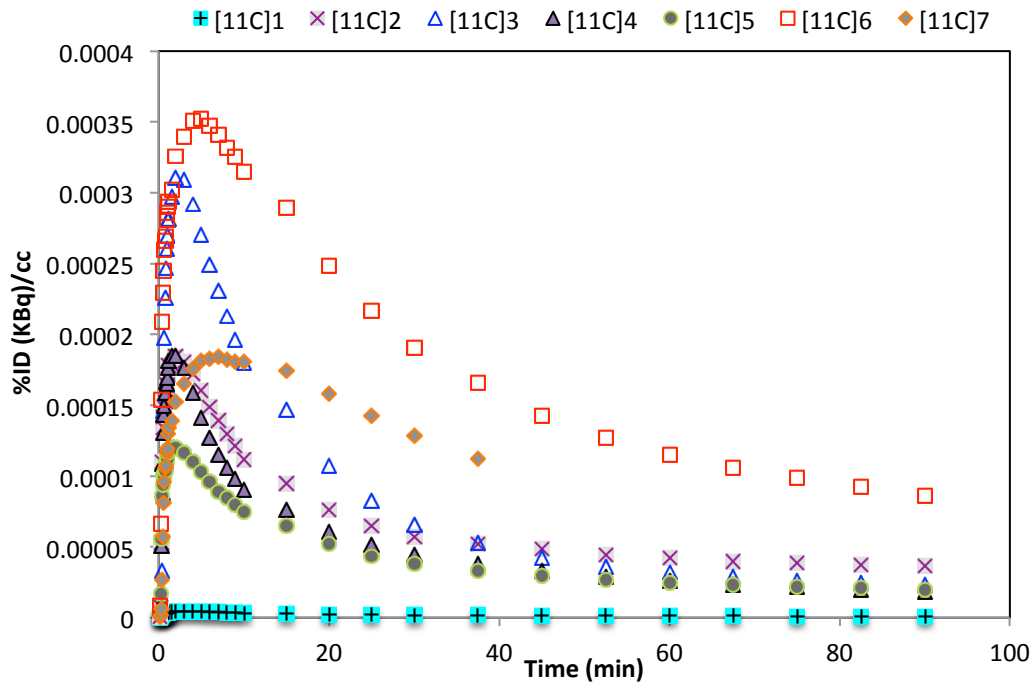
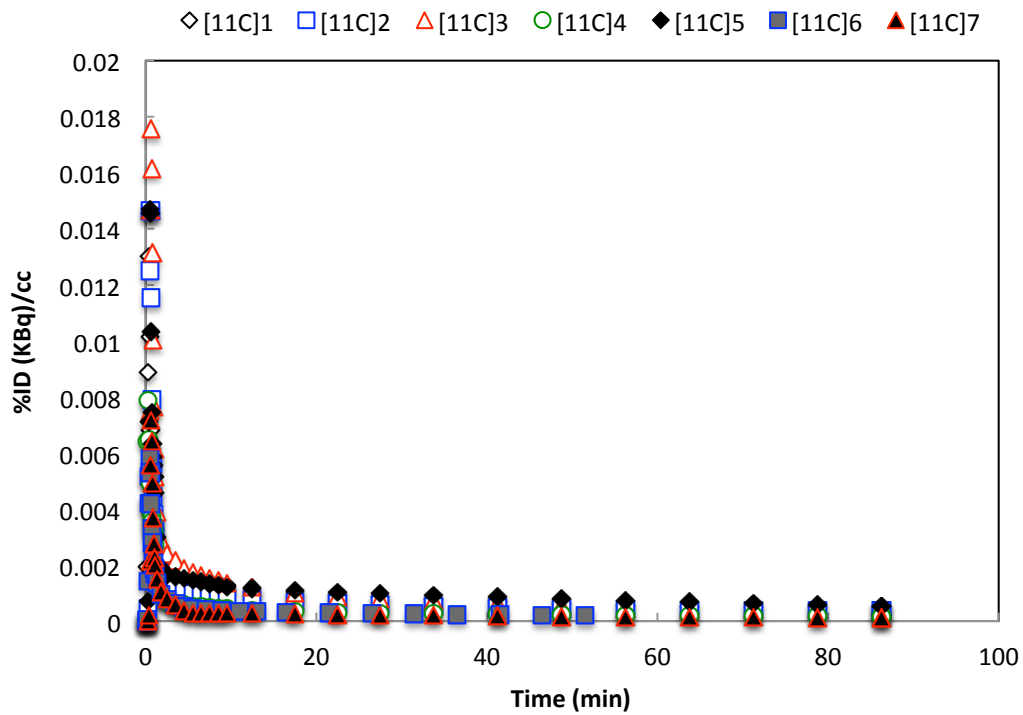


Figure 5. Blood time-activity curve of seven [^{11}C]benzamides through [^{11}C]1 to [^{11}C]7



5.2. Application to kinetic modeling

A QSPR model to predict K_1 and k_2 in blood brain barrier penetration using systematically synthesized [^{11}C]benzamides ($[^{11}\text{C}]\mathbf{1} - [^{11}\text{C}]\mathbf{7}$) was constructed. The high-correlated descriptors were Van der Waals volume (VDW_{vol}) and topological polar surface area (TPSA). The predicted K_1 and k_2 were compared with measured value from PET.

6. Conclusion

Seven well-defined candidate benzamides with different numbers of hydrogen bonds by PSA order were designed and targeted for synthesis and radiolabeling with carbon -11 (half life; 20.4 min). Cold nor-precursors and reference compounds based on our strategy (through **nor-1** to **nor-7** and through **1** to **7**) were successfully synthesized via parallel synthesis in moderate yield (~70%).

Seven C-11 labeled benzamides were synthesized successfully. Reaction condition for radiosynthesis was optimized in terms of synthesis time and yield. The radiosynthesis time was 30 min ranged from end-of-bombardment (EOB) and high radiochemical yield was ranged from 32 to 55%. Experimental details are shown in the section **3. Experimental details**.

O-Methylation with [^{11}C]MeI in radiosynthesis showed higher radiochemical yield than N-methylation. By using [^{11}C]MeOTf in radiosynthesis milder reaction conditions (low temperature without base) was used to achieve higher radiochemical yield.

Baboon PET studies revealed BBB penetration imaging and estimated experimental K_1 and k_2 . The representative time-activity curve of seven benzamide compounds labeled with C-11 was from PET study controlling for individual variability by performing all studies in the same

baboon and allowing time between scans for recovery. Brain time-activity data was measured to calculate the dynamic model terms of interest: plasma-to-brain transfer term (K_1) and brain-to-plasma efflux term (k_2) by using 1-tissue-compartment model.

The main criteria driving QSPR were TPSA and Van der Waals volume with K_1 being highly correlated with TPSA and k_2 being affected mainly by VDW_{vol} . We demonstrated, for the first time an experimentally validated K_1 and k_2 prediction model for PET radiotracers in the particular structure. Even though it is limited to structurally well-defined benzamides we suggest that it will be generalizable to other structural motifs.

7. Appendix

7.1. Plasma-protein binding (PPB) assay

The plasma-protein binding assay of seven [^{11}C]benzamides was performed based on adapted method previously published¹⁶. An aliquot of [^{11}C]metergoline in saline (10 μl) was added to a sample of baboon plasma (0.8-mL). The mixture was gently mixed by repeated inversion and incubated for 10 min at room temperature. Following incubation a small sample (20 μl) was removed to determine the total radioactivity in the plasma sample (A_T ; $A_T=A_{\text{bound}}+A_{\text{unbound}}$). An additional 0.2 mL of the plasma sample was placed in the upper compartment of a Centrifree® tube (Amicon, Inc., Beverly, MA) and then centrifuged for 10 min. The upper part of the Centrifree tube was discarded and an aliquot (20 μl) from the bottom part of the tube was removed to determine the amount of radioactivity that passed through the membrane (A_{unbound}). Plasma protein binding was derived by the following equation: $\% \text{ unbound}=A_{\text{unbound}}\times 100/A_T$.

7.2. Determination of log D value of seven [¹¹C]benzamides

The distribution of [¹¹C]benzamides between 1-octanol and 0.2 M phosphate buffer (pH 7.4) was measured in triplicate at room temperature by adapting a method previously described¹⁷. Briefly, 1 mL of 1 mCi/mL solution of [¹¹C]benzamides in 0.2 M phosphate buffer (pH = 7.4) was mixed vigorously with 1 mL 1-octanol for 1 min at room temperature using a vortex. After centrifugation for 5 min at 4,000 rpm and a settling period of 30 min, five aliquots of 100 μ L were taken from both layers, carefully avoiding cross contamination between the phases. Five aliquots of 100 μ L of the 1 mCi/mL solution of [¹¹C]benzamides in 0.2 M phosphate buffer (pH = 7.4) were taken as reference for determining recovery. All aliquots were counted for radioactivity using a Capintec CRC-712MV radioisotope calibrator (Capintec, Ramsey, NJ, USA). The logD value was calculated according to $\log D = \text{Log}(A_{\text{oct}} / A_{\text{buffer}})$, with A_{buffer} as the average radioactivity of five buffer samples and A_{oct} as the average radioactivity of five 1-octanol samples.

7.3. In vivo metabolite study with baboon plasma (Analysis was performed by Payton King and Colleen Shea)

Arterial blood samples were centrifuged and an aliquot of plasma was pipetted and counted and then the plasma was subjected to radioHPLC analysis to determine the fraction of total C-11 which was present as the parent injected radiolabeled compound (Table 1). Sample tubes were prepared with 500 μ L of methanol or acetonitrile depending on solvent if solvent is \geq 50% organic solvent. 300 μ L of organic solvent was used if more aqueous. Tubes for supernatant were prepared empty if using 500 μ L of organic solvent (methanol or acetonitrile) in sample tubes, with 300 μ L of water if using 300 μ L of the organic solvent in sample tubes. For each

baboon plasma sample; 1 min, 5 min, 10 min, 30 min, 60 min samples total activity was counted by a well counter. Supernatant and pellet was separated by sonication and centrifuge and then counted by wellcounter. 400 – 500 μ L of supernatant was injected into HPLC. Retention time was divided by 3 and collected peaks into picker vial to count the activity based on UV changes. Standard compound (3 μ L) was dispensed into the picker vial measuring accurately.

Table 2. In vivo metabolite study with baboon plasma by analytical HPLC*.

Date	Comp.	Flow rate (mL/min)	Retention time (min)
01-23-12	17	0.8	6 - 7
01-23-12	18	1.0	7 - 8
02-23-12	19	1.0	8 - 9
02-23-12	20	1.0	9 - 10
03-09-12	21	1.5	8 - 9
04-12-12	22	2.0	12 - 13
04-26-12	23	0.9	11 - 12

*Analytical HPLC Column (Waters®, Bondapak C18, 4.6 mm \times 250 mm, 10 μ m) with isocratic solvent (1.0M aq. ammonium formate/MeCN = 50/50) at UV 254 nm.

7.4. Using quantitative structure-property relationship (QSPR) as a prediction tool for dynamic modeling of BBB permeability (QSAR modeling study was performed by Yeona Kang)

To calculate parameters from PET study, we used a 1-tissue-compartment model (1TCM) to approximate the total brain uptake. The in vivo performance of candidate compounds was estimated through PMOD® (PMOD Technologies, Ltd). To calculate various chemical and structural properties of candidate compounds and to evaluate possible QSPR models, MOE and

Shrödinger were used. In silico and in vivo datasets were introduced, and the validation of the individual model components and their overall performance was investigated.

7.4.1. PET studies and data analysis

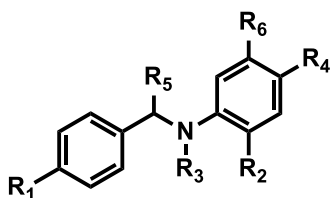
All animal studies were reviewed and approved by Brookhaven Institutional Animal Use and Care committee. 9 different female baboons were used for these experiments. Twenty two C-11 labeled benzamides including seven [¹¹C]benzamide compounds ([¹¹C]1 – [¹¹C]7) were prepared for baboon PET studies (Table 3 and Figure 6).

Table 3. To do QSPR K_1 and k_2 prediction modeling study, the interesting/high-correlated descriptors are molecular volume and topological polar surface area (TPSA).

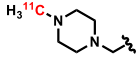
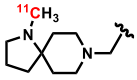
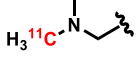
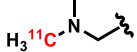
Compd	K_1	k_2	logD (pH:7.4)	logP	clogBB	TPSA	Vdw_vol	Weight
H10-1	0.047	0.012	0.65	1.76	0.202	61.60	468.89	324.43
H10-3	0.189	0.034	-0.62	2.23	0.184	58.36	391.60	269.35
H10-5	0.104	0.015	1.39	2.39	0.336	61.60	484.85	358.87
H10-9	0.111	0.010	1.6	2.59	0.368	61.60	497.88	403.32
H10-12	0.079	0.010	2.96	3.76	0.615	61.60	583.86	400.53
H10-16	0.072	0.012	1.68	2.99	0.511	61.60	501.46	450.32
H10-18	0.118	0.016	0.76	1.949	0.235	61.60	472.03	342.41
H10-20	0.024	0.011	1.41	3.96	0.353	67.15	480.52	331.42
H10-21	0.162	0.015	1.45	4.23	0.598	58.36	506.57	345.45
H10-24	0.069	0.010	3.04	3.91	0.636	61.60	587.01	418.52
H10-38	0.014	0.000	3.07	5.36	1.055	61.60	667.68	454.62
H10-27	0.222	0.012	1.84	4.38	0.618	58.36	509.71	363.44
H10-32	0.134	0.008	0.47	3.88	0.516	58.36	486.00	351.47

[¹¹ C]1	0.283	0.112	2.31	3.05	0.669	20.30	311.78	211.26
[¹¹ C]2	0.357	0.141	2.38	2.97	0.830	23.54	378.54	254.33
[¹¹ C]3	0.368	0.131	2.49	3.01	0.613	29.54	346.87	241.28
[¹¹ C]4	0.190	0.113	2.93	2.80	0.327	47.56	355.92	257.29
[¹¹ C]5	0.179	0.125	1.78	2.37	0.177	55.56	361.54	256.30
[¹¹ C]6	0.316	0.060	3.46	2.61	1.055	3.24	310.60	197.28
[¹¹ C]7	0.140	0.042	5.64	8.51	1.772	20.30	639.44	419.56
NICOT								
INE	0.472	0.046	-0.649	0.76	0.397	16.13	204.63	162.34
MS275	0.009	0.000	1.05	2.45	-0.220	106.34	507.72	376.42

Figure 6. Structures of the 15 benzamide compounds besides 7 benzamides ([¹¹C]1 – [¹¹C]7 shown on **Table 1**) contained in **Table 3**.



Compd	R ₁	R ₂	R ₃	R ₄	R ₅	R ₆	H-bonds
H10-1		-NH ₂	-H	-H	Carbonyl	-H	7
H10-3		-NH ₂	-H	-H	Carbonyl	-H	6
H10-5		-NH ₂	-H	-H	Carbonyl	-Cl	7
H10-9		-NH ₂	-H	-H	Carbonyl	-Br	7
H10-12		-NH ₂	-H	-H	Carbonyl	Phenyl	7
H10-16		-NH ₂	-H	-H	Carbonyl	-I	7
H10-18		-NH ₂	-H	-H	Carbonyl	-F	7
H10-20		-NH ₂	-H	-H	Carbonyl	Phenyl	7
H10-21		-NH ₂	-H	-H	Carbonyl	Phenyl	6

H10-24		-NH ₂	-H	-H	Carbonyl	4-fluorophenyl	7
H10-38		-NH ₂	-H	-H	Carbonyl	phenyl	7
H10-27		-NH ₂	-H	-H	Carbonyl	4-fluorophenyl	6
H10-32		-NH ₂	-H	-H	Carbonyl	2-thienyl	7

7.4.2. Blood flow

One of common assumption is the blood flow effect to penetrate radiotracers¹⁸. In this study, blood flow stability among different scans over different days in the several animals was checked using [¹¹C]-(R)nicotine studies. Since the extraction fraction of nicotine can be assumed to be as 1¹⁹, uptake value K₁ of [¹¹C]-(R)nicotine equals the blood flow. To confirm the blood flow stability, we used four different baboons and each test run different study days and times as showed by Table 4. Although different scans over different days in the several animals were used, all K₁ values are consistent (0.47±0.1) and these results supported to prove that the blood flow is stable for our studies.

Table 4. Summary of baboon PET studies

Radiotracer	Study #	Baboon	Injection Dose (mCi)	Weight (kg)	K ₁	k ₂
[¹¹ C]nicotine	BEJ426DY3	Spicey	4.26	18.2	0.3266	0.0398
	BEH288DY2	Pearl	4.68		0.4726	0.0464
	BEH289DY1	Lulu	0.97		0.5089	0.0420
	BEH290DY3	Chloe	3.2	18.8	0.5626	0.0883
	MEAN				0.4676	0.0539
	STD				0.1010	0.0230

7.4.3. QSPR mode

For development new QSAR model related to apparent K_1 and k_2 , the performance of our approach is evaluated on a dataset containing 22 compounds including seven [^{11}C]benzamide compounds for which the in silico and in vivo data exist (Table 3). For each compound, the in silico descriptors such as TPSA or vdw_vol were obtained from MOE or Schrodinger commercial software. For in vivo, all animal studies were reviewed and approved by Brookhaven Institutional Animal Use and Care committee. 6 different female baboons were used for these experiments.

7.4.4. Results

Prior to data verification or any subsequent fitting procedures, preliminary analysis of the relationship between calculated logBB (clogBB) and apparent uptake values (K_1) was performed. The well-known QSAR model using some MOE and Schrodinger descriptors calculated the clogBB²⁰. Those clogBB values were plotted against apparent K_1 (or uptake) and k_2 values as shown in Figure 7 and Figure 8. There seem to be no correlations between clogBB and apparent K_1 and k_2 although the model for clogBB was employed with logP and TPSA as important descriptors. These findings clearly demonstrate that clogBB is not enough to explain brain uptake driven BBB permeability at least for early time point events.

Figure 7. The correlation between clogBB and apparent uptake value K_1

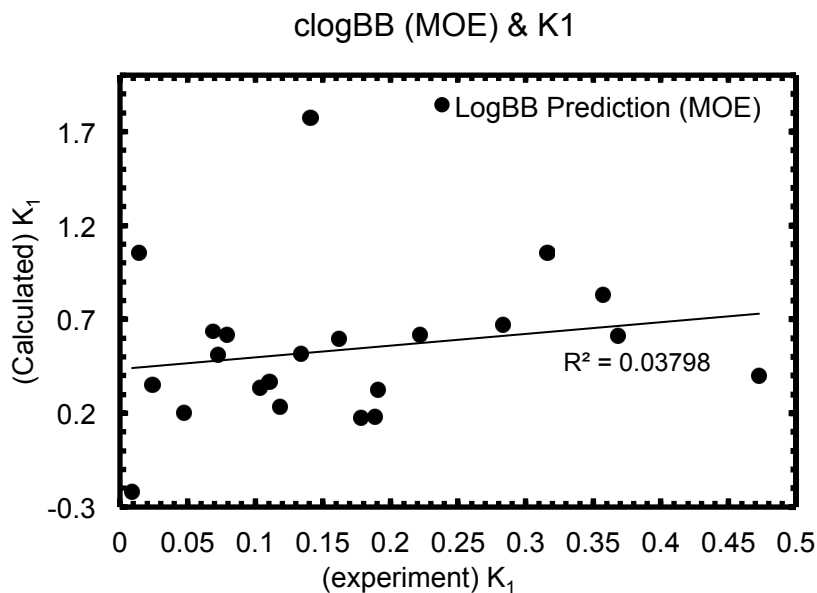
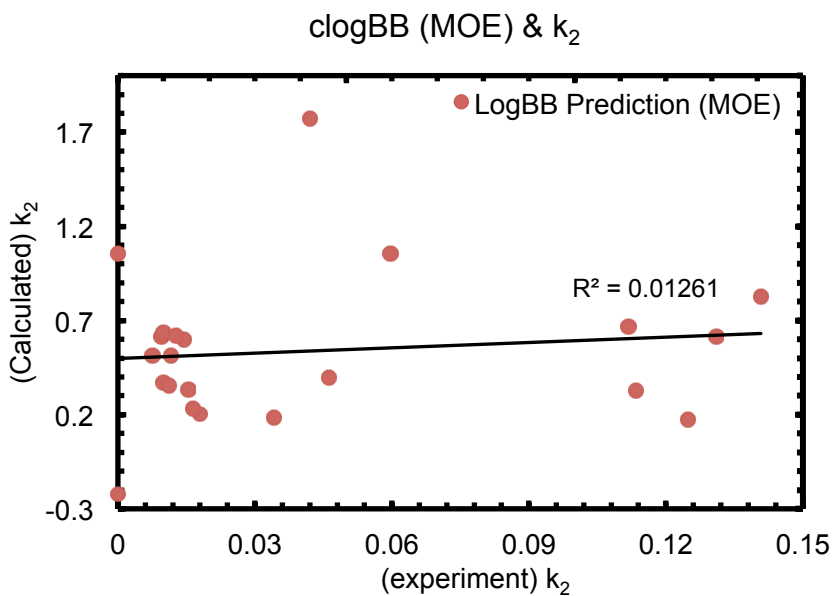


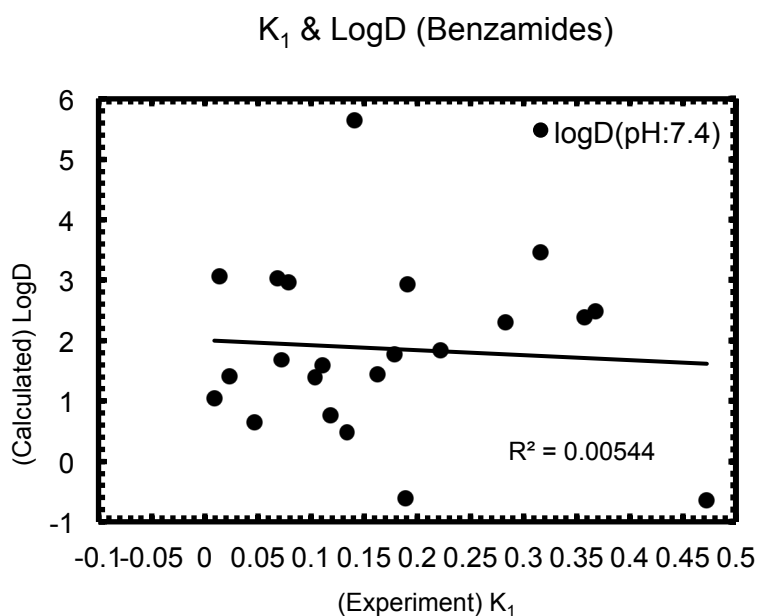
Figure 8. The relation between clogBB and efflux rate k_2 : there is not correlation each other.



As known parameter, logD can deal with an assumption that ionic species have the same affinity to BBB as to octanol, which is quite disputable. To compute clogD, we used the online

chemical database and modeling environment²¹ to calculate clogD and showed no correlation between (ex) K_1 and clogD. However in our result, there is still low correlation between apparent K_1 and clogD as shown Figure 9.

Figure 9. The comparison between apparent uptake value K_1 and calculated logD: there is almost no correlation.



1-compartment kinetic analysis was applied to the time-activity curves to derive regional estimates of the influx rate constant (K_1). The least-squares fitting procedure included a fixed 5% blood volume and was performed with a Levenberg-Marquadt optimizer in PMOD.

For the QSAR prediction model, the K_1 values of the 22 compounds in the dataset (Table 3) were predicted using Equation 1., with TPSA and v_{dw_vol} as considered descriptors. Before to test with completed 22 dataset, some criteria for relationship between TPSA and K_1 were built. In early stage, most benzamide compound's TPSA values were 58 or 61 and so more diversity to validate TPSA's role for K_1 prediction was necessary. In Table 3, the seven [¹³C]benzamide

compounds ($[^{11}\text{C}]\mathbf{1} - [^{11}\text{C}]\mathbf{7}$) were specifically designed and synthesized for in silico and in vivo PET study.

$$P = 10^{-0.121(c\log D - 2.298)^2 - 2.544 \log\left(V_x^{\frac{1}{3}}\right) - 2.525} \quad (1)$$

$$K_1 = F(1 - e^{PS/F}) \quad (2)$$

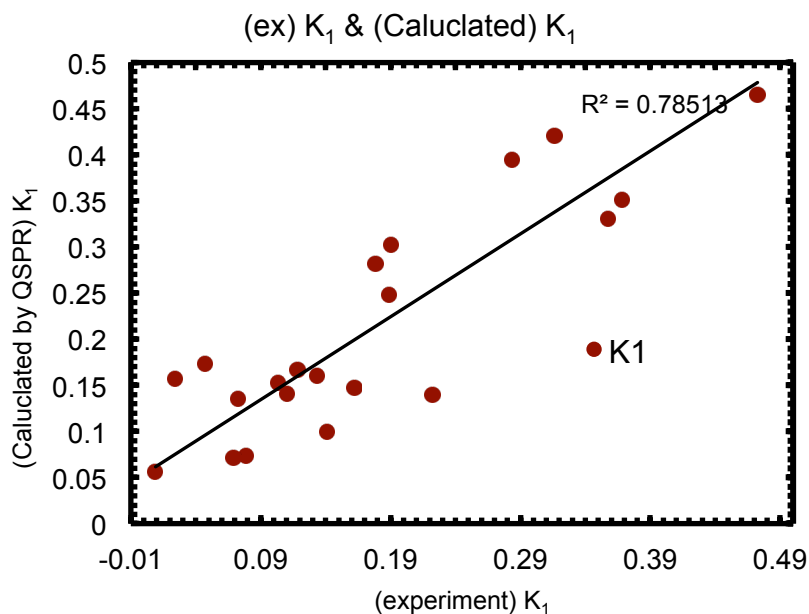
Furthermore, one of the interesting descriptors was molecular weight (MW) and the correlation among TPSA, MW and K1 was one of most important thing. Early benzamide compound's MW was approximately from 320 to 450. Those numbers were fitted to Lipinski's rule of five but still there still existed some more diversity in near marginal area. the seven $[^{11}\text{C}]$ benzamide compounds ($[^{11}\text{C}]\mathbf{1} - [^{11}\text{C}]\mathbf{7}$) considerably overcame this point of view.

The QuaSAR module in MOE was used to perform the 2D-QSAR PLS regression analysis on the data set. Two molecular descriptors with top contingency coefficients were picked that fit to the experiment dataset. This resulted in a model with the following statistics: N=22, $r^2=0.833$, cross validated (leave one out) $Q^2=0.733$:

$$K_{1_{predict}} = 0.572 - 0.0029 * TPSA - 0.00057 * vdw_{vol}$$

Where TPSA is topological polar surface area and vdw_vol is van der Walls volume. The normalized linear model shows the relative importance of the two descriptors in the model to be 1 for TPSA and 0.97 for vdw_vol. Linear model is very good fitting relative to alternative methods as well as less descriptors involving. For this QSAR model we tried to make validate 2-fold cross-validation. Also Q^2 is more than 0.7 and it is very consistent result (Figure 10).

Figure 10. QSAR result for K_1 apparent: high correlation is shown (correlation value = 0.78).



As well as K_1 , k_2 is also very important parameter to determine drug-able compound. In fact, k_2 is affected in equilibrium state because this number is wash-out factor related. Therefore k_2 might have some correlation with $\log BB$.

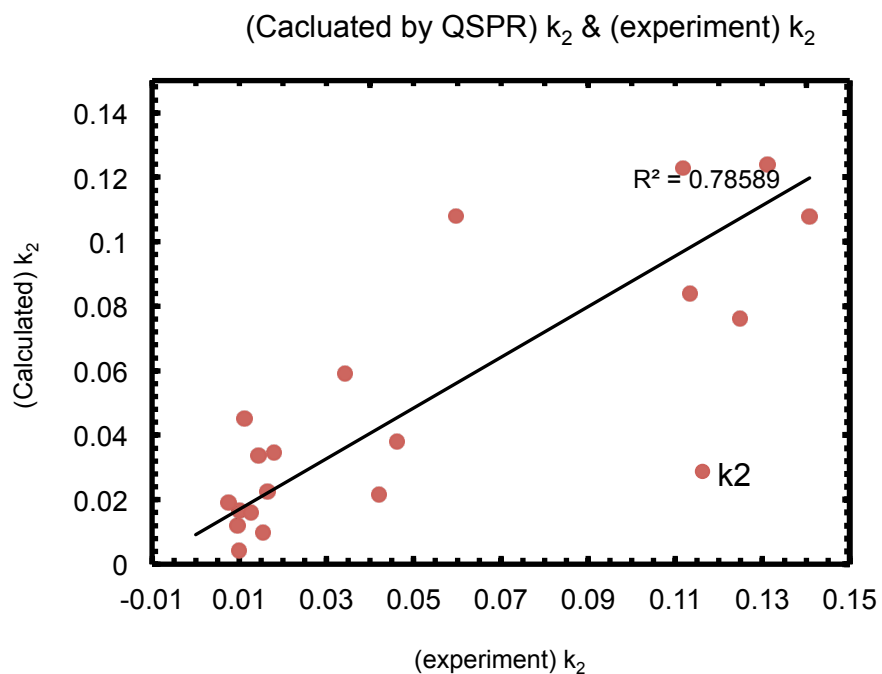
For k_2 prediction, there are three descriptors involved: TPSA, MV (molecular volume), and vdw_vol . Similar with K_1 model, three molecular descriptors with top contingency coefficients were picked that fit to the experiment dataset (Figure 11). This resulted in a model with the following statistics: $N=22$, $r^2=0.786$, cross validated (leave one out) $r^2=0.68$:

$$k_{2_{predict}} = 0.214 - 0.00054 * TPSA - 0.0045 * vol + 0.0029 * vdw_{vol}$$

For k_2 , the normalized linear model shows the relative importance of the three descriptors in the model to be 1 for vol , 0.93 for vdw_vol and 0.034 for TPSA. Relative to two other

descriptors, TPSA is relative low importance of descriptors but for marginal area prediction, TPSA plays as a key role.

Figure 11. Correlation between in house calculated k_2 values and experimental k_2 values: correlation value is approximately 0.79 and they have very high correlation.



8. Reference

1. Guo, Q.; Brady, M.; Gunn, R. N., A biomathematical modeling approach to central nervous system radioligand discovery and development. *Journal of nuclear medicine : official publication, Society of Nuclear Medicine* **2009**, *50* (10), 1715-23.
2. Pike, V. W., PET radiotracers: crossing the blood-brain barrier and surviving metabolism. *Trends in pharmacological sciences* **2009**, *30* (8), 431-40.
3. Fan, Y.; Unwalla, R.; Denny, R. A.; Di, L.; Kerns, E. H.; Diller, D. J.; Humblet, C., Insights for predicting blood-brain barrier penetration of CNS targeted molecules using QSPR approaches. *Journal of chemical information and modeling* **2010**, *50* (6), 1123-33.
4. (a) Fowler, J. S.; Volkow, N. D.; Logan, J.; Alexoff, D.; Telang, F.; Wang, G. J.; Wong, C.; Ma, Y.; Kriplani, A.; Pradhan, K.; Schlyer, D.; Jayne, M.; Hubbard, B.; Carter, P.; Warner, D.; King, P.; Shea, C.; Xu, Y.; Muench, L.; Apelskog, K., Fast uptake and long-lasting binding of methamphetamine in the human brain: comparison with cocaine. *NeuroImage* **2008**, *43* (4), 756-63; (b) Volkow, N. D.; Ding, Y. S.; Fowler, J. S.; Wang, G. J.; Logan, J.; Gatley, J. S.; Dewey, S.; Ashby, C.; Liebermann, J.; Hitzemann, R.; Wolf, A. P., Is Methylphenidate Like Cocaine - Studies on Their Pharmacokinetics and Distribution in the Human Brain. *Arch Gen Psychiat* **1995**, *52* (6), 456-463; (c) Fowler, J. S.; Volkow, N. D.; Wolf, A. P.; Dewey, S. L.; Schlyer, D. J.; Macgregor, R. R.; Hitzemann, R.; Logan, J.; Bendriem, B.; Gatley, S. J.; et al., Mapping cocaine binding sites in human and baboon brain in vivo. *Synapse* **1989**, *4* (4), 371-7.
5. (a) Isakovic, A. J.; Abbott, N. J.; Redzic, Z. B., Brain to blood efflux transport of adenosine: blood-brain barrier studies in the rat. *Journal of neurochemistry* **2004**, *90* (2), 272-86; (b) Reichel, A., The role of blood-brain barrier studies in the pharmaceutical industry. *Current drug metabolism* **2006**, *7* (2), 183-203.
6. (a) Katritzky, A. R.; Kuanar, M.; Slavov, S.; Dobchev, D. A.; Fara, D. C.; Karelson, M.; Acree, W. E., Jr.; Solov'ev, V. P.; Varnek, A., Correlation of blood-brain penetration using structural descriptors. *Bioorganic & medicinal chemistry* **2006**, *14* (14), 4888-917; (b) Winkler, D. A., The role of quantitative structure--activity relationships (QSAR) in biomolecular discovery. *Briefings in bioinformatics* **2002**, *3* (1), 73-86.
7. Kononov, D. A.; Coomans, D.; Deconinck, E.; Heyden, Y. V., Benchmarking of QSAR models for blood-brain barrier permeation. *Journal of chemical information and modeling* **2007**, *47* (4), 1648-56.
8. Hansch, C.; Bjorkroth, J. P.; Leo, A., Hydrophobicity and central nervous system agents: on the principle of minimal hydrophobicity in drug design. *Journal of pharmaceutical sciences* **1987**, *76* (9), 663-87.
9. Norinder, U.; Haeberlein, M., Computational approaches to the prediction of the blood-brain distribution. *Advanced drug delivery reviews* **2002**, *54* (3), 291-313.
10. (a) Martin, I., Prediction of blood-brain barrier penetration: are we missing the point? *Drug discovery today* **2004**, *9* (4), 161-2; (b) Pardridge, W. M., Log(BB), PS products and in silico models of drug brain penetration. *Drug discovery today* **2004**, *9* (9), 392-3.

11. Mensch, J.; Oyarzabal, J.; Mackie, C.; Augustijns, P., In vivo, in vitro and in silico methods for small molecule transfer across the BBB. *Journal of pharmaceutical sciences* **2009**, *98* (12), 4429-68.
12. Abraham, M. H., The factors that influence permeation across the blood-brain barrier. *European journal of medicinal chemistry* **2004**, *39* (3), 235-40.
13. (a) Renkin, E. M., Transport of potassium-42 from blood to tissue in isolated mammalian skeletal muscles. *The American journal of physiology* **1959**, *197*, 1205-10; (b) Crone, C., The Permeability of Capillaries in Various Organs as Determined by Use of the 'Indicator Diffusion' Method. *Acta physiologica Scandinavica* **1963**, *58*, 292-305.
14. Chabaud, L.; Clayden, J.; Helliwell, M.; Page, A.; Raftery, J.; Vallverdu, L., Conformational studies of tertiary oligo-m-benzanilides and oligo-p-benzanilides in solution. *Tetrahedron* **2010**, *66* (34), 6936-6957.
15. Baures, P. W.; Kaliyan, K.; Desper, J., N alpha-urocanylhistamine: A natural histamine derivative. *Molecules* **2002**, *7* (11), 813-816.
16. Hooker, J. M.; Kim, S. W.; Alexoff, D.; Xu, Y.; Shea, C.; Reid, A.; Volkow, N.; Fowler, J. S., Histone deacetylase inhibitor, MS-275, exhibits poor brain penetration: PK studies of [C]MS-275 using Positron Emission Tomography. *ACS chemical neuroscience* **2010**, *1* (1), 65-73.
17. Windhorst, A. D.; Timmerman, H.; Klok, R. P.; Custers, F. G.; Menge, W. M.; Leurs, R.; Stark, H.; Schunack, W.; Gielen, E. G.; van Kroonenburgh, M. J.; Herscheid, J. D., Radiosynthesis and biodistribution of 123I-labeled antagonists of the histamine H3 receptor as potential SPECT ligands. *Nucl Med Biol* **1999**, *26* (6), 651-9.
18. Yokoi, F.; Komiyama, T.; Ito, T.; Hayashi, T.; Lio, M.; Hara, T., Application of carbon-11 labelled nicotine in the measurement of human cerebral blood flow and other physiological parameters. *European journal of nuclear medicine* **1993**, *20* (1), 46-52.
19. (a) Tomida, S.; Wagner, H. G.; Klatzo, I.; Nowak, T. S., Jr., Effect of acute electrode placement on regional CBF in the gerbil: a comparison of blood flow measured by hydrogen clearance, [3H]nicotine, and [14C]iodoantipyrine techniques. *Journal of cerebral blood flow and metabolism : official journal of the International Society of Cerebral Blood Flow and Metabolism* **1989**, *9* (1), 79-86; (b) Suzuki, R.; Yamaguchi, T.; Kirino, T.; Orzi, F.; Klatzo, I., The effects of 5-minute ischemia in Mongolian gerbils: I. Blood-brain barrier, cerebral blood flow, and local cerebral glucose utilization changes. *Acta neuropathologica* **1983**, *60* (3-4), 207-16; (c) Ohno, K.; Pettigrew, K. D.; Rapoport, S. I., Local cerebral blood flow in the conscious rat as measured with 14C-antipyrine, 14C-iodoantipyrine and 3H-nicotine. *Stroke; a journal of cerebral circulation* **1979**, *10* (1), 62-7.
20. Vilar, S.; Chakrabarti, M.; Costanzi, S., Prediction of passive blood-brain partitioning: straightforward and effective classification models based on in silico derived physicochemical descriptors. *Journal of molecular graphics & modelling* **2010**, *28* (8), 899-903.
21. Oprisiu, I.; Novotarskyi, S.; Tetko, I. V., Modeling of non-additive mixture properties using the Online CHEmical database and Modeling environment (OCHEM). *Journal of cheminformatics* **2013**, *5* (1), 4.

Supplementary Information for CHAPTER 2.

Part 1. HPLC: analytical HPLC & semi-preparative HPLC

Part 2. $^1\text{H}/^{13}\text{C}$ NMR spectroscopy and Mass spectrometry (ESI)

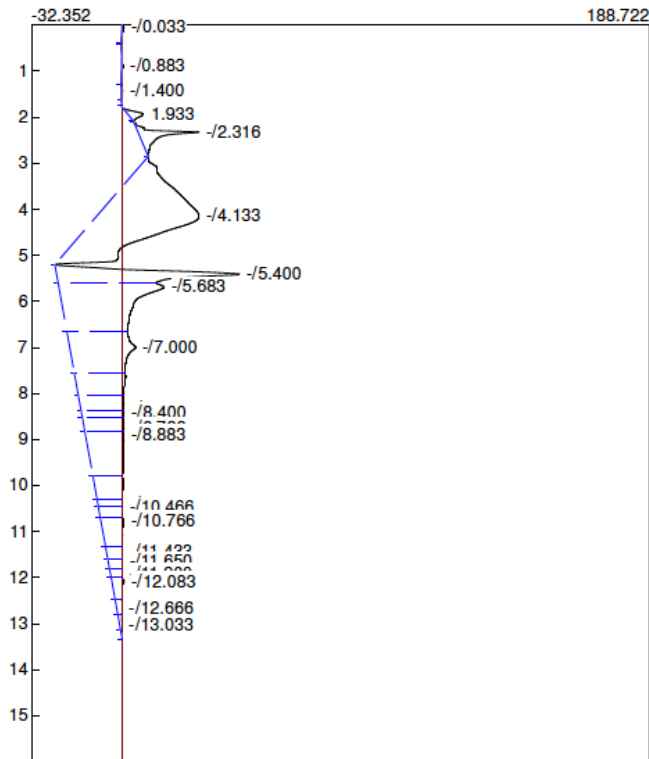
Part 1. HPLC analysis

1.1. [¹¹C]1

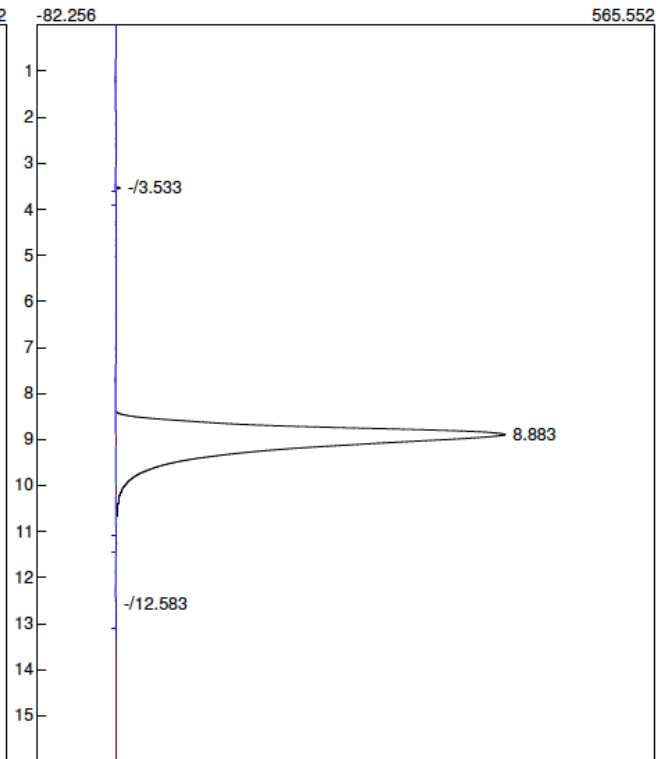
Analytical HPLC of [¹¹C]1

Lab name: SRI Instruments
 Collected: 11/07/2011
 Data file: H11-2_baboon_110711_anaU01.CHR (c:\documents and settings\hp
 Operator: So Jeong Lee
 Comments: FDG-P 100uL
 60 min 2 --> 21%

Lab name: SRI Instruments
 Collected: 11/07/2011
 Data file: H11-2_baboon_110711_anaR01.CHR (c:\documents and settings\hp
 Operator: So Jeong Lee
 Comments: FDG-P 100uL
 60 min 2 --> 21%



Number	Retention	Area	Type	Area %	External	Units
0	1.933	831.6510		8.3055	0.0000	
0	0.000	0.0000		0.0000	0.0000	
0	0.000	0.0000		0.0000	0.0000	
1		831.6510		100.0000	0.0000	

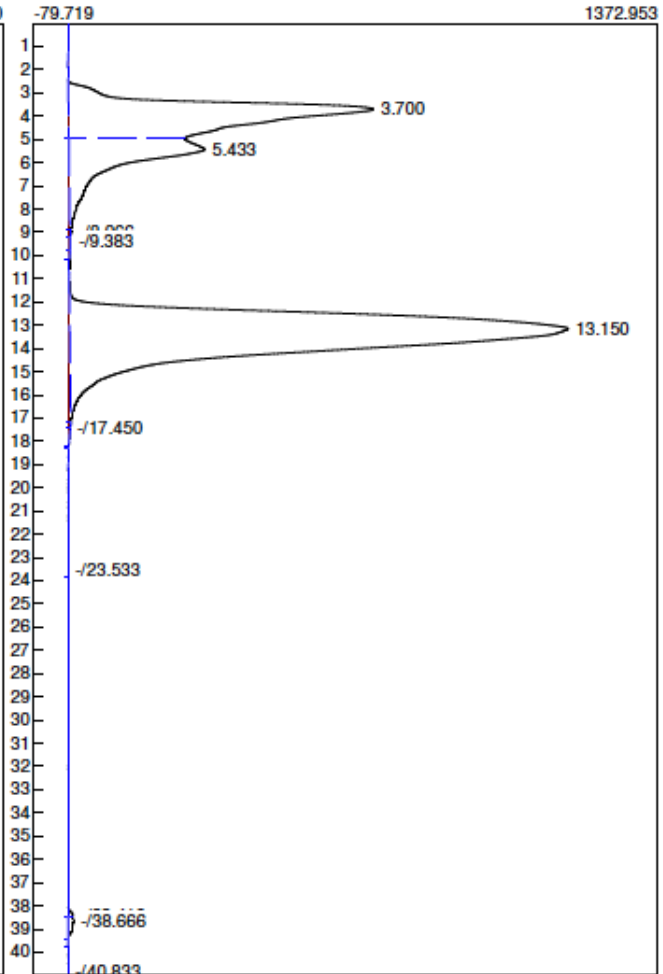
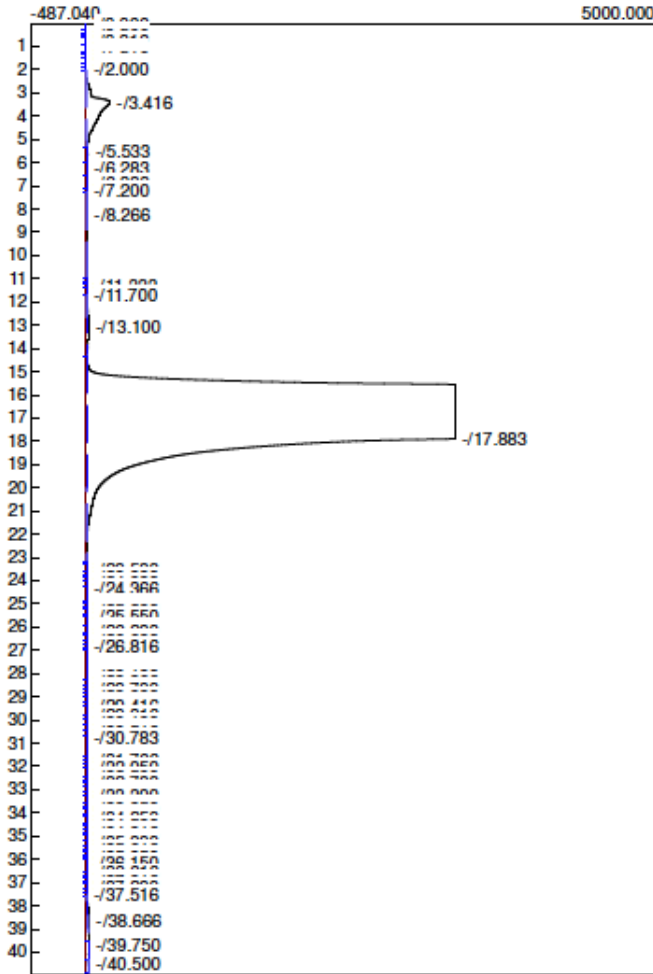


Number	Retention	Area	Type	Area %	External	Units
1	8.883	13305.1355		99.8280	0.0000	
1		13305.1355		100.0000	0.0000	

Semi-preparative HPLC

Lab name: SRI Instruments
 Collected: 11/07/2011
 Data file: H11-2_baboon_110711_U01.CHR (c:\documents and settings\hplc11
 Operator: So Jeong Lee
 Comments:

Lab name: SRI Instruments
 Collected: 11/07/2011
 Data file: H11-2_baboon_110711_R01.CHR (c:\documents and settings\hplc11
 Operator: So Jeong Lee
 Comments:



Number	Retention	Area	Type	Area %	External	Units
0		0.0000		100.0000	0.0000	

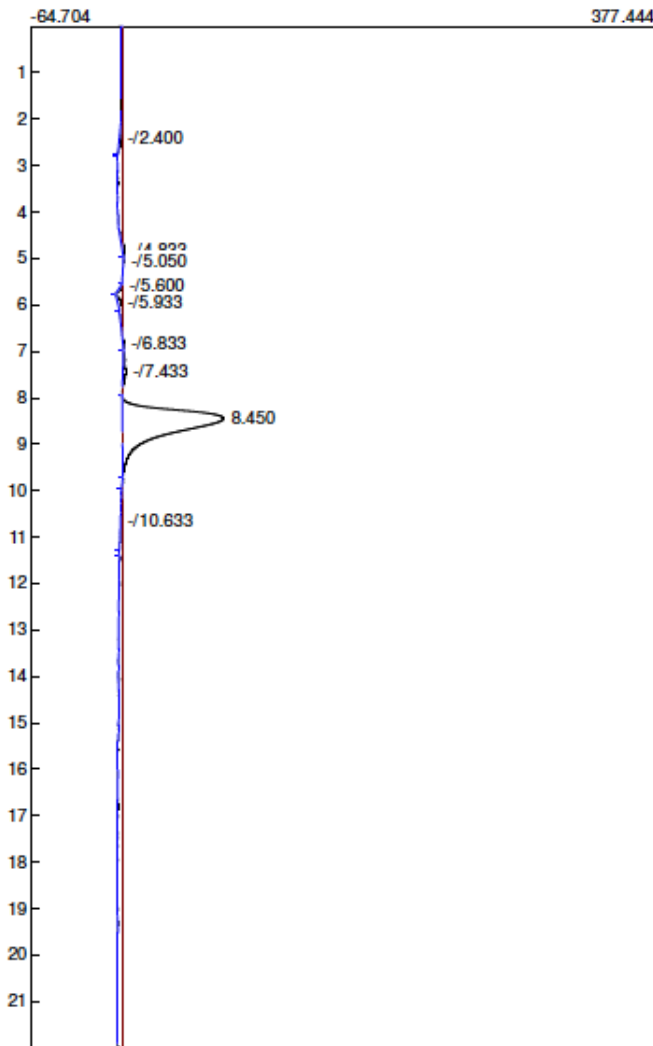
Number	Retention	Area	Type	Area %	External	Units
2	3.700	49597.1620		25.4077	0.0000	
3	5.433	23085.7875		11.8264	0.0000	
1	13.150	121713.4155		62.3515	0.0000	
3		194396.3650		100.0000	0.0000	

1.2. [¹¹C]2

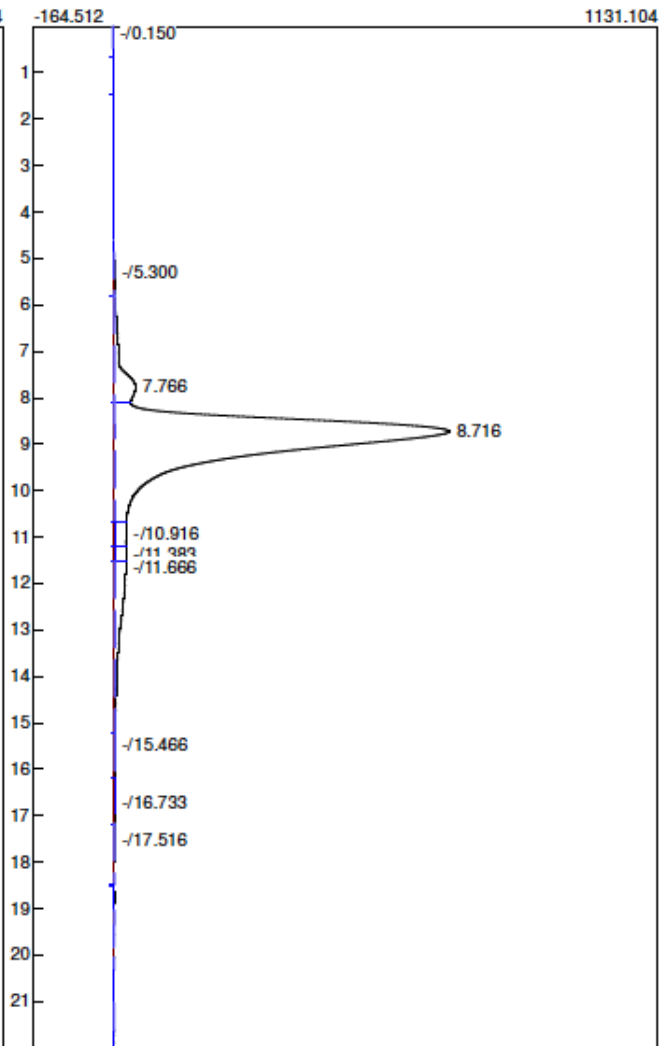
Analytical HPLC

Lab name: SRI Instruments
 Collected: 01/18/2012
 Data file: 012312_baboon_H11_3_ana_U01.CHR (c:\documents and settings\l
 Operator: So Jeong Lee
 Comments:

Lab name: SRI Instruments
 Collected: 01/18/2012
 Data file: 012312_baboon_H11_3_ana_R01.CHR (c:\documents and settings\l
 Operator: So Jeong Lee
 Comments:



Number	Retention	Area	Type	Area %	External	Units
0	0.000	0.0000		0.0000	0.0000	
1	8.450	2400.5820		91.7415	0.0000	
0	0.000	0.0000		0.0000	0.0000	
0	0.000	0.0000		0.0000	0.0000	
1		2400.5820		100.0000	0.0000	

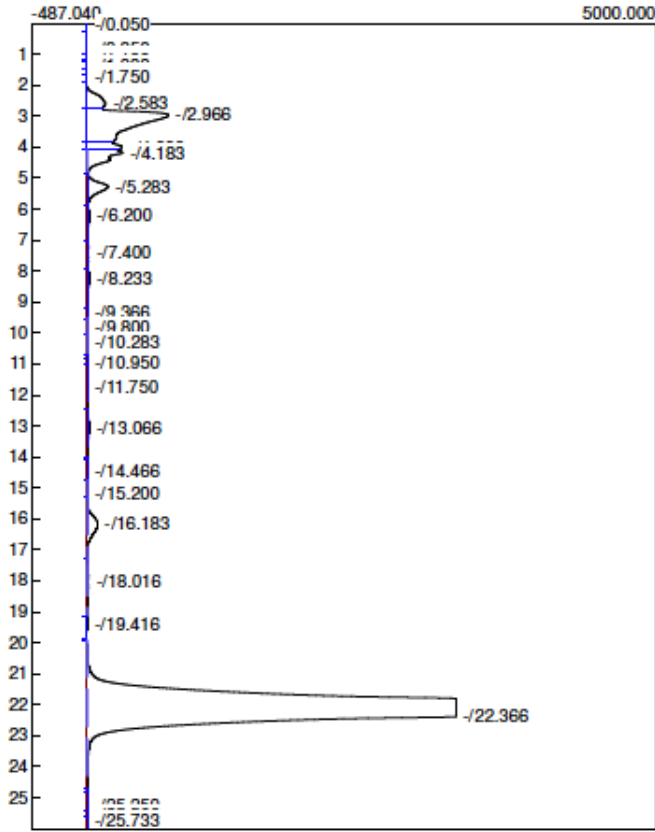


Number	Retention	Area	Type	Area %	External	Units
2	7.766	2003.6170		4.9702	0.0000	
1	8.716	34793.0785		86.3077	0.0000	
2		36796.6955		100.0000	0.0000	

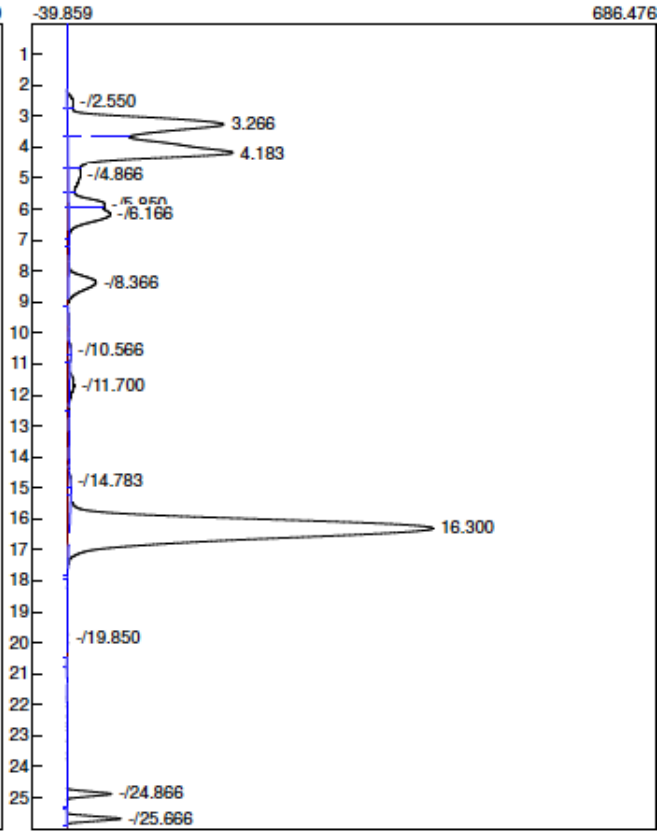
Semi-preparative HPLC

Lab name: SRI Instruments
 Collected: 01/18/2012
 Data file: 011812_H11_3_U01.CHR (c:\documents and settings\hplc112\my do
 Operator: So Jeong Lee
 Comments:

Lab name: SRI Instruments
 Collected: 01/18/2012
 Data file: 011812_H11_3_R01.CHR (c:\documents and settings\hplc112\my d
 Operator: So Jeong Lee
 Comments:



Number	Retention	Area	Type	Area %	External	Units
0		0.0000		100.0000	0.0000	



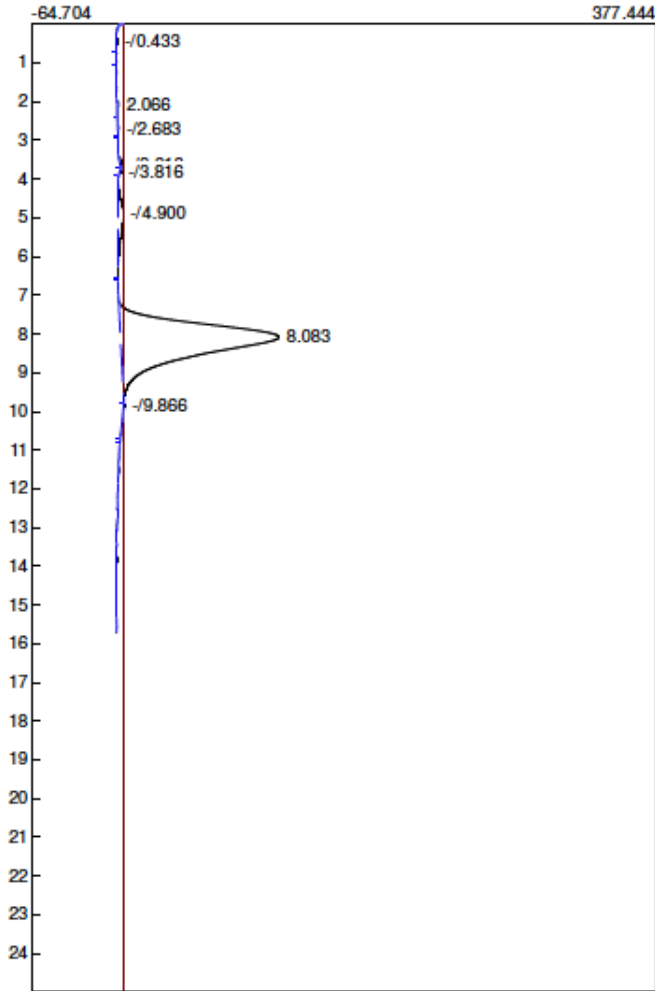
Number	Retention	Area	Type	Area %	External	Units
3	3.266	5540.1025		15.8420	0.0000	
2	4.183	6405.0350		18.3153	0.0000	
1	0.000	0.0000		0.0000	0.0000	
1	16.300	17763.3120		50.7945	0.0000	
3		29708.4495		100.0000	0.0000	

1.3. [¹¹C]3

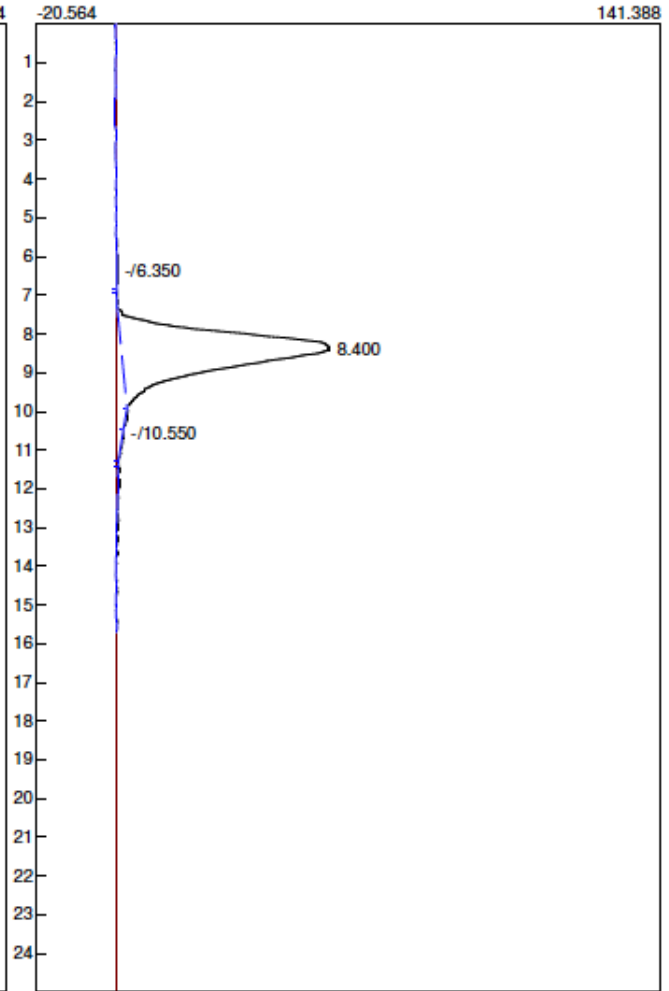
Analytical HPLC

Lab name: SRI Instruments
 Collected: 02/23/2012
 Method: syringe Injection
 Data file: 022312 SJ4 ana_baboon_U01.CHR (c:\documents and settings\hpl
 Operator: So Jeong Lee
 Comments:

Lab name: SRI Instruments
 Collected: 02/23/2012
 Method: syringe Injection
 Data file: 022312 SJ4 ana_baboon_R01.chr (c:\documents and settings\hpl
 Operator: So Jeong Lee
 Comments:



Number	Retention	Area	Type	Area %	External	Units
0	2.066	14.3715		0.2282	0.0000	
1	8.083	5977.5995		94.9013	0.0000	
0	0.000	0.0000		0.0000	0.0000	
0	0.000	0.0000		0.0000	0.0000	
2		5991.9710		100.0000	0.0000	

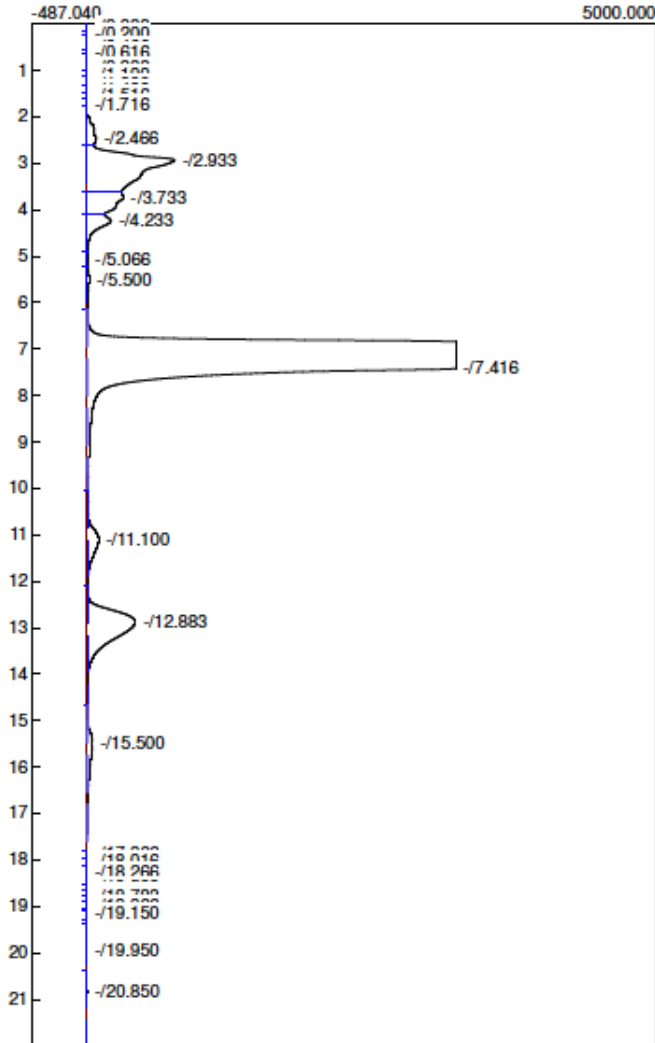


Number	Retention	Area	Type	Area %	External	Units
1	8.400	3272.6670		99.2003	0.0000	
1		3272.6670		100.0000	0.0000	

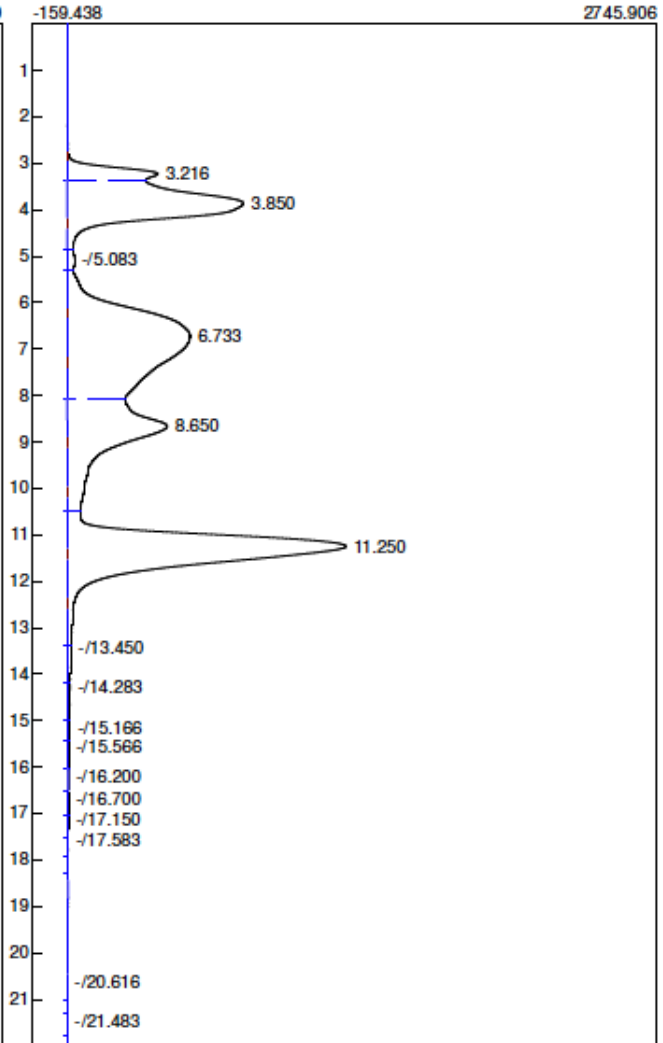
Semi-Preparative HPLC

Lab name: SRI Instruments
 Collected: 02/23/2012
 Method: Loop Injection
 Data file: 02232012_SJ4_Baboon_U01.CHR (c:\documents and settings\hplc1
 Operator: So Jeong Lee
 Comments:

Lab name: SRI Instruments
 Collected: 02/23/2012
 Method: Loop Injection
 Data file: 02232012_SJ4_Baboon_R01.CHR (c:\documents and settings\hplc1
 Operator: So Jeong Lee
 Comments:



Number	Retention	Area	Type	Area %	External	Units
0		0.0000		100.0000		0.0000



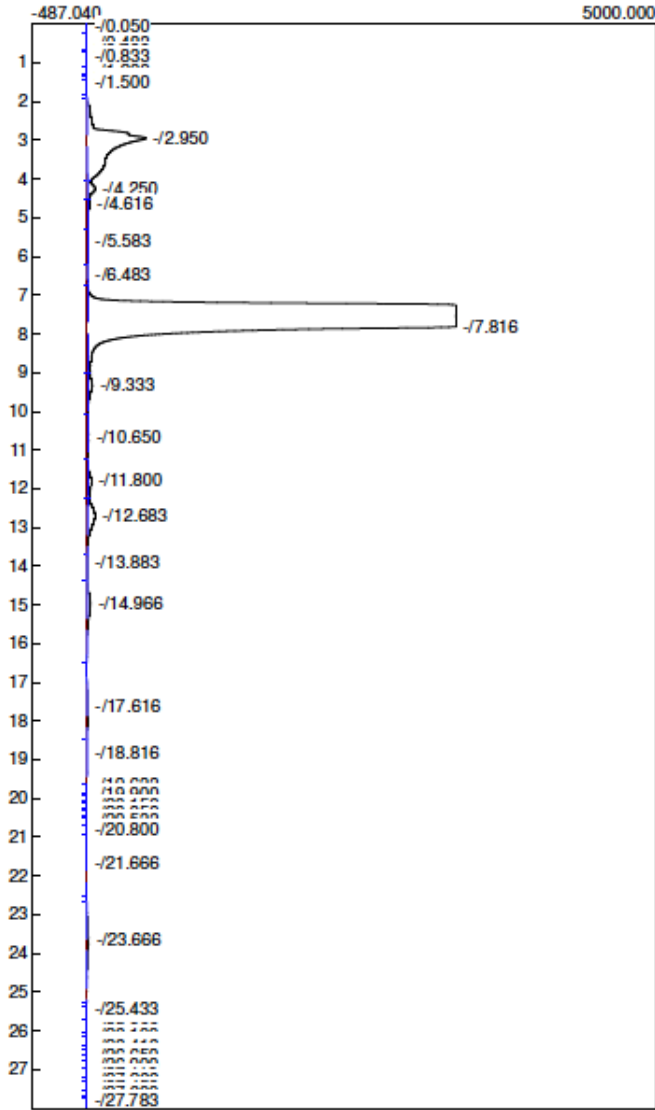
Number	Retention	Area	Type	Area %	External	Units
1	3.216	7276.8860		3.8923		0.0000
2	3.850	35327.8515		18.8966		0.0000
3	6.733	56945.9790		30.4600		0.0000
4	8.650	29410.5850		15.7315		0.0000
5	11.250	55161.2690		29.5053		0.0000
5		184122.5705		100.0000		0.0000

1.4. [¹¹C]4

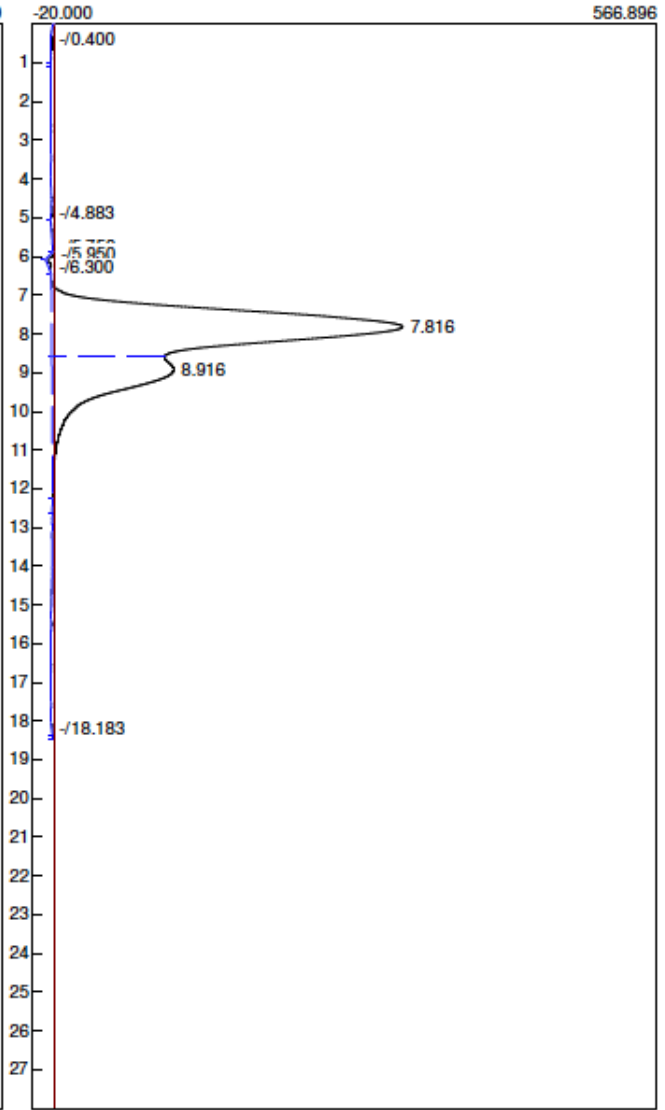
Analytical HPLC

Lab name: SRI Instruments
 Collected: 02/22/2012
 Method: Loop Injection
 Data file: 022212_newH11_5_5050_U01.CHR (c:\documents and settings\hplc
 Operator: So Jeong Lee
 Comments:

Lab name: SRI Instruments
 Collected: 02/22/2012
 Method: Loop Injection
 Data file: 02142012_ana_new H11_5_2_4060_U02.CHR (c:\documents and
 Operator: So Jeong Lee
 Comments:



Number	Retention	Area	Type	Area %	External	Units
0		0.0000		100.0000	0.0000	

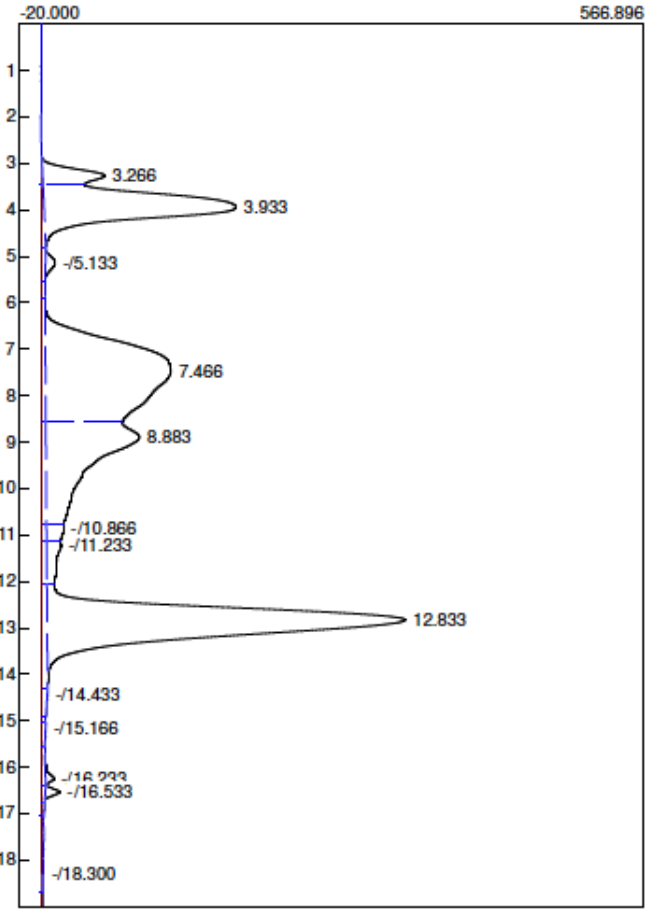
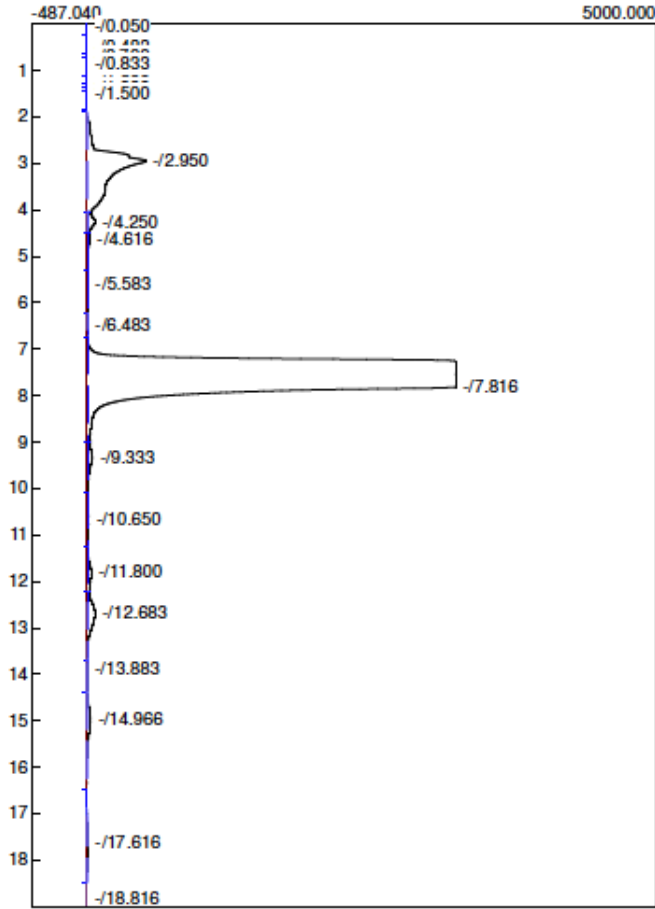


Number	Retention	Area	Type	Area %	External	Units
1	0.000	0.0000		0.0000	0.0000	
2	0.000	0.0000		0.0000	0.0000	
4	7.816	18910.2930		72.4178	0.0000	
4	8.916	7054.9470		27.0172	0.0000	
5	0.000	0.0000		0.0000	0.0000	
2		25965.2400		100.0000	0.0000	

Semi-preparative HPLC

Lab name: SRI Instruments
 Collected: 02/22/2012
 Method: Loop Injection
 Data file: 022212 newH11_5_5050_U01...chr (c:\documents and settings\hplc1
 Operator: So Jeong Lee
 Comments:

Lab name: SRI Instruments
 Collected: 02/22/2012
 Method: Loop Injection
 Data file: 022212 newH11_5_5050_R01.CHR (c:\documents and settings\hplc1
 Operator: So Jeong Lee
 Comments:



Number	Retention	Area	Type	Area %	External	Units
0		0.0000		100.0000	0.0000	

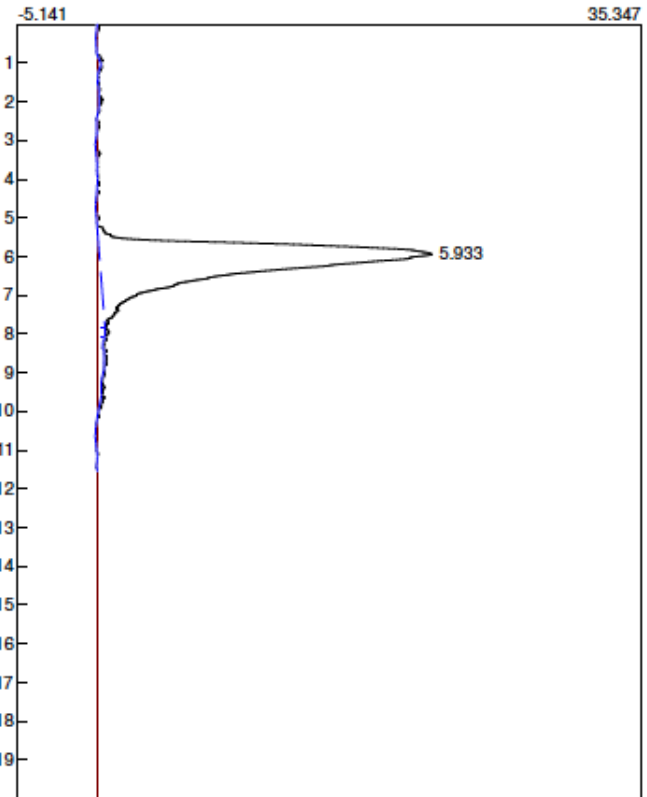
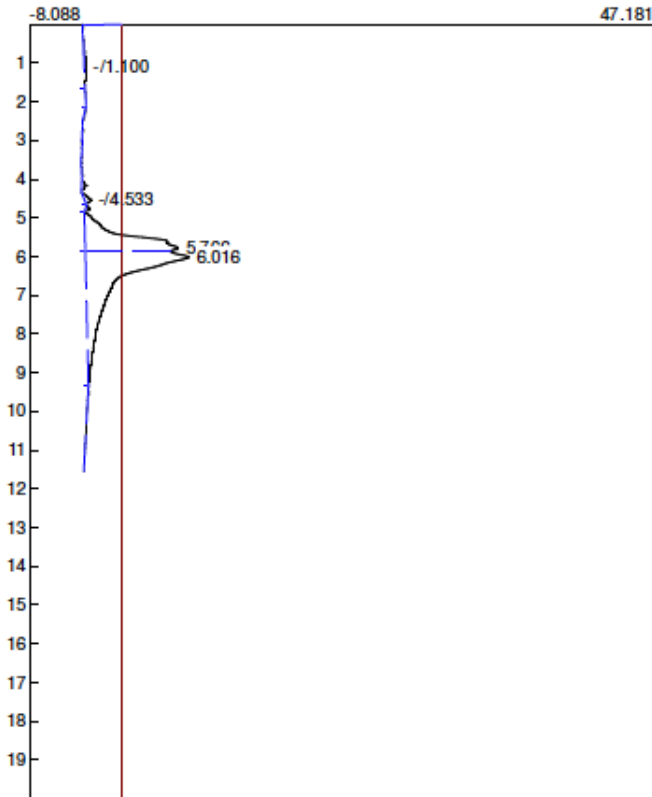
Number	Retention	Area	Type	Area %	External	Units
1	3.266	1099.3020		2.7819	0.0000	
2	3.933	6486.7100		16.4151	0.0000	
4	7.466	11901.1635		28.5984	0.0000	
4	8.883	5974.1805		15.1181	0.0000	
5	12.833	13282.7675		33.6130	0.0000	
5		38144.1235		100.0000	0.0000	

1.5. [¹¹C]5

Analytical HPLC

Lab name: SRI Instruments
 Collected: 03/08/12
 Method: syringe Injection
 Data file: 030912 baboon SJ6_ana_U01.CHR (c:\documents and settings\hpl
 Sample: [11C]5 for baboon
 Operator: So Jeong Lee
 CQC batch:

Lab name: SRI Instruments
 Collected: 03/08/12
 Method: syringe Injection
 Data file: 030912 baboon SJ6_ana_R01.CHR (c:\documents and settings\hpl
 Sample: [11C]5 for baboon
 Operator: So Jeong Lee
 CQC batch:

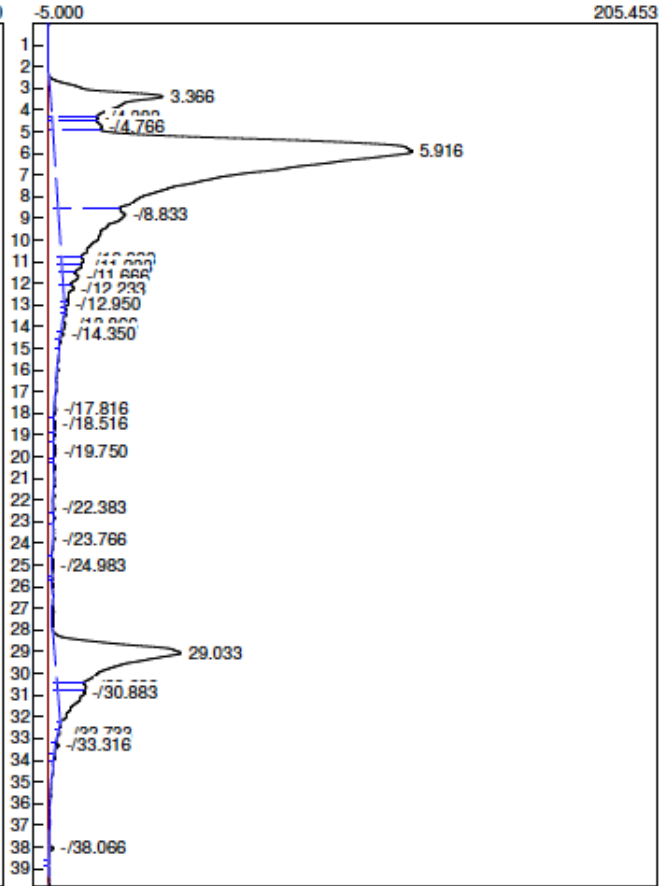
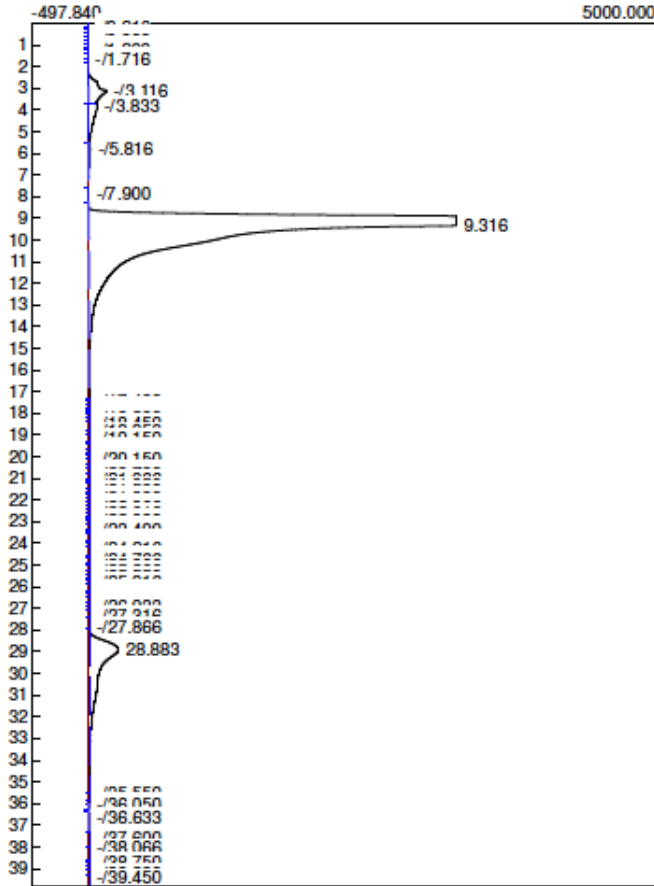


Number	Retention	Area	Type	Area %	External	Units	Sample	Number	Retention	Area	Type	Area %	External	Units	Sample
1	5.766	220.6405		33.2106	0.0000		[11C]5 for baboon	1	5.933	1039.8030		100.0000	0.0000		[11C]5 for baboon
1	6.016	429.1870		64.6008	0.0000		[11C]5 for baboon	1		1039.8030		100.0000	0.0000		
2		649.8275		100.0000	0.0000										

Semi-preparative HPLC

Lab name: SRI Instruments
 Collected: 03/08/12
 Method: Syringe Injection
 Data file: 030812_SJ6_ACNAF_3565_U01.CHR (c:\documents and settings\h
 Sample: [11C]5
 Operator: So Jeong Lee
 Comments:

Lab name: SRI Instruments
 Collected: 03/08/12
 Method: Syringe Injection
 Data file: 030812_SJ6_ACNAF_3565_R01..chr (c:\documents and settings\hp
 Sample: [11C]5
 Operator: So Jeong Lee
 Comments:



Number	Retention	Area	Type	Area %	External	Units	Sample
1	0.000	0.0000		0.0000	0.0000		[11C]5
2	0.000	0.0000		0.0000	0.0000		[11C]5
3	9.316	228663.0420		85.7304	0.0000		[11C]5
7	28.883	25593.9775		9.5957	0.0000		[11C]5
2		254257.0195		100.0000	0.0000		

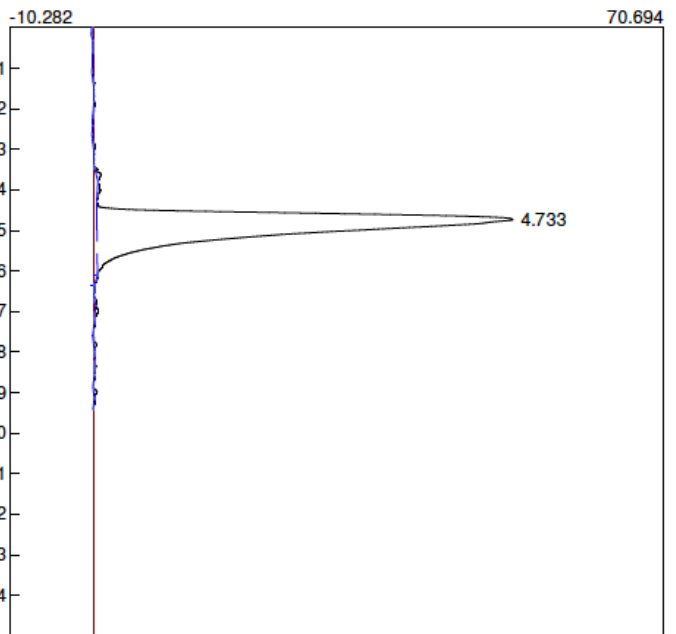
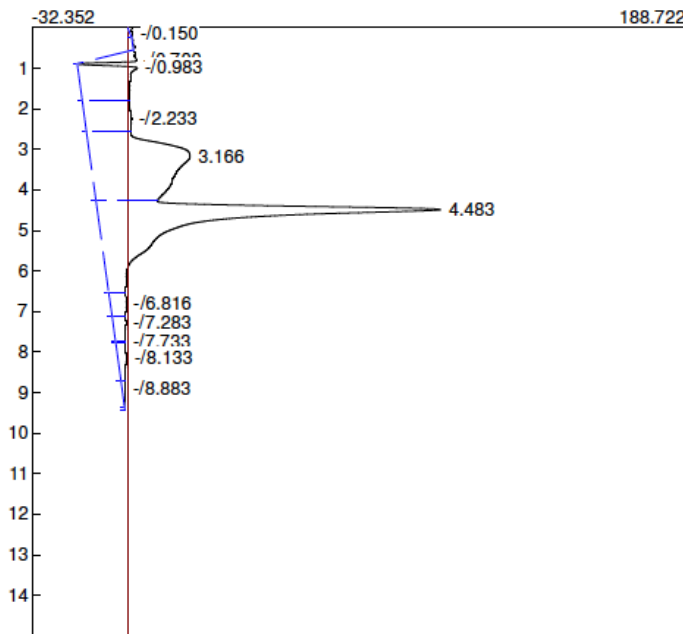
Number	Retention	Area	Type	Area %	External	Units	Sample
1	3.366	2001.0230		8.8058	0.0000		[11C]5
4	5.916	13881.2360		61.0868	0.0000		[11C]5
7	29.033	2918.6050		12.8438	0.0000		[11C]5
3		18800.8640		100.0000	0.0000		

1.6 [¹¹C]6

Analytical HPLC

Lab name: SRI Instruments
 Collected: 04/12/12
 Method: syringe Injection
 Data file: 041212_baboon_SJ7ana_U01.CHR (c:\documents and settings\hplc
 Sample: [¹¹C]6 for baboon
 Operator: So Jeong Lee
 CQC batch:

Lab name: SRI Instruments
 Collected: 04/12/12
 Method: syringe Injection
 Data file: 041212_baboon_SJ7ana_r01.chr (c:\documents and settings\hplc11
 Sample: [¹¹C]6 for baboon
 Operator: So Jeong Lee
 CQC batch:

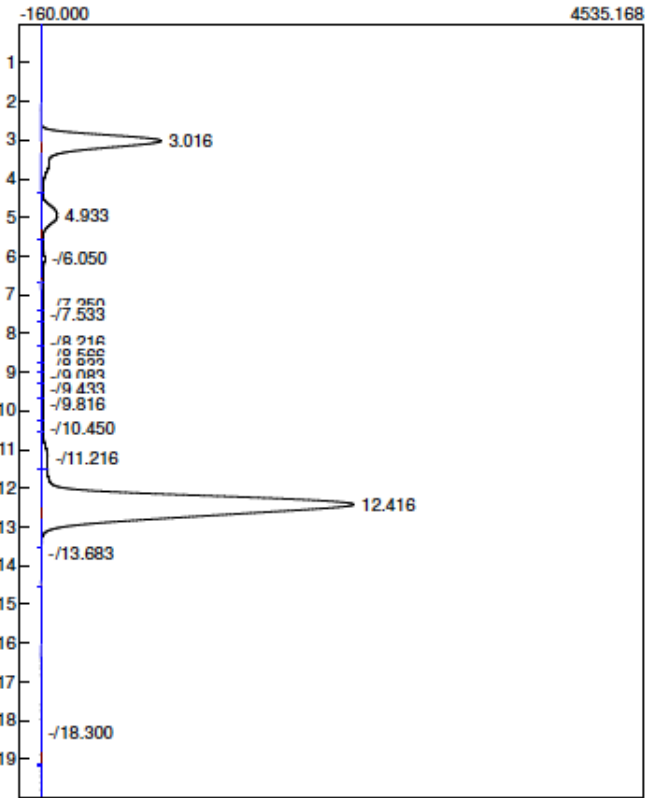
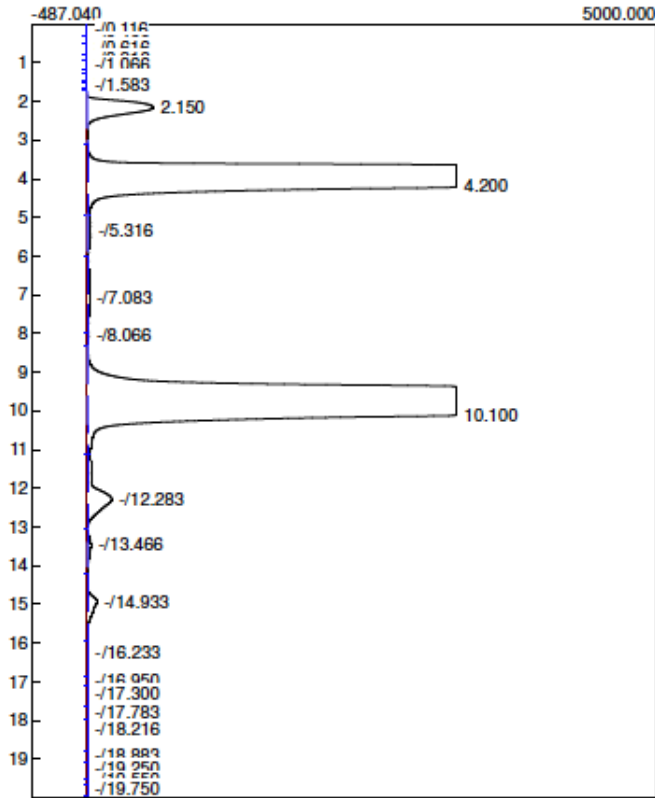


Number	Retention	Area	Type	Area %	External	Units	Sample	Number	Retention	Area	Type	Area %	External	Units	Sample
3	3.166	2718.8405		32.3838	0.0000		[¹¹ C]6 for baboon	1	4.733	1713.3145		100.0000	0.0000		[¹¹ C]6 for baboon
1	4.483	3381.4950		40.2766	0.0000		[¹¹ C]6 for baboon	1		1713.3145		100.0000	0.0000		
2		6100.3355		100.0000	0.0000										

Semi-preparative HPLC

Lab name: SRI Instruments
 Collected: 04/12/12
 Method: Loop Injection
 Data file: 041212_BABOON_SJ7_GRADIENT_U01..chr (c:\documents and se
 Sample: [11C]6 for baboon
 Operator: So Jeong Lee
 CQC batch:

Lab name: SRI Instruments
 Collected: 04/12/12
 Method: Loop Injection
 Data file: 041212_BABOON_SJ7_GRADIENT_R01.CHR (c:\documents and s
 Sample: [11C]6 for baboon
 Operator: So Jeong Lee
 CQC batch:



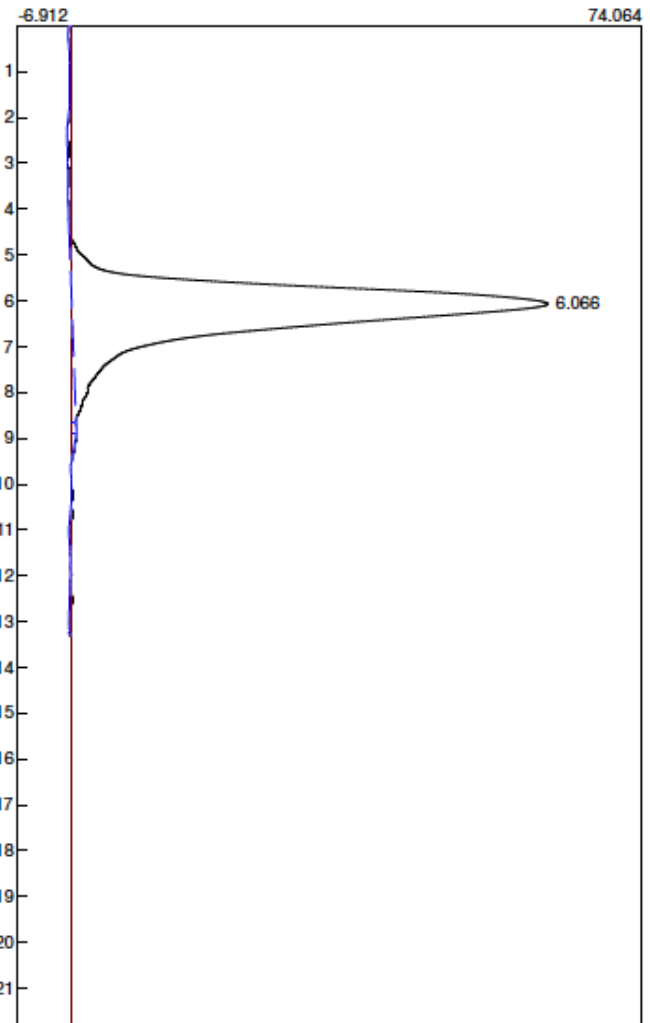
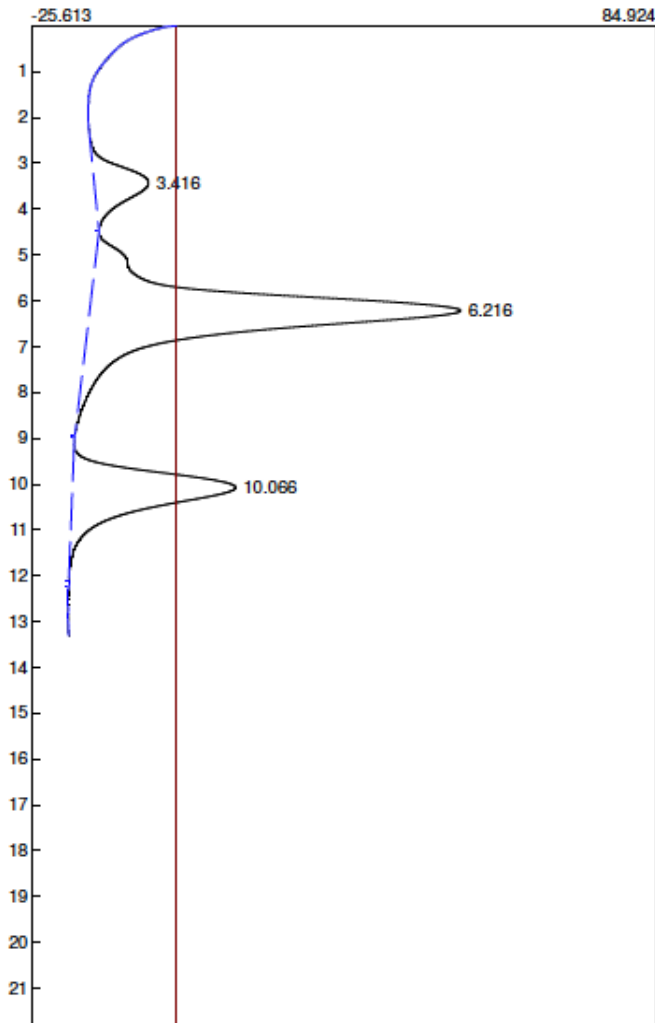
Number	Retention	Area	Type	Area %	External	Units	Sample	Number	Retention	Area	Type	Area %	External	Units	Sample
1	2.150	12838.1255		3.6358	0.0000		[11C]6 for baboon	1	3.016	22222.6280		19.7784	0.0000		[11C]6 for baboon
2	4.200	138714.4230		39.2840	0.0000		[11C]6 for baboon	4	4.933	4253.7680		3.7859	0.0000		[11C]6 for baboon
3	10.100	187108.7830		52.9893	0.0000		[11C]6 for baboon	3	12.416	80300.3380		71.4683	0.0000		[11C]6 for baboon
7	28.816	0.1695		0.0000	0.0000		[11C]6 for baboon	7	0.000	0.0000		0.0000	0.0000		[11C]6 for baboon
7	28.950	0.4100		0.0001	0.0000		[11C]6 for baboon	3	106776.7340			100.0000	0.0000		
5		338661.9110		100.0000	0.0000										

1.7 [¹¹C]7

Analytical HPLC

Lab name: SRI Instruments
 Collected: 07/14/2011
 Method: Syringe Injection
 Data file: 040612_SJ8_ana_U08.CHR (c:\documents and settings\hplc112\my
 Sample: slow gradient 100uL
 Operator: Youwen
 Comments: FDG-P 200uL
 5min 2% ACN
 60 min 2 --> 21% ACN
 QC batch:

Lab name: SRI Instruments
 Collected: 07/14/2011
 Method: Syringe Injection
 Data file: 040612_SJ8_ana_R08.CHR (c:\documents and settings\hplc112\my
 Sample: slow gradient 100uL
 Operator: Youwen
 Comments: FDG-P 200uL
 5min 2% ACN
 60 min 2 --> 21% ACN
 QC batch:

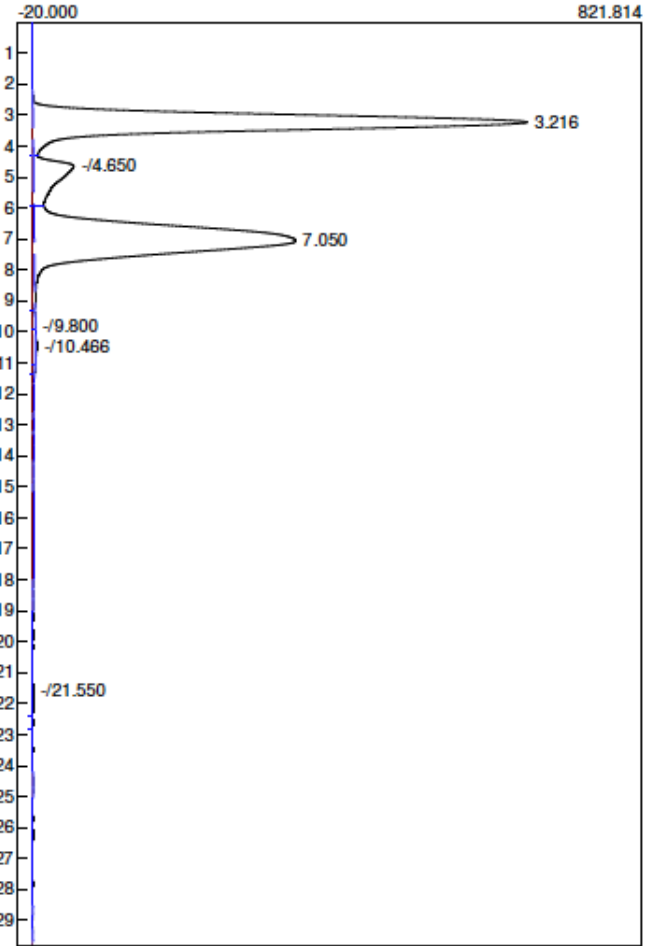
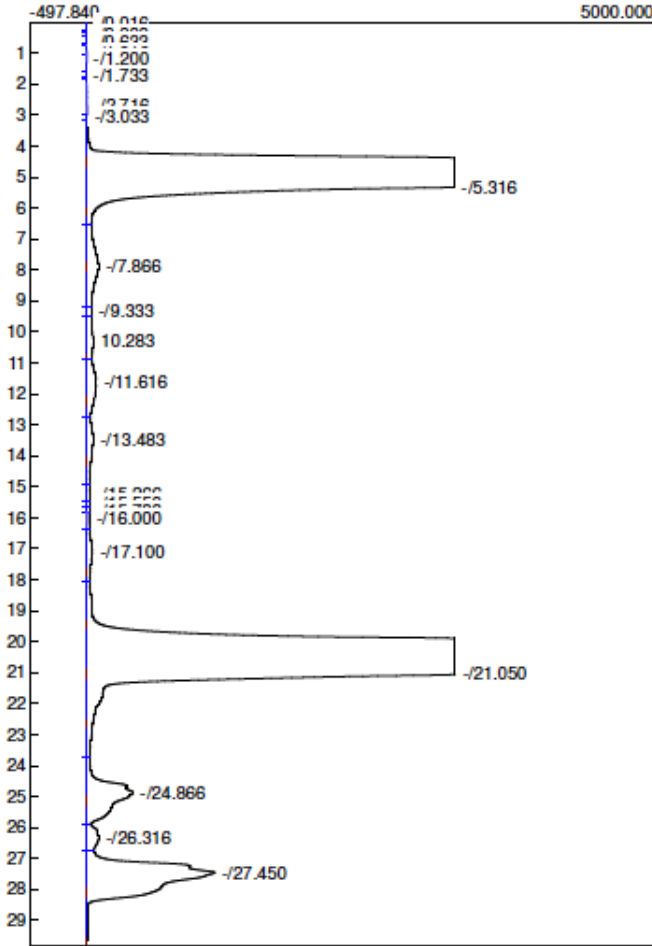


Number	Retention	Area	Type	Area %	External	Units	Sample	Number	Retention	Area	Type	Area %	External	Units	Sample
3	3.416	476.8470		8.3689	0.0000		slow gradient 100uL	1	6.066	3678.7560		100.0000	0.0000		slow gradient 100
1	6.216	3726.7960		65.3918	0.0000		slow gradient 100uL	1	6.066	3678.7560		100.0000	0.0000		slow gradient 100
0	10.066	1495.5375		26.2413	0.0000		slow gradient 100uL								
3		5699.1805		100.0000	0.0000										

Semi-preparative HPLC

Lab name: SRI Instruments
 Collected: 04/05/2012
 Method: Loop Injection
 Data file: 040512_SJB_gradient_U01.CHR (c:\documents and settings\hplc112
 Sample: [11C]7
 Operator: So Jeong Lee
 CQC batch:

Lab name: SRI Instruments
 Collected: 04/05/2012
 Method: Loop Injection
 Data file: 040512_SJB_gradient_R01.CHR (c:\documents and settings\hplc112
 Sample: [11C]7
 Operator: So Jeong Lee
 CQC batch:



Number	Retention	Area	Type	Area %	External	Units	Sample
1	0.000	0.0000	0.0000	0.0000	0.0000		[11C]7
2	0.000	0.0000	0.0000	0.0000	0.0000		[11C]7
3	10.283	3889.3040	0.6014	0.0000	0.0000		[11C]7
7	0.000	0.0000	0.0000	0.0000	0.0000		[11C]7
1		3889.3040	100.0000	0.0000			

Number	Retention	Area	Type	Area %	External	Units	Sample
1	3.216	21947.2525	48.0765	0.0000	0.0000		[11C]7
4	7.050	20690.4575	45.3234	0.0000	0.0000		[11C]7
7	0.000	0.0000	0.0000	0.0000	0.0000		[11C]7
2		42637.7100	100.0000	0.0000			

Part 2. $^1\text{H}/^{13}\text{C}$ NMR spectroscopy and Mass spectrometry (ESI)

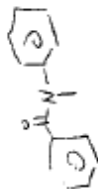
1.1. ^1H NMR

1.2. ^{13}C NMR

1.3. Mass spectrometry



sj1-2 comp/

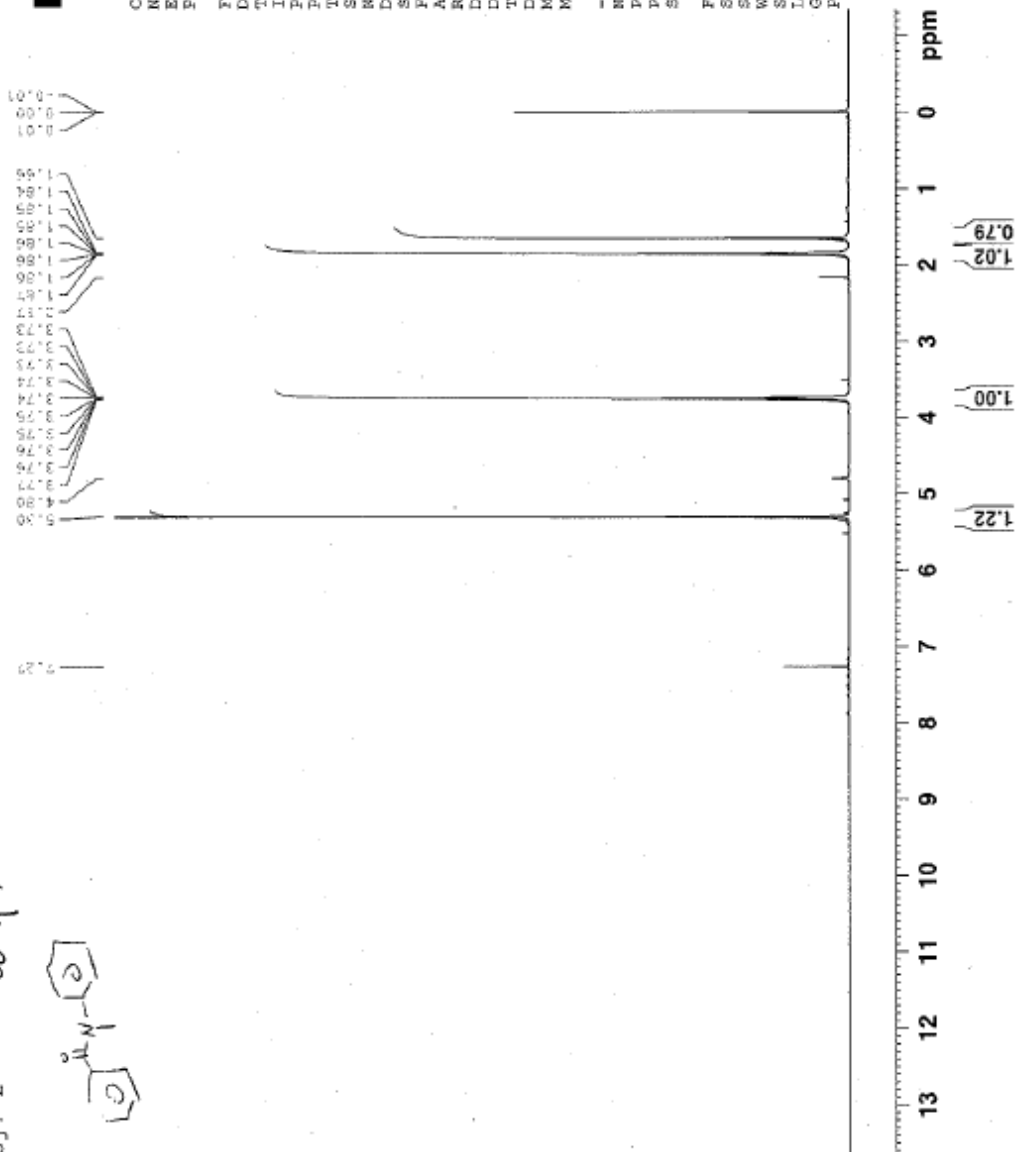


Current Data Parameters
NAME sj1-2
EXPNO 1
PROCNO 1

F2 - Acquisition Parameters
Date_ 20110616
Time 12.00
INSTRUM spect
PROBHD 5 mm QNP 1H/13
PULPROG zgpg30
TD 32768
SOLVENT CDCl3
RS 16
DS 2
SWH 6009.615 Hz
FIDRES 0.187800 Hz
AQ 2.5625333 sec
RG 406.4
ICW 83.200 usec
DE 6.00 usec
TE 294.2 K
D1 1.00000000 sec
MCRET 0.00000000 sec
MCRRK 0.01500000 sec

----- CHANNEL f1 -----
NUC1 1H
P1 10.90 usec
PL1 -1.00 dB
SFO1 400.1324710 MHz

F2 - Processing parameters
SI 32768
SF 400.1300064 MHz
WDW EM
SSB 0
LB 0.30 Hz
GB 0
PC 1.00





Current Data Parameters
NAME S7-1-6-final-06
EXPNO 1
PROCNO 1

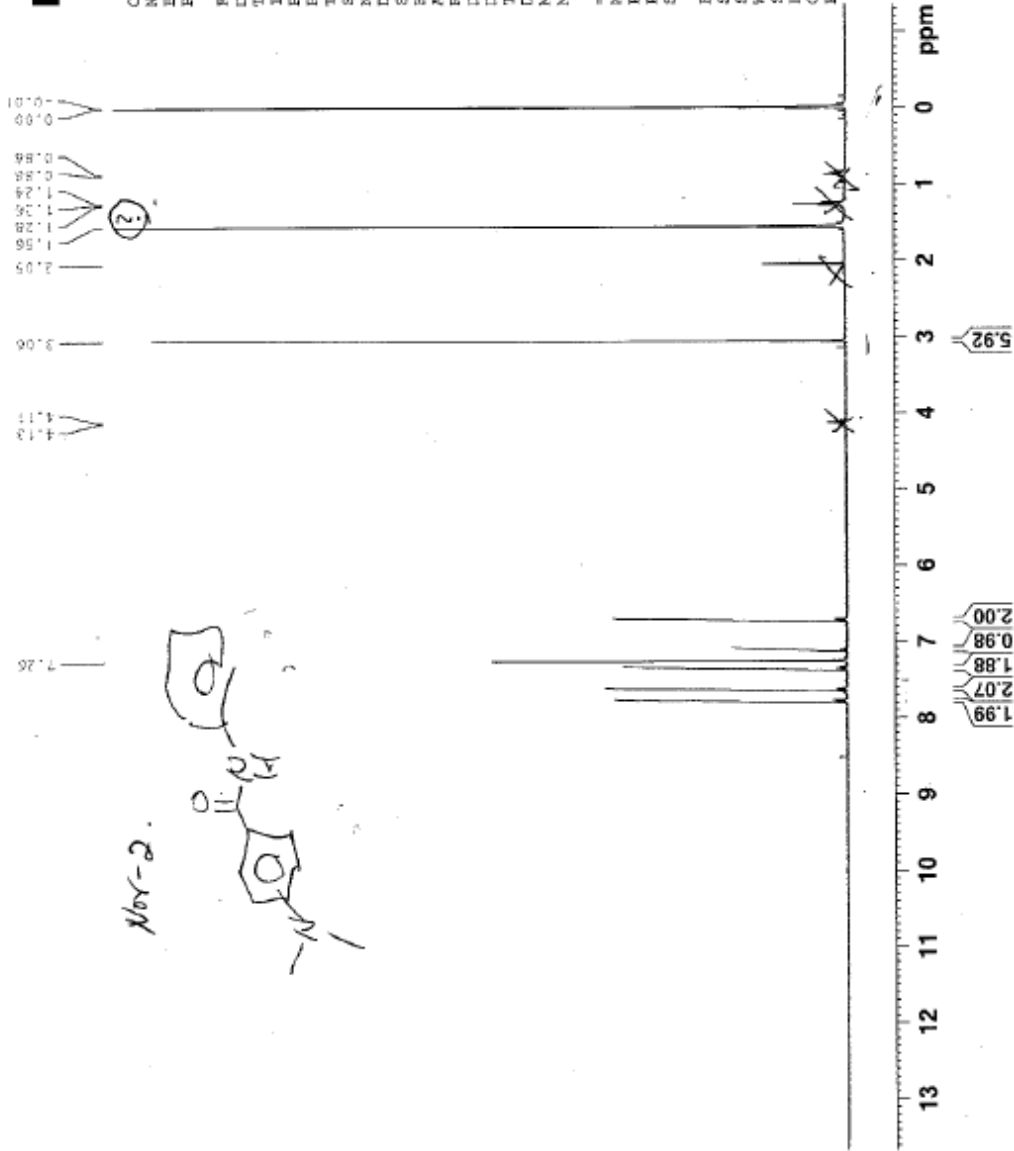
Nov-2

F2 - Acquisition Parameters

Date_ 20110629
Time 16:40
INSTRUM spect
PROBHD 5 mm QNP 1H/13
PULPROG zg30
TD 32000
SOLVENT CDCl3
NS 16
DS 2
SWH 6009.615 Hz
FIDRES 0.187800 Hz
AQ 2.6625333 sec
RG 912.3
DM 83.200 usec
DE 6.00 usec
TE 295.2 K
D1 1.0000000 sec
MCREST 0.0000000 sec
MCMRK 0.0150000 sec

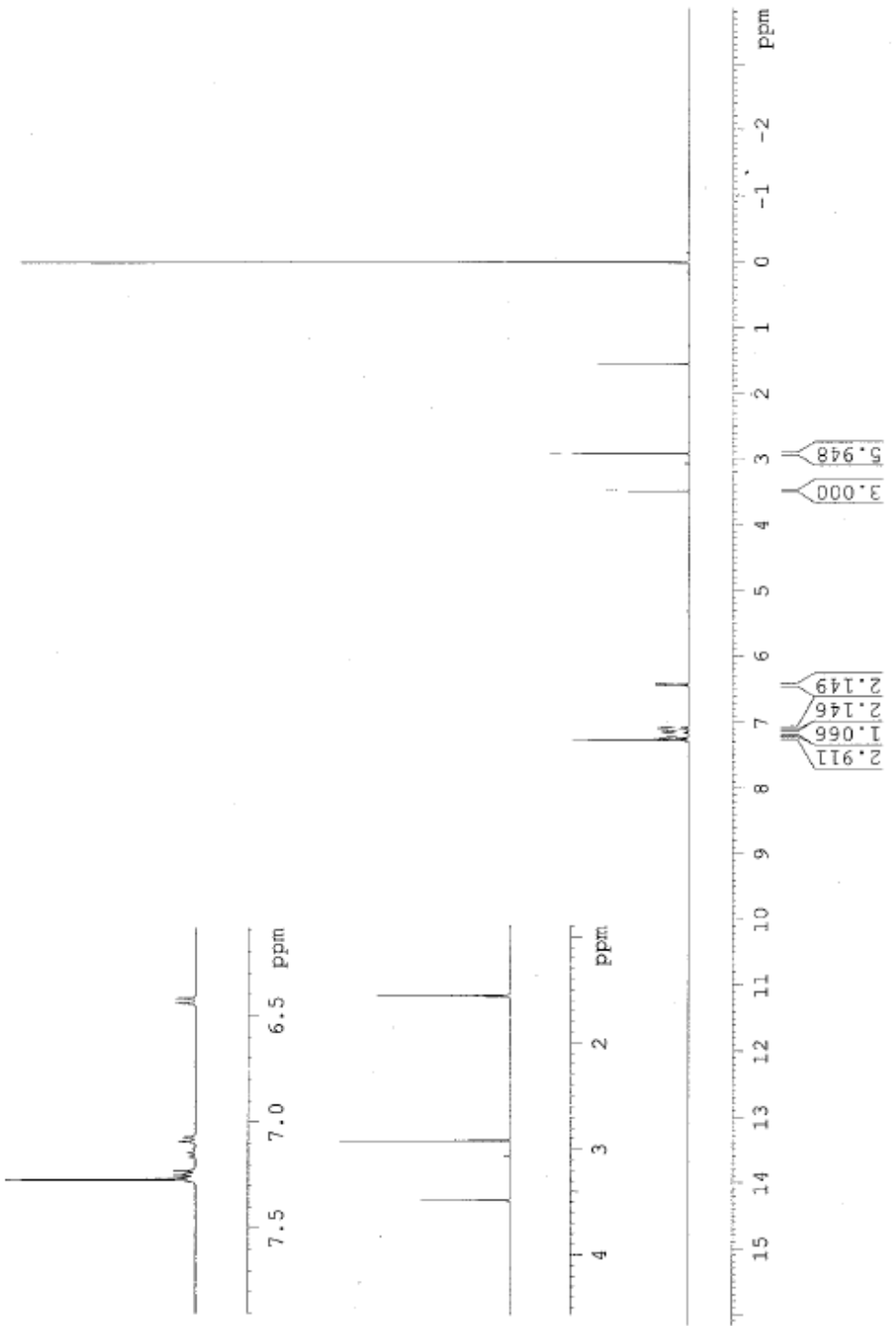
==== CHANNEL f1 =====
NUC1 1H
P1 10.90 usec
PC1 -1.00 dB
SFO1 400.1324710 MHz

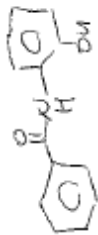
F2 - Processing Parameters
SI 32768
SF 400.1300086 MHz
WDW EM
SSB 0
LB 0.30 Hz
GB 0
PC 1.00



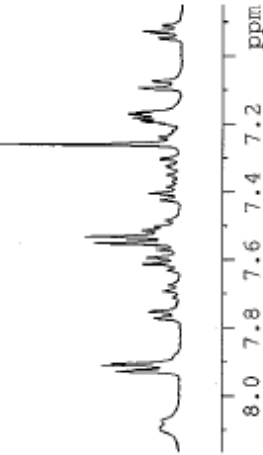


7.279
7.261
7.249
7.241
7.232
7.226
7.219
7.163
7.160
7.149
7.145
7.140
-7.126
7.093
7.090
7.085
7.072
6.448
6.441
6.435
6.423
6.418
6.411
3.484
2.920





S14 pre
Nov-3



Current Data Parameters
 NAME pre_S14
 EXPNO 1
 PROCNO 1

F2 - Acquisition Parameters
 Date_ 20120228
 Time 11.27
 INSTRUM spect
 PROBD 5 mm QNP 1H/13
 PULPROG zg30
 TD 32000
 SOLVENT CDCl3
 NS 16
 DS 2
 SWH 6009.615 Hz
 FIDRES 0.187800 Hz
 AC 2.662533 sec
 RG 912.3
 EN 83.200 usec
 DE 6.00 usec
 TE 294.2 K
 D1 1.0000000 sec
 MCREST 0.0000000 sec
 MCKRK 0.0150000 sec

===== CHANNEL f1 =====
 NUC1 13
 P1 10.90 usec
 PL1 -1.80 dB
 SFO1 400.1324710 MHz

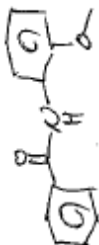
F2 - Processing parameters
 SI 32768
 SP 400.1300081 MHz
 MDW EM
 SSB 0
 LB 0.30 Hz
 GB 0
 PC 1.00

1.37
2.00
3.20
0.92
0.92
1.11
Nov

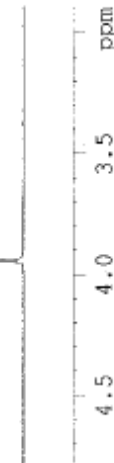
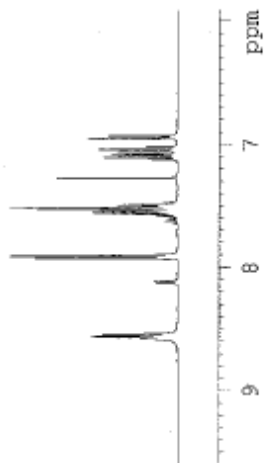
~~2.00~~

compd 3

SS-1-49



8.560
8.556
8.541
8.537
7.922
7.909
7.904
7.900
7.584
7.580
7.573
7.565
7.559
7.551
7.548
7.544
7.529
7.529
7.515
7.510
7.498
7.493
7.489
7.466
7.270
7.123
7.119
7.104
7.099
7.084
7.080
7.059
7.055
7.039
7.036
7.020
7.017
6.951
6.947
6.931
6.927
3.943



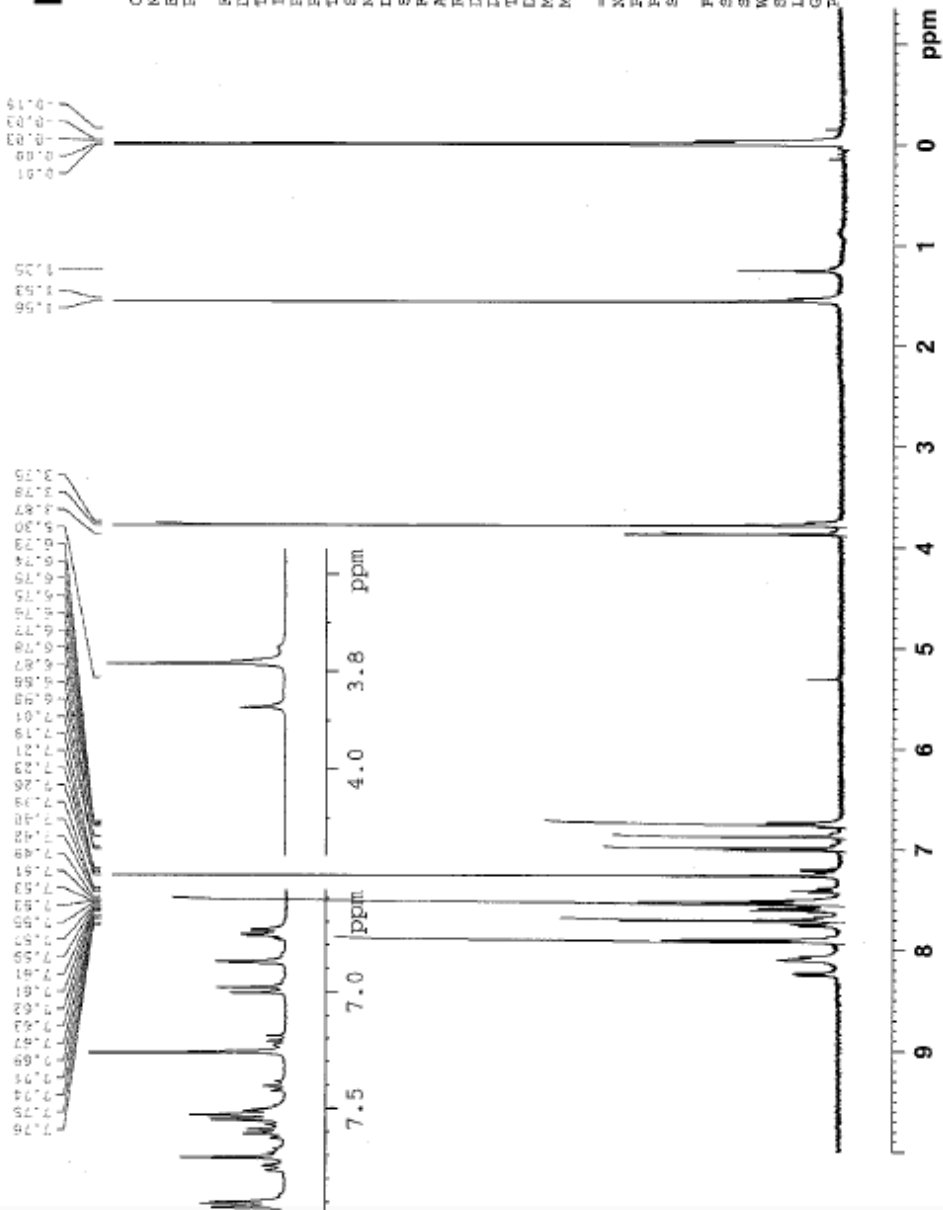
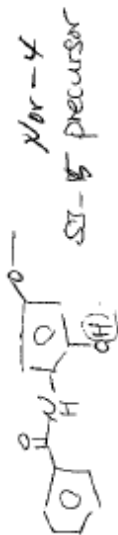


Current Data Parameters
NAME pre_SJ_5
EXNO 1
PROCNO 1

F2 - Acquisition Parameters
Date_ 20120228
Time 11.11
INSTRUM spect
PROBHD 5 mm QNP 1H/13
PULPROG zg30
TD 32000
SOLVENT CDCl3
NS 16
DS 2
SWH 6009.615 Hz
FIDRES 0.187800 Hz
AQ 2.6625333 sec
RG 1149.4
DM 83.200 usec
DE 6.00 usec
TE 294.2 K
D1 1.00000000 sec
MCREST 0.00000000 sec
MCWRR 0.01500000 sec

===== CHANNEL F1 =====
NUC1 1H
P1 10.90 usec
PL1 -1.00 dB
SFO1 400.1324710 MHz

F2 - Processing parameters
SI 32768
SF 400.1300000 MHz
WDW EM
SSB 0
LB 0.30 Hz
GB 0
PC 1.00



2.86
0.77
1.24
0.97
1.00
2.77
2.10

100%
100%

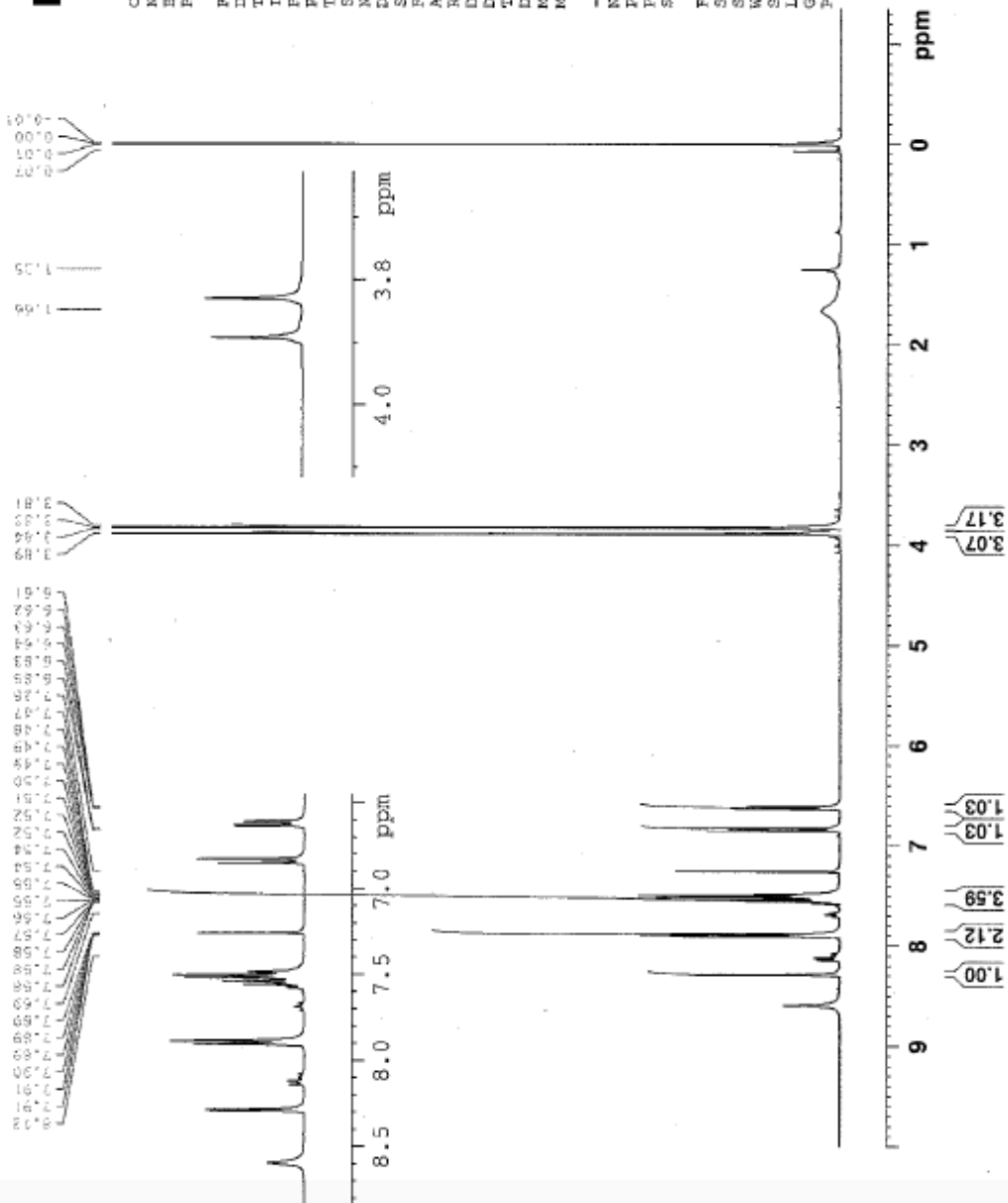


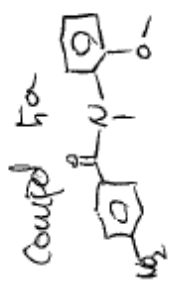
Current Data Parameters
 NAME 021012_SJ1_62
 EXPNO 1
 PROCNO 1

F2 - Acquisition Parameters
 Date_ 20120210
 Time 16.30
 INSTRUM spect
 PROBRD 5 mm QNP 1H/13
 PULPROG zg30
 TD 32000
 SOLVENT CDCl3
 NS 16
 DS 2
 SHF 6005.615 Hz
 FIDRES 0.187800 Hz
 AQ 2.6625333 sec
 RG 456.1
 DW 83.200 usec
 DE 6.00 usec
 TE 295.2 K
 D1 1.00000000 sec
 MCREST 0.00000000 sec
 MCKEK 0.01500000 sec

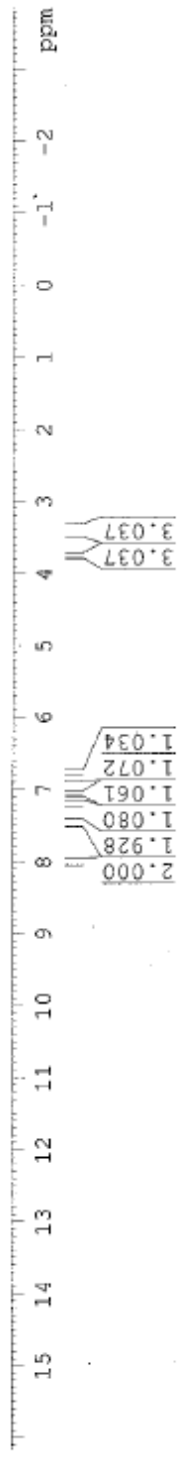
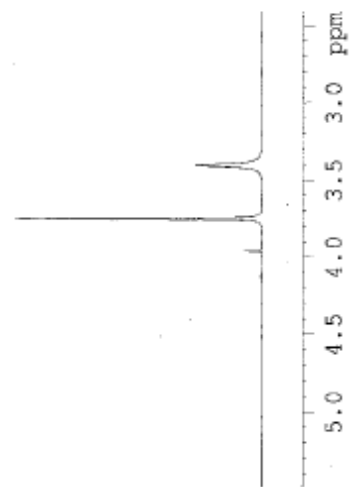
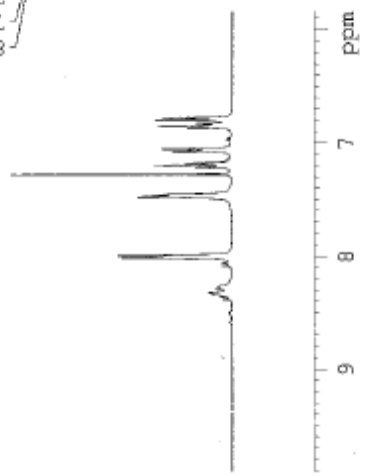
***** CHANNEL f1 *****
 NUC1 1H
 P1 10.90 usec
 PL1 -1.00 dB
 SFO1 400.1324710 MHz

F2 - Processing parameters
 SI 32768
 SF 400.1300087 MHz
 WDW EM
 SSB 0
 LB 0.30 Hz
 GB 0
 PC 1.00





- 8.008
- 7.988
- 7.473
- 7.452
- 7.270
- 7.210
- 7.191
- 7.171
- 7.068
- 7.050
- 6.861
- 6.842
- 6.823
- 6.794
- 6.773
- 3.748
- 3.403



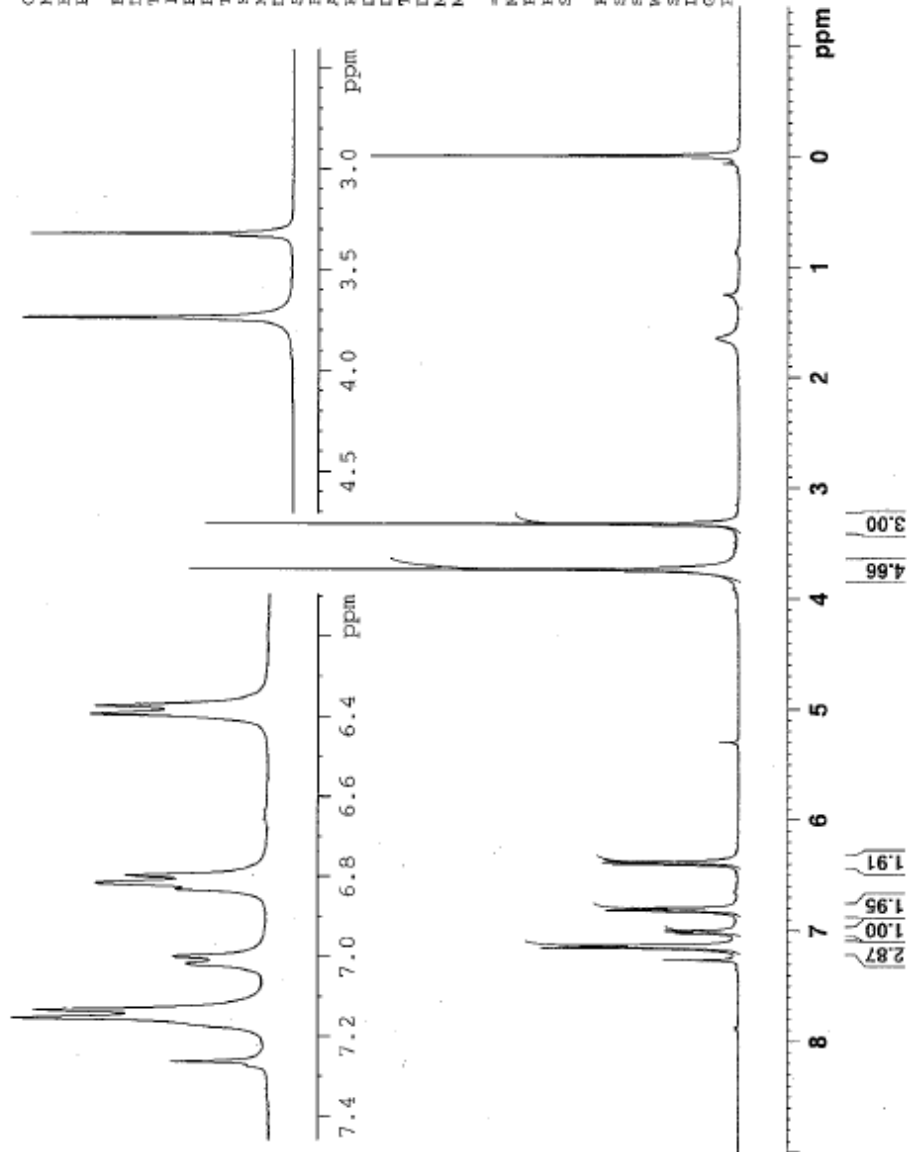


Comp 5.

7.26
7.27
7.28
7.29
7.30
7.31
7.32
7.33
7.34
7.35
7.36
7.37
7.38
7.39
7.40
7.41
7.42

5.30

4.66
3.00



Current Data Parameters
 NAME std_SJ_6
 EXPNO 1
 PROCNO 1

F2 - Acquisition Parameters
 Date_ 20120229
 Time 14.36
 INSTRUM spect
 PROSHD 5 mm QNP 1H/13
 PULPROG zg30
 TD 32000
 SOLVENT CDCl3
 NS 16
 DS 2
 SMR 6009.615 Hz
 FIDRES 0.187800 Hz
 AQ 2.6625333 sec
 RG 362
 DM 83.200 usec
 DE 5.00 usec
 TE 298.2 K
 D1 1.00000000 sec
 MCKRST 0.00000000 sec
 MCKRCK 0.01500000 sec

===== CHANNEL f1 =====
 NUC1 1H
 P1 10.90 usec
 PL1 -1.00 dB
 SFO1 400.1324710 MHz

F2 - Processing parameters
 SI 32768
 SF 400.1300079 MHz
 WDM 0
 SSB 0
 LB 0.30 Hz
 GB 0
 PC 1.00



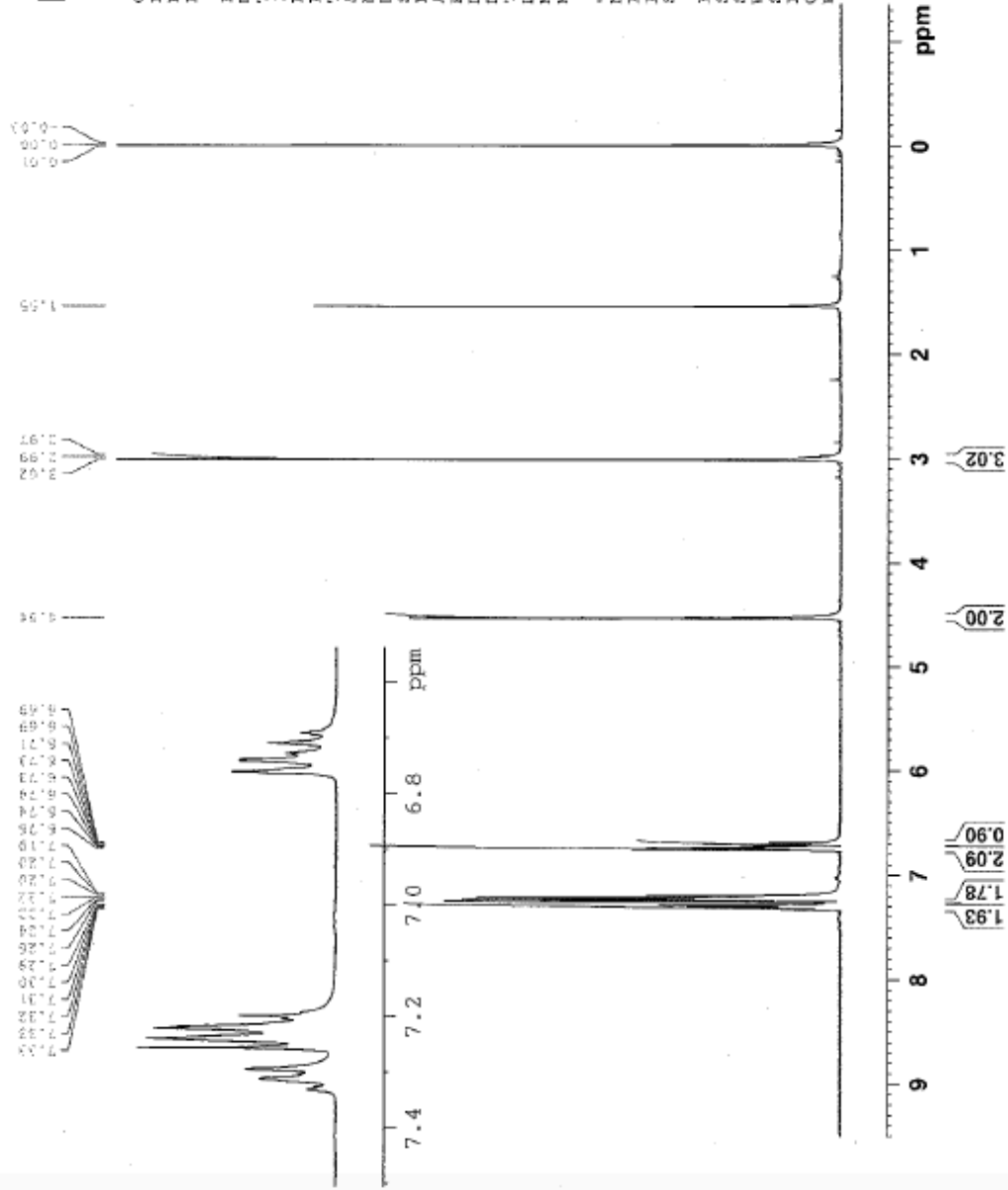
Current Data Parameters
NAME SJ7_std
EXPNO 1
PROCNO 1

F2 - Acquisition Parameters
Date_ 20120402
Time 20.03
INSTRUM spect
PROBHD 5 mm QNP 1H/13
PULPROG zg30
TD 32000
SOLVENT CDCl3
NS 16
DS 2
SWH 6009.615 Hz
FIDRES 0.167800 Hz
AQ 2.6625333 sec
RG 645.1
CW 83.200 usec
DE 6.00 usec
TE 293.2 K
D1 1.00000000 sec
MCREST 0.00000000 sec
MCNPK 0.01500000 sec

***** CHANNEL f1 *****
NUC1 1H
P1 10.90 usec
PL1 -1.00 dB
SFO1 400.1324710 MHz

F2 - Processing parameters
SI 32768
SF 400.1300107 MHz
WDW EM
SSB 0
LB 0.30 Hz
GB 0
PC 1.00

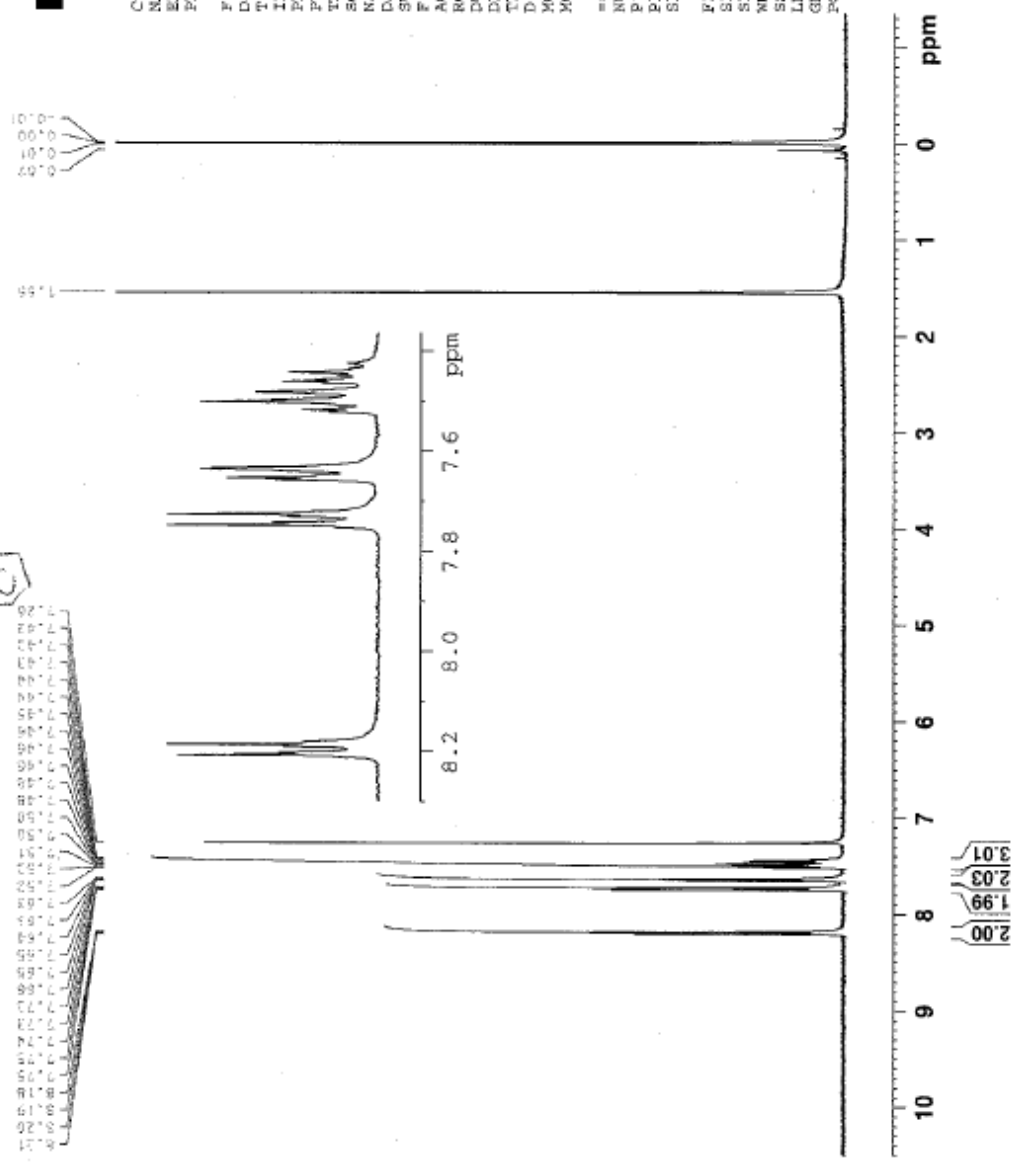
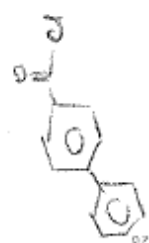
Compd
SJ7 Std

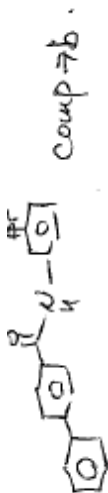




Current Data Parameters
NAME 031912_SJ67
EXPNO 1
PROCNO 1
F2 - Acquisition Parameters
Date_ 20120319
Time 11.28
INSTRUM spect
PROBHD 5 mm QNP 1H/13
PULPROG zg30
TD 32000
SOLVENT CDCl3
NS 16
DS 2
SWH 6009.615 Hz
FIDRES 0.187800 Hz
AQ 2.6625333 sec
RG 1825.5
DW 83.200 usec
DE 6.00 usec
TE 295.2 K
D1 1.00000000 sec
MCREST 0.00000000 sec
MCWRK 0.01500000 sec
***** CHANNEL f1 *****
NUC1 13
P1 10.90 usec
PL1 -1.00 dB
SFO1 400.1324710 MHz
F2 - Processing parameters
SI 32768
SF 400.1300090 MHz
WDW EM
SSB 0
LB 0
GB 0
PC 1.00

Comp Fa.
SJ-1-67



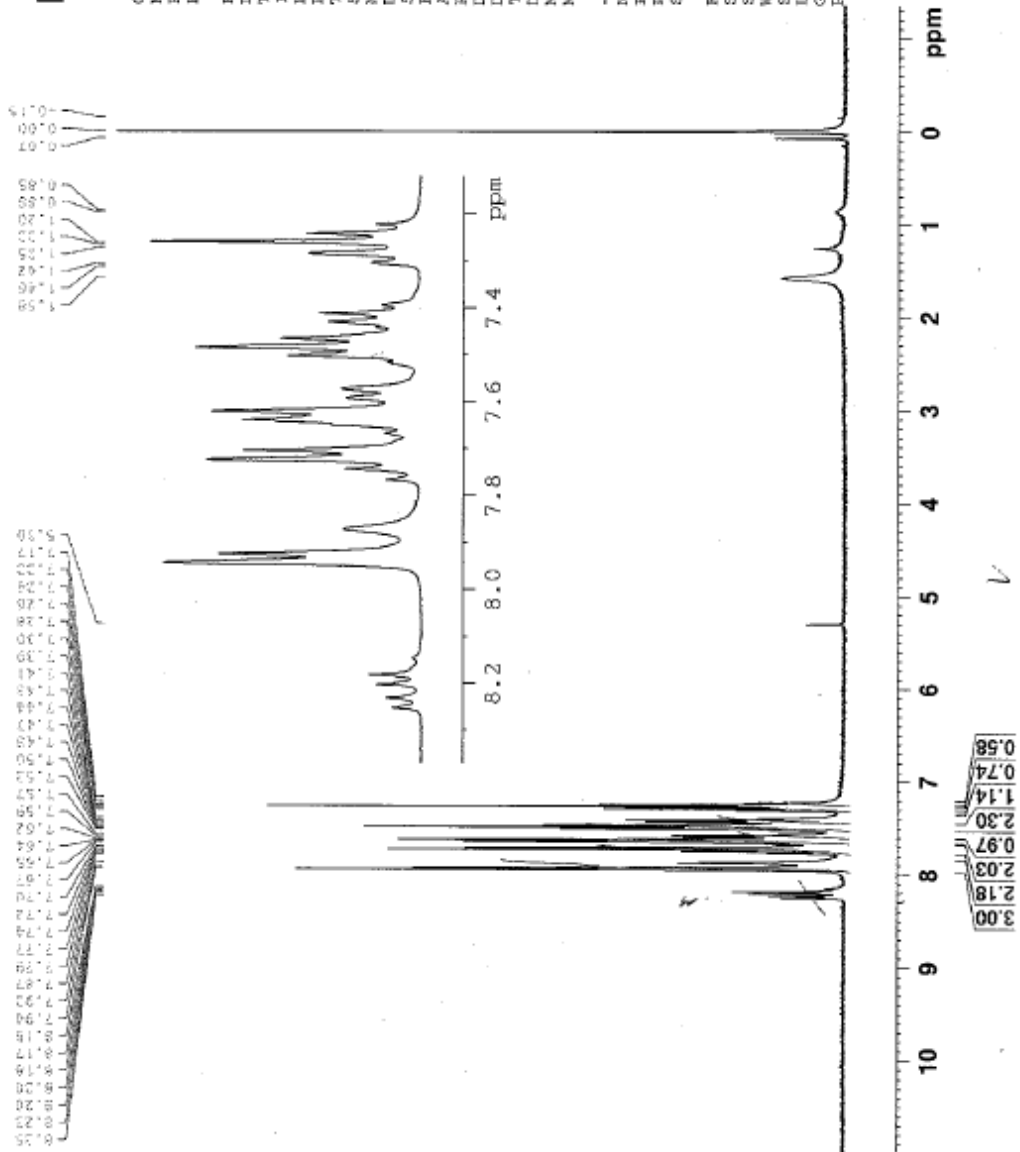


Current Data Parameters
 NAME 032612_871_68
 EXPNO 1
 PROCNO 1

F2 - Acquisition Parameters
 Date_ 20120326
 Time 20.00
 INSTRUM spect
 PROBHD 5 mm QNP 1H/13
 PULPROG zg30
 TD 32000
 SOLVENT CDCl3
 NS 16
 DS 2
 SWH 6009.615 Hz
 FIDRES 0.167800 Hz
 AQ 2.662533 sec
 RG 456.1
 DW 83.200 usec
 DE 6.00 usec
 TR 293.2 K
 D1 1.00000000 sec
 MCREST 0.00000000 sec
 MCNRK 0.01500000 sec

----- CHANNEL f1 -----
 NUC1 1H
 P1 10.90 usec
 PL1 -1.00 dB
 SFO1 400.1324710 MHz

F2 - Processing parameters
 SI 32768
 SF 400.1300036 MHz
 MDW EM
 SSB 0
 LB 0.30 Hz
 GB 0
 PC 1.00



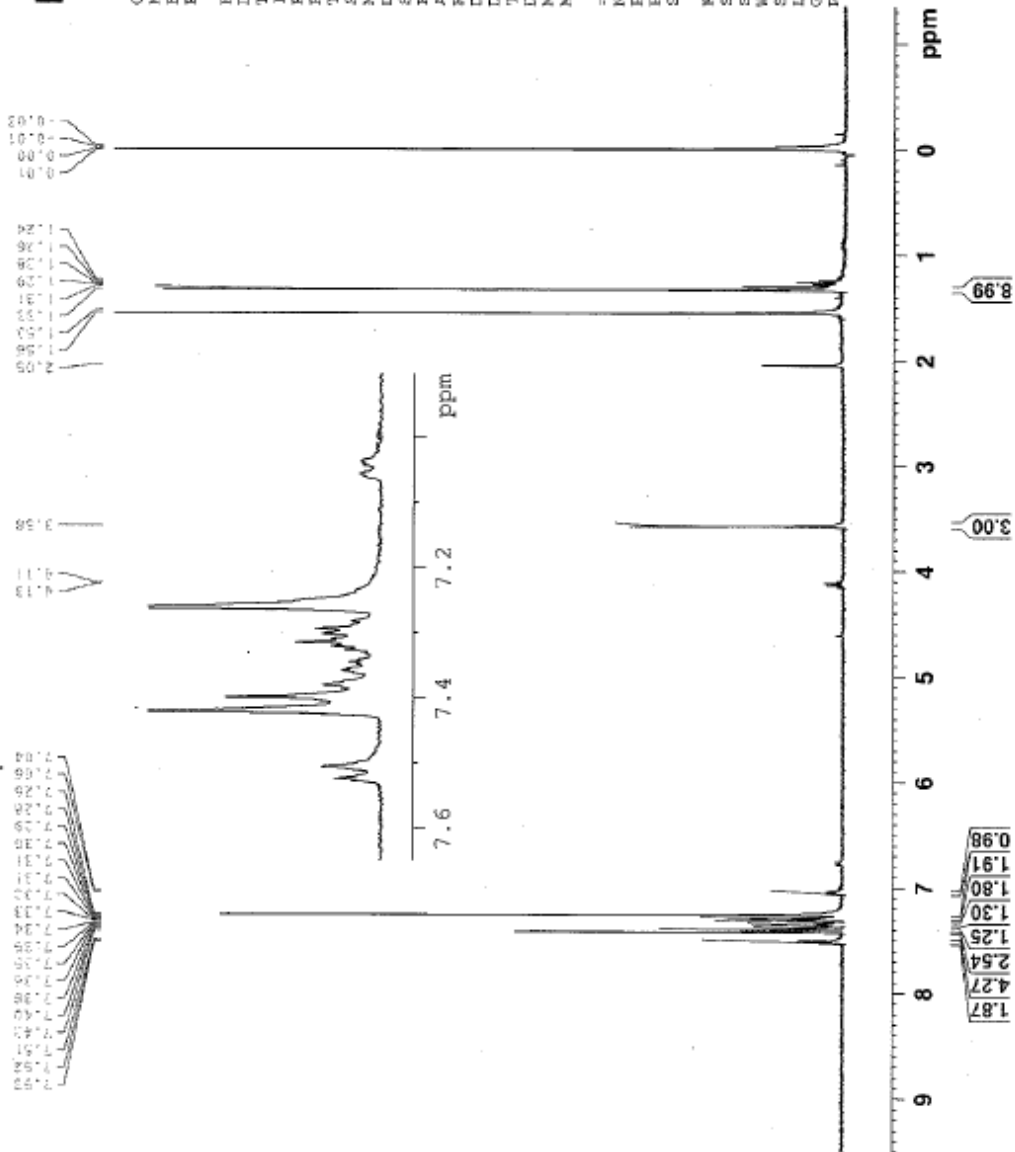


Current Data Parameters
 NAME SJ8_std
 EXPNO 1
 PROCNO 1

F2 - Acquisition Parameters
 Date_ 20120402
 Time 20.11
 INSTRUM spect
 PROBHD 5 mm QNP 1H/13
 PULPROG zg30
 TD 32000
 SOLVENT CDC13
 NS 16
 DS 2
 SWH 6009.615 Hz
 FIDRES 0.187800 Hz
 AQ 2.6625333 sec
 RG 312.3
 CW 83.200 usec
 DE 6.00 usec
 TR 293.2 K
 D1 1.0000000 sec
 MCREST 0.0000000 sec
 MCRX 0.0150000 sec

===== CHANNEL f1 =====
 NUC1 1H
 P1 10.90 usec
 PL1 -1.00 dB
 SFO1 400.1324710 MHz

F2 - Processing parameters
 SI 32768
 SF 400.1300087 MHz
 WDW EM
 SSB 0
 LB 0.30 Hz
 GB 0
 PC 1.00



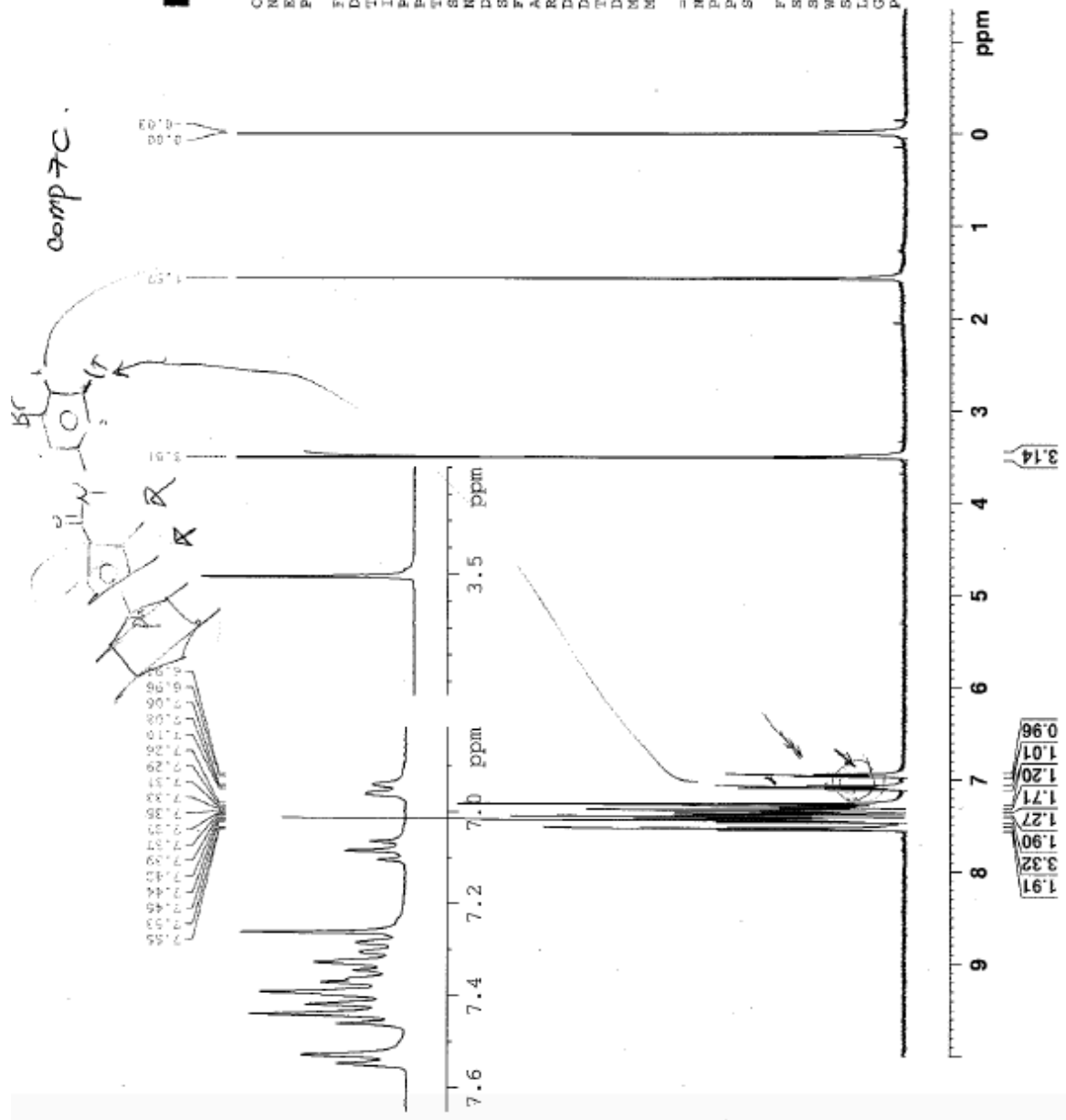


Current Data Parameters
 NAME 032612_SJ1_69
 EXPNO 1
 PROCNO 1

F2 - Acquisition Parameters
 Date_ 20120326
 Time 19.31
 INSTRUM spect
 PROBDW 5 mm QNP 1H/13
 PULPROG zg30
 TD 32000
 SOLVENT CDCl3
 NS 16
 DS 2
 SWH 6009.615 Hz
 FIDRES 0.187800 Hz
 AQ 2.6625333 sec
 RG 724.1
 DW 83.200 usec
 DE 6.00 usec
 TE 293.2 K
 D1 1.00000000 sec
 MCREST 0.00000000 sec
 MCWRR 0.01500000 sec

===== CHANNEL f1 =====
 NUC1 1H
 P1 10.90 usec
 PL1 -1.00 dB
 SFO1 400.1324710 MHz

F2 - Processing parameters
 SI 32768
 SF 400.1300084 MHz
 WDW EM
 SSB 0
 LB 0.30 Hz
 GB 0
 PC 1.00





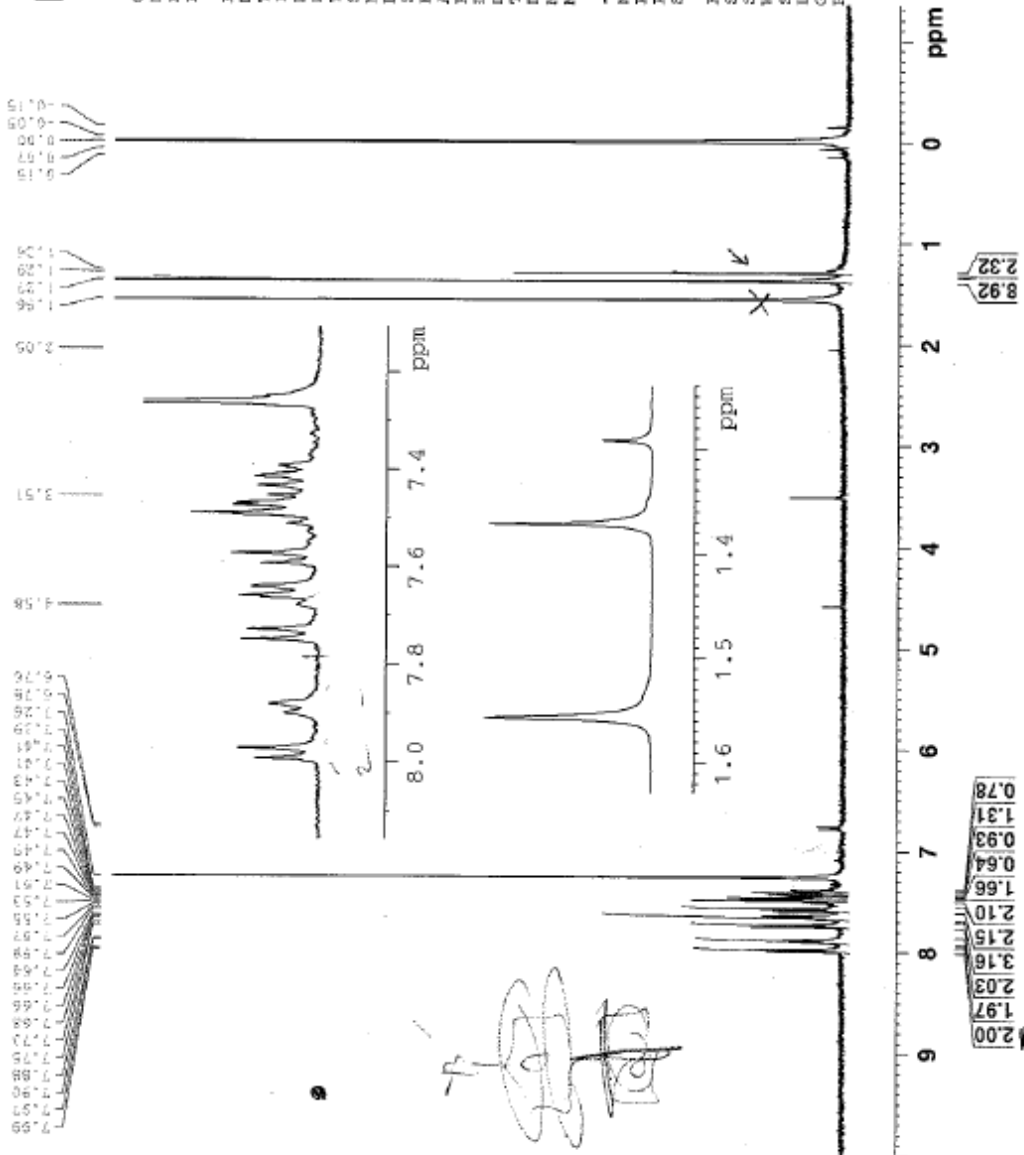
Current Data Parameters
NAME 032612_808pre_2
EXPNO 1
PROCNO 1

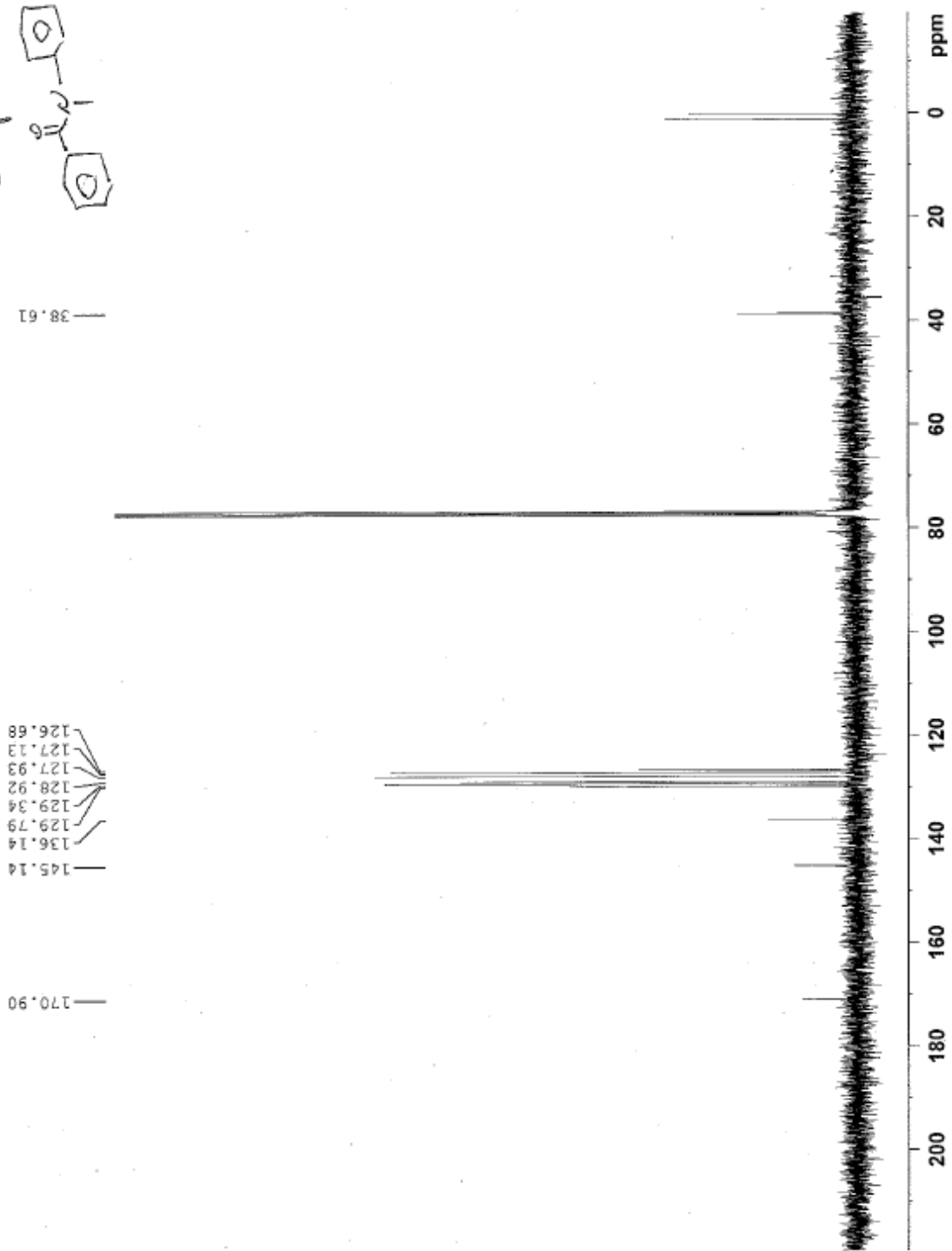
F2 - Acquisition Parameters
Date_ 20120326
Time 19.47
INSTRUM spect
PROBHD 5 mm QNP 1H/13
PULPROG zg30
TD 32000
SOLVENT CDCl3
NS 16
DS 2
SWH 6009.615 Hz
FIDRES 0.187800 Hz
AQ 2.6625333 sec
RG 512.3
DM 83.200 usec
DE 6.00 usec
TE 293.2 K
D1 1.00000000 sec
MCREST 0.00000000 sec
MCNCRK 0.01500000 sec

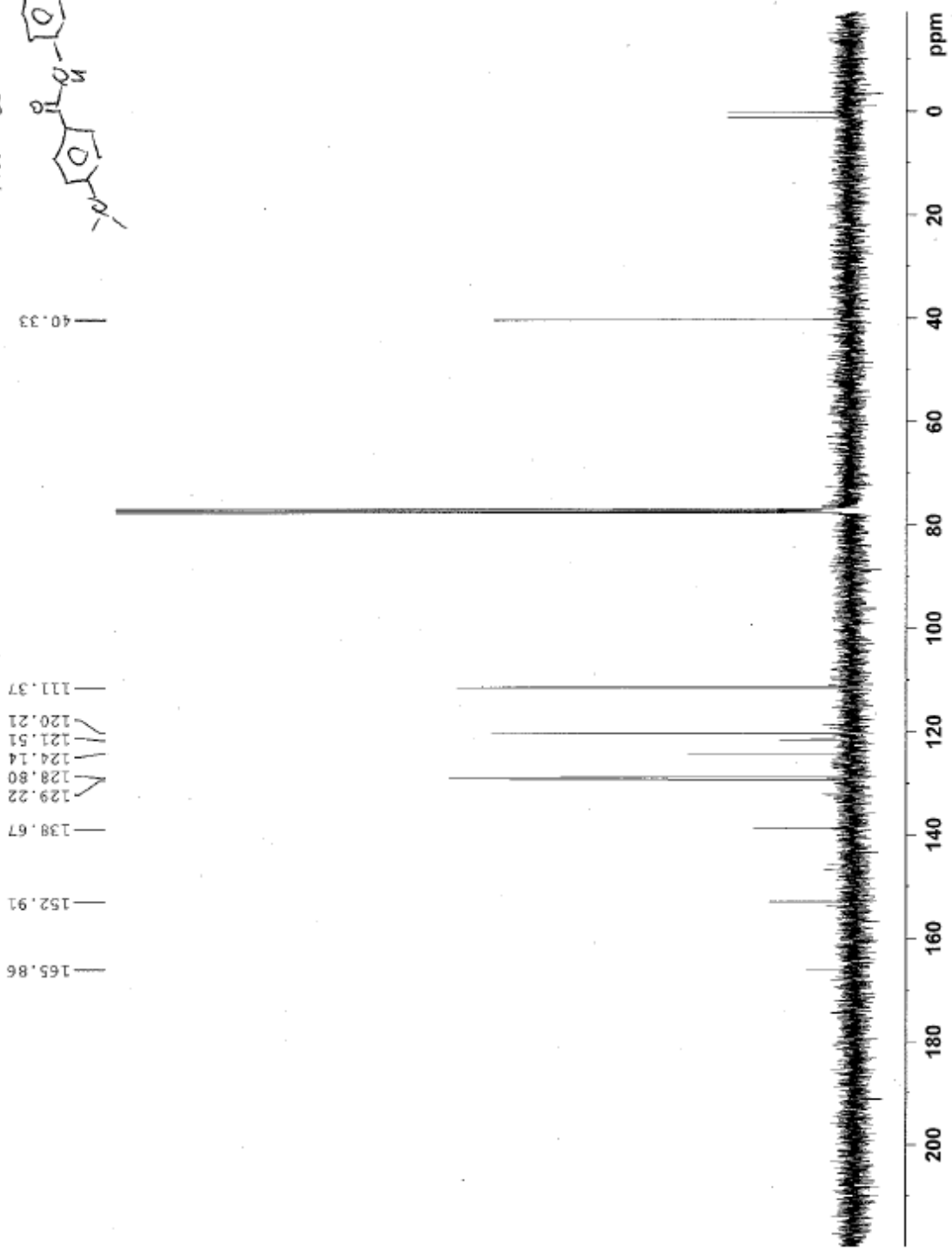
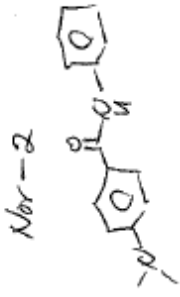
----- CHANNEL f1 -----
NUC1 1H
P1 10.90 usec
PL1 -1.00 dB
SFO1 400.1324710 MHz

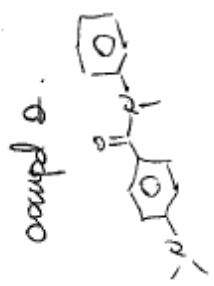
F2 - Processing parameters
SI 32768
SF 400.1300087 MHz
WDW EM
SSB 0
LB 0.30 Hz
GB 0
PC 1.00

~~P~~ Coupl →



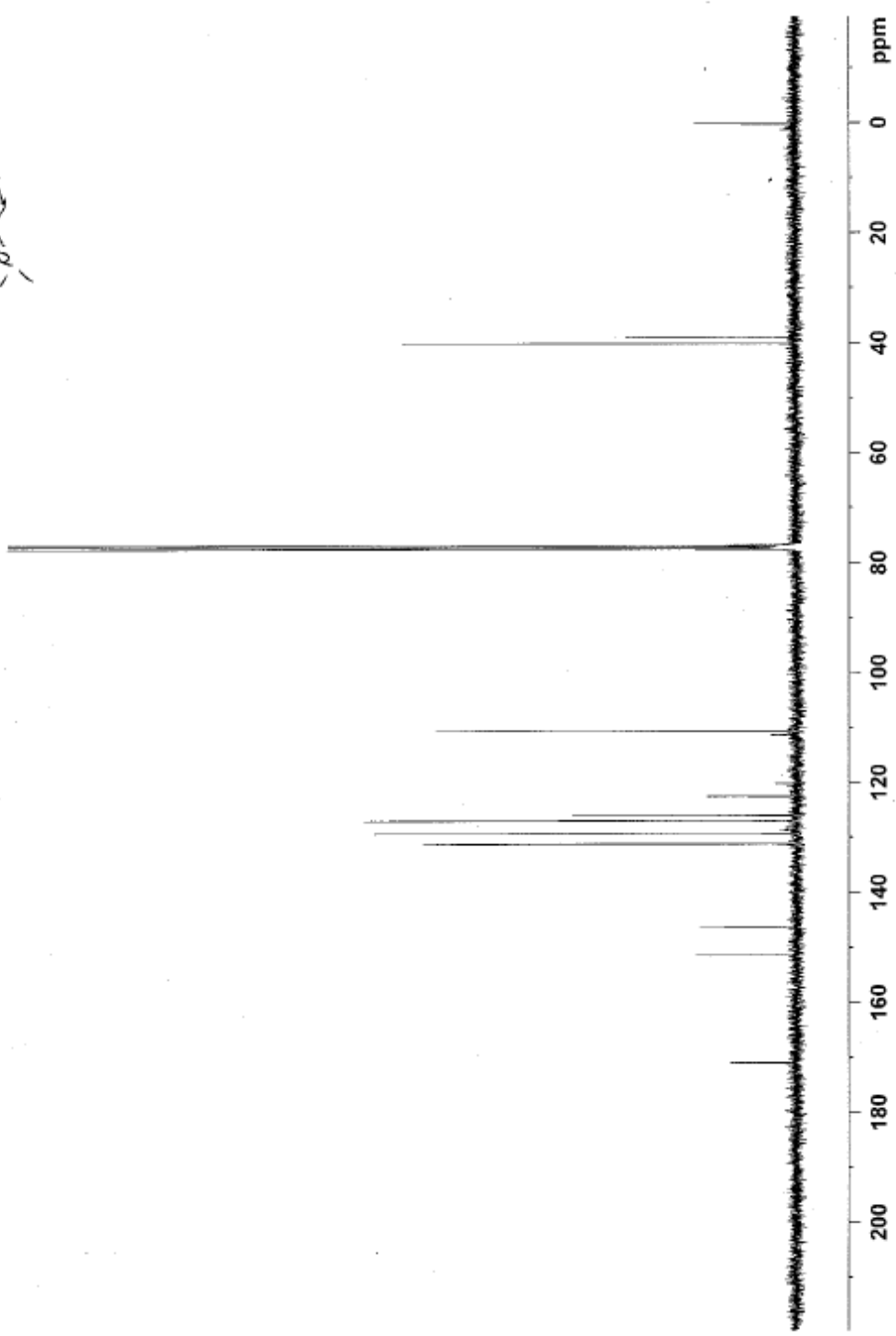


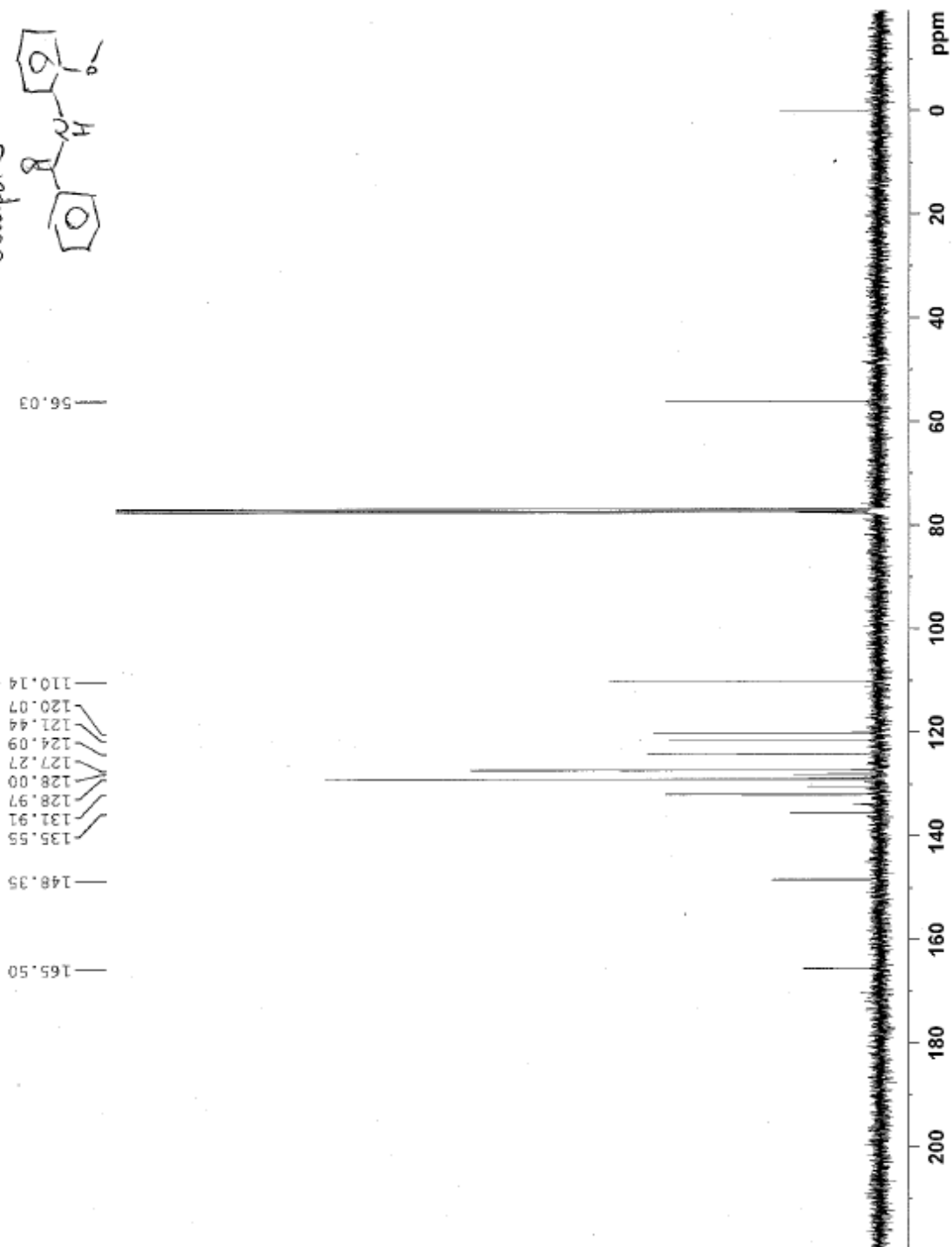
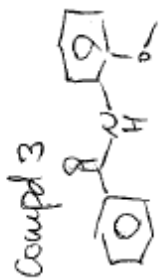


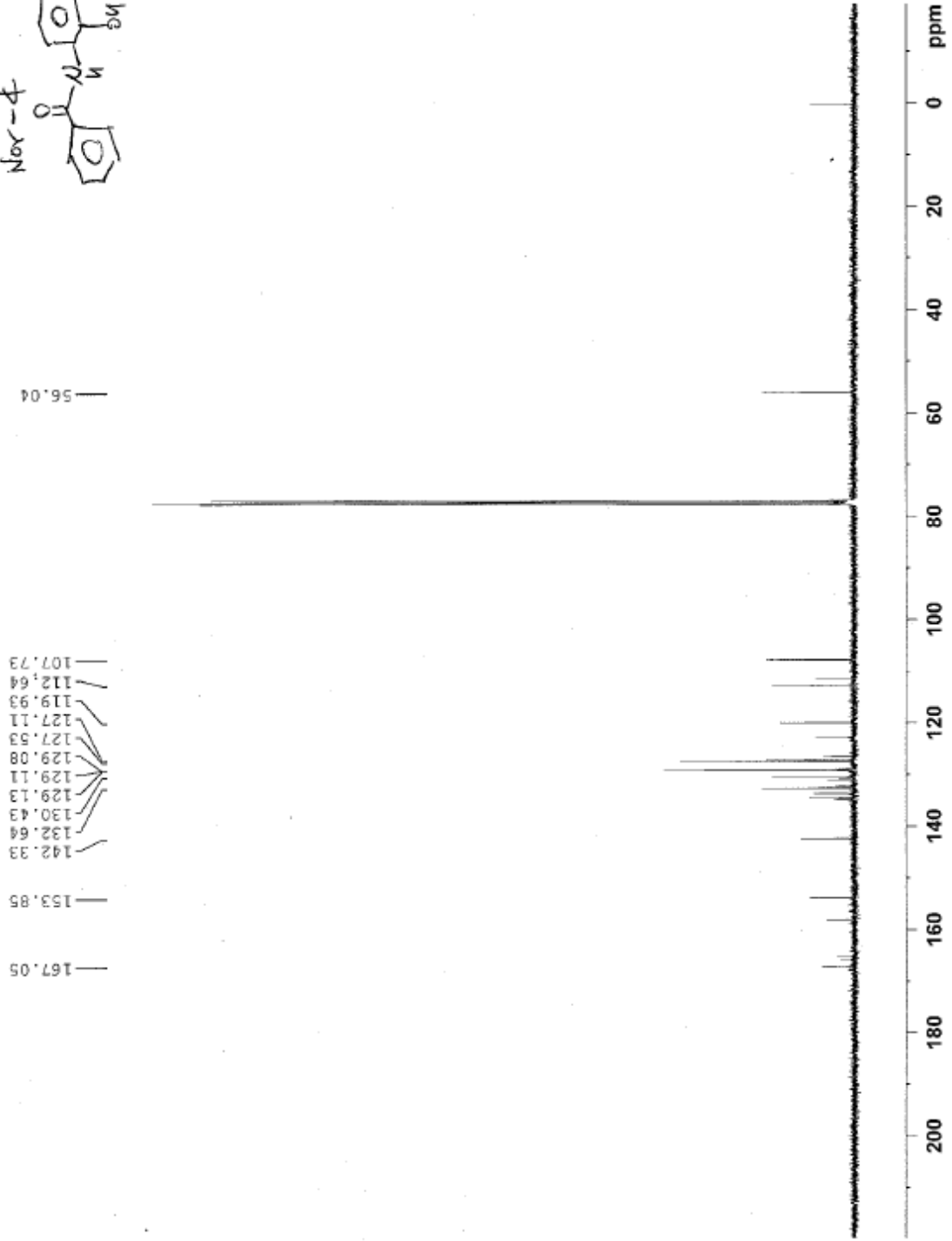
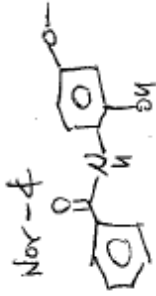


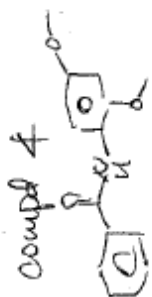
40.21
38.99

170.92
151.37
146.37
131.24
129.31
126.99
126.06
122.53
110.61









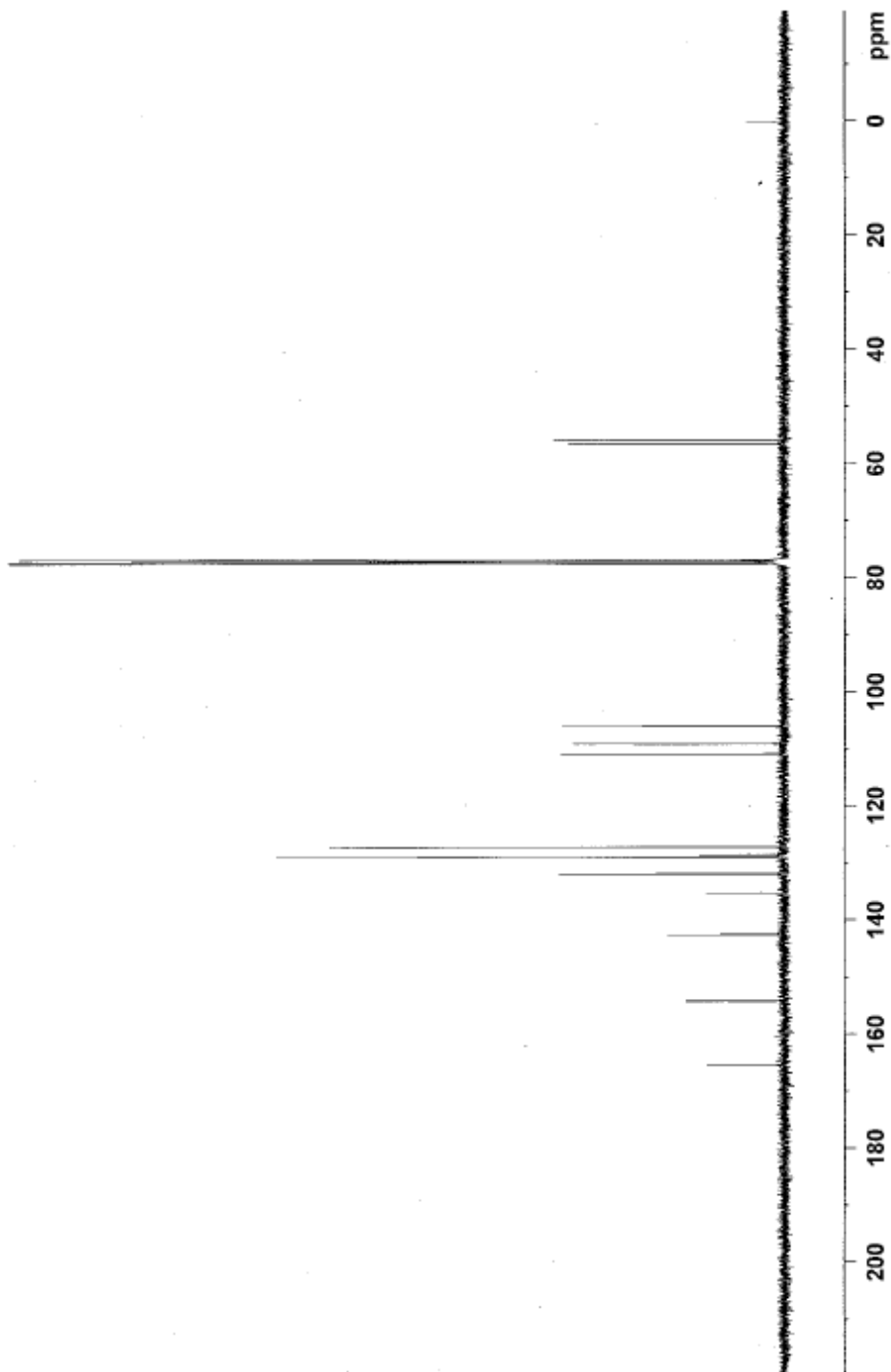
56.54
56.04

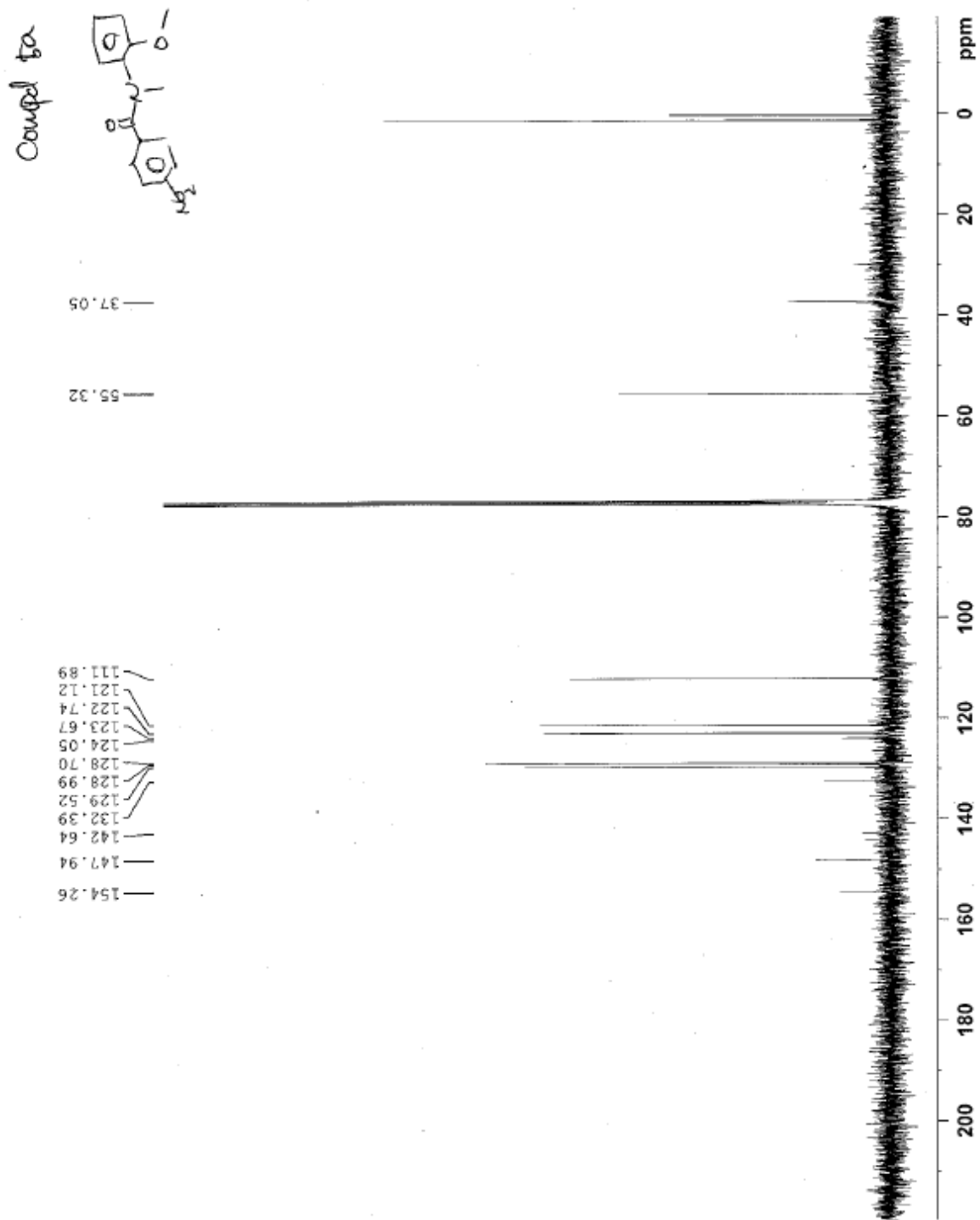
106.07
109.13
110.94

127.23
128.99
131.99
135.40
142.56

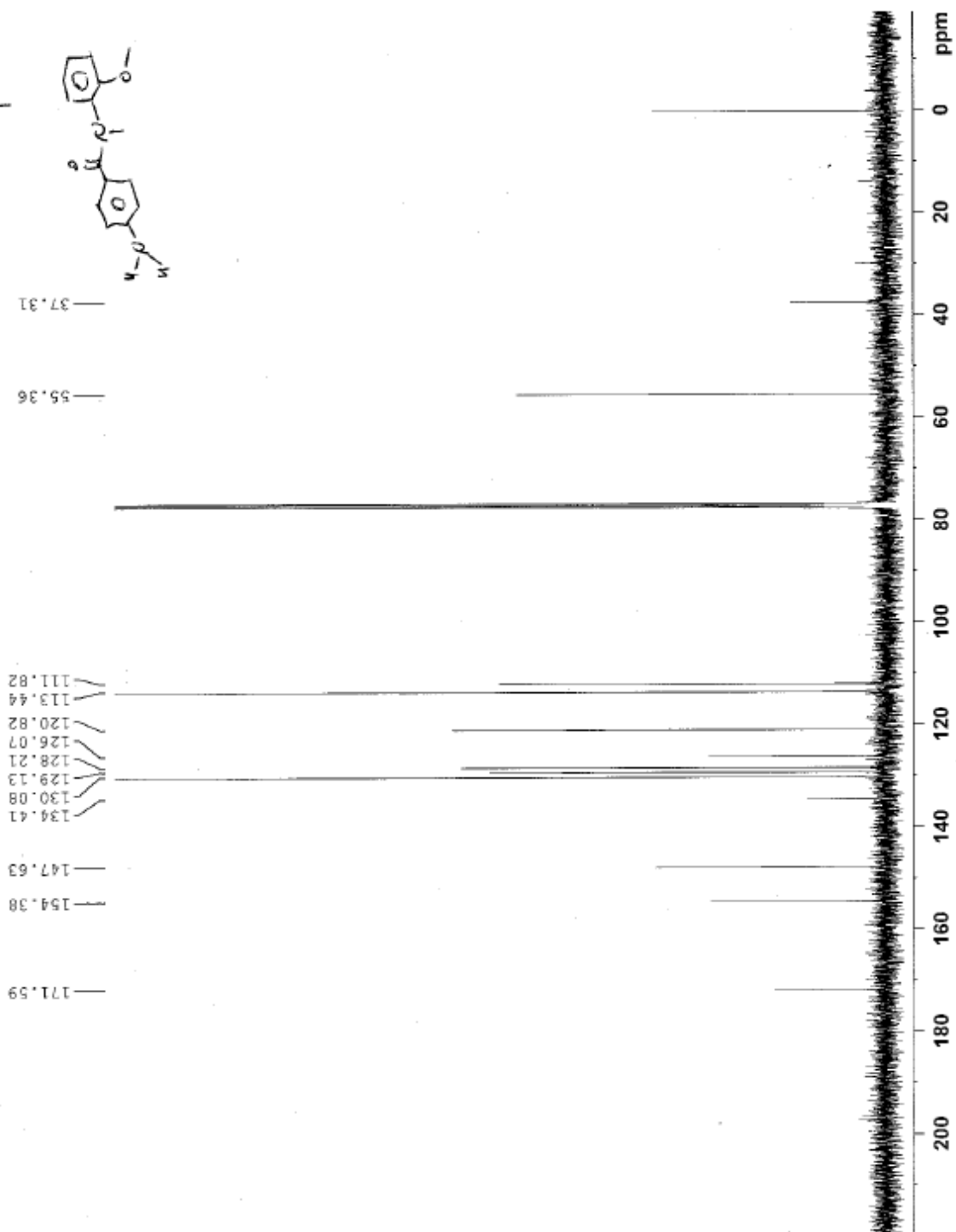
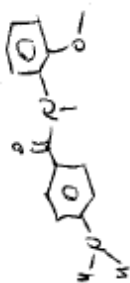
154.17

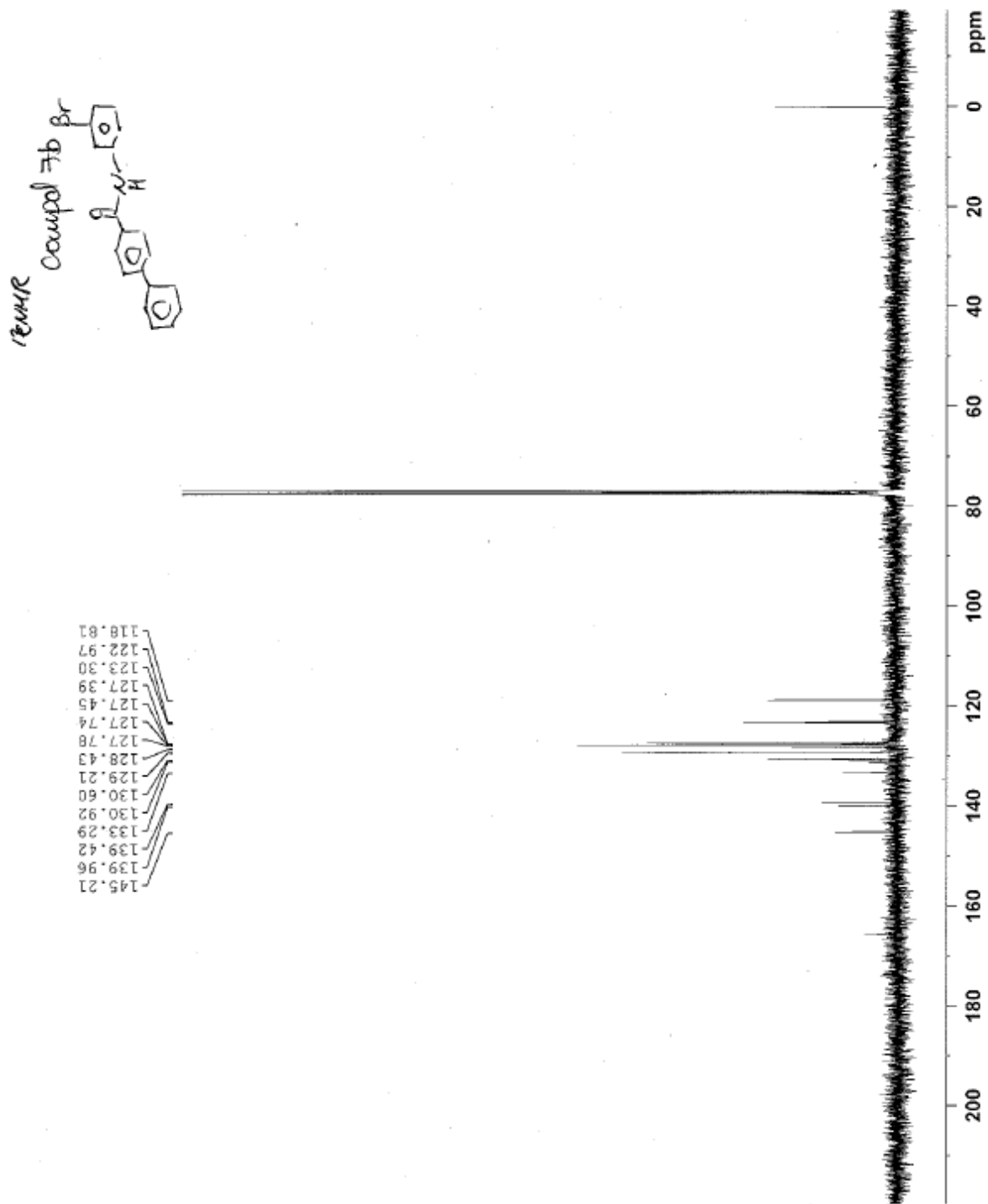
165.45





13C NMR
Compound 5





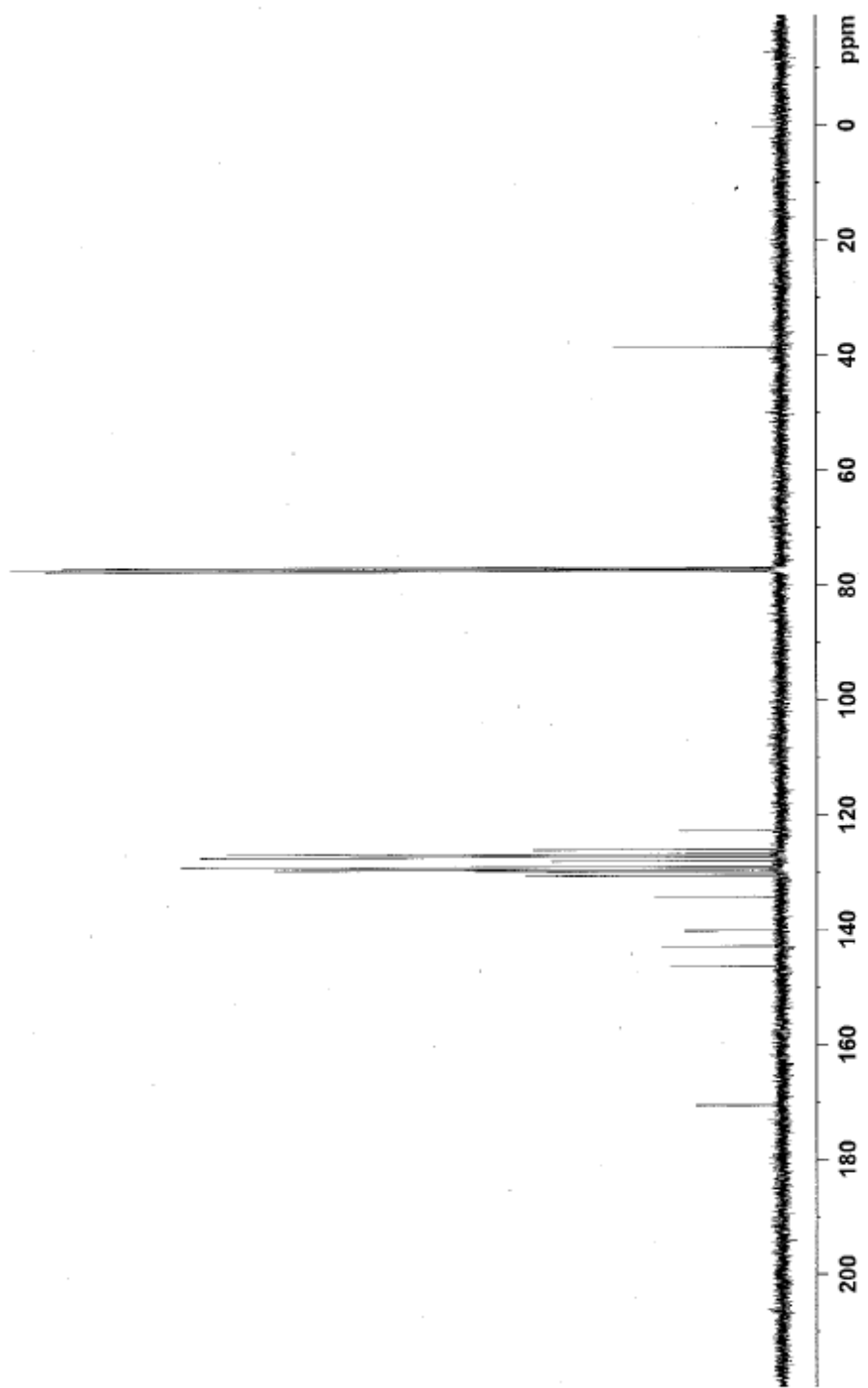
¹³C NMR



38.67

122.71
126.02
126.76
127.28
128.00
129.01
129.49
129.79
129.81
130.55
134.28
140.18
142.86
146.47

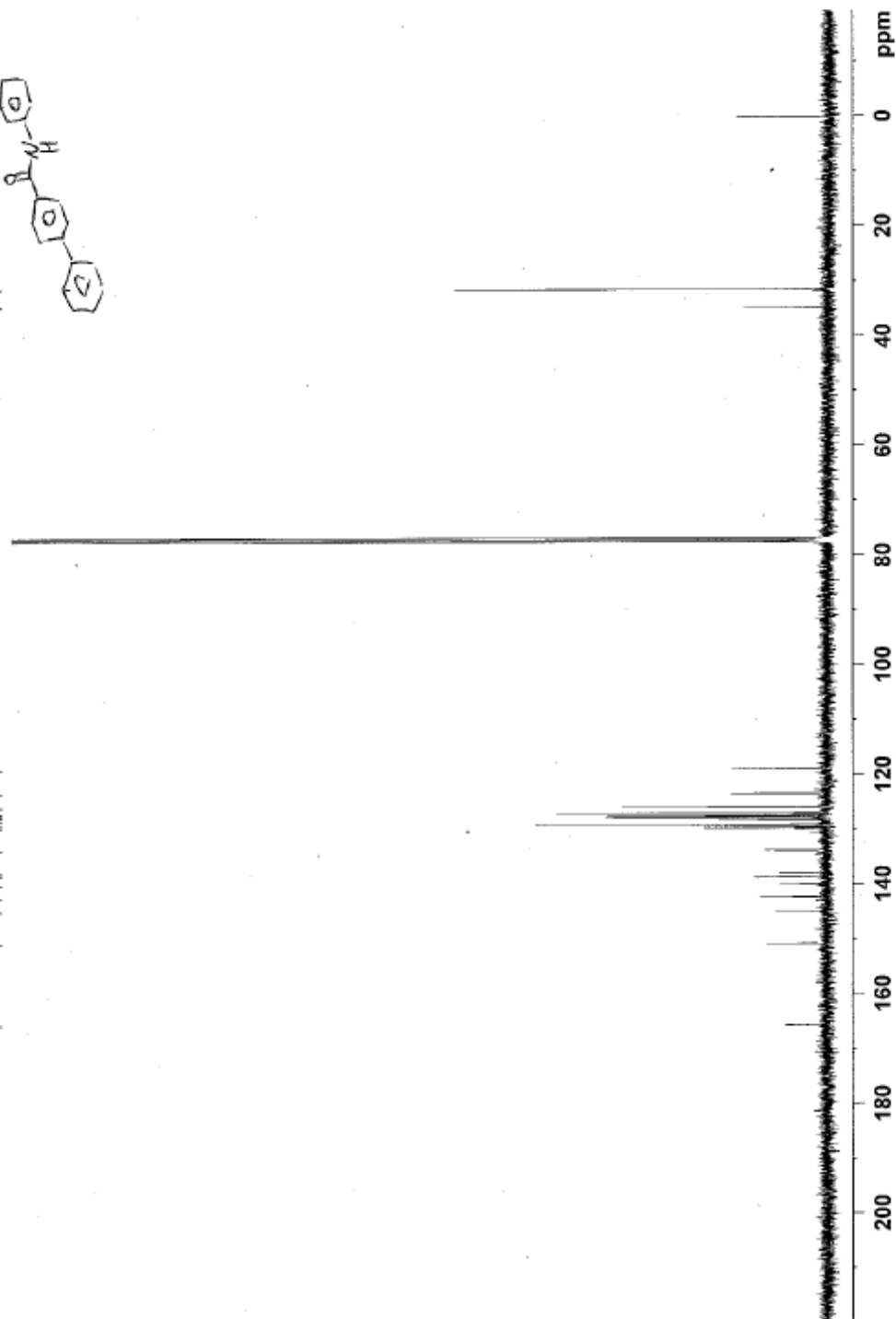
170.47



¹³C NMR



- 165.66
- 150.82
- 144.95
- 142.32
- 140.09
- 138.53
- 137.91
- 133.80
- 129.68
- 129.19
- 128.35
- 127.80
- 127.69
- 127.46
- 127.05
- 125.95
- 123.49
- 119.05
- 119.00



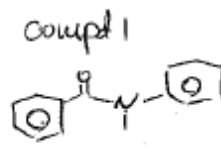
Print of window 80: MS Spectrum

Data File : D:\CHEM32\DATA\FOWLER\061215_COMPD 1.D

Sample Name : 061215_COMPD 1.D

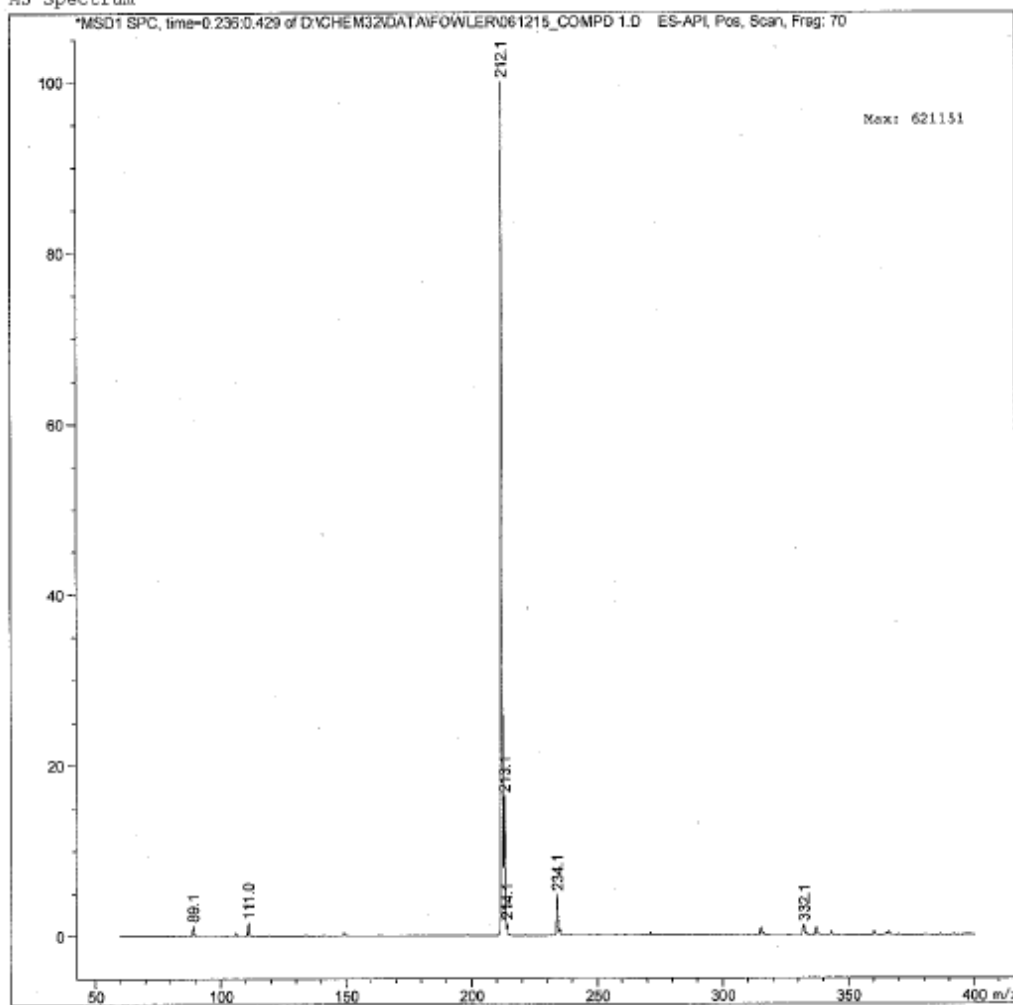
=====

Acq. Operator	: So Jeong	Location	: Vial 1
Acq. Instrument	: Instrument 1	Inj	: 1
Injection Date	: 6/12/2015 5:32:44 PM	Inj Volume	: 1.0 µl



Acq. Method	: D:\CHEM32\METHODS\DIR-INJ-POS.M
Last changed	: 6/12/2015 5:31:38 PM by So Jeong (modified after loading)
Analysis Method	: D:\CHEM32\DATA\FOWLER\061215_COMPD 1.D\DA.M (DIR-INJ-POS.M, From Data File)
Last changed	: 6/12/2015 5:34:20 PM by So Jeong
Method Info	: Direct-inject (FIA) ESI positive A1 (0.1%Ac): B1 (MeOH); 25:75(v:v); 0.25ml/min

MS Spectrum



Instrument 1 6/12/2015 5:42:07 PM rajesh

Page 1 of 1

Print of window 80: MS Spectrum

Data File : D:\CHEM32\DATA\FOWLER\061215_NOR 2.D

Sample Name : 061215_nor 2.D

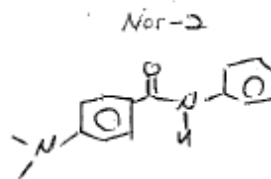
Acq. Operator : So Jeong
Acq. Instrument : Instrument 1 Location : Vial 1
Injection Date : 6/12/2015 5:38:22 PM Inj : 1
Inj Volume : 1.0 µl

Acq. Method : D:\CHEM32\METHODS\DIR-INJ-POS.M
Last changed : 6/12/2015 5:34:22 PM by So Jeong
(modified after loading)

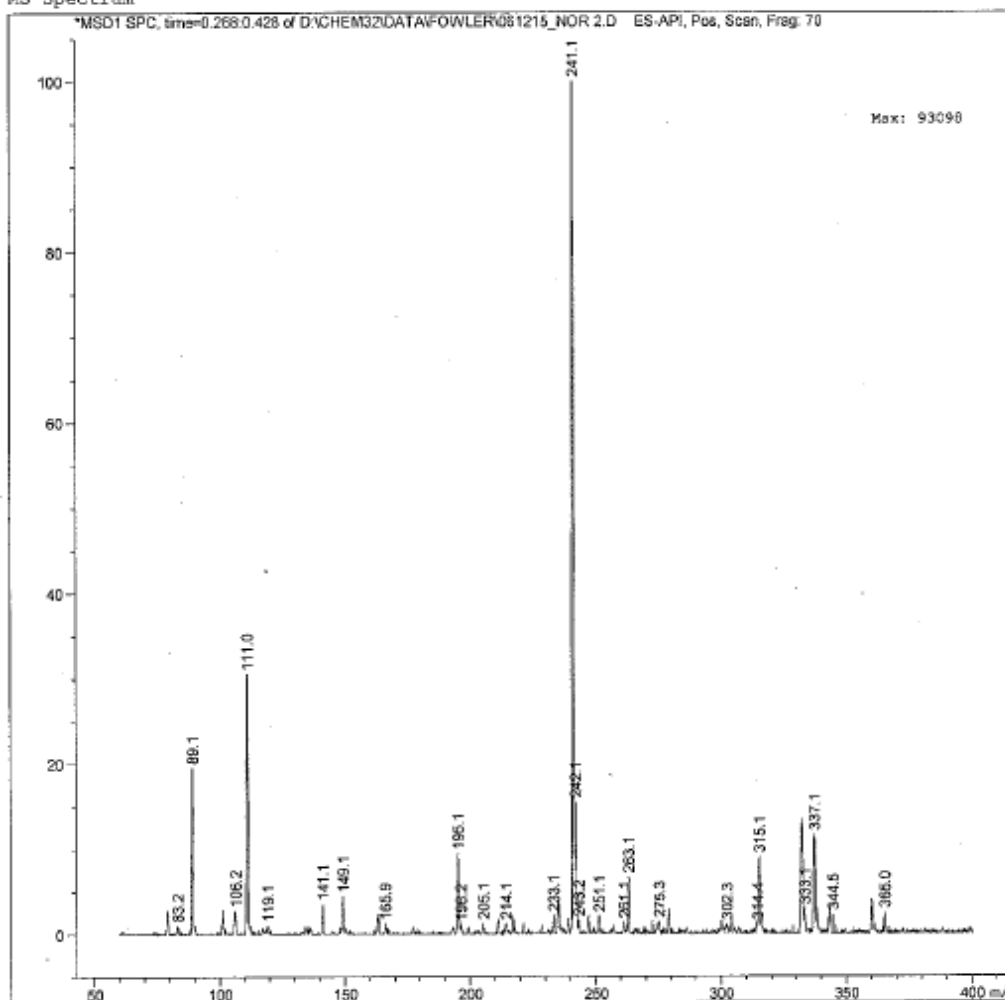
Analysis Method : D:\CHEM32\DATA\FOWLER\061215_NOR 2.D\DA.M (DIR-INJ-POS.M, From Data File)

Last changed : 6/12/2015 5:39:58 PM by So Jeong

Method Info : Direct-inject (FIA) ESI positive
A1 (0.1%Ac): B1 (MeOH); 25;75(v:v); 0.25ml/min



MS Spectrum



Instrument 1 6/12/2015 5:41:45 PM rajesh

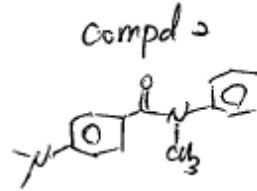
Page 1 of 1

Print of window 80: MS Spectrum

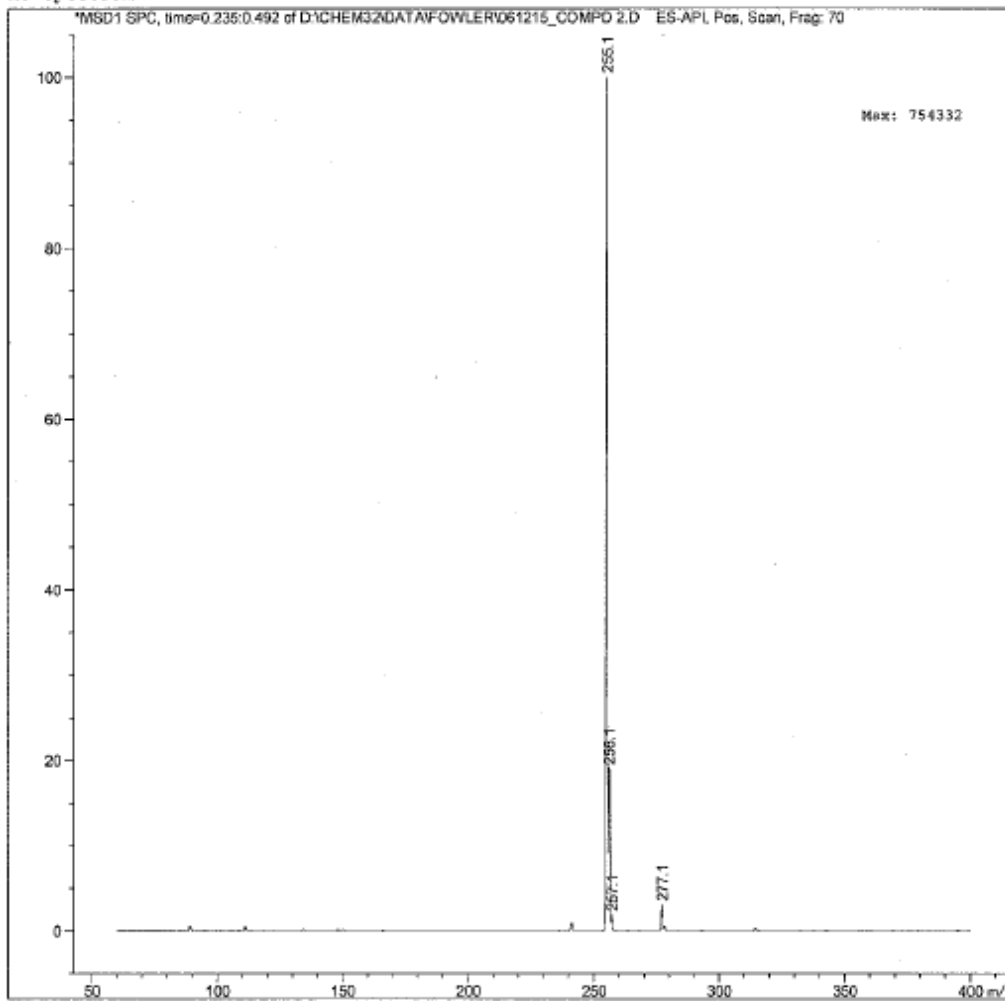
Data File : D:\CHEM32\DATA\FOWLER\061215_COMPD 2.D

Sample Name : 061215_compd 2.D

=====
Acq. Operator : So Jeong
Acq. Instrument : Instrument 1 Location : Vial 1
Injection Date : 6/12/2015 5:43:50 PM Inj : 1
Inj Volume : 1.0 µl
Acq. Method : D:\CHEM32\METHODS\DIR-INJ-POS.M
Last changed : 6/12/2015 5:40:00 PM by So Jeong
(modified after loading)
Analysis Method : D:\CHEM32\DATA\FOWLER\061215_COMPD 2.D\DA.M (DIR-INJ-POS.M, From Data File)
Last changed : 6/12/2015 5:45:26 PM by So Jeong
Method Info : Direct-inject (FIA) ESI positive
A1 (0.18Ac): B1 (MeOH): 25:75(v:v); 0.25ml/min



MS Spectrum



Instrument 1 6/12/2015 5:45:45 PM rajesh

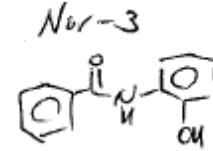
Page 1 of 1

Print of window 80: MS Spectrum

Data File : D:\CHEM32\DATA\FOWLER\061215_NOR 3_2.D

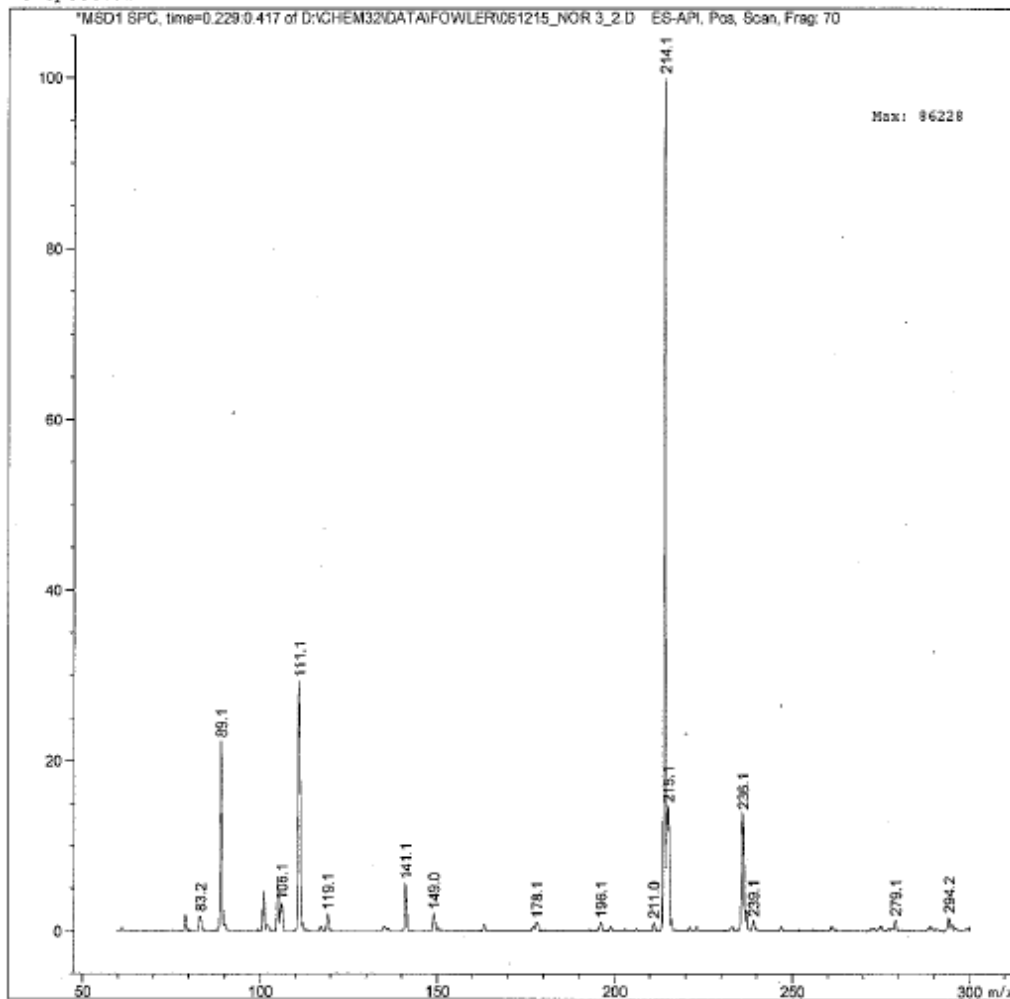
Sample Name : 061215_nor 3_2.D

Acq. Operator : So Jeong
Acq. Instrument : Instrument 1 Location : Vial 1
Injection Date : 6/12/2015 6:00:13 PM Inj : 1
Inj Volume : 1.0 µl



Acq. Method : D:\CHEM32\METHODS\DIR-INJ-POS.M
Last changed : 6/12/2015 5:59:15 PM by So Jeong
(modified after loading)
Analysis Method : D:\CHEM32\DATA\FOWLER\061215_NOR 3_2.D\DA.M (DIR-INJ-POS.M, From Data File)
Last changed : 6/12/2015 6:01:49 PM by So Jeong
Method Info : Direct-inject (FIA) ESI positive
A1 (0.1%Ac): B1 (MeOH); 25:75(v:v); 0.25ml/min

MS Spectrum



Instrument 1 6/12/2015 6:02:02 PM rajesh

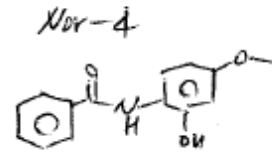
Page 1 of 1

Print of window 80: MS Spectrum

Data File : D:\CHEM32\DATA\FOWLER\061215_NOR_4_2.D

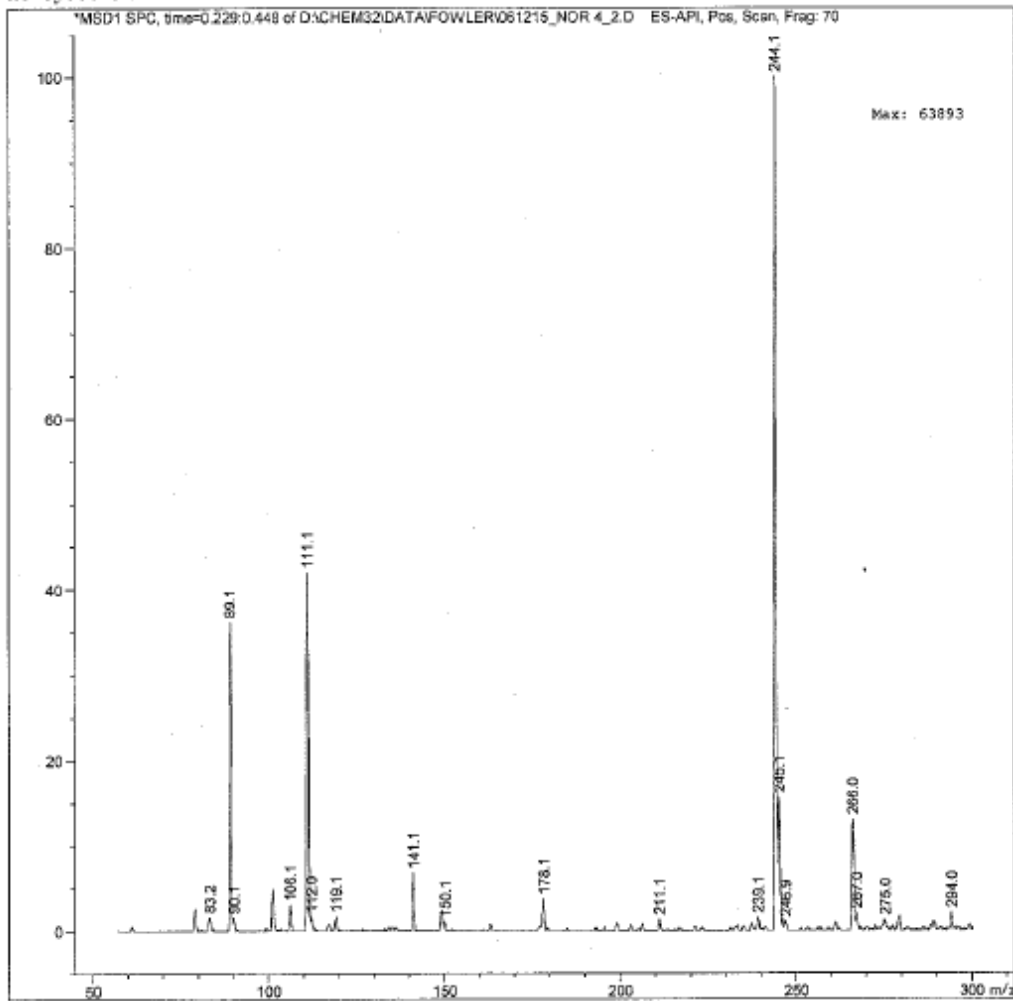
Sample Name : 061215_nor_4_2.D

Acq. Operator : So Jeong
Acq. Instrument : Instrument 1 Location : Vial 1
Injection Date : 6/12/2015 6:12:08 PM Inj : 1
Inj Volume : 1.0 µl



Acq. Method : D:\CHEM32\METHODS\DIR-INJ-POS.M
Last changed : 6/12/2015 6:11:27 PM by So Jeong
(modified after loading)
Analysis Method : D:\CHEM32\DATA\FOWLER\061215_NOR_4_2.D\DA.M (DIR-INJ-POS.M, From Data File)
Last changed : 6/12/2015 6:13:44 PM by So Jeong
Method Info : Direct-inject (FIA) ESI positive
A1 (0.1%Ac): B1 (MeOH); 25:75(v:v); 0.25ml/min

MS Spectrum



Instrument 1 6/12/2015 6:14:01 PM rajesh

Page 1 of 1

Print of window 80: MS Spectrum

Data File : D:\CHEM32\DATA\FOWLER\061215_COMPD 4.D

Sample Name : 061215_COMPD 4.D

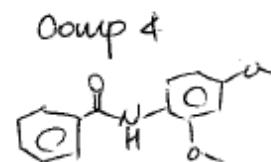
Acq. Operator : So Jeong
Acq. Instrument : Instrument 1 Location : Vial 1
Injection Date : 6/12/2015 6:16:06 PM Inj : 1
Inj Volume : 1.0 µl

Acq. Method : D:\CHEM32\METHODS\DIR-INJ-POS.M
Last changed : 6/12/2015 6:15:15 PM by So Jeong
(modified after loading)

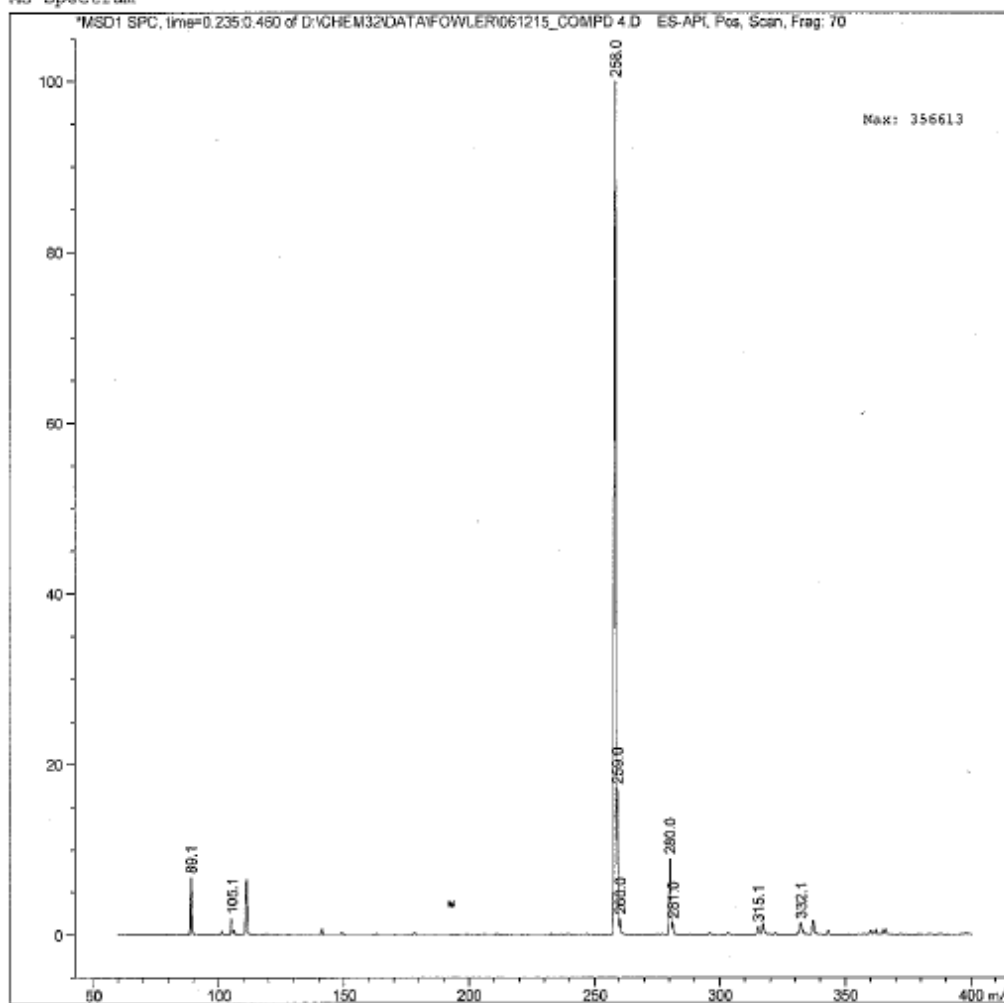
Analysis Method : D:\CHEM32\DATA\FOWLER\061215_COMPD 4.D\DA.M (DIR-INJ-POS.M, From Data File)

Last changed : 6/12/2015 6:17:42 PM by So Jeong

Method Info : Direct-inject (FIA) ESI positive
A1 (0.1%Ac); B1 (MeOH); 25:75(v:v); 0.25ml/min



MS Spectrum



Instrument 1 6/12/2015 6:18:27 PM rajesh

Page 1 of 1

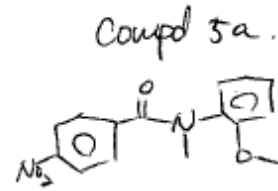
Print of window 80: MS Spectrum

Data File : D:\CHEM32\DATA\FOWLER\061215_COMPD 5A.D

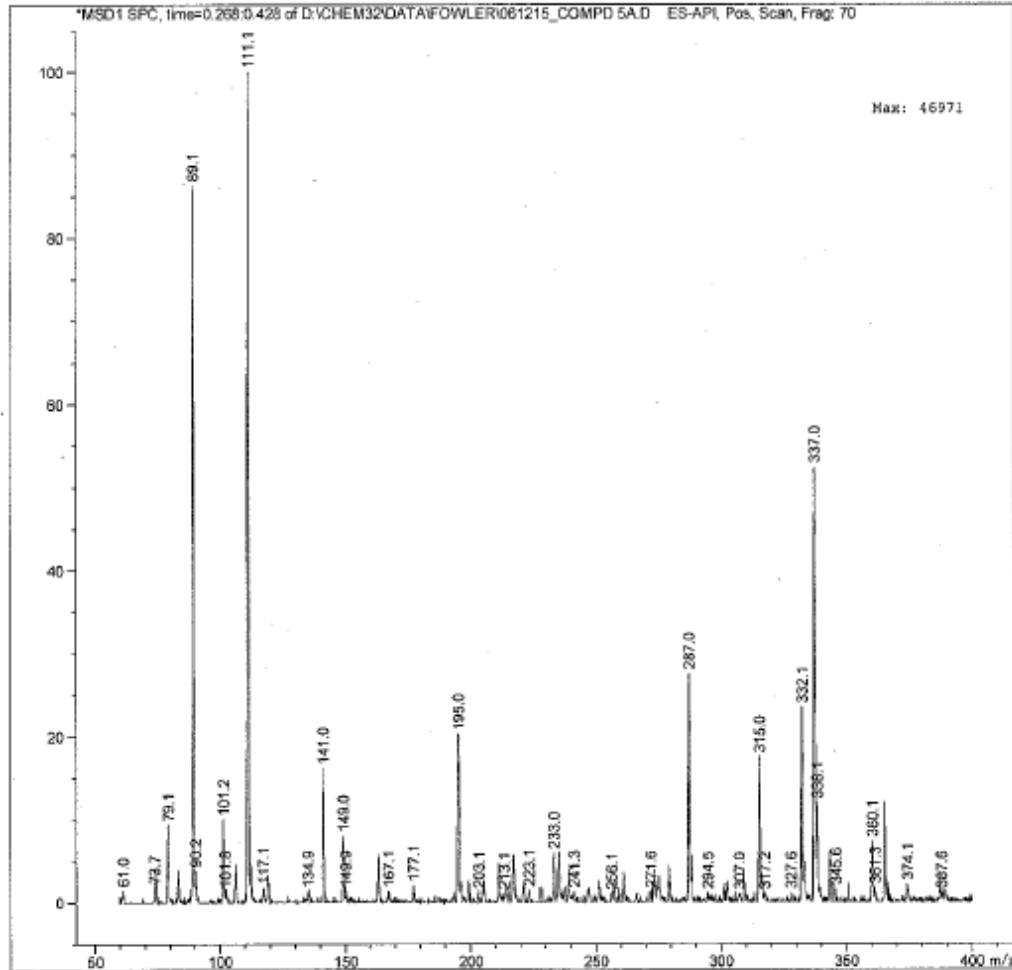
Sample Name : 061215_COMPD 5a.D

Acq. Operator : So Jeong
Acq. Instrument : Instrument 1 Location : Vial 1
Injection Date : 6/12/2015 6:19:39 PM Inj : 1
Inj Volume : 1.0 µl

Acq. Method : D:\CHEM32\METHODS\DIR-INJ-POS.M
Last changed : 6/12/2015 6:17:43 PM by So Jeong
(modified after loading)
Analysis Method : D:\CHEM32\DATA\FOWLER\061215_COMPD 5A.D\DA.M (DIR-INJ-POS.M, From Data
File)
Last changed : 6/12/2015 6:21:16 PM by So Jeong
Method Info : Direct-inject (FIA) ESI positive
A1 (0.1%Ac): B1 (MeOH); 25:75(v:v); 0.25ml/min



MS Spectrum



Instrument 1 6/12/2015 6:21:52 PM rajesh

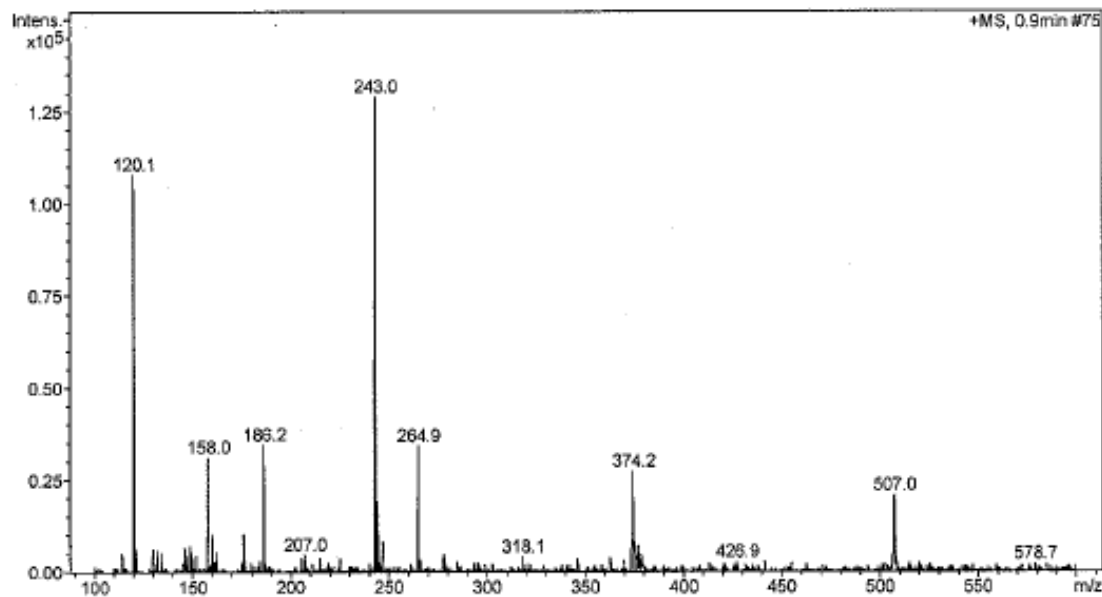
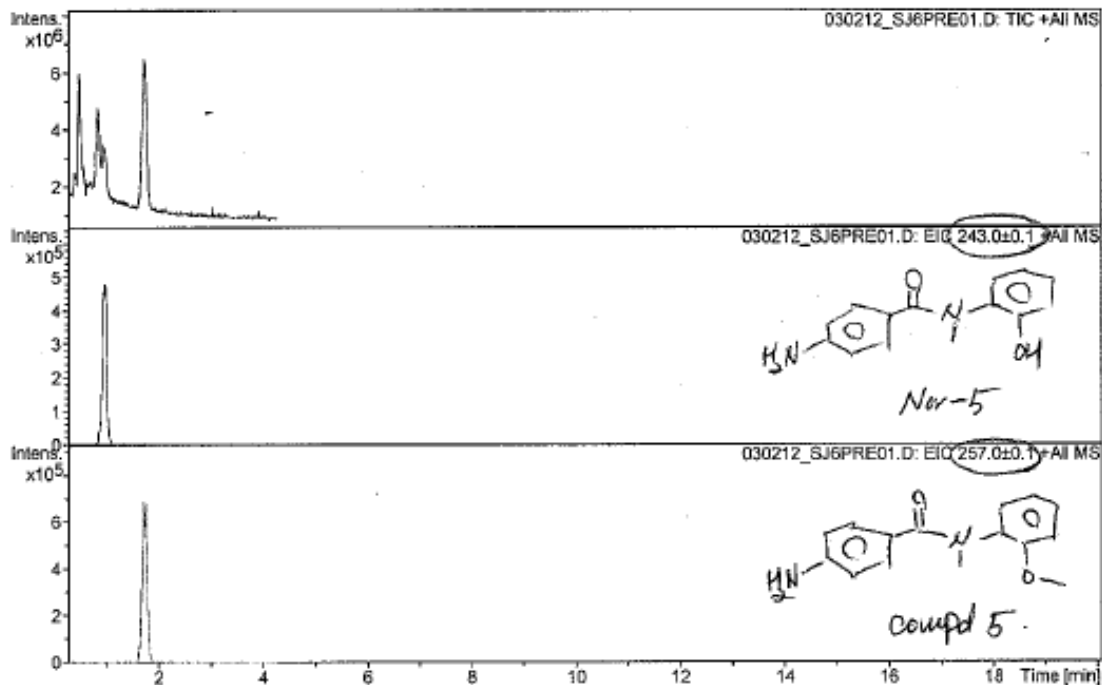
Page 1 of 1

Display Report - All Windows All Analyses

Operator: agilent

Instrument: Agilent 6310 Ion Trap

Print Date: 6/13/2015 2:57:51 PM



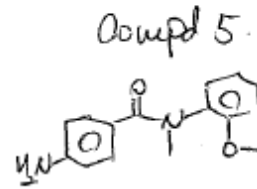
Print of window 80: MS Spectrum

Data File : D:\CHEM32\DATA\FOWLER\061215_COMPD 5.D

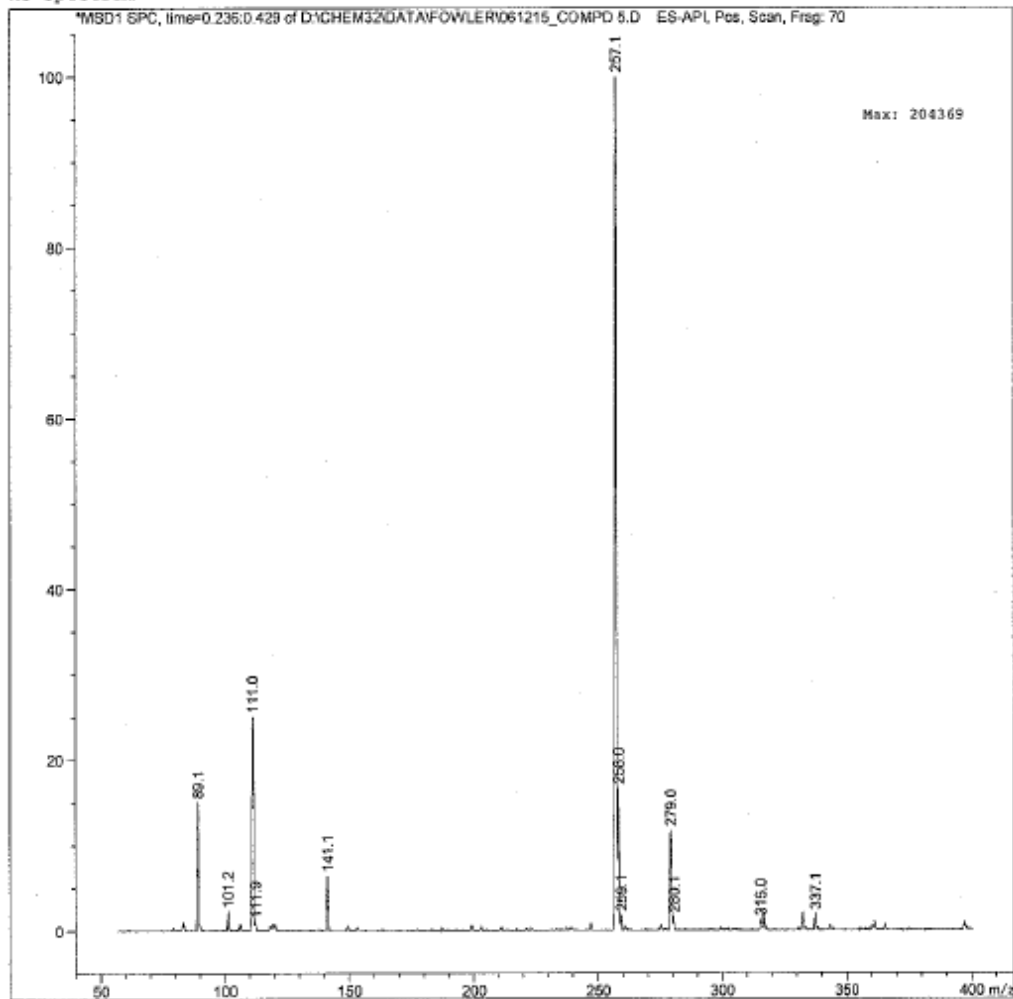
Sample Name : 061215_compd 5.D

=====
Acq. Operator : So Jeong
Acq. Instrument : Instrument 1 Location : Vial 1
Injection Date : 6/12/2015 6:27:30 PM Inj : 1
Inj Volume : 1.0 µl

Acq. Method : D:\CHEM32\METHODS\DIR-INJ-POS.M
Last changed : 6/12/2015 6:25:56 PM by So Jeong
(modified after loading)
Analysis Method : D:\CHEM32\DATA\FOWLER\061215_COMPD 5.D\DA.M (DIR-INJ-POS.M, From Data File)
Last changed : 6/12/2015 6:29:07 PM by So Jeong
Method Info : Direct-inject (FIA) ESI positive
A1 (0.18Ac): B1 (MeOH); 25:75(v:v); 0.25ml/min



MS Spectrum



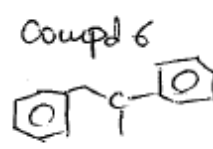
Instrument 1 6/12/2015 6:29:32 PM rajesh

Page 1 of 1

Print of window 80: MS Spectrum

Data File : D:\CHEM32\DATA\FOWLER\061215_COMPD 6.D

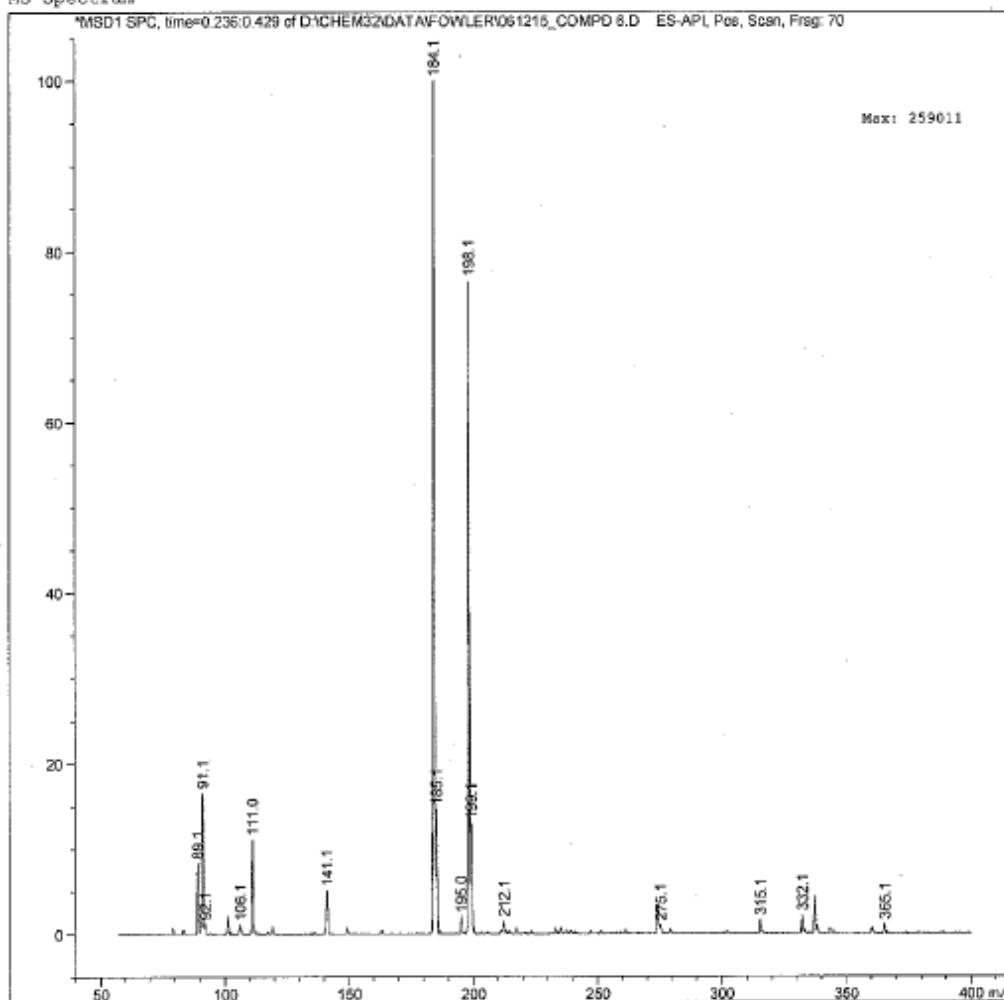
Sample Name : 061215_compd 6.D



Acq. Operator : So Jeong
Acq. Instrument : Instrument 1 Location : Vial 1
Injection Date : 6/12/2015 6:30:42 PM Inj : 1
Inj Volume : 1.0 µl

Acq. Method : D:\CHEM32\METHODS\DIR-INJ-POS.M
Last changed : 6/12/2015 6:29:08 PM by So Jeong
(modified after loading)
Analysis Method : D:\CHEM32\DATA\FOWLER\061215_COMPD 6.D\DA.M (DIR-INJ-POS.M, From Data File)
Last changed : 6/12/2015 6:32:18 PM by So Jeong
Method Info : Direct-inject (FIA) ESI positive
A1 (0.1%Ac): B1 (MeOH); 25:75(v:v); 0.25ml/min

MS Spectrum



Instrument 1 6/12/2015 6:32:53 PM rajesh

Page 1 of 1

Print of window 80: MS Spectrum

Data File : D:\CHEM32\DATA\FOWLER\061215_COMPD 7B.D

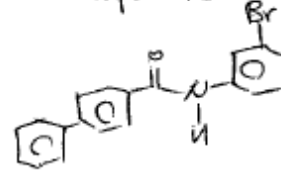
Sample Name : 061215_compd 7b.D

Acq. Operator : So Jeong
Acq. Instrument : Instrument 1 Location : Vial 1
Injection Date : 6/12/2015 6:34:30 PM Inj : 1
Inj Volume : 1.0 µl

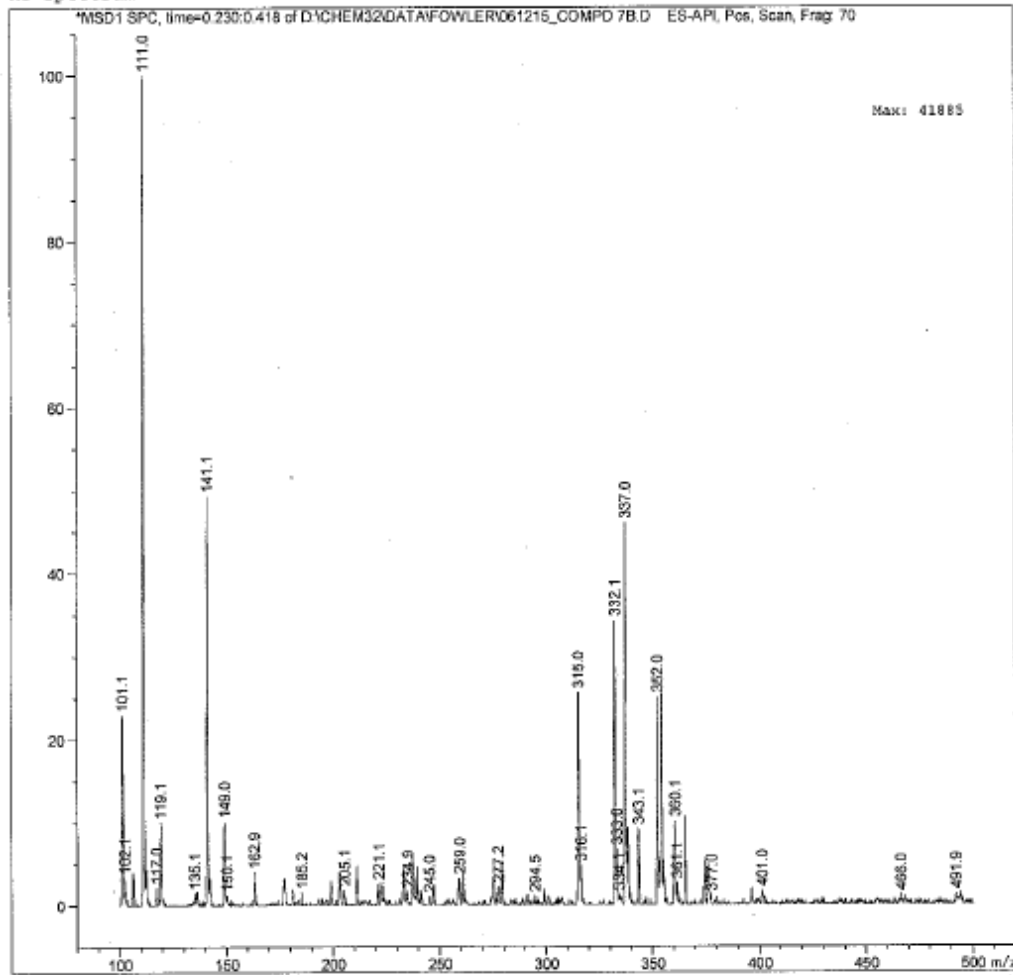
Acq. Method : D:\CHEM32\METHODS\DIR-INJ-POS.M
Last changed : 6/12/2015 6:33:45 PM by So Jeong
(modified after loading)
Analysis Method : D:\CHEM32\DATA\FOWLER\061215_COMPD 7B.D\DA.M (DIR-INJ-POS.M, From Data File)

Last changed : 6/12/2015 6:36:06 PM by So Jeong
Method Info : Direct-inject (FIA) ESI positive
AL (0.18Ac): B1 (MeOH); 25:75 (v:v); 0.25ml/min

Compd 7b



MS Spectrum



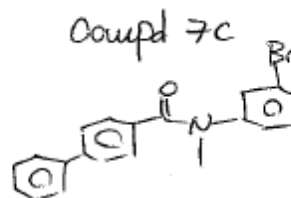
Instrument 1 6/12/2015 6:38:08 PM rajesh

Page 1 of 1

Print of window 80: MS Spectrum

Data File : D:\CHEM32\DATA\FOWLER\061215_COMPD 7C.D

Sample Name : 061215_compd 7c.D



Acq. Operator : So Jeong
Acq. Instrument : Instrument 1 Location : Vial 1
Injection Date : 6/12/2015 6:39:07 PM Inj : 1
Inj Volume : 1.0 µl

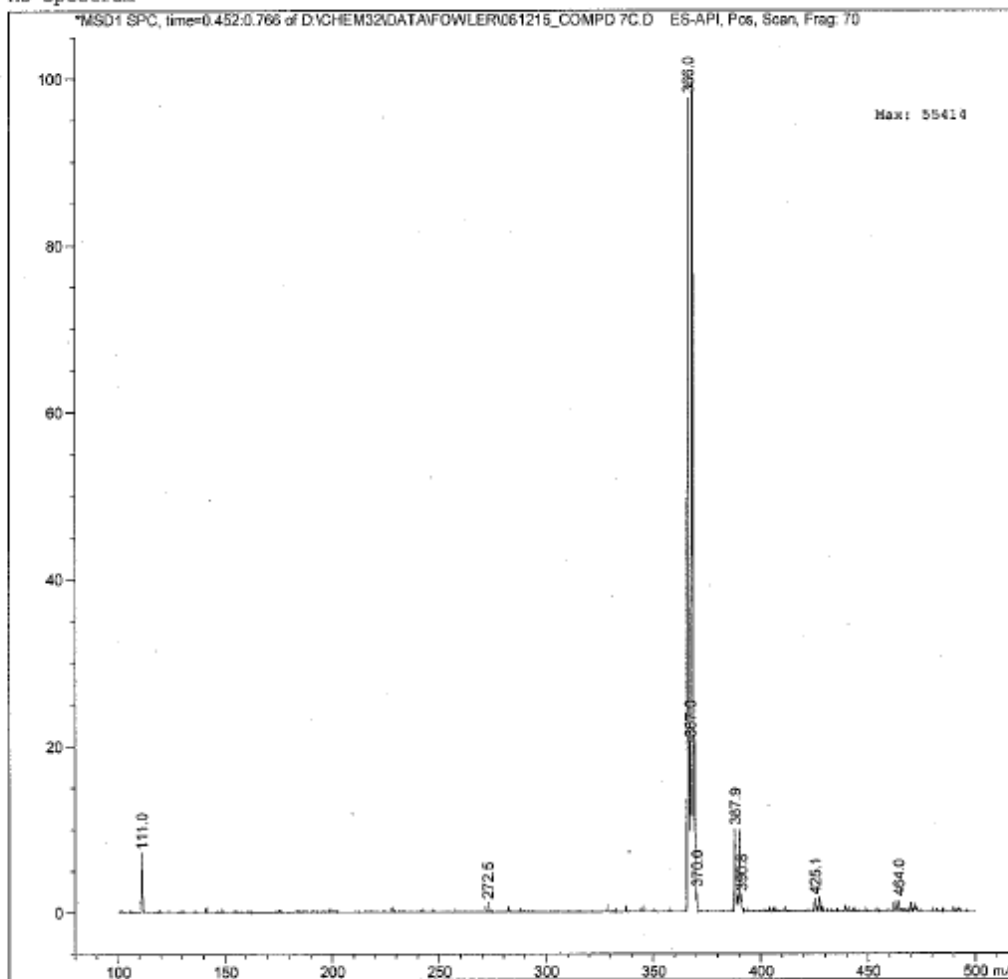
Acq. Method : D:\CHEM32\METHODS\DIR-INJ-POS.M
Last changed : 6/12/2015 6:36:08 PM by So Jeong
(modified after loading)

Analysis Method : D:\CHEM32\DATA\FOWLER\061215_COMPD 7C.D\DA.M (DIR-INJ-POS.M, From Data File)

Last changed : 6/12/2015 6:40:43 PM by So Jeong

Method Info : Direct-inject (FIA) ESI positive
A1 (0.1%Ac): B1 (MeOH); 25:75(v:v); 0.25ml/min

MS Spectrum



Instrument 1 6/12/2015 6:41:04 PM rajesh

Page 1 of 1

Print of window 80: MS Spectrum

Data File : D:\CHEM32\DATA\FOWLER\061215_NOR 7.D

Sample Name : 061215_nor 7.D

Acq. Operator : So Jeong

Acq. Instrument : Instrument 1

Location : Vial 1

Injection Date : 6/12/2015 6:46:22 PM

Inj : 1

Inj Volume : 1.0 µl

Acq. Method : D:\CHEM32\METHODS\DIR-INJ-POS.M

Last changed : 6/12/2015 6:44:04 PM by So Jeong

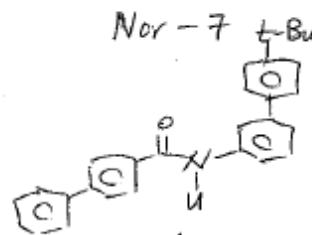
(modified after loading)

Analysis Method : D:\CHEM32\DATA\FOWLER\061215_NOR 7.D\DA.M (DIR-INJ-POS.M, From Data File)

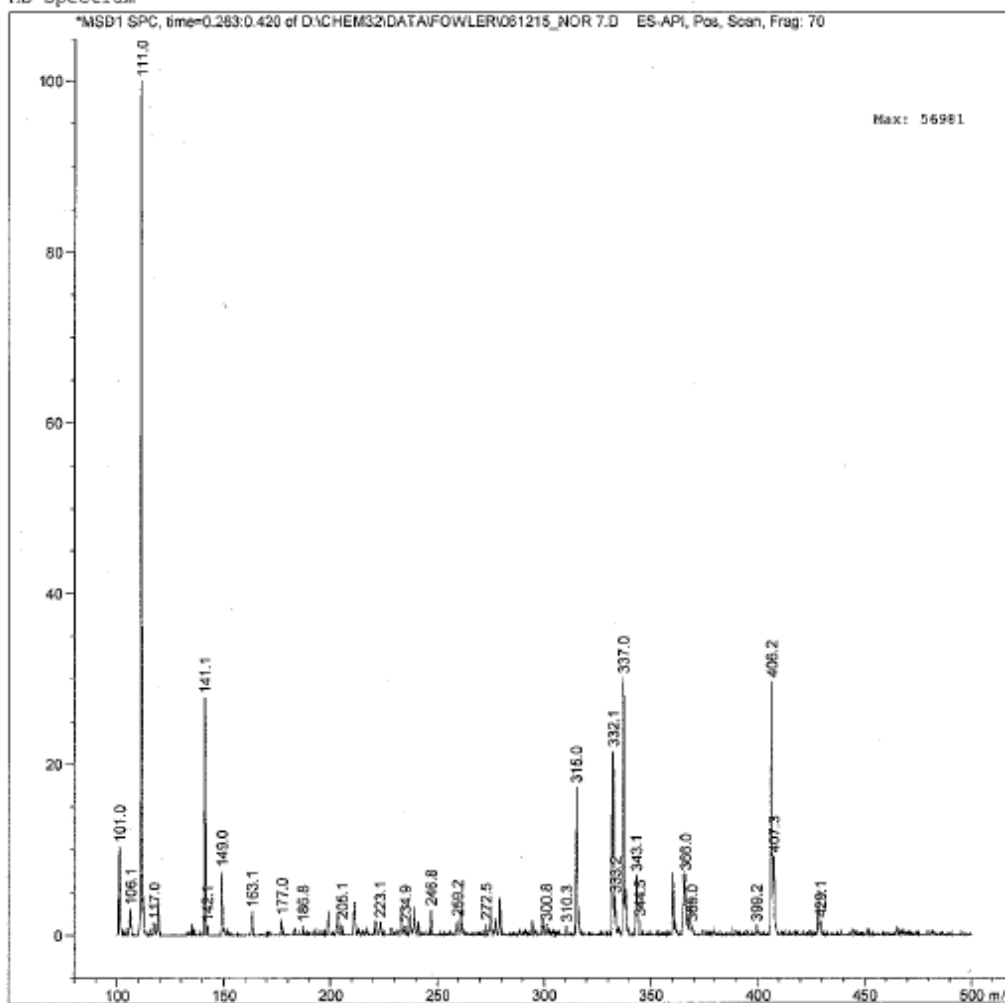
Last changed : 6/12/2015 6:47:58 PM by So Jeong

Method Info : Direct-inject (FIA) ESI positive

AI (0.1%Ac): B1 (MeOH); 25:75(v:v); 0.25ml/min



MS Spectrum



Instrument 1 6/12/2015 6:48:18 PM rajesh

Page 1 of 1

CHAPTER 3.

Tetraethylene Glycol Promoted Two-Step, One-Pot Rapid Synthesis of Indole-3-[1-¹¹C]Acetic Acid

1. Abstract

Auxins are plant hormones which are essential in plant growth and development. Indole-3-acetic acid (IAA) is the most abundant naturally occurring auxin. However the biosynthetic pathway for IAA and the in vivo transformation pathway and mechanism for its biological activity is still unclear. IAA labeled with carbon-11 has been developed as a radiotracer to better understand its involvement in plant growth and development. Herein we describe rapid synthesis of [¹¹C]IAA from radiocyanation of gramine with radioprecursor, [¹¹C]HCN, in boiling tetraethylene glycol (TEG) under no-carrier-added conditions to form the [¹¹C]indole acetonitrile followed by basic hydrolysis to form [¹¹C]IAA. The use of TEG enabled both cyanation and hydrolysis steps to be performed in the same pot. By optimizing both steps, [¹¹C]IAA was produced with total synthesis time (including HPLC purification) of 40 min and total production cycle including formulation in a small volume for plant studies of 50 – 55 min. Radiochemical purity was > 98% and specific activity was 47.4 ± 12.5 GBq/ μ mol.

2. Introduction

Auxins are important plant hormones that play an essential role in plant cell growth and are involved in a wide variety of developmental processes, including initiation of leaf primordia,

apical dominance, phototropism, fruit development, and lateral root production¹. In particular, the plant hormone auxin directs many developmental responses including the elaboration of branching patterns in the root by ubiquitylation and degradation of transcriptional co-repressor proteins called Aux/IAAs². Auxin signaling components are distributed throughout the plant and proliferate via several different biosynthetic pathways to control specific developmental processes.

Indole-3-acetic acid (IAA) is the most common and potent among naturally occurring auxins³. Although IAA was structurally characterized in the 1930s, its translocation in the whole plant in response to growth and environmental stimuli is still not completely understood⁴. There are four tryptophan-dependent pathways which have been proposed for the biosynthesis of IAA. These include indole-3-aldoxime, indole-3-pyruvic acid, indole-3-acetamide and tryptamine pathways, none of which has been characterized⁵.

Positron emission tomography (PET) has been used as an efficient tool to monitor the translocation of plant signaling molecules and carbon and nitrogen resource distribution in real time via *in vivo* imaging of whole plants⁶. The use of PET to study plant metabolism has stimulated the development of rapid synthetic procedures for the radiosynthesis of PET radioisotopes (e.g. carbon-11: $t_{1/2} = 20.4$ min, nitrogen-13: $t_{1/2} = 10$ min.) and labeled small organic radiotracers designed to study plant metabolism and signaling pathways⁷. The development and application of PET radiotracers to probe the auxin biosynthesis pathway, to study sites of auxin biosynthesis, and auxin distribution and metabolism builds on our recent development of a rapid synthesis of [¹¹C]IAA.

Most radiotracers for plants, with the exception of the radioactive gases (e.g. ¹¹CO₂, ¹³NH₃, ¹³N₂), require formulation in appropriate vehicles and volumes for administration to roots and

leaves. We previously reported the radiosynthesis of indole-3- ^{11}C acetic acid (^{11}C IAA) and its biosynthetic precursor, ^{11}C indole-3-acetonitrile (^{11}C IAN) as well as indole-3- ^{11}C acetamide (^{11}C IAM) as tools to examine signaling pathways for plant development^{7c}. The basic strategy for the synthesis of IAA was derived from the first publication describing cyanation of gramine with sodium cyanide followed by hydrolysis to IAA in high yield (~90%) for synthesis of tryptophol by H.R. Snyder in 1948⁸. Gramine was converted to ^{11}C indole-3-acetonitrile (^{11}C IAN) then to ^{11}C IAA via ^{11}C cyanide displacement followed by hydrolysis. However there were critical constraints for ^{11}C IAA production for plant PET imaging including the need for the removal of a large excess of gramine after cyanation and final formulation of pure ^{11}C IAA in microliter volume ($> 50 \mu\text{L}$). This required optimization of the thereby it required to optimize synthesis conditions and the development of appropriate formulation methods for practical and frequent ^{11}C IAA production for plant studies.

In the past year, we further polished the original synthesis method and also developed a reliable and remotely controllable formulation method to support our routine production of a solution of ^{11}C IAA which is concentrated enough for in vivo plant imaging purposes (0.2 – 0.4 GBq/0.15 – 0.3 mL , **Figure 1**)⁹. Even though both overall radiochemical yield and concentration of ^{11}C IAA were doubled and specific activity was improved by a factor three via this reinvestigated strategy, several drawbacks still existed and limited the routine production including (1) requirement for massive amounts of starting radioactivity (500 to 600 mCi at EOB) causing high radiation exposure to the production radiochemists; (2) complicated procedures and many manipulations for production requiring extra time. According to this method, the total production time with this method ranges from 80 – 85 min, which is four half-lives of carbon-11. In order to compensate for the radioactive decay due to the long radiosynthesis and formulation

times and assure enough radioactivity for a plant imaging study, previous production generally required a 15 – 25 GBq (you switched from mCi to MBq) of starting $H^{11}CN$ radioactivity. The large amount of starting radioactivity and considerable handling during formulation resulted in unacceptably high radiation exposure to chemistry personnel.

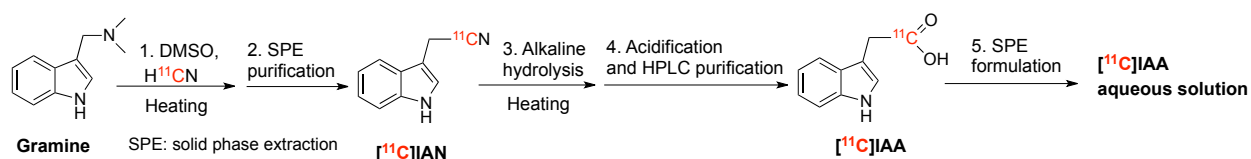


Figure 1. Previously reported radiosynthesis process of $[^{11}C]IAA$ ⁹

With the aim of developing an efficient radiosynthesis method, i.e. the total process time at 60 min or less (*rule-of thumb of carbon-11 labeled radiotracer production: overall time < 3 half-lives*), as well as reducing radiation exposure to the production radiochemists, we developed a simplified two-step, one-pot method for the radiosynthesis of $[^{11}C]IAA$ which is significantly faster and which requires far less starting radioactivity.

3. Experimental details

3.1. General

All commercial chemical reagents, 3-(dimethylaminomethyl)indole (gramine), indole-3-acetic acid, indole-3-acetonitrile and indole-3-acetamide, and solvents for synthesis and analysis were purchase from Sigma-Aldrich Chemical Co. (St. Louis, MO, USA) with a minimum of ACS reagent grade and used without further purification. Solid phase extraction (SPE) cartridges (SepPak® C18 plus) manufactured by Waters (Waters® Association, MA, USA) were used. The reaction was carried out in a 10cc microwave reaction vial (Biotage® INC., VA, USA) to endure high pressure and sealed by a particular cap and septa (Biotage® Inc., VA, USA). Thus, semi-

reflux reaction system was maintained with a variety of alcoholic solvent/water solvent for hydrolysis and water was condensed on the cap.

Preliminary model reactions performed without radioisotope labeling were characterized by ultra-high performance liquid chromatography (UHPLC) using an Agilent model 1200 system (Agilent Technologies Inc., Santa Clara, CA). High and low levels of radioactivity were measured using a Capintec CRC-712MV and a Capintec CRC-ultra radioisotope dose calibrator (Capintec Inc. NJ, USA) respectively. Semi-preparative high performance liquid chromatography (HPLC) was performed using a Knauer HPLC system equipped with a model K-1001 pump, a model 87 variable wavelength monitor, a NaI detector and a SRI peak simple integration system. Analytical HPLC was performed using a Knauer model K-1001 pump, a Knauer model K2501 UV detector (254nm), a Geiger Muller ionization detector and a SRI Peak simple integration System. Radiochemical yields (decay-corrected back to end of cyclotron bombardment (EOB)) were obtained based on the total radioactivity trapped in the reaction vessel at the start of the reaction. Specific activities, decay corrected back to EOB and recorded in mCi/nmol, were determined from the C-11 activity in the product peak in the HPLC and the mass of compound. Total synthesis times were calculated from EOB to the end of radiotracer formulation.

3.2. Production of [¹¹C]CO₂ and [¹¹C]HCN

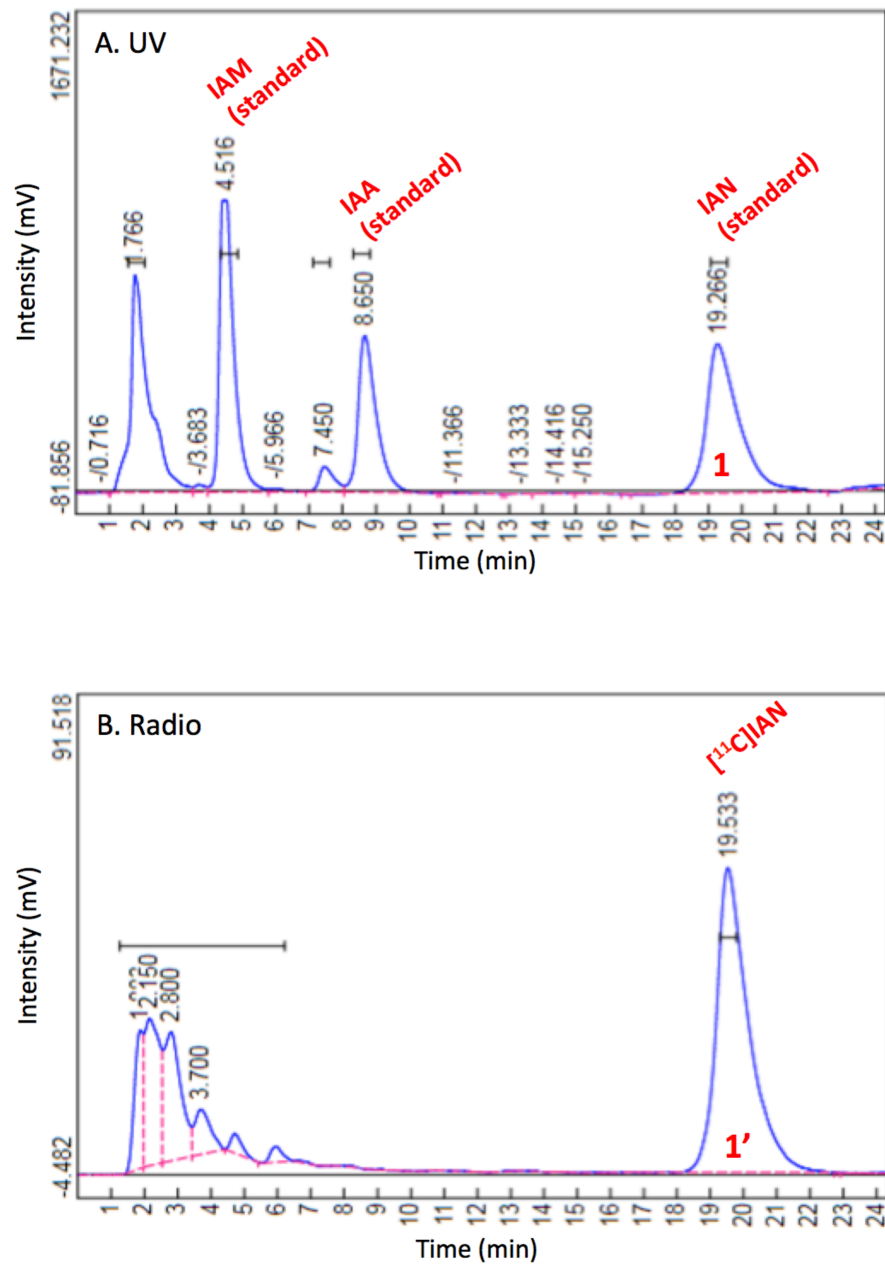
Carbon-11 was generated as [¹¹C]CO₂ using 17.4 MeV proton irradiation of N₂ gas target containing 100 ppm O₂ to induce the ¹⁴N(p, α)¹¹C nuclear reaction. Irradiations were carried out on the BNL EBCO TR-19 cyclotron. The [¹¹C]HCN was produced via automated gas phase synthesis by a homemade system¹⁰. Briefly, [¹¹C]CO₂ produced from this process was collected

over molecular sieves, catalytically reduced to $[^{11}\text{C}]\text{CH}_4$ with H_2 over Ni at 420°C . The $[^{11}\text{C}]\text{CH}_4$ was converted to $\text{H}[^{11}\text{C}]\text{CN}$ by adding gaseous ammonia and passage through a Pt furnace at 950°C at a flow rate of $350\sim 400\text{mL}/\text{min}$. Radioactivity measurements were made in a Capintec CRC-712MV radioisotope dose calibrator (Capintec Inc., Ramsey, NJ).

3.3. General radioanalytical procedures for optimizing the $[^{11}\text{C}]$ cyanation and hydrolysis steps

During the optimization, the radiochemical yield of the $[^{11}\text{C}]$ cyanation reaction was determined by HPLC analysis of a $50\mu\text{L}$ aliquot of the crude mixture from the $[^{11}\text{C}]$ cyanation reaction. HPLC conditions: acetonitrile/water containing formic acid (0.1% v/v) (25/75) at a flow rate of $1.5\text{mL}/\text{min}$ on Phenomenex Gemini NX C18 column ($250 \times 4.6\text{ mm}$). The C-11 labeled intermediate, $[^{11}\text{C}]\text{IAN}$, was eluted at 19.5 min (Figure 2). For optimizing the hydrolysis step, the same HPLC conditions as above were used. Radiochemical yields in Table 1 and Table 2 are calculated by comparing the radioactivity eluted in the product peak to the total radioactivity injected. The chemical identities of resulting compounds were determined by co-injection with commercially available standards of IAN and IAA.

Figure 2. A typical analytical HPLC profile of [^{11}C]cyanation of gramine to [^{11}C]IAN

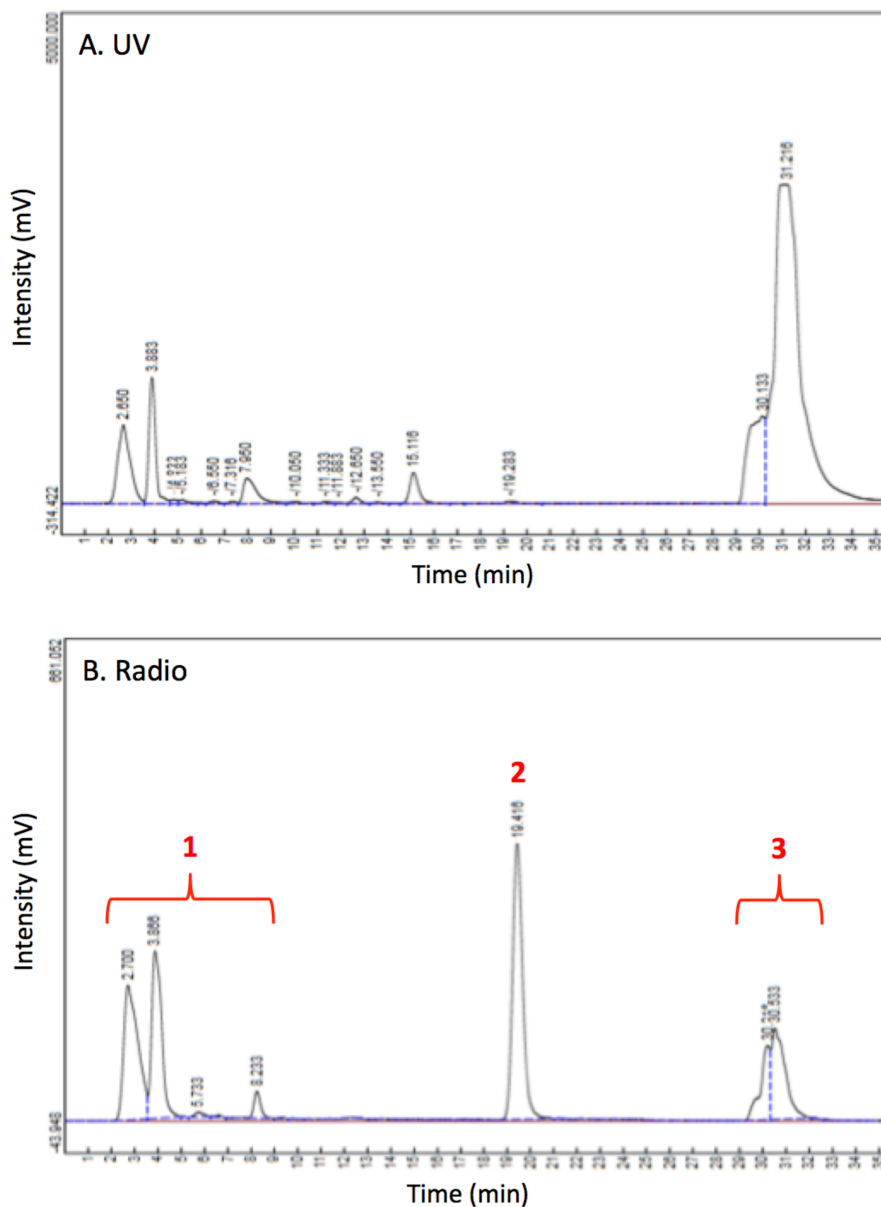


The chemical identities of crude mixture from [^{11}C]cyanation of gramine were determined by co-injection with commercially available standards of IAM, IAA and IAN. Peak 1 in UV profile (A) indicates IAN without C-11 labeling; correspondent peak 1' in Radio profile (B) shows [^{11}C]IAN yield by [^{11}C]cyanide displacement.

3.4. Radiosynthesis of [¹¹C]indole-3-acetic acid via two-step, one-pot method based on optimized conditions

Radiosynthesis was performed based on the optimized conditions shown on entry 8 in table 1 and entry 15 in table 2. Gramine (2 mg, 11.5 μ mol), K₂CO₃ (2 mg, 14.5 μ mol) was prepared in the U-shape reaction vessel with a stir bar and dissolved in 0.3 mL of TEG containing 20 μ L of water. After trapping the [¹¹C]cyanide directly into the reaction vessel for 3 min at room temperature, the cyanation reaction was performed at 145 $^{\circ}$ C for 5 min. To the crude reaction mixture, 3 mmol of NaOH aqueous solution (10 M solution, 0.3 mL) and water (0.43 mL) was added. The reaction vessel was submitted into 145 $^{\circ}$ C oil bath again and reaction mixture was vigorously stirred for 8min at the same temperature. The hydrolysis was quenched with 1.4 equivalent of conc. HCl (0.35 mL, 4.2mmol). The resulting mixture containing reddish colored residue was diluted with 1 mL of HPLC solvent and injected into semi-preparative HPLC for purification. Pure [¹¹C]IAA was eluted at 19 min using a Phenomenex Gemini C18 column (250 \times 10.00mm) with isocratic solvent system (acetonitrile/water containing formic acid (v/v 0.1%)=25/75) and flow rate set at 5.5mL/min (Figure 3). Total synthesis time including semi-prep purification was 45~50 min.

Figure 3. A typical semi-preparative HPLC purification profile of [^{11}C]IAA



The crude mixture from the synthesis of [^{11}C]IAA via two-steps-one-pot method was purified by preparative HPLC: highly polar C-11 labeled impurities was eluted from 2 min to 8min (1); [^{11}C]IAA (2) was eluted at 19.4 min and separated; Isocratic solvent system (acetonitrile/water containing formic acid (v/v 0.1%)=25/75) was switched at 22min to 100% of acetonitrile to elute all organic C-11 labeled impurities (3) left inside the HPLC column.

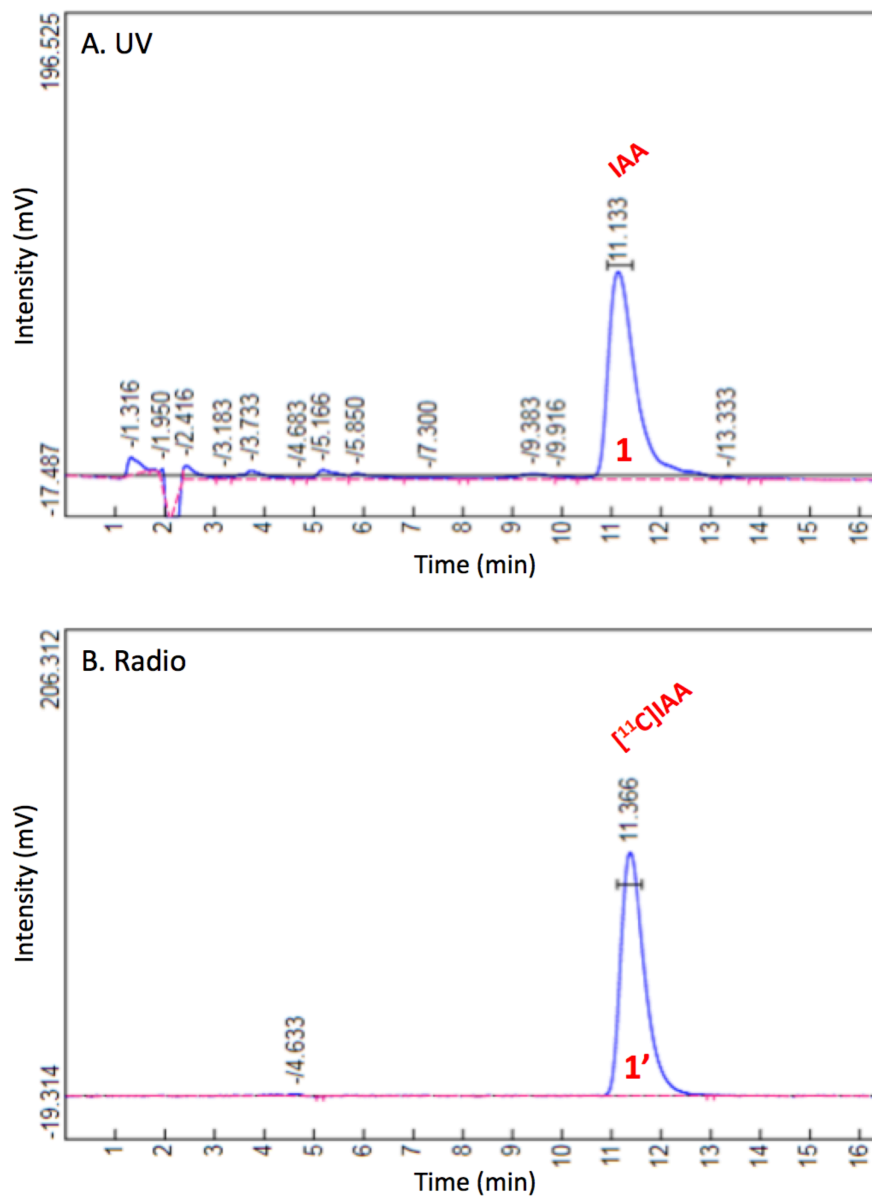
3.5. Formulation of [¹¹C]indole-3-acetic acid ([¹¹C]IAA)

The formulation procedure was modified and optimized based on our previous study⁹. The pure [¹¹C]IAA, from the semi-preparative HPLC was diluted with aqueous formic acid solution (0.1% v/v, 40 mL) then passed through a C18 plus SepPak cartridge. The cartridge holding [¹¹C]IAA was rinsed with 5 mL of deionized water and then dried with air to minimize dead volume of water left. The [¹¹C]IAA was eluted with diethyl ether (1.5mL) into the final product vial containing 20 μ L of MES buffer solution (2-(N-morpholino)ethanesulfonic acid, 5% w/v). The product was concentrated by drying diethyl ether with a stream of Ar at 50°C for 1min. One production cycle from EOB to the formulation procedure required 55~60 min.

3.6. Quality control and specific activity determination

Quality control and specific activity determination was determined as described previously⁹. Briefly the radiochemical purity and specific activity of [¹¹C]IAA was determined by an analytical HPLC system with a Gemini C18 analytical HPLC column (250 \times 4.6 mm, 5 μ m, Phenomenex) using acetonitrile/water containing formic acid (0.1% v/v) (25/75) at a flow rate of 1.5mL/min. The [¹¹C]IAA eluted at 11 min. A UV standard calibration curve was established using an authentic sample of IAA and used for the mass determination (Figure 4-A). The injected radioactivity was measured in the range of MBq using a low dose Capintec radioisotope dose calibrator. The specific activity was determined as the ratio of the injected radioactivity (GBq, decay-corrected to EOB) and mass (μ mol). The radiochemical purity (%) was determined by integrating radio peaks on the analytical HPLC profile (Figure 4-B). The chemical identity of the product was determined by co-injection with a standard indole-3-acetic acid sample.

Figure 4. A typical analytical HPLC for quality control of [^{11}C]IAA



After purification and formulation of final product [^{11}C]IAA, radiochemical purity and specific activity of the final product was determined by analytical HPLC without coinjection of unlabeled IAA. The integration area of peak 1 in the UV profile (A) indicates mass of a known amount of purified [^{11}C]IAA; radiochemical purity of [^{11}C]IAA was determined by integration of peak 1' in the radio profile (B)

4. Results and discussion

When considering the whole synthetic process of [^{11}C]IAA (Figure 1), we first focused on eliminating the step of solid phase extraction (SPE) purification of intermediate [^{11}C]IAN. In our previous report^{7c, 9}, dimethyl sulfoxide was used in nucleophilic [^{11}C]cyanation for synthesizing [^{11}C]IAN from gramine and H^{11}CN . Except for the residual amount of ammonia (NH_3) from production of H^{11}CN , there was no other base involved in the nucleophilic [^{11}C]cyanation. Although DMSO provided a very good yield for $^{11}\text{CN}^-$ substitution, it inhibited the alkaline hydrolysis of [^{11}C]IAN and required removal by an SPE step^{7c}. In order to switch to another solvent system, which could be compatible with both efficient nucleophilic [^{11}C]cyanation and alkaline hydrolysis reactions, we resorted to the conditions reported by Snyder and Pilgrim over six decades ago.⁸ In their synthesis of IAA, gramine and NaCN were reacted in boiling aqueous ethanol solution for over eight hours to give IAN and IAM with ~ 90% overall yield.

Inspired by this original process, we designed a two-step, one-pot method for the radiosynthesis of [^{11}C]IAA (Figure 5). In the initial test of the one-pot IAA synthesis, gramine, K_2CO_3 and KCN were added into aqueous ethanol solution and the reaction mixture was boiled for 10 min; after which concentrated base NaOH was immediately added into this mixture and maintained at boiling status for an additional 10 min. The results from the analysis of the reaction mixture by analytical HPLC proved that a trace amount of IAA was formed. Encouraged by these results, we immediately conducted the [^{11}C]cyanation reaction under similar conditions. Analysis by radio-HPLC showed an 8% yield of [^{11}C]IAN from the [^{11}C]cyanation reaction. In addition, the detection of a trace amount of [^{11}C]IAA also proved the

feasibility of the radiosynthesis of [^{11}C]IAA without the purification of the intermediate [^{11}C]IAN (Table 1, Entry 1). We then carried out a series of radiosynthesis experiments utilizing this two-step, one-pot strategy.

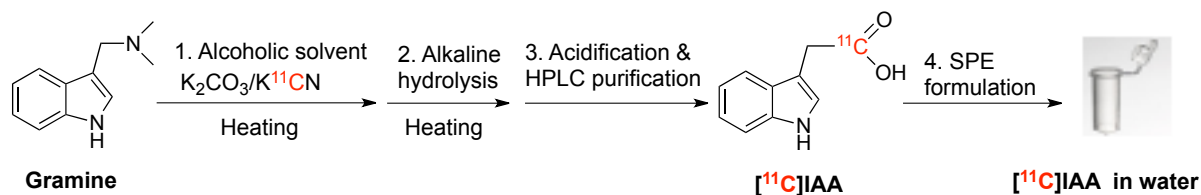
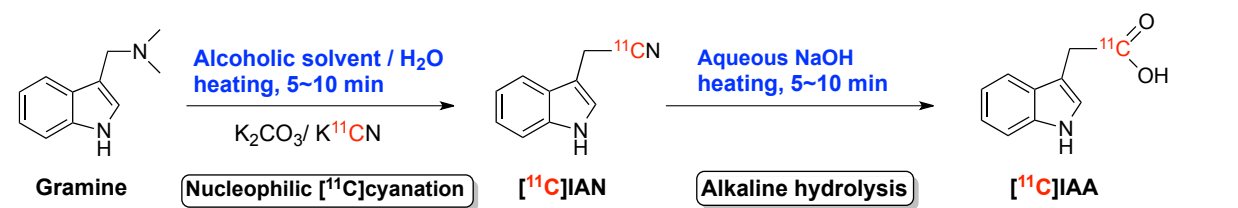


Figure 5. Scheme of designed two-step-one-pot method

Hoping to improve the yield of the [^{11}C]cyanation reaction, ethanol was replaced with ethylene glycol (EG) and a higher reaction temperature (145 °C) was tested and the results showed that these changes clearly benefited the reaction (Entry 2). At this moment, another alcoholic solvent, tetraethylene glycol (TEG), was brought to our attention because it showed very good compatibility with nucleophilic substitution reactions¹¹. Presumably, this bis-terminal hydroxyl oligoether can act as a general $\text{S}_{\text{N}}2$ reaction promoter by chelating with metallic cations and decreasing their interaction with the anion. Therefore, the nucleophilicity of an anion, such as cyanide ion, will be greatly enhanced. The next radiolabeling experiment, in which TEG and water were used as solvents, provided very promising results and the yield of [^{11}C]cyanation reaction dramatically improved to 68% (Entry 3). The overall yield of entire synthesis process, however, was still not adequate. An additional experiment showed that a shorter reaction time was better for the [^{11}C]cyanation reaction (Entry 4). The more meaningful result was that the overall yield sharply increased to 38% by increasing the base concentration (from 2 mmol to 3 mmol) and water volume in the hydrolysis step. At this stage, we investigated the effect of temperature on the [^{11}C]cyanation reaction. The lower reaction temperature was less favored

since it decreased the reaction yield (Entry 5). Increased temperature did not benefit the reaction, either (Entries 6 – 7). When water was removed entirely from the [^{11}C]cyanation reaction, the yield clearly dropped (Entry 8). When only a small portion of water (0.02 mL) added, the [^{11}C]cyanation reaction yield increased to 81% (Entry 9). We speculate that the addition of water helped to dissolve the K_2CO_3 salt and that bringing potassium cation into the reaction system improved the solubility of [^{11}C]cyanide anion in organic solvent. Presumably, increasing the amount of gramine precursor would improve the [^{11}C]cyanation reaction yield. However, since we eliminated the purification of the [^{11}C]IAN intermediate by SPE, the total mass of crude reaction mixture loaded onto the semi-prep HPLC column when purifying the final product [^{11}C]IAA already exceeded that of our previous reported method^{11,12}. In order to assure adequate resolution for purification of the final product [^{11}C]IAA and to extend the lifetime of the semi-prep HPLC column, we opted not to attempt to improve the yield by simply increasing the amount of starting material.

Table 1. Screen of better reaction conditions^{a, b}



Entry	[^{11}C]Cyanation reaction conditions ^c	[^{11}C]IAN ^d RCY (%)	Alkaline hydrolysis conditions ^e	[^{11}C]IAA Overall RCY ^f (%)
1	EtOH/H ₂ O (0.6 mL/0.2 mL) 120 °C, 10 min	8	0.6 mL, 4 mmol 120 °C, 10 min	0.06
2	EG/H ₂ O (0.3 mL/0.1 mL) 145 °C, 10 min	20	0.3 mL, 2 mmol 145 °C, 10 min	4
3	TEG/H ₂ O (0.3 mL/0.1 mL) 145 °C, 10 min	68	0.3 mL, 2 mmol 145 °C, 10 min	3

4	TEG/H ₂ O (0.3 mL/0.1 mL) 145 °C, 5 min	75	0.6 mL, 3 mmol 145 °C, 5 min	38
5	TEG/H ₂ O (0.3 mL/0.1 mL) 140 °C, 5 min	56	0.6 mL, 3 mmol 140 °C, 5 min	29
6	TEG/H ₂ O (0.3 mL/0.1 mL) 150 °C, 5 min	73	0.6 mL, 3 mmol 145 °C, 8 min	37
7	TEG/H ₂ O (0.3 mL/0.1 mL) 160 °C, 5 min	75	N/A	N/A
8	TEG (0.3 mL) 145 °C, 5 min	62	0.75 mL, 3 mmol 145 °C, 8 min	33
9	TEG/H₂O (0.3 mL/0.02 mL) 145 °C, 5 min	81	0.75 mL, 3 mmol 145 °C, 8 min	25

^a A series of radiolabeling experiments was performed with a 2 min proton beam produced by a cyclotron. The ¹⁴N(p,α)¹¹C nuclear reaction was induced by the proton irradiation to generate the radioisotope ¹¹C (refer to **2. Experimental Section, General**).

^b Hydrogen [¹¹C]cyanide was produced by our in-house built H¹¹CN production system and trapped with K₂CO₃ in reaction vial efficiently as K¹¹CN form.¹²

^c Solvent, T (°C), t (min); EG (ethylene glycol); TEG (tetraethylene glycol)

^d RCY (radiochemical yield, decay-corrected) of [¹¹C]IAN was calculated based on HPLC analysis of a measured aliquot of the crude reaction mixture.

^e Total H₂O (mL), NaOH (mmol); temperature (°C), reaction time (min)

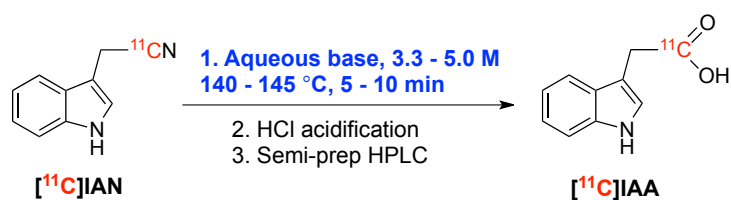
^f Overall RCY of [¹¹C]IAA was calculated based on HPLC analysis of measured aliquot of the crude product mixture for entry **1**, **2**, **3** and **6**; hydrolysis step was not applicable for entry **7**; overall RCY of [¹¹C]IAA was obtained after semi-prep HPLC purification for entry **4**, **5**, **8** and **9**.

At this stage, in addition to having optimized the [¹¹C]cyanation reaction conditions (Table 1, Entry 9), we had also gained important information about improving the alkaline hydrolysis reaction. There were two critical factors affecting hydrolysis of [¹¹C]IAN. The first was that a sufficient amount of water was needed for hydrolysis, which is clear when comparing results of two experiments (Table 1, Entries 3 and 4). Secondly, in order to assure a rapid hydrolysis compatible with the short half-life of carbon-11 isotope, a high reaction temperature (140 -160

°C) is needed. During the experimental process (Table 1, Entry 3), we found that a small amount of water condensed at the top of the reaction vessel. We attributed the removal of H₂O from the reaction mixture as the main cause of the low overall reaction yield (3%). On one hand, it decreased the amount of H₂O for the hydrolysis reaction; on the other hand, it clearly increased the concentration of NaOH, which could possibly cause more side reactions. After increasing total water amount to 0.6 mL, better reflux was observed and overall reaction yield was dramatically improved (Table 1, Entry 4).

With the optimized [¹¹C]cyanation reaction conditions in hand, we further scrutinized the alkaline hydrolysis conditions by fine-tuning several reaction parameters including the base strength, reaction time and reaction temperature (Table 2, Entries 10 to 15). The results showed that the combination of 0.75 mL of H₂O, 4 M NaOH and 8 min reaction time increased the hydrolysis reaction yield to 55% (Table 2, Entry 15). In addition to NaOH, LiOH, which could be a mild basic hydrolysis agent¹³, was also tested for the alkaline hydrolysis reaction and only gave 31% yield and so is less favored for this reaction (Table 2, Entry 16).

Table 2. Further optimization of hydrolysis reaction of [¹¹C]IAN to ¹¹C]IAA^a



Entry	Solvent ^b	NaOH (mmol)	Reaction time (min)	RCY [¹¹ C]IAA ^c (%)
10	TEG / H ₂ O (0.3 mL/0.6 mL)	2	10	19
11	TEG / H ₂ O (0.3 mL/0.6 mL)	3	8	46
12	TEG / H ₂ O (0.3 mL/0.6 mL)	3	10	42
13	TEG / H ₂ O (0.3 mL/0.6 mL)	3	5	35
14 ^d	TEG / H ₂ O (0.3 mL/0.6 mL)	3	8	34

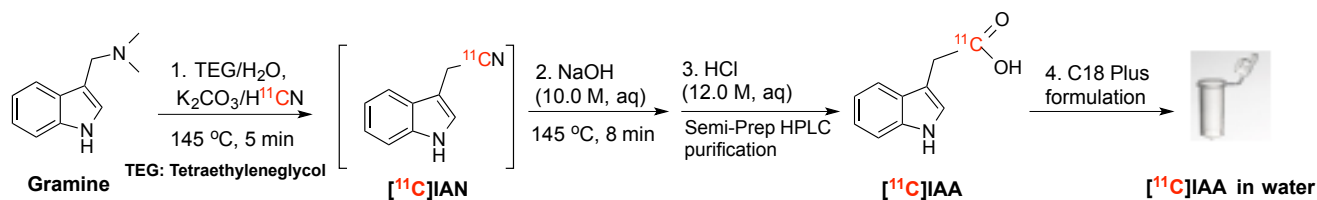
15	TEG / H₂O (0.3 mL/0.75 mL)	3	8	55
16	TEG / H ₂ O (0.3 mL/0.75 mL)	3	8	31

(LiOH)

^a Hydrolysis and [¹¹C]cyanation were carried out in the same reaction vessel without intermediate purification. ^b The solvents for hydrolysis came from the [¹¹C]cyanation reaction and extra water and NaOH were added. ^c [¹¹C]IAA was purified by semi-prep HPLC and RCY (decay-corrected) in this table refers to conversion in the hydrolysis step only ($100 \times [\text{¹¹C]IAA} / [\text{¹¹C]IAN}$). ^d All the experiments above were performed at 145 °C except for entry 14 which was conducted at 140 °C.

Once conditions for both the [¹¹C]cyanation and hydrolysis steps were optimized, a new two-step, one-pot method was established for rapidly synthesizing the PET radiotracer [¹¹C]IAA. By replacing the polar aprotic solvent DMSO with tetraethylene glycol, the SPE purification of reaction intermediate [¹¹C]IAN was successfully eliminated from the whole synthesis process. Both the nucleophilic [¹¹C]cyanation and alkaline hydrolysis reactions can be consecutively performed in one pot. This change obviously simplified the synthesis process and shortened the total synthesis time from 80 -85 min to 55 – 60 min. In addition, the investigation of several reaction parameters for both reactions, such as reaction temperature, reaction time, solvent amount and base strength, etc., helped to further polish the whole synthetic process. To confirm the robustness of our newly developed synthetic method, we combined the optimum reaction conditions for both reactions (Table 1, Entry 8 and Table 2, Entry 15) and repeated the synthesis of [¹¹C]IAA five times under the optimized reaction conditions (Figure 6). The results show the high reliability of this newly established synthetic process. With a two-min cyclotron beam time, which generates ~ 8.1 GBq (220 mCi) of ¹¹CO₂, 0.22-0.46 GBq (6.1-12.4 mCi) of [¹¹C]IAA product was obtained at the end of synthesis (EOS). The overall radiochemical yield (ORCY) for both steps was $33 \pm 9.5\%$ (calculated from H¹¹CN radioactivity collected in reaction vessel)

and was $18.9 \pm 6.4\%$ (calculated from $^{11}\text{C}\text{O}_2$ radioactivity generated from a two-min cyclotron beam). The radiochemical purity of final product was 98% and the specific activity of final product was 47.4 ± 12.5 GBq/ μmol . The complete processing time, calculated from end of bombardment (EOB) to the end of formulation, ranged from 55 to 60 min.



Overall radiochemical yield (ORCY, decay-corrected): $33 \pm 9.5\%$; range from 24 - 51 % (n = 5, calculated from H^{11}CN activity)
 ORCY (decay-corrected): $18.9 \pm 6.4\%$; range from 14.9 - 30.9 % (n = 5, calculated from $^{11}\text{C}\text{O}_2$ activity)
 Radiochemical purity > 98 %, Specific activity: 47.4 ± 12.5 GBq/ μmol (n = 5, range from 44.4 - 96.2 GBq/ μmol)
 Total production time (including purification and formulation): 55 - 60 min

Figure 6. Reaction parameters of the optimized two-step, one-pot method

5. Conclusion

In summary, we successfully developed a two-step, one-pot method for routine production of $[\text{ }^{11}\text{C}]\text{IAA}$ to support plant imaging research. By replacing the polar aprotic solvent DMSO with protic tetraethylene glycol, both $[\text{ }^{11}\text{C}]\text{cyanation}$ and alkaline hydrolysis reactions were performed in same pot without purification of the $[\text{ }^{11}\text{C}]\text{IAN}$ intermediate and whole process successfully yielded $[\text{ }^{11}\text{C}]\text{IAA}$ with high radiochemical purity and high specific activity with reasonable radiochemical yield. The total synthesis time required is 40 min and the entire production cycle including HPLC purification and formulation product into a small volume of aqueous solution (0.15 – 0.3 mL) was complete in 55 min. Considering the short half-life of carbon-11 (20.4 min), reducing the total production time to less than 60 min and simplifying the synthesis

procedure is exceedingly beneficial to the practical use of this tracer for in vivo PET imaging studies. Furthermore, the efficient [^{11}C]cyanation procedure specifically using tetraethylene glycol with potassium salts as a nucleophilic substitution promoter is potentially useful for the development of other [^{11}C]cyanation reactions when preparing PET radiotracers containing the [^{11}C]cyano group. Research utilizing the radiotracer [^{11}C]IAA for in vivo plant studies via PET imaging is in progress.

6. References

1. Ludwig-Muller, J., Indole-3-butyric acid in plant growth and development. *Plant Growth Regul.* **2000**, *32* (2-3), 219-230.
2. (a) Chapman, E. J.; Estelle, M., Mechanism of Auxin-Regulated Gene Expression in Plants. *Annu Rev Genet* **2009**, *43*, 265-285; (b) Chapman, E. J.; Estelle, M., Cytokinin and auxin intersection in root meristems. *Genome Biol* **2009**, *10* (2).
3. Thimann, K. V.; Koepfli, J. B., Identity of the growth-promoting and root-forming substances of plants. *Nature (London, U. K.)* **1935**, *135*, 101-2.
4. Pollmann, S.; Duechting, P.; Weiler, E. W., Tryptophan-dependent indole-3-acetic acid biosynthesis by 'IAA-synthase' proceeds via indole-3-acetamide. *Phytochemistry (Elsevier)* **2009**, *70* (4), 523-531.
5. (a) Tivendale, N. D.; Davies, N. W.; Molesworth, P. P.; Davidson, S. E.; Smith, J. A.; Lowe, E. K.; Reid, J. B.; Ross, J. J., Reassessing the role of N-hydroxytryptamine in auxin biosynthesis. *Plant Physiol.* **2010**, *154* (4), 1957-1965; (b) Normanly, J., Approaching cellular and molecular resolution of auxin biosynthesis and metabolism. *Cold Spring Harb Perspect Biol* **2010**, *2* (1), a001594; (c) Phillips, K. A.; Skirpan, A. L.; Liu, X.; Christensen, A.; Slewinski, T. L.; Hudson, C.; Barazesh, S.; Cohen, J. D.; Malcomber, S.; McSteen, P., Vanishing tassel2 encodes a grass-specific tryptophan aminotransferase required for vegetative and reproductive development in maize. *Plant Cell* **2011**, *23* (2), 550-566.
6. (a) Robert, C. A. M.; Ferrieri, R. A.; Schirmer, S.; Babst, B. A.; Schueller, M. J.; Machado, R. A. R.; Arce, C. C. M.; Hibbard, B. E.; Gershenzon, J.; Turlings, T. C. J.; Erb, M., Induced carbon reallocation and compensatory growth as root herbivore tolerance mechanisms. *Plant, Cell and Environment* **2014**, *37* (11), 2613-2622; (b) Hanik, N.; Gomez, S.; Schueller, M.; Orians, C. M.; Ferrieri, R. A., Use of gaseous $^{15}\text{NH}_3$ administered to intact leaves of *Nicotiana tabacum* to study changes in nitrogen utilization during defence induction. *Plant, Cell and Environment* **2010**, *33* (12), 2173-2179; (c) Gomez, S.; Ferrieri, R. A.; Schueller, M.; Orians, C. M., Methyl jasmonate elicits rapid changes in carbon and nitrogen dynamics in tomato. *New Phytologist* **2010**, *188* (3), 835-844; (d) Thorpe, M. R.; Ferrieri, R. A.; Herth, M. M.; Ferrieri, R. A., ^{11}C -imaging: Methyl jasmonate moves in both phloem and xylem, promotes transport of jasmonate, and of photoassimilate even after proton transport is decoupled. *Planta* **2007**, *226* (2), 541-551; (e) Ferrieri, R. A.; Gray, D. W.; Babst, B. A.; Schueller, M. J.; Schlyer, D. J.; Thorpe, M. R.; Orians, C. M.; Lerdau, M., Use of carbon-11 in *Populus* shows that exogenous jasmonic acid increases biosynthesis of isoprene from recently fixed carbon. *Plant, Cell and Environment* **2005**, *28* (5), 591-602.
7. (a) Herth, M. M.; Thorpe, M. R.; Ferrieri, R. A., Synthesis of the phytohormone [^{11}C]methyl jasmonate via methylation on a C18 Sep Pak cartridge. *Journal of Labelled Compounds and Radiopharmaceuticals* **2005**, *48* (5), 379-386; (b) Kasel, M. C. K.; Schueller, M. J.; Ferrieri, R. A., Optimizing [^{13}N]N $_2$ radiochemistry for nitrogen-fixation in root nodules of legumes. *Journal of Labelled Compounds and Radiopharmaceuticals* **2010**, *53* (9), 592-597; (c) Reid, A. E.; Kim, S. W.; Seiner, B.; Fowler, F. W.; Hooker, J.; Ferrieri, R.; Babst, B.; Fowler, J. S., Radiosynthesis of C-11 labeled auxin (3-indolyl[1- ^{11}C]acetic acid) and its derivatives from gramine. *J. Labelled Compd. Radiopharm.* **2011**, *54* (8), 433-437.

8. Snyder, H. R.; Pilgrim, F. J., The preparation of 3-indoleacetic acid; a new synthesis of tryptophol. *J Am Chem Soc* **1948**, *70* (11), 3770.
9. Xu, Y.; Alexoff, D. L.; Kunert, A. T.; Qu, W.; Kim, D.; Paven, M.; Babst, B. A.; Ferrieri, R. A.; Schueller, M. J.; Fowler, J. S., Radiosynthesis of 3-indolyl[1-11C]acetic acid for phyto-PET-imaging: An improved production procedure and formulation method. *Appl. Radiat. Isot.* **2014**, *91*, 155-160.
10. Kim, D.; Alexoff, D.; Kim, S. W.; Hooker, J.; Ferrieri, R. A. 11C-Labeled cyanide production system. US20130045151A1, 2013.
11. Lee, J. W.; Yan, H.; Jang, H. B.; Kim, H. K.; Park, S.-W.; Lee, S.; Chi, D. Y.; Song, C. E., Bis-Terminal Hydroxy Polyethers as All-Purpose, Multifunctional Organic Promoters: A Mechanistic Investigation and Applications. *Angewandte Chemie, International Edition* **2009**, *48* (41), 7683-7686, S7683/1-S7683/39.
12. Kim, D.; Alexoff, D.; Kim, S. W.; Hooker, J.; Ferrieri, R. A. 11C-Labeled cyanide production system. 2012-13584033 20130045151, 20120813., 2013.
13. Dayal, B.; Salen, G.; Toome, B.; Tint, G. S.; Shefer, S.; Padia, J., Lithium hydroxide/aqueous methanol: mild reagent for the hydrolysis of bile acid methyl esters. *Steroids* **1990**, *55* (5), 233-7.

4. Radiosynthesis of [2-¹¹C]indole via rapid nucleophilic [¹¹C]cyanation followed by reductive cyclization

1. Abstract

A practical and efficient method for synthesis of Carbon-11 (¹¹C, β⁺ emitter, t_{1/2} = 20.4 min) labeled indole was developed using [¹¹C]cyanide as radiolabeling precursor. Based upon a report for synthesis of 2-nitrophenylacetonitrile, a highly reactive substrate 2-nitrobenzylbromide was tested for nucleophilic [¹¹C]cyanation and related reaction conditions were explored for quickly obtaining of 2-nitrophenyl [¹¹C]acetonitrile. Next, a Raney Nickel catalyzed reductive cyclization method was utilized for synthesizing desired [2-¹¹C]indole with hydrazinium monoformate as active reducing agent. After the extensive investigation for both reactions in several parameters, which including basicity, temperature and stoichiometry, an efficient and two-step method was established to reliably provide [2-¹¹C]indole with an overall radiochemical yield of 21 ± 2.2% (n = 5, ranging from 18 – 24%). The radiochemical purity of the final product was > 98% and specific activity was 176 ± 24.8 GBq/μmol (n = 5, ranging from 141 – 204 GBq/μmol). The total radiosynthesis time including product purification by semi-preparative HPLC was 50 – 55 min from end-of-bombardment.

2. Introduction

The synthesis of indole and its derivatives has played a prominent role in organic chemistry because of the importance of the indole ring containing natural products, such as alkaloids and

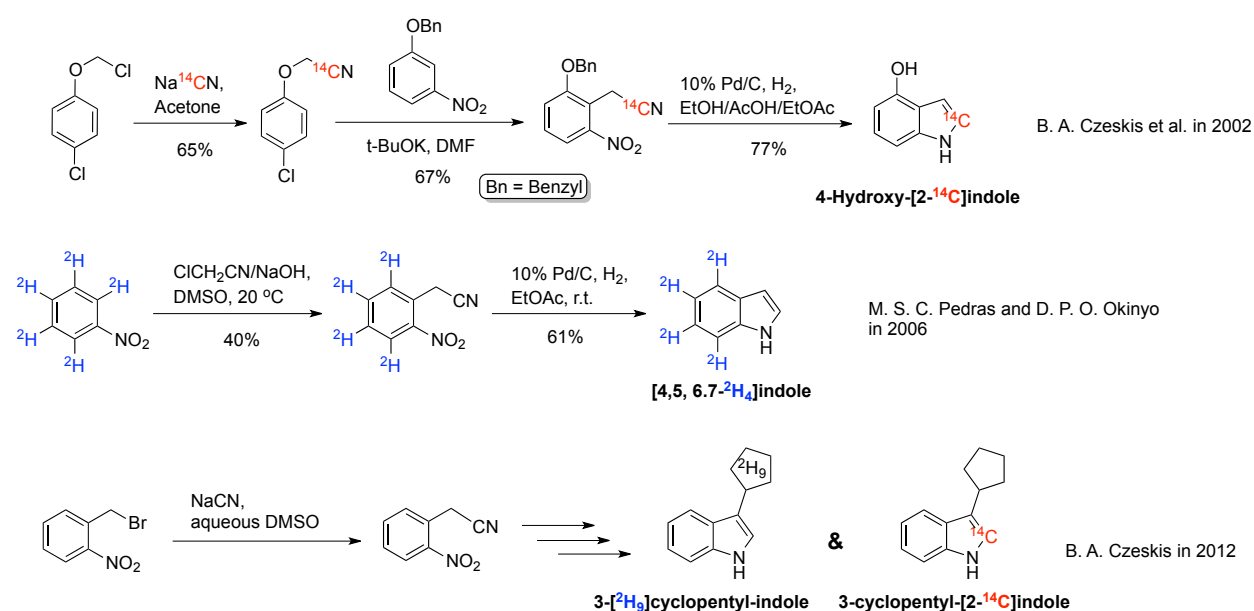
other biologically active molecules¹. One of the most important plant hormone, indole-3-acetic acid (auxin or IAA), is such an example and it plays a pivotal role in plant growth and development². It is known that indole is the core precursor for all five known auxin biosynthetic pathways including tryptophan-dependent and tryptophan-independent pathways³. Tracking the downstream flow of indole, could help us to understand some questions, such as the relative importance of the different auxin biosynthesis pathways in different plant tissues as well as the role of auxin biosynthesis in plant-microbe interactions⁴.

Our group has been interested in developing practical methods for synthesizing carbon-11 (¹¹C, $t_{1/2} = 20.4$ min) radiolabeled auxin and its biosynthetic intermediates and using them for investigation of plant metabolisms and for plant in vivo imaging study. Using [¹¹C]cyanide as radiolabeling precursor, we had reported the radiosynthesis of indolyl-3-[1-¹¹C]acetonitrile ([¹¹C]IAN), indolyl-3-[1-¹¹C]acetamide ([¹¹C]IAM), as well as indolyl-3-[1-¹¹C]acetic acid ([¹¹C]IAA) using DMSO⁴. Recently, we further developed a fast and more efficient method for the synthesis [¹¹C]IAA in a two-step, one-pot manner by replacing DMSO with tetraethylene glycol as reaction solvent⁵. In addition to labeled auxin, we were also very interested in synthesizing ¹¹C-labeled indole since this radiotracer could help us to better map and understand the biosynthetic pathways for auxin in different plant tissues.

The synthesis of molecules containing indole ring as core structure has been extensively investigated and well developed, and the related work has been summarized⁶. In contrast, there are only limited reports related to the incorporation of isotopes into the indole ring. In 2002, Czeskis and colleagues reported an elegant method for synthesis of 4-hydroxy [2-¹⁴C]indole⁷. Starting from Na¹⁴CN, they first synthesized *p*-chlorophenoxy [1-¹⁴C]acetonitrile in 65% yield. Next, this carbon-14 (¹⁴C) labeled acetonitrile was reacted with benzyl-protected 3-nitrophenol

via a vicarious nucleophilic substitution reaction to afford a 2-nitrophenyl acetonitrile derivative. Finally, palladium catalyzed triple hydrogenation reduction and cyclization provided desired ^{14}C -labeled 4-hydroxyindole. (need to know the mechanism) Four years later, Pedras and Okinyo reported a synthesis of stable isotope deuterium labeled [5,6,7,8- $^2\text{H}_4$]indole using chloroacetonitrile direct alkylation and reductive cyclization reactions⁸. More recently, two isotopically labeled indole compounds had been reported by Czeskis⁹. First of all, 2-nitrophenyl acetonitrile was obtained with 52% yield by reacting 2-nitrobenzylbromide with NaCN in aqueous DMSO. Further transformation from this intermediate provide both deuterium and ^{14}C labeled indole derivatives (Scheme 1).

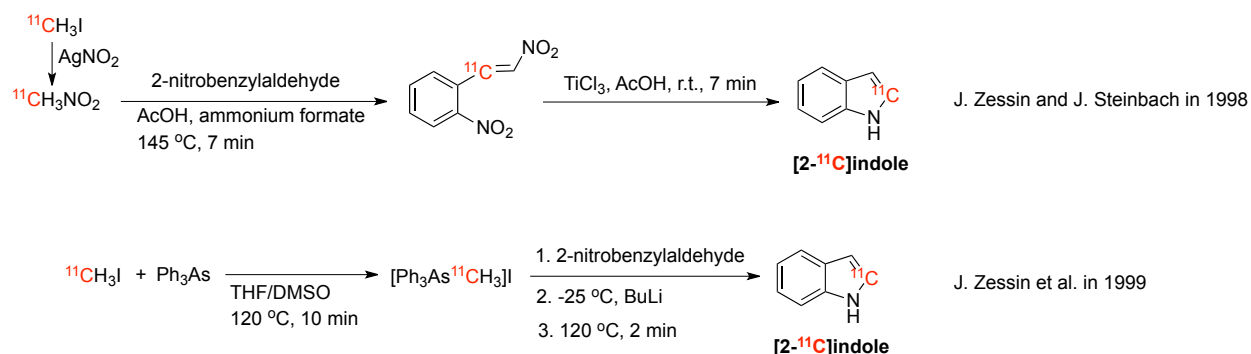
Scheme 1. Three reports of synthesis of deuterium or ^{14}C labeled indole derivatives



Additionally, two methods for synthesis of ^{11}C -labeled indole, [2- ^{11}C]indole, had been reported in 1998 and 1999 by same research group (Scheme 2)¹⁰: in the first report, the [^{11}C]CH₃NO₂ was used as radiolabeling precursor and titanium(III) chloride was used as reducing agent for second step – reductive cyclization to form desired [2- ^{11}C]indole. The more

common radiolabeling precursor $^{11}\text{C}\text{H}_3\text{I}$ was used in the second report. Once $[^{11}\text{C}]\text{CH}_3\text{I}$ reacted with triphenylarsine to form the $[^{11}\text{C}]\text{methyltriphenylarsonium iodide}$, 2-nitrobenzaldehyde was immediately added into reaction mixture. After cooling to $-25\text{ }^\circ\text{C}$, the strong base butyl lithium was added to convert arsonium salt to $[^{11}\text{C}]\text{triphenylarsoniummethylide}$. Next, the reaction mixture was heated to $120\text{ }^\circ\text{C}$ for 2 min to give expected $[2\text{-}^{11}\text{C}]\text{indole}$. Although both reports showed that $[2\text{-}^{11}\text{C}]\text{indole}$ could be synthesized successfully, the latter method, in which $^{11}\text{C}\text{H}_3\text{I}$ was directly used as radiolabeling precursor, seems more attractive since all reactions could be run with an one pot manner. Surprisingly, both reports only showed the analytic HPLC data for the reaction mixture. Neither the description about the purification of reaction mixture nor the radiochemical yield of $[2\text{-}^{11}\text{C}]\text{indole}$ was reported.

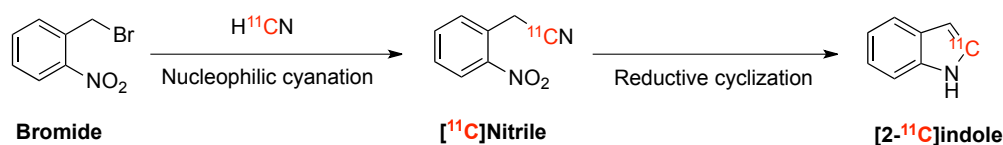
Scheme 2. Previous reports for synthesis of ^{11}C -labeled indole



Given the long history of utilization of H^{11}CN as radiolabeling precursor to synthesize various ^{11}C -labeled bioactive radiotracers¹¹ and above-mentioned successful examples of cyanide based methods for synthesizing various isotopically labeled indole derivatives¹², we envisioned to synthesize $[2\text{-}^{11}\text{C}]\text{indole}$ by using $[^{11}\text{C}]\text{HCN}$ as radiolabeling precursor (Scheme 3). Starting from 2-nitrobenzylbromide (*bromide*), nucleophilic cyanation with $[^{11}\text{C}]\text{cyanide}$

($[^{11}\text{C}]\text{CN}^-$) could provide us with 2-nitrophenyl $[^{11}\text{C}]$ acetonitrile ($[^{11}\text{C}]\text{nitrile}$). Reductive cyclization, if successful, should provide us desired radiotracer, $[2-^{11}\text{C}]\text{indole}$.

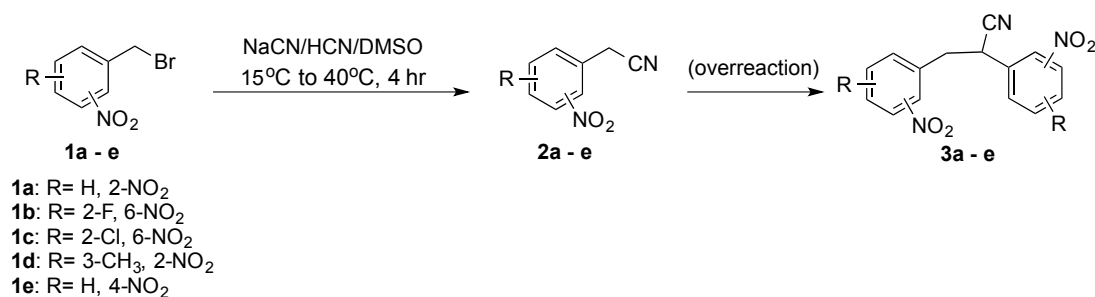
Scheme 3. Our design of synthesis $[2-^{11}\text{C}]\text{indole}$ using H^{11}CN as radiolabeling precursor



We were optimistic that the cyanation strategy followed by reductive cyclization could be translated to carbon-11 based on many previous examples showing that nucleophilic $[^{11}\text{C}]$ cyanation with H^{11}CN is a practical and reliable method to prepare C-11 labeled nitrile intermediates for a variety of compounds. However, we also anticipated problems based on reports of that nitro-substituted benzyl halides react with cyanide to form the benzyl cyanide which readily undergoes further alkylation reactions with the benzylic halide to produce the known 2,3-bis-(2-nitrophenyl)propanenitrile at the expense of the 2-nitro benzyl cyanide under basic conditions (Scheme 4).

Scheme 4. Reaction of nitrobenzyl bromide with NaCN to form 2-nitrobenzyl cyanide

(*nitrile*) and side-product (*dimer*) under basic conditions¹²



Kalir and Mualem minimized the formation of *dimer* by reducing the pH and increasing the ratio of cyanide to *nitrile*. Adapting these conditions to cyanation with no-carrier-added $[^{11}\text{C}]$ cyanide was challenging because the chemical quantity of cyclotron-produced $[^{11}\text{C}]$ cyanide

is fixed and very small ($< 0.03 \mu\text{mol}$, $< 0.06 \text{ mM}$) whereas mg quantities (10 mg, $46.3 \mu\text{mol}$, 93 mM) of the benzyl halide precursor is typically used to drive the nucleophilic substitution reaction resulting in a ratio of benzyl halide to $[^{11}\text{C}]$ cyanide of 1550:1 in the typical reaction volume of 0.5 mL. Though this high ratio of substrate to radioprecursor greatly favors the nucleophilic substitution reaction, it also favors side product formation and interferes with subsequent steps in the synthesis and in product purification where a very small chemical mass of labeled product must be separated from unreacted starting material and/or decomposition products within 60 min practical time frame for carbon-11 ($t_{1/2}$: 20.4 min),

Herein we report the screening and development of various conditions to optimize nitrile formation vs side-product formation using with NaCN (referred to as carrier-added) and the adaptation of these conditions to the radiosynthesis synthesis of 2-nitro-benzyl $[^{11}\text{C}]$ cyanide from the reaction of 2-nitro-benzyl bromide with no-carrier-added H^{11}CN followed by rapid reductive cyclization and purification.

3. Experimental details

3.1. General

All commercial chemical reagents, 2-nitrobenzyl bromide, 2-nitrophenylacetonitrile, 18-crown-6, potassium bicarbonate, potassium carbonate, Raney-nickel in water (60% slurry), hydrazine monohydrate, formic acid (98%) and solvents for synthesis and analysis were purchase from Sigma-Aldrich Chemical Co. (St. Louis, MO, USA) with a minimum of ACS reagent grade and used without further purification. Solid phase extraction (SPE) cartridges (SepPak® C18 plus) manufactured by Waters (Waters® Association, MA, USA) were used.

The reaction was carried out in a 10 cc microwave reaction vial sealed by a cap and septum to withstand high pressure (Biotage® INC., VA, USA). Thus, semi-reflux reaction system was maintained with a variety of alcoholic solvent/water solvents for hydrolysis and water was condensed on the cap.

Preliminary model reactions performed without radioisotope labeling were characterized by ultra-high performance liquid chromatography (UHPLC) using an Agilent model 1200 system (Agilent Technologies Inc., Santa Clara, CA). High and low levels of radioactivity were measured using a Capintec CRC-712MV and a Capintec CRC-ultra radioisotope dose calibrator (Capintec Inc. NJ, USA) respectively. Semi-preparative high performance liquid chromatography (HPLC) was performed using a Knauer HPLC system equipped with a model K-1001 pump, a model 87 variable wavelength monitor, a NaI detector and a SRI peak simple integration system. Analytical HPLC was performed using a Knauer model K-1001 pump, a Knauer model K2501 UV detector (254nm), a Geiger Muller ionization detector and a SRI Peak simple integration System. Radiochemical yields (decay-corrected back to end of cyclotron bombardment (EOB)) were obtained based on the total radioactivity trapped in the reaction vessel at the start of the reaction. Specific activities, decay corrected back to EOB and recorded in mCi/nmol, were determined from the C-11 activity in the product peak in the HPLC and the mass of compound. Total synthesis times were calculated from EOB to the end of radiotracer formulation.

3.2. Controlled production system for anhydrous [¹¹C]HCN

3.2.1. Production of [¹¹C]CO₂ and [¹¹C]HCN

Carbon-11 was generated as [^{11}C]CO₂ using 17.4 MeV proton irradiation of N₂ gas target containing 100 ppm O₂ to induce the $^{14}\text{N}(\text{p}, \alpha)^{11}\text{C}$ nuclear reaction. Irradiations were carried out on the BNL EBCO TR-19 cyclotron. The [^{11}C]HCN was produced via automated gas phase synthesis by a homemade system¹³. Briefly, [^{11}C]CO₂ produced from this process was collected over molecular sieves, catalytically reduced to [^{11}C]CH₄ over reduced Ni at 420°C. The [^{11}C]CH₄ was converted to the [^{11}C]HCN by adding gaseous ammonia and passage through a Pt furnace at 950°C at a flow rate of 350~400mL/min. Radioactivity measurements were made in a Capintec CRC-712MV radioisotope dose calibrator (Capintec Inc., Ramsey, NJ).

3.2.2 Purification of [^{11}C]HCN

The purification procedure for delivering anhydrous [^{11}C]HCN was modified and optimized based on previously published method¹⁴. [^{11}C]HCN was transferred from the cyclotron vault in a gas stream in the presence of NH₃ and H₂O. Before trapping of the [^{11}C]cyanide, it was passed through 5 mL of 50% sulphuric acid heated to 65 °C followed by 1 – 2 g of phosphorous pentoxide. Anhydrous [^{11}C]cyanide was trapped in reaction vessel containing reaction solvent (0.3 mL), cation source (0.3 mmol) in presence of 18-C-6 (0.6 mmol) and magnetic stirring bar.

3.3. Nucleophilic [^{11}C]cyanation for [^{11}C]benzyl nitrile intermediate

3.3.1. General radioanalytical procedure for analysis of [^{11}C]cyanation

50 μL of aliquot from the crude mixture was used for confirmation of the formation of [^{11}C]2-nitrophenyl acetonitrile (**[^{11}C]nitrile**) via cyanation by analytical HPLC using an isocratic system with aqueous formic acid solution (0.1%)/methanol=50/50 at a flow rate of 1 mL/min on a Eclipse XDB-C8 column (Agilent, 4.6 \times 150 mm, 5 μm). The **[^{11}C]nitrile** eluted at 3-4 min under these conditions. HPLC solvent was switched to 100% methanol at 4-5 min and [^{11}C]2,3-

bis-(2-nitrophenyl)propanenitrile ($[^{11}\text{C}]\text{dimer}$) was eluted at 8-9 min. Radiochemical yield (decay-corrected) of $[^{11}\text{C}]\text{nitrile}$ was obtained based on eluted radioactivity after aqueous workup by solid phase extraction using SepPak® C18 plus cartridge. The proportion of $[^{11}\text{C}]\text{nitrile}$ and $[^{11}\text{C}]\text{dimer}$ (9/1, m/m) extracted from SepPak C18 plus was determined by analytical HPLC analysis of an aliquot of the Sep-pak eluate. Analysis of $[^{11}\text{C}]\text{cyanation}$ result by analytical HPLC was shown in Supplementary Part 2.

3.3.2. Optimized radiosynthesis of $[^{11}\text{C}]\text{2-nitrophenylacetonitrile}$ ($[^{11}\text{C}]\text{nitrile}$) from 2-nitrobenzyl bromide (bromide)

$\text{K}_2\text{CO}_3/\text{KHCO}_3/18\text{-crown-6}$ (5 $\mu\text{mol}/10 \mu\text{mol}/30 \mu\text{mol}$) were dissolved in 0.3 mL of dimethylacetamide (DMA) in a U-shape reaction vessel with a stirring bar. After trapping the anhydrous $[^{11}\text{C}]\text{HCN}$ directly into the reaction vessel for 3 min at r.t, 2-nitrobenzyl bromide (0.2 mg, 0.926 μmol) dissolved in 0.2 mL of DMA was added then the cyanation reaction was performed at 40 °C for 35 second. To the crude reaction mixture, aqueous formic acid solution (0.1% v/v, 1 mL) was added for quenching the reaction. The resulting mixture was diluted with 9 mL of 0.1% of aqueous formic acid solution (0.1% v/v, 9 mL) and loaded to a C18 plus SepPak cartridge. The cartridge holding C-11 labeled organic compounds such as $[^{11}\text{C}]\text{nitrile}$ and $[^{11}\text{C}]\text{2,3-bis-(2-nitrophenyl)propanenitrile}$ ($[^{11}\text{C}]\text{dimer}$) was rinsed with 5 mL of deionized water and dried with air to minimize dead volume of residual water. The $[^{11}\text{C}]\text{nitrile}$ and $[^{11}\text{C}]\text{dimer}$ are eluted with EtOH (1.5 mL) into the second reaction vessel for analysis of the $[^{11}\text{C}]\text{cyanation}$ products and for the reductive cyclization to $[^{11}\text{C}]\text{indole}$.

3.4. Reductive cyclization of [¹¹C]nitrile to [2-¹¹C]indole

The mixture of [¹¹C]nitrile and [¹¹C]dimer from [¹¹C]cyanation dissolved in EtOH (1.3 mL in presence of dead volume of water in 0.2 mL) from the sep Pak separation described above was eluted into a U-shape reaction vessel with a stir bar. To the mixture, Raney-nickel (0.16 mg, 60 % slurry in water) and hydrazinium monoformate (0.05 mmol, N₂H₄/HCO₂H = 1:1 mol ratio) was added and the reaction vessel was capped. Hydrogenation was performed for 10 min at 40 °C. The resulting mixture was diluted with water (1 mL) and Raney-nickel was filtered out and then the resulting crude containing [2-¹¹C]indole was injected into semi-preparative HPLC for purification.

The reaction mixture was purified with semi-preparative HPLC using aqueous formic acid solution (0.1%)/methanol = 45/55 at flow rate of 5 mL/min on a Luna C18 column (Phenomenex, 10 × 250 mm, 5 μm). [2-¹¹C]indole eluted at 12 – 13 min. The fraction containing [2-¹¹C]indole was collected. The overall radiochemical yield of [2-¹¹C]indole based on total [¹¹C]cyanide trapped was 21 ± 2.2% (n = 5, ranging from 18 – 24%). Radiochemical purity as determined by analytical HPLC was > 97%. Total synthesis time was 40 – 45 min, while specific activity at EOB was 129.5 ± 48 GBq/μmol (n = 8, decay-corrected).

3.5. Formulation of [2-¹¹C]indole for plant studies

The pure [2-¹¹C]indole, from the semi-preparative HPLC was diluted with aqueous formic acid solution (0.1% v/v, 40 mL) then passed through a C18 plus SepPak® cartridge. The cartridge retaining the [2-¹¹C]indole was rinsed with 5 mL of deionized water and then dried with air to minimize dead volume of water. The [2-¹¹C]indole was eluted with diethyl ether (1.5 mL) into the final product vial containing 0.1 mL of water. The product was concentrated

by drying diethyl ether with a stream of Ar at 50 °C for 10 min. One production cycle from EOB to the formulation procedure required 40 – 45 min.

3.6. Quality control and specific activity determination

Briefly the radiochemical purity and specific activity of [2-¹¹C]indole was determined by an analytical HPLC system with a Eclipse XDB-C8 analytical HPLC column (Agilent, 4.6 × 150 mm, 5 μm) using aqueous formic acid solution (0.1%)/methanol = 50/50 at a flow rate of 1 mL/min. The [2-¹¹C]indole eluted at 6 min. A UV standard calibration curve was measured using an authentic sample of indole for the mass determination (**Supplementary data**). The injected radioactivity was measured in the range of MBq using a low dose Capintec radioisotope dose calibrator. The specific activity was determined as the ratio of the injected radioactivity (GBq, decay-corrected to EOB) and mass (μmol). The radiochemical purity (%) was determined by integrating radio peaks on the analytical HPLC profile (**Supplementary data**). The chemical identity of the product was determined by co-injection with a standard indole sample.

3.7. Cold chemistry

3.7.1. Preparation of 2,3-bis(2-nitrophenyl)propanenitrile (dimer)

2,3-bis(2-nitrophenyl)propanenitrile was synthesized according to a literature method¹². 2-nitrobenzyl bromide (0.1 g, 0.46 mmol) was added to a stirred suspension of sodium cyanide (30 mg, 0.46 mmol) in DMSO (2 mL). The mixture was stirred for 1 hr at r.t and 1 hr at 45 °C and poured into water (10 mL). Organic crude mixture was extracted with AcOEt by separation and purified by isolera with gradient system. The desire product, **dimer**, in white powder was given in 78 % yield. ¹H NMR (400 MHz, CDCl₃): δ 8.05 (dt, J=8, 1.2 HZ, 2H), 7.76 – 7.70 (m, 2H),

7.65-7.44 (m, 4H), 5.19 (dd, 8.8, 6 Hz, 1H), 3.84 (dd, 13.6, 8.8 Hz, 1H), 3.51 (dd, 13.6, 6 Hz, 1H). ¹³C NMR (100 MHz, CDCl₃): δ 134.53, 133.92, 133.14, 130.93, 130.87, 130.15, 129.95, 129.40, 125.97, 125.76, 119.01. MS (ESI): m/z [M+H⁺] calcd for C₁₅H₁₁N₃O₄ 297.07 found 315.0 (+H₂O).

3.7.2. Preparation of indole from the nitrile without C-11

The experimental procedure for hydrogenation of **nitrile** to **indole** was modified and optimized based on previously published method¹⁵. Hydrazinium monoformate was prepared by neutralizing equal moles of hydrazine monohydrate and 98% formic acid in an ice water bath. The hydrazinium monoformate thus prepared was used directly for hydrogenation. A suspension of commercially available 2-nitrophenylacetonitrile (2 mg, 12.3 μmol) and Raney-nickel (0.4 mg) in EtOH/H₂O (1.5 mL, v/v = 4/1) was stirred with hydrazinium monoformate (0.5 μmol, 41 μL), for 15 min at r.t. The reaction mixture was filtered through celite and injected to analytical HPLC to be monitored and analyzed by using isocratic system with aqueous formic acid solution (0.1%)/methanol=50/50 at a flow rate of 1 mL/min on a XSelect HSS PEP column (Waters, 4.6 × 30 mm, 5 μm). An unidentified byproduct eluted at 1 min. Unreacted **nitrile** eluted at 1.2 min and **indole** eluted at 1.7 min. The yield of indole (60 %) was determined by integrating peaks on the analytical UV-UHPLC profile (**Supplementary data Part 2**).

3.7.3. Reductive cyclization of the nitrile in presence of the bromide

Hydrazinium monoformate was prepared by the same procedure described above. A suspension of commercially available 2-nitrophenylacetonitrile (2 mg, 12.3 μmol), 2-nitrobenzyl bromide (2 mg, 9.26 μmol) and Raney-nickel (0.4 mg) in EtOH/H₂O (1.5 mL, v/v = 4/1) was stirred with hydrazine monoformate (0.5 μmol, 41 μL), for 15 min at r.t. The reaction mixture was filtered through celite and injected to analytical UHPLC to be monitored and analyzed by

using isocratic system with aqueous formic acid solution (0.1%)/methanol=50/50 at a flow rate of 1 mL/min on a XSelect HSS PEP column (Waters, 4.6 × 30 mm, 5 μm). **Nitrile** eluted at 1.2 min but no indole was formed.

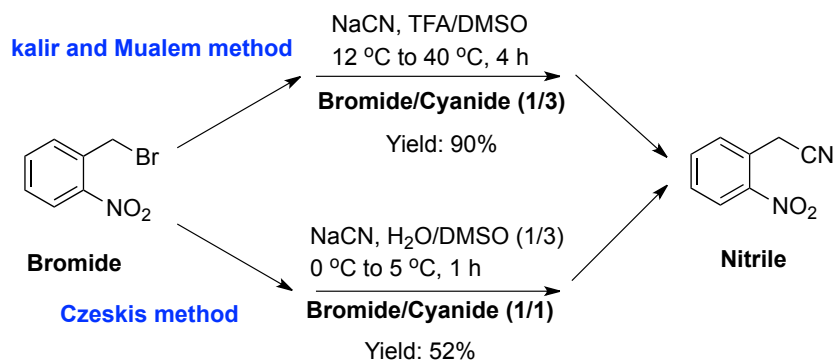
4. Results and discussion

We started by testing the feasibility of synthesizing the intermediate 2-(2-nitrophenyl)acetonitrile (**nitrile**). One report by Kalir and Mualem in 1987¹² disclosed a reliable method using NaCN plus HCN (for pH adjustment) using **bromide** as starting material, which provided **nitrile** with yields up to 90%. A later report showed that this compound was also synthesized in 52% yield in aqueous DMSO at near neutral conditions for 1 h at 0 – 5 °C (Scheme 5)⁹. Following these reports, we initiated the “cold” test for synthesis of **nitrile** intermediate and we found, with slightly modified conditions (Scheme 6), that 10 – 60% **nitrile** could be synthesized by reacting **bromide** with KCN or KCN/HCN combined conditions.

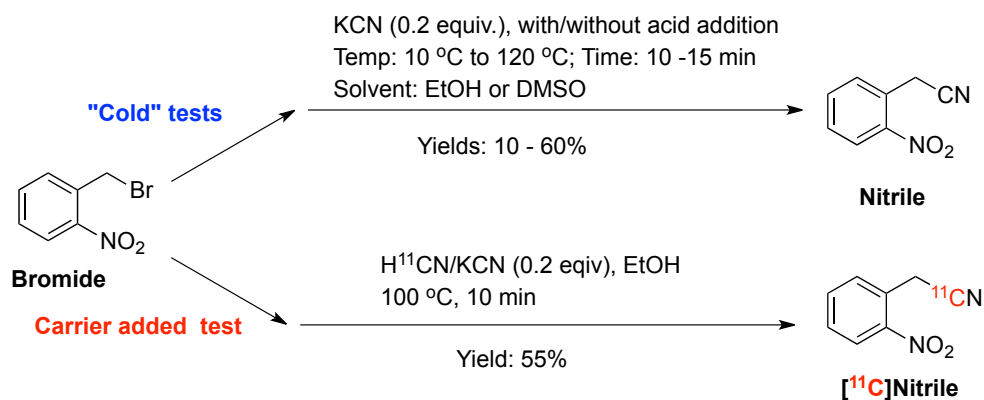
Next, we added radioactive [¹¹C]HCN into the reaction system and tested carrier added (CA) [¹¹C]cyanation reaction (Scheme 6). The radio-HPLC analysis was very encouraging, it showed that 55% of radioactivity converted to desired [¹¹C]**nitrile** in the presence of KCN in EtOH for 10 min at 100 °C. We then removed the carrier KCN from the reaction to develop the conditions for the synthesis of the no-carrier-added (NCA) [¹¹C]**nitrile** (Scheme 7). Under slightly acidic conditions, no [¹¹C]**nitrile** was detected. Increasing the reaction temperature (from 50 °C to 150 °C) gave only 2,3-bis(2-nitrophenyl)-[1-¹¹C]propanenitrile (“¹¹C**dimer**”), which was formed by the further alkylation (here called “**dimerization**”) of [¹¹C]**nitrile** with the starting material **bromide**. When KHCO₃ was used to trap radioactivity [¹¹C]HCN and the reaction mixture was

maintained at slight basic, radio-HPLC analysis showed that the NCA [^{11}C]nitrile was formed in yields up to 46% yield but attempts to repeat the experiments always gave disappointing results. In most cases, only small amount of [^{11}C]nitrile could be detected and the majority of radioactivity in the reaction mixture was [^{11}C]CN $^-$, [^{11}C]dimer and an unidentified low polarity labeled compound (Scheme 7).

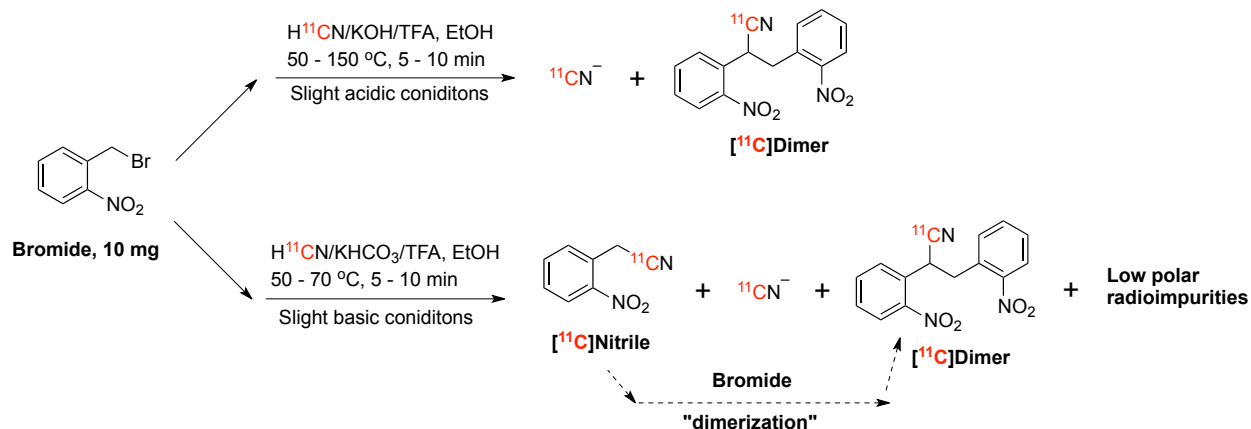
Scheme 5. Reference reports for the synthesis nitrile^{9,12}



Scheme 6. Results for the synthesis of nitrile and carrier added [^{11}C]nitrile



Scheme 7. Preliminary results for the radiosynthesis of [^{11}C]nitrile

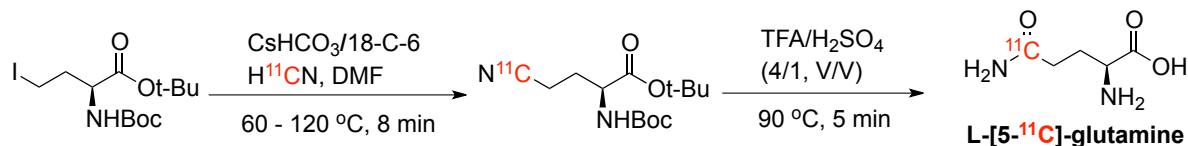


These initial results were not surprising nor were they unprecedented. Kalir and Mualem also observed the formation of 2,3-bis-(2-nitrophenyl)propanenitrile (*dimer*) and minimized it by carefully controlling the reaction stoichiometry with excess NaCN to obtain a ratio of 3:1 (NaCN : **bromide**) and conducting the reaction under acidic conditions¹². Czeskis reduced **dimer** formation by using aqueous DMSO and quenching the reaction after 1 h reaction at 0 – 5 °C (Scheme 5)⁹. Adapting these conditions to [^{11}C]cyanation with no-carrier-added [^{11}C]cyanide was challenging because the chemical quantity of cyclotron-produced [^{11}C]cyanide is fixed and very small (0.03 μmol - 0.06 μmol) whereas milligram quantities (10 mg, 46.3 μmol , of the **bromide** is typically used to drive the nucleophilic substitution reaction). This results in a ratio of **bromide** to [^{11}C]cyanide of 1550:1 in a typical radiosynthesis. Though this high ratio of substrate to radioprecursor greatly favors the nucleophilic cyanation reaction, it also favors dimer formation from further alkylation once a certain amount of [^{11}C]nitrile has accumulated in the reaction mixture (Scheme 7). At this stage, we speculated that it was necessary to carefully examine the NCA [^{11}C]cyanation conditions. Only well-refined reaction conditions could,

potentially, provide enough desired [^{11}C]nitrile intermediate for the next reductive cyclization reaction.

Because we anticipated that careful pH adjustment would be necessary to avoid further alkylation of the [^{11}C]nitrile, we envisioned that it was necessary to remove trace amounts of ammonia and water which were formed during the gas phase production of our radioprecursor [^{11}C]HCN¹³. For this purpose, a [^{11}C]HCN purification method which was first introduced by Långström¹⁴ was adapted in our [^{11}C]HCN delivery system: the helium flow containing radioactivity was first purged through 50% H_2SO_4 acid bath heated at 65 °C to remove NH_3 , and then was passed through a newly packed P_2O_5 drying tube for further removal of the trace amount of H_2O . With this purified [^{11}C]HCN in hand, we started to screen the nucleophilic [^{11}C]cyanation conditions for the synthesis of NCA [^{11}C]nitrile following the [^{11}C]cyanation conditions of our recent report of optimized synthesis of carbon-11 labeled L-glutamine (Scheme 8)¹⁶, and, the preliminary exploration results were listed in Table 1.

Scheme 8. Optimized L-[5- ^{11}C]-glutamine synthesis method ¹⁶



We also reduced the amount of **bromide** substrate from 10 mg to 1 mg for this set of experiments since the larger amount of **bromide** would also facilitate further alkylation to form the **dimer**. Although directly following the L-[5- ^{11}C]-glutamine synthesis method gave a 79% overall radiochemical yield (ORCY, includes total radioactivity of [^{11}C]nitrile and [^{11}C]dimer, decay corrected) (entry 1), only [^{11}C]dimer was detected from radio-HPLC analysis. Clearly the milder reaction conditions were needed to avoid the side reaction of [^{11}C]nitrile with excess

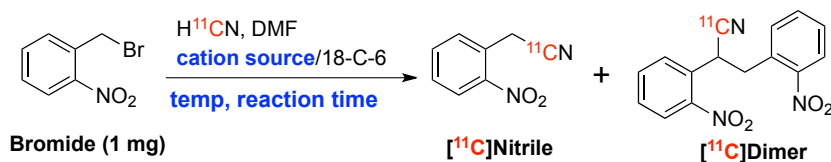
bromide, which formed undesired [^{11}C]**dimer**. Reducing the reaction temperature from 60 °C to 30 – 35 °C gave similar results (entry 2). The further reduction of the temperature to 18 – 20 °C not only provided us with 90% ORCY but also 4% of the desired [^{11}C]**nitrile** (entry 3). One step further, the reaction mixture was cooled with ice bath and the [^{11}C]cyanation reaction was clearly slow down. Although the ORCY was only 22% with an 8 min reaction time (entry 4), the results were quite encouraging since all detected radioactivity was desired [^{11}C]**nitrile** intermediate. The extended reaction time (from 8 min to 25 min) provided higher ORCY (58%), but further alkylation occurred at the expense of [^{11}C]**nitrile**. Only 9% of the total radioactivity was [^{11}C]**nitrile** and the rest was [^{11}C]**dimer**. Based upon these results (Table 1, entry 1 to 4), it was clear that **bromide** is a highly reactive substrate, and the ORCY reached 90% after a 8 min reaction time even at room temperature. From this set of experiments it was clear that conditions which favored a high ratio of nitrile to dimer also dramatically reduced the ORCY and that we would need to adjust other reaction parameters to facilitate both the nitrile formation and ORCY.

We next set out investigated the effect of basicity on ORCY and radiolabeled product distribution. The results listed in entries 5 and 6 showed that no [^{11}C]cyanation reaction occurred when the pH was <8. Neither the direct use of NCA [^{11}C]HCN (pH = 5) nor the addition of near neutral form salt KBr (pH = 7.7) initiated any [^{11}C]cyanation reaction. With the introduction of more basic K_2CO_3 into the reaction (entry 8 and 7 compared with entry 6), the [^{11}C]cyanation reaction rate was dramatically improved. Adjusting the pH to 8.4 resulted in a 26% ORCY with a mixture of [^{11}C]**nitrile** and [^{11}C]**dimer** (ratio at 23 : 77) favoring the formation of [^{11}C]**dimer** (entry 7). Increasing the pH to 8.7 increased the ORCY to 60% but only side product [^{11}C]**dimer** was formed (entry 8). These initial experiments showed that basic conditions were required to initiate the [^{11}C]cyanation reaction but also indicated that the formation of

[¹¹C]**dimer** was very favorable. Encouraged by the increase in ORCY we further adjusted the cation source and elevated the pH to 9.6, reduced the temperature to 0 °C and then carefully monitored the reaction by analytical radio-HPLC (entry 9). The results showed that this reaction was very fast. The ORCY reached to 73% even after 0.2 min with product distribution favoring the nitrile (92 : 8). Further extension of the reaction time only changed the product distribution to favor the dimer. When K₂CO₃ was chosen as cation source and pH was increased to 11.2 (entry 10), the radio-HPLC analysis results of different time point reaction solution samples showed the similar trend as the results listed in entry 9: the short reaction (0.6 min) provided the higher [¹¹C]**nitrile** yield and the extended reaction time favored further alkylation to form the [¹¹C]**dimer**. Finally, the solvent N,N-dimethylacetamide (DMA), a sibling of DMF, was tested and the results also showed that the ORCY plateaued to 76% even after 0.2 min with a ratio of [¹¹C]**nitrile** and [¹¹C]**dimer** at 78 : 22 (entry 11). It is very interesting to find that the rate of “dimerization” reaction is relatively slower with DMA as reaction solvent when comparing the results from entry 11 with the results listed in entry 10.

This series of experiments showed that it was hard to avoid further alkylation of the [¹¹C]**nitrile** with the excess **bromide** to form the [¹¹C]**dimer**. However, by carefully control several reaction parameters, i.e., reaction temperature, basicity as well as reaction time, it is possible to obtain a good conversion of [¹¹C]cyanide to product [¹¹C]**nitrile**, while maintains minimum formation of side product [¹¹C]**dimer**. Eventually, to approach the better operation consistency and to reach higher yield of [¹¹C]**nitrile**, the [¹¹C]cyanation reaction conditions listed in entry 11 (medium pH 9.6, **bromide** 1 mg, DMA as solvent, reaction at 0 °C for 0.6 min) were selected for the synthesis of [¹¹C]**nitrile** intermediate. We also switched our attention to the exploration of reductive cyclization reaction.

Table 1. Exploratory results of [^{11}C]cyanation based upon recent update of the synthesis of L-[5- ^{11}C]-glutamine ¹⁶



Entry	Cation Source ^a	pH ^b	Time (min)	Temp (°C)	ORCY ^c	Radioactivity ratio ([^{11}C]nitrile : [^{11}C]dimer ^d)
1	CsHCO ₃	8.5	8	60	79	0:100
2	CsHCO ₃	8.5	8	30~35	73	0:100
3	CsHCO ₃	8.5	8	18~20	90	4:96
4	CsHCO ₃	8.5	8	0	22	100:0
			25		58	9:91
5 ^e	None	5	8	60	0	nd
6	KBr (0.1 M)	7.7	10	18	0	nd
7	K ₂ CO ₃ /KBr (1/98)	8.4	10	18	26	23:77
8	K ₂ CO ₃ /KBr (5/90)	8.7	10	18	67	0:100
9	K ₂ CO ₃ /KHCO ₃ (1/4)	9.6	0.2	0	73	92:8
			0.6		72	71:29
			2		76	21:79
			5		77	16:84
			15		69	7:93
10	K ₂ CO ₃ (0.1 M)	11.2	0.6	0	68	85:15
			2		81	49:51
			10		70	28:72
11 ^f	K₂CO₃/KHCO₃ 9.6 (1/4)		0.2	0	76	78:22
			0.6		77	78:22
			2		77	39:61
			5		74	28:72
			15		64	22:28

^aAll the experiments were performed with 2-nitrobenzyl bromide (1 mg, 4.63 μmol) with different cation sources (15 μmol) in presence of 18-C-6 (30 μmol) dissolved in 0.5 mL of DMF; if two different cation sources were used, the numbers listed in parenthesis were the mole ratios; ^bpH was measured with the cation source dissolved in aqueous solution (give the volume of water because pH is concentration dependent); ^cOverall radiochemical yield (% ORCY, decay-corrected) of [¹¹C]cyanation was determined by analytical radio-HPLC and included both [¹¹C]nitrile and [¹¹C]dimer (entry 1 – 11); ^dThis number is the radioactivity ratio of [¹¹C]nitrile : [¹¹C]dimer (decay-corrected), nd: not detected; ^eA solution of H¹¹CN in DMF was weakly acidic without addition of a cation source and 18-C-6; ^fReaction solvent was changed to N,N-dimethylacetamide (DMA).

We initially tested several reducing agents for the reductive cyclization of [¹¹C]nitrile to [2-¹¹C]indole including: Pd-C/H₂ in ethyl acetate¹⁷ and in alcoholic solvents¹⁸; Pd-C/H₂ in ethanol/acetic acid^{7, 19}; Pd-C in the presence of *in situ* H₂²⁰; Raney-nickel or Pd-C in the presence of NH₄CO₂H/HCO₂H²¹; Al-NiCl₂ · 6H₂O²²; Zn/acetic acid²³. Results were generally disappointing: they either only provided trace amount of desired [2-¹¹C]indole or none at all under NCA conditions. Later, a report by Gowda et al using Raney-Nickel based rapid reduction (both nitro and nitrile groups) caught our attention¹⁵. This method quickly reduced various nitro or nitrile group containing compounds to the corresponding amines in high yield (70 – 94%) with hydrazinium monoformate as hydrogen donor and Raney-nickel as catalyst at r.t. in 2 – 6 min. Given the time limitation of the carbon-11 radiochemistry, i.e. “Working Against Time”²⁴, we felt that above nitro and nitrile moieties reduction method is especially fit for our radiochemistry research. We confirmed that this method rapidly converted the nitrile to indole

under “cold” conditions and set out to adapt it to our [2-¹¹C]indole synthesis process (Table 2).

The procedure of entire radiosynthesis of [2-¹¹C]indole is described in Figure 1.

Figure 1. Procedure of total radiosynthesis of [2-¹¹C]indole

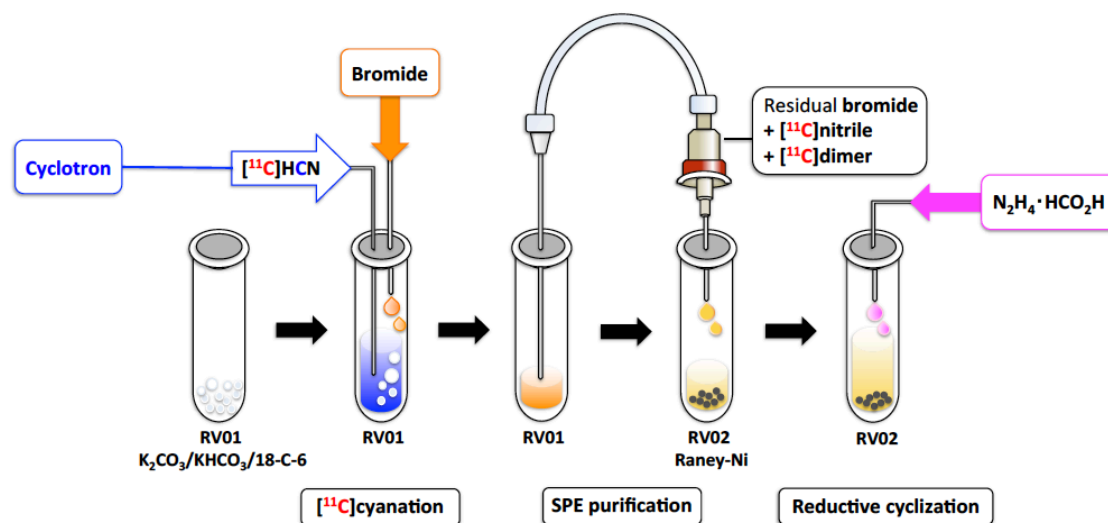
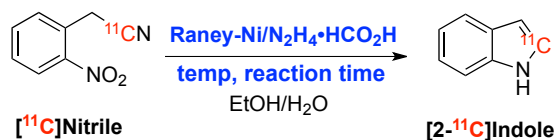


Table 2. Exploration of reductive cyclization method to convert [¹¹C]nitrile to [2-¹¹C]indole catalyzed by Raney Ni with hydrazinium monoformate as hydrogen donor



Entry	Time (min)	N ₂ H ₄ ·HCO ₂ H ^a (mmol)	Raney-Ni ^b (mg)	Temp ^c (°C)	RCY ^d (%)
12	5	5	48	r.t	25
13	10	5	48	r.t	26
14	15	5	48	r.t	33
15	5	10	48	r.t	9
16	15	10	48	r.t	19
17	15	2.5	48	r.t	38
18	15	2.5	96	r.t	10

19	5	5	48	40	18
20	10	5	48	40	30
21	15	5	48	40	24
22	10	0.5	48	40	35
23	10	0.5	38	40	41
24^e	10	0.5	48	40	n/a

^aThe mole ratio of hydrazine monohydrate and formic acid was 1/1; ^bRaney-nickel slurry in water (50%) was used for reactions; ^cRoom temperature indicates 18 ~ 20 °C; ^dRCY (decay-corrected) (%) was determined by radio-HPLC analysis of filtered crude mixture; ^e2 mg of **bromide** was used for synthesis of [¹¹C]**nitrile**; After the Sep-Pak purification, the ORCY was 51% and 42% of radioactivity was [¹¹C]**nitrile**; n/a: no [**2-¹¹C**]**indole** was detected.

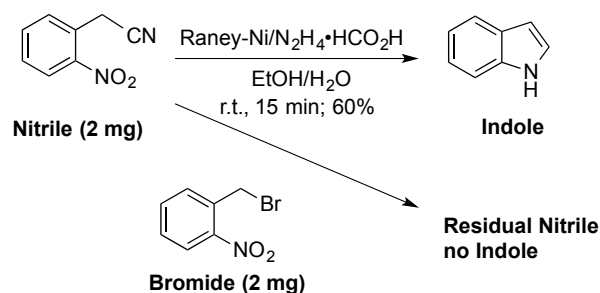
The initial test result was quite promising (Table 2, entry 12). We obtained 25% of desired [**2-¹¹C**]**indole** by using 5 mmol N₂H₄•HCO₂H and 48 mg Raney Ni at r.t. for 5 min. The results from next two experiments (entries 13 & 14) showed that the longer reaction times of 15 min resulted in a moderate increase in yield to 33%. When the amount of N₂H₄•HCO₂H, was increased to 10 mmol, the yield was surprisingly decreased (entries 15 and 16) and only afforded less than 20% of [**2-¹¹C**]**indole** even after 15 min. In contrast, reducing the N₂H₄•HCO₂H from 5 mmol to 2.5 mmol increased the reaction yield to 38% (entry 17). A two-fold increase in the Raney-Ni catalyst negatively affected the yield (entry 18). Moreover, a large amount of radioactivity remained in the filtration solid cake after the filtering off the catalyst from reaction mixture and only 10% of [**2-¹¹C**]**indole** was detected in the filtrate. When the reaction temperature was raised to 40 °C, we found that the reaction yield was reached to peak at 10 min (30%) and further extension of reaction time decreased the reaction yield to 24% (entries 19 – 21). Next, a sharp reduction of N₂H₄•HCO₂H from 5 mmol to 0.5 mmol clearly helped to

improve the reaction and gave a 35% yield (entry 22). A 20% cut of Raney-Ni catalyst also showed positive impact and increased reaction yield to 41% (entry 23) which was the highest reductive cyclization yield so far we had reached after this series of experiments.

At this time, we were wondering if we could further improve the [^{11}C]cyanation yield by simply increasing the amount of starting material **bromide** and so to help to increase the two steps overall yields. We doubled the amount of **bromide** for the [^{11}C]cyanation and 42% of [^{11}C]**nitrile** was obtained after the Sep-Pak purification. However, when this solution was submitted to reductive cyclization, we were disappointed to find that no [$2\text{-}^{11}\text{C}$]**indole** was detected (entry 24). It looks like that the increase of **bromide** for the [^{11}C]cyanation totally inhibited the following reductive cyclization reaction. This phenomenon led us to speculate that the presence of **bromide** in the reaction mixture may be responsible for the yield ceiling on the reductive cyclization.

For all of our reactions, we incorporated a Sep-Pak solid phase extraction (SPE) method to quickly remove the reaction solvent DMF, unreacted [^{11}C]cyanide ion, inorganic salt, phase transfer catalyst (PTC) 18-crown-6 as well as H_2O after the [^{11}C]cyanation step. After that, the ethanol flush process not only eluted radioactive [^{11}C]**nitrile** and [^{11}C]**dimer** but also a large amount of the unreacted **bromide** into the reduction vessel from this Sep-Pak cartridge. To test our hypothesis that the residual **bromide** would interfere or even totally inhibit the reductive cyclization, a “cold” test for reductive cyclization step was tested again with the addition of extra bromide (2 mg) and the results proved that the formation of indole from **nitrile** intermediate was totally inhibited (Scheme 9).

Scheme 9. Reductive cyclization inhibition test



To determine how much **bromide** starting material could be introduced into the reductive cyclization reaction, we next carried out a series of “cold” cyanation reactions with different starting amount of **bromide** and following Sep-Pak SPE purification process and then analyzed the ethanol elute samples (Figure 2). Analytical results showed that there was 55 – 78% portion of starting material **bromide** was eluted into the second reaction vessel after the Sep-Pak SPE purification. When 0.1 mg of **bromide** was used for cyanation reaction, there was only 0.06 mg bromide residue being introduced the next reaction vessel with the elution of EtOH.

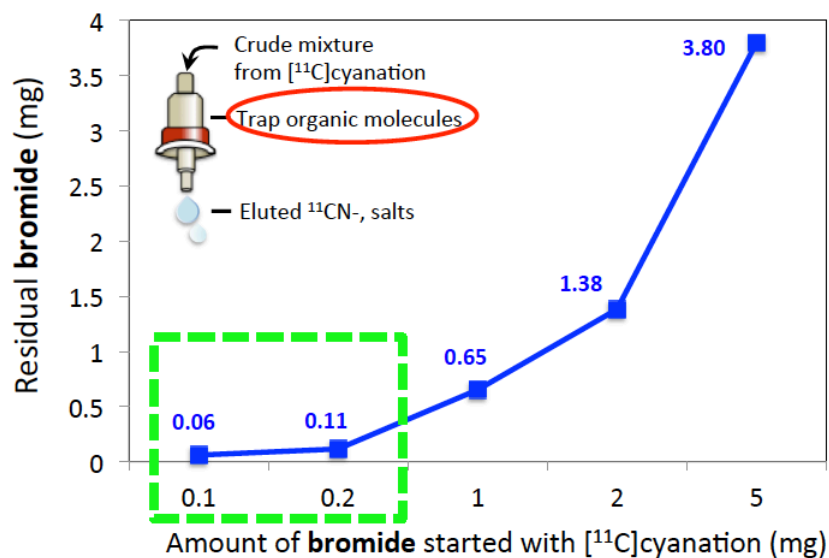


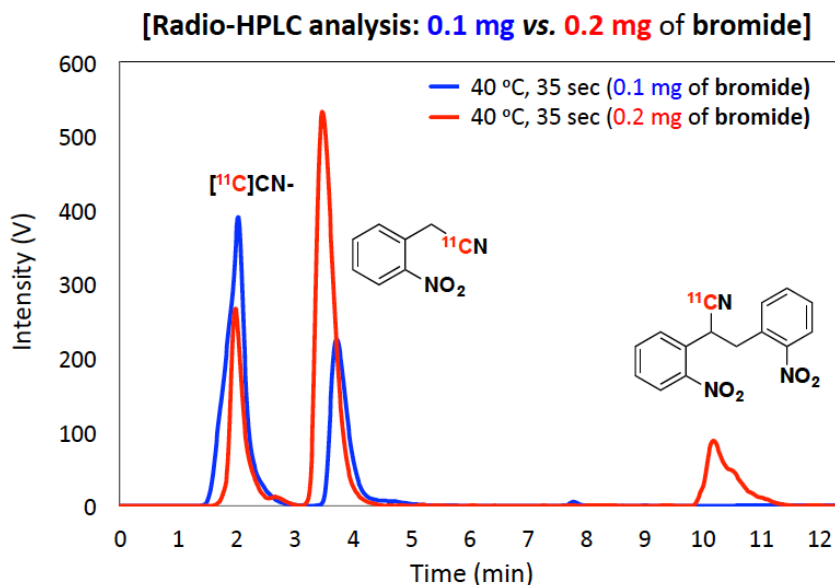
Figure 2. The amount of residual **bromide** after purification of “cold” cyanation reaction mixture by SPE method

Based upon the high reactivity of the **bromide** to S_N2 [^{11}C]cyanation (Table 1), we predicted that it would be possible to get comparable RCY of [^{11}C]nitrile using less **bromide** by simply modifying the [^{11}C]cyanation reaction conditions. We next designed a series of experiments to measure RCY and product distribution using less amount of **bromide** (Table 3). With the decrease of **bromide** from 1 mg to 0.1 mg, the reaction rate was clearly decreased (Entry 25). At 0.6 min time interval, only 25% radioactivity converted to desired [^{11}C]nitrile. Longer times only decreased the amount of [^{11}C]nitrile. Increasing the reaction temperature clearly improved the RCY (entry 26 – 28). The best conditions were found at 40 °C with 0.6 min reaction time (Figure 3). Further increase reaction temperature to 60 °C did not improve the reaction. One important finding was only negligible amount of [^{11}C]dimer was found in all experiments which was consistent with the role of the **bromide** in consuming [^{11}C]nitrile once it accumulated. Reducing the amount of **bromide** effectively increases the ratio of cyanide to **bromide** which is similar to the strategy that Kalir and Mualem used to improve the yield of nitrile¹². To see if the yield of [^{11}C]nitrile could be further improved. The [^{11}C]cyanation reaction was next tested at 40 °C with the amount of **bromide** increasing from 0.1 mg to 0.2 mg. The results were delightful: the ORCY reached 78% with ratio of [^{11}C]nitrile and [^{11}C]dimer at 77/23 (entry 29, Figure 3). Further extension of reaction time only decreased the amount of [^{11}C]nitrile and increased the undesired [^{11}C]dimer.

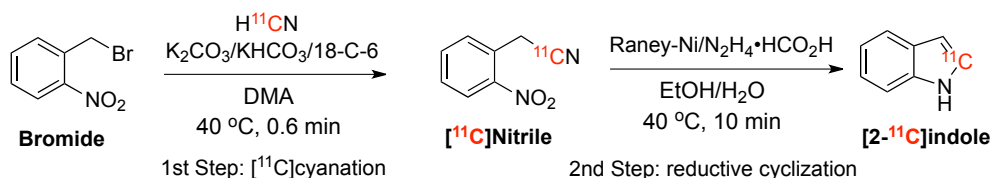
Table 3. Further exploration of the [^{11}C]cyanation reaction with reduced amount of **bromide**

Entry	Bromide ^a (mg)	Temp (°C)	Ratio of [^{11}C]nitrile / [^{11}C]dimer (ORCY) ^b			
			0.6 min	2 min	5 min	15 min
25	0.1	0	100/0 (25)	100/0 (12)	100/0 (6)	100/0 (3)
26	0.1	20	97/3 (37)	96/4 (26)	93/7 (15)	83/7 (6)
27	0.1	40	96/4 (48)	91/9 (43)	95/5 (19)	91/9 (11)
28 ^c	0.1	60	96/4 (47)	98/2 (41)	97/3 (33)	94/6 (16)
29	0.2	40	77/23 (78)	72/28 (78)	42/58 (71)	27/73 (62)

^aAll the experiments were performed with 2-nitrobenzyl bromide (**bromide**); ^bThe ratio of [^{11}C]nitrile / [^{11}C]dimer was calculated based upon radio-HPLC analysis of reaction solution samples at different time point (decay-corrected); ORCY (% , overall radiochemical yield, decay-corrected) included radioactive peaks of both [^{11}C]nitrile and [^{11}C]dimer; ^c[^{11}C]cyanation for 0.3 min was also monitored and gave the ratio of [^{11}C]CN⁻ / [^{11}C]nitrile / [^{11}C]dimer (ORCY) as 98/2 (41).

**Figure 3.** Analytical radio-HPLC profiles of two reaction samples from the reaction of 0.1 mg and 0.2 mg of **bromide** with [^{11}C]cyanide in DMA solution for 0.6 min at 40 °C

With above [^{11}C]cyanation reaction investigation results in hand, We restarted the synthesis of [$2\text{-}^{11}\text{C}$]indole with decreased amount of **bromide** as starting material. Once a superfast (0.6 min) [^{11}C]cyanation was performed, the reaction mixture was quickly purified with a SPE Sep-Pak. Following elution with EtOH, the obtained radioactive intermediate was submitted to reductive cyclization reaction using optimized reaction conditions (Table 2, entry 23). When 0.1 mg of **bromide** was used for [^{11}C]cyanation reaction, only 21% of desired [^{11}C]nitrile was obtained (Table 4, entry 30). The subsequent reductive cyclization as well as semi-prep HPLC purification process yielded 57% of [$2\text{-}^{11}\text{C}$]indole and the two steps entire preparative RCY for this synthesis was 12% (entry 30). When the 0.2 mg of **bromide** was used, 48% of desired [^{11}C]nitrile was obtained after the SPE purification. The second reaction gave 54% of [$2\text{-}^{11}\text{C}$]indole and the two steps entire preparative RCY reached 26% (Table 4, entry 31). These two experiments showed that the reductive cyclization reaction was clearly benefited from decreasing the amount of bromide and the preparative (isolated) yield of the reductive cyclization step was over 50%. In addition, the [^{11}C]cyanation reaction with 0.2 mg of **bromide** was better than just 0.1 mg since it yielded over doubled amount of [^{11}C]nitrile intermediate and also a significantly higher entire RCY (26% vs. 12%) of [$2\text{-}^{11}\text{C}$]indole (Table 4, entry 31).

Table 4. Further exploration of hydrogenation with reduced starting amount of **bromide***

Entry	Bromide (mg)	1 st step RCY (%)	2 nd step RCY (%)	Entire RCY (%)
30	0.1	21	57	12
31	0.2	48	54	26

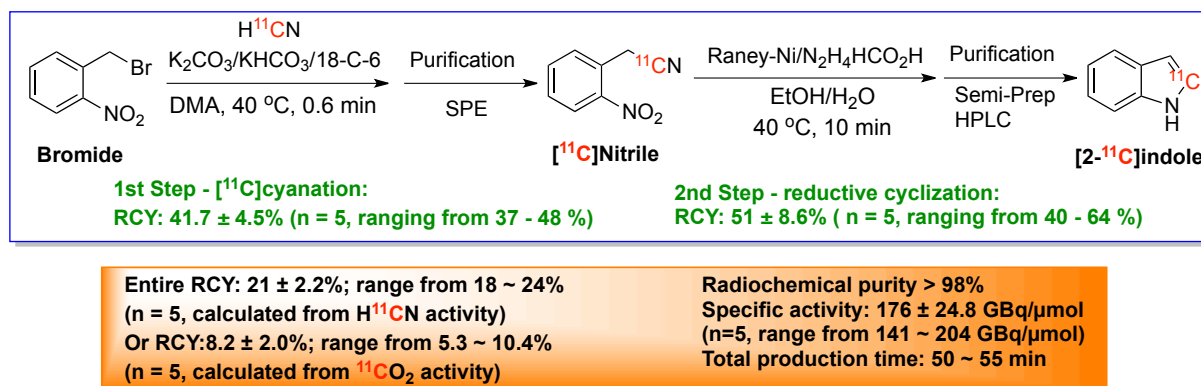
*Both 1st step and 2nd step RCYs were preparative results (purified by SPE and semi-prep HPLC method, respectively).

With the combination of reduced amount of starting material **bromide** (0.2 mg), strictly controlled and also superfast reaction time (0.6 min), mild temperature (40 °C) as well as polar aprotic solvent DMA, the [¹¹C]cyanation reaction provided us nearly 50% yield of [¹¹C]nitrile intermediate. Next, the reductive cyclization of [¹¹C]nitrile intermediate with selected conditions (0.5 mmol N₂H₄·HCO₂H, 38 mg Raney-Ni in EtOH/H₂O solution at 40 °C for 10 min) presented over 50% of [**2-¹¹C**]indole. Over 25% of [**2-¹¹C**]indole (calculated from starting [¹¹C]HCN, decay-corrected) was synthesized in 54 min (counted from the time of end-of-bombardment to the end of semi-prep HPLC purification of [**2-¹¹C**]indole).

To further confirm the robustness of this newly developed synthetic method, we repeated the synthesis of [**2-¹¹C**]indole five times under above described optimized reaction conditions. The results show the high reliability of this synthetic process (Scheme 10). With a six-min cyclotron beam time, which generates ~ 24.4 GBq (660 mCi) of [¹¹C]CO₂, 0.17-0.40 GBq (4.7 – 10.9 mCi) of [**2-¹¹C**]indole product was obtained at the end of synthesis (EOS). The entire yield (RCY) for both steps was 21 ± 2.2% (calculated from [¹¹C]HCN radioactivity collected in first reaction

vessel) and was $8.2 \pm 2.0\%$ (calculated from $[^{11}\text{C}]\text{CO}_2$ radioactivity generated from a six-min cyclotron beam). The radiochemical purity of final product was $> 98\%$ and the specific activity of final product was $176 \pm 24.8 \text{ GBq}/\mu\text{mol}$. The complete processing time, calculated from EOB to the EOS, ranged from 50 to 55 min.

Scheme 10. Optimized reaction parameters for synthesis of $[2\text{-}^{11}\text{C}]\text{indole}$



5. Conclusion

In summary, we successfully developed a practical and efficient method for synthesis of a biologically interesting PET tracer $[2\text{-}^{11}\text{C}]\text{indole}$ with high specific activity. The overall process illustrates the challenges in developing the conditions for controlling a superfast $[^{11}\text{C}]\text{cyanation}$ reaction that lead to a highly reactive intermediate, 2-(2-nitrophenyl)-[1- ^{11}C]acetonitrile. More specifically, under NCA conditions, the amount of $[^{11/12}\text{C}]\text{HCN}$ is very low ($0.03 - 0.06 \mu\text{mol}$) and fixed biasing the stoichiometry in favor of other reactants. In this case the amount of 2-nitrobenzylbromide used in the formation of the intermediate $[^{11}\text{C}]\text{nitrile}$ both further consumed the desired $[^{11}\text{C}]\text{nitrile}$ by further alkylation reaction with it and also poisoned the next reductive cyclization step. However, a systematic investigation and optimization of each step resulted in a

robust, rapid and reproducible method for the radiosynthesis of **[2-¹¹C]indole**. In addition, the conditions that we describe here could be adapted to commercially available radiosynthesizer for full-scale automation. Furthermore, it is reasonable to postulate that this [¹¹C]cyanation and reductive cyclization combined method could be quickly adapted to synthesize carbon-11 labeled indole derivatives with functional groups attached at phenyl ring of indole. Currently, we are working on plant and bacteria imaging study using **[2-¹¹C]indole** tracer and these results will be reported separately.

6. Reference

1. Kaushik, N. K.; Kaushik, N.; Attri, P.; Kumar, N.; Kim, C. H.; Verma, A. K.; Choi, E. H., Biomedical importance of indoles. *Molecules* **2013**, *18*, 6620-6662.
2. Woodward, A. W.; Bartel, B., Auxin: Regulation, action, and interaction. *Ann. Bot. (Oxford, U. K.)* **2005**, *95* (5), 707-735.
3. (a) Tivendale, N. D.; Davies, N. W.; Molesworth, P. P.; Davidson, S. E.; Smith, J. A.; Lowe, E. K.; Reid, J. B.; Ross, J. J., Reassessing the role of N-hydroxytryptamine in auxin biosynthesis. *Plant Physiol.* **2010**, *154* (4), 1957-1965; (b) Normanly, J., Approaching cellular and molecular resolution of auxin biosynthesis and metabolism. *Cold Spring Harb Perspect Biol* **2010**, *2* (1), a001594; (c) Phillips, K. A.; Skirpan, A. L.; Liu, X.; Christensen, A.; Slewinski, T. L.; Hudson, C.; Barazesh, S.; Cohen, J. D.; Malcomber, S.; McSteen, P., Vanishing tassel2 encodes a grass-specific tryptophan aminotransferase required for vegetative and reproductive development in maize. *Plant Cell* **2011**, *23* (2), 550-566; (d) McSteen, P., Auxin and monocot development. *Cold Spring Harb Perspect Biol* **2010**, *2* (3), a001479.
4. (a) Reid, A. E.; Kim, S. W.; Seiner, B.; Fowler, F. W.; Hooker, J.; Ferrieri, R.; Babst, B.; Fowler, J. S., Radiosynthesis of C-11 labeled auxin (3-indolyl[1-11C]acetic acid) and its derivatives from gramine. *J. Labelled Compd. Radiopharm.* **2011**, *54* (8), 433-437; (b) Xu, Y.; Alexoff, D. L.; Kunert, A. T.; Qu, W.; Kim, D.; Paven, M.; Babst, B. A.; Ferrieri, R. A.; Schueller, M. J.; Fowler, J. S., Radiosynthesis of 3-indolyl[1-11C]acetic acid for phyto-PET-imaging: An improved production procedure and formulation method. *Appl. Radiat. Isot.* **2014**, *91*, 155-160.
5. Lee, S.; Alexoff, D. L.; Shea, C.; Kim, D.; Schueller, M.; Fowler, J. S.; Qu, W., Tetraethylene glycol promoted two-step, one-pot rapid synthesis of indole-3-[1-11C]acetic acid. *Tetrahedron Lett.* **2015**, *56* (3), 517-520.
6. (a) Humphrey, G. R.; Kuethe, J. T., Practical methodologies for the synthesis of Indoles. *Chem. Rev. (Washington, DC, U. S.)* **2006**, *106* (7), 2875-2911; (b) Shukla, G.; Verma, R. K.; Verma, G. K.; Singh, M. S., Solvent-free sonochemical one-pot three-component synthesis of 2H-indazolo[2,1-b]phthalazine-1,6,11-triones and 1H-pyrazolo[1,2-b]phthalazine-5,10-diones. *Tetrahedron Lett.* **2011**, *52* (52), 7195-7198.
7. Czeskis, B. A.; Clodfelter, D. K.; Wheeler, W. J., Synthesis of 14C-labeled 4-hydroxyindole as an intermediate for the preparation of (S)-2-[4-[2-[3-(indol-2-[14C]-4-yloxy)-2-hydroxypropylamino]-2-methylpropyl]-phenoxy]pyridine-5-carboxamide (LY368842-[indole-14C]) glycolate. *J. Labelled Compd. Radiopharm.* **2002**, *45* (13), 1143-1152.
8. Pedras, M. S. C.; Okinyo, D. P. O., Syntheses of perdeuterated indoles and derivatives as probes for the biosynthesis of crucifer phytoalexins. *J. Labelled Compd. Radiopharm.* **2006**, *49* (1), 33-45.
9. Czeskis, B. A., Syntheses of two isotopically labeled CB1 receptor antagonists. *J. Labelled Compd. Radiopharm.* **2012**, *55* (5), 171-179.
10. (a) Zessin, J.; Steinbach, J., 11C-labeling of heterocyclic aromatic compounds in ring positions: synthesis of [2-11C]indole. *J. Labelled Compd. Radiopharm.* **1998**, *41* (7), 669-676; (b) Zessin, J.; Steinbach, J.; Johannsen, B., Synthesis of triphenylarsonium [11C]methylide, a

new ¹¹C-precursor. Application in the preparation of [2-¹¹C]indole. *J. Labelled Compd. Radiopharm.* **1999**, 42 (8), 725-736.

11. (a) Lamb, J. F.; James, R. W.; Winchell, H. S., Recoil synthesis of high specific activity ¹¹C cyanide. *Int. J. Appl. Radiat. Isotop.* **1971**, 22 (8), 475-9; (b) Christman, D. R.; Finn, R. D.; Karlstrom, K. I.; Wolf, A. P., Production of carrier-free hydrogen cyanide (carbon-11) for medical use and radiopharmaceutical syntheses. IX. *J. Nucl. Med.* **1973**, 14 (11), 864-6; (c) Miller, P. W.; Long, N. J.; Vilar, R.; Gee, A. D., Synthesis of ¹¹C, ¹⁸F, ¹⁵O, and ¹³N radiolabels for positron emission tomography. *Angew. Chem., Int. Ed.* **2008**, 47 (47), 8998-9033; (d) Lee, H. G.; Milner, P. J.; Placzek, M. S.; Buchwald, S. L.; Hooker, J. M., Virtually instantaneous, room-temperature [(¹¹C)-cyanation using biaryl phosphine Pd(0) complexes. *J Am Chem Soc* **2015**, 137 (2), 648-51.

12. Kalir, A.; Mualem, R., One-step synthesis of 2- and 4-nitrobenzyl cyanides. *Synthesis* **1987**, (5), 514-15.

13. Kim, D.; Alexoff, D.; Kim, S. W.; Hooker, J.; Ferrieri, R. A. ¹¹C-Labeled cyanide production system. US20130045151A1, 2013.

14. Antoni, G.; Omura, H.; Bergstrom, M.; Furuya, Y.; Moulder, R.; Roberto, A.; Sundin, A.; Watanabe, Y.; Langstrom, B., Synthesis of L-2,4-diamino[4-¹¹C]butyric acid and its use in some in vitro and in vivo tumor models. *Nucl. Med. Biol.* **1997**, 24 (6), 595-601.

15. Gowda, S.; Gowda, D. C., Application of hydrazinium monoformate as new hydrogen donor with Raney nickel: a facile reduction of nitro and nitrile moieties. *Tetrahedron* **2002**, 58 (11), 2211-2213.

16. Gleede, T.; Riehl, B.; Shea, C.; Kersting, L.; Cankaya, A. S.; Alexoff, D.; Schueller, M.; Fowler, J. S.; Qu, W., Investigation of SN2 [¹¹C]cyanation for base-sensitive substrates: an improved radiosynthesis of L-[5-¹¹C]-glutamine. *Amino Acids* **2015**, 47 (3), 525-533.

17. (a) Snyder, H. R.; Merica, E. P.; Force, C. G.; White, E. G., Synthesis of indoles by catalytic reduction of o-nitrobenzyl cyanides. *J. Am. Chem. Soc.* **1958**, 80, 4622-5; (b) Walker, G. N., Synthesis of α -(p-aminophenyl)- and α -(p-chlorophenyl)- β -arylpropionitriles by catalytic reduction of stilbenenitriles. *J. Med. Chem.* **1965**, 8 (5), 583-8.

18. (a) Macor, J. E.; Froman, J. T.; Post, R. J.; Ryan, K., Synthesis and reactivity of pyrrolo[3,2-e]indole: removal of a N-BOM group from an unactivated indole. *Tetrahedron Lett.* **1997**, 38 (10), 1673-1676; (b) Sajiki, H.; Ikawa, T.; Hirota, K., Reductive and catalytic monoalkylation of primary amines using nitriles as an alkylating reagent. *Org. Lett.* **2004**, 6 (26), 4977-4980.

19. (a) Walker, G. N., Synthesis of 5,6-dimethoxyindoles and 5,6-dimethoxyoxindoles. A new synthesis of indoles. *J. Am. Chem. Soc.* **1955**, 77, 3844-50; (b) Groszek, G.; Bednarski, M.; Dybala, M.; Filipek, B., Synthesis and adrenolytic activity of 1-(1H-indol-4-yloxy)-3-{[2-(2-methoxyphenoxy)ethyl]amino}propan-2-ol and its enantiomers. Part 1. *Eur. J. Med. Chem.* **2009**, 44 (2), 809-817.

20. (a) Mandal, P. K.; McMurray, J. S., Pd-C-induced catalytic transfer hydrogenation with triethylsilane. *The Journal of organic chemistry* **2007**, 72 (17), 6599-601; (b) Khdour, O.; Ouyang, A.; Skibo, E. B., Design of a Cyclopropyl Quinone Methide Reductive Alkylating Agent. 2. *J. Org. Chem.* **2006**, 71 (16), 5855-5863.

21. Johnstone, R. A. W.; Wilby, A. H.; Entwistle, I. D., Heterogeneous catalytic transfer hydrogenation and its relation to other methods for reduction of organic compounds. *Chem. Rev.* **1985**, 85 (2), 129-70.

22. Sarmah, B. K.; Barua, N. C., Al-NiCl₂·6H₂O-THF: a new, mild and neutral system for selective reduction of organic functional groups. *Tetrahedron* **1991**, *47* (40), 8587-600.
23. Reader, J. C.; Matthews, T. P.; Klair, S.; Cheung, K.-M. J.; Scanlon, J.; Proisy, N.; Addison, G.; Ellard, J.; Piton, N.; Taylor, S.; Cherry, M.; Fisher, M.; Boxall, K.; Burns, S.; Walton, M. I.; Westwood, I. M.; Hayes, A.; Eve, P.; Valenti, M.; de Haven Brandon, A.; Box, G.; van Montfort, R. L. M.; Williams, D. H.; Aherne, G. W.; Raynaud, F. I.; Eccles, S. A.; Garrett, M. D.; Collins, I., Structure-Guided Evolution of Potent and Selective CHK1 Inhibitors through Scaffold Morphing. *J. Med. Chem.* **2011**, *54* (24), 8328-8342.
24. Fowler, J. S.; Wolf, A. P., Working against Time: Rapid Radiotracer Synthesis and Imaging the Human Brain. *Acc. Chem. Res.* **1997**, *30* (4), 181-188.

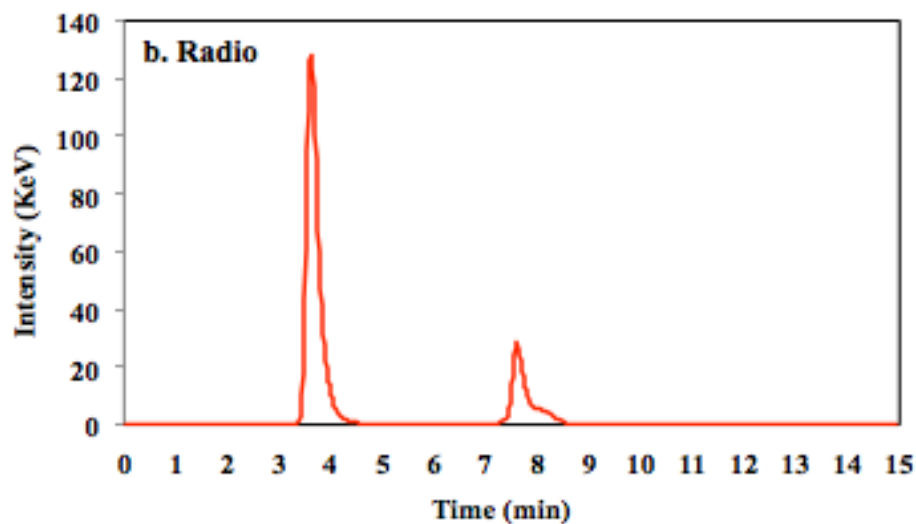
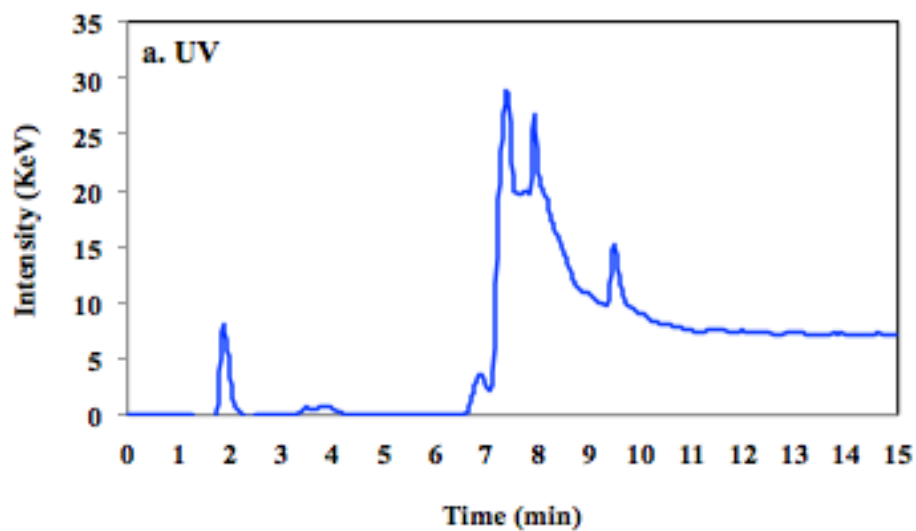
Supplementary Information for CHAPTER 4.

Part 1. HPLC: analytical HPLC & semi-preparative HPLC

Part 2. $^1\text{H}/^{13}\text{C}$ NMR spectroscopy and Mass spectrometry (ESI)

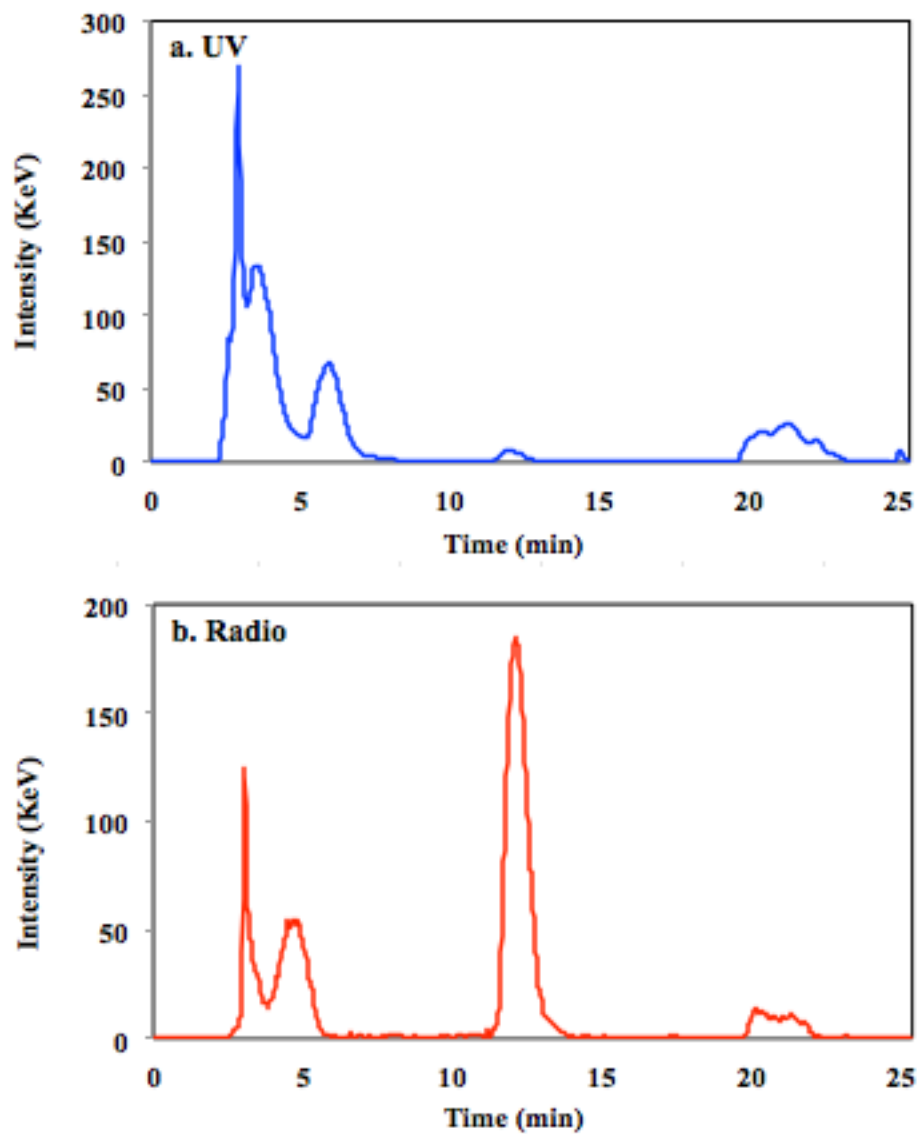
Part 1. HPLC: analytical HPLC & semi-preparative HPLC

1.1. [^{13}C]cyanation analysis



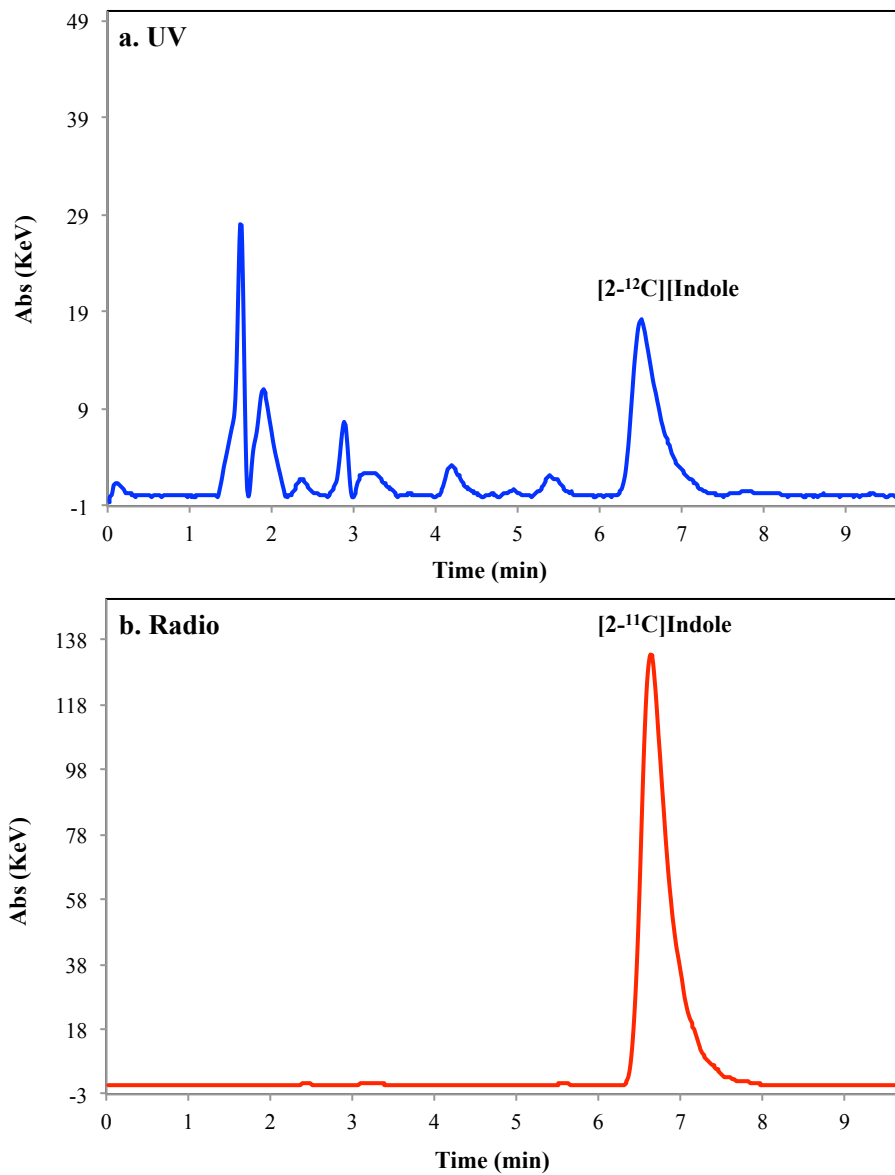
Peak at 3.5 min: [^{13}C]nitrile; peak at 7.7 min: [^{13}C]dimer

1.2. Semi-preparative HPLC for [^{11}C] indole purification



Peak at 12 min: [^{11}C]indole

1.3. Product [2-¹¹C]indole quality analysis



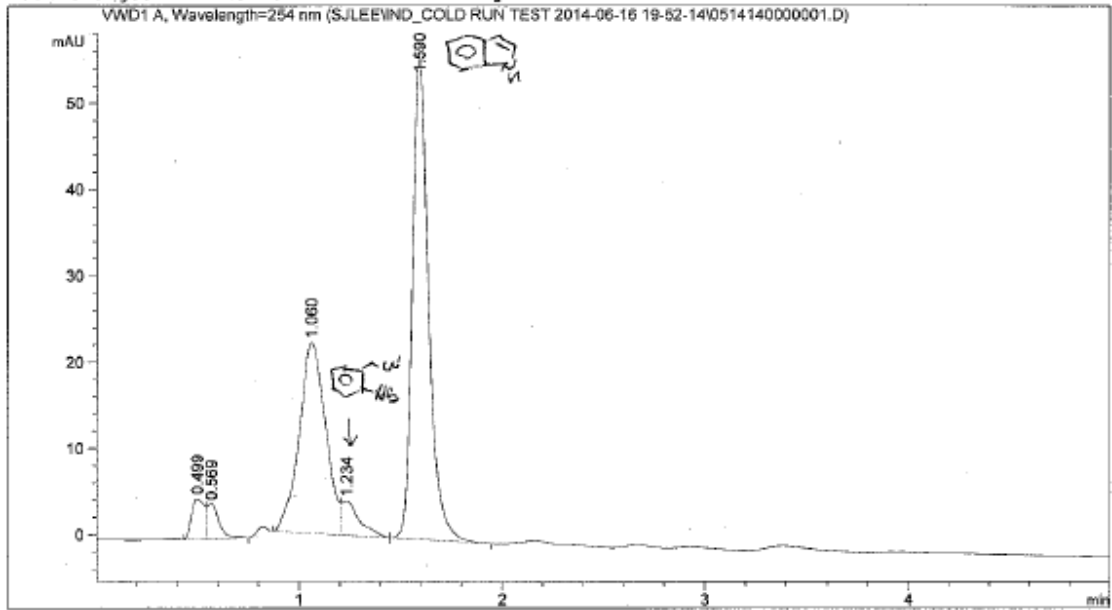
Peak at 6.5 min (a. UV): pure mass of [2-¹²C]indole; peak at 6.8 min (b. Radio): desired product [2-¹¹C]indole

1.4. Cold reductive cyclization without 2-nitrobenzyl bromide

Data File C:\CHEM32\1\DATA\SJLEE\IND_COLD RUN TEST 2014-06-16 19-52-14\0514140000001.D
 Sample Name: 10min

```

=====
Acq. Operator   : SYSTEM                               Seq. Line :    1
Acq. Instrument : HPLC555                             Location  : Vial 54
Injection Date  : 6/16/2014 7:52:58 PM                Inj       :    1
                                                    Inj Volume: 3.000 µl
Acq. Method     : C:\CHEM32\1\DATA\SJLEE\IND_COLD RUN TEST 2014-06-16 19-52-14\ISO_5050_
                  4.6X30.M
Last changed    : 6/16/2014 7:52:15 PM by SYSTEM
Analysis Method : C:\CHEM32\1\DATA\SJLEE\IND_COLD RUN TEST 2014-05-14 16-02-04\ISO_5050_
                  4.6X30.M (Sequence Method)
Last changed    : 5/14/2014 4:02:04 PM by SYSTEM
=====
  
```



Area Percent Report

```

=====
Sorted By      : Signal
Multiplier     : 1.0000
Dilution      : 1.0000
Use Multiplier & Dilution Factor with ISTDs
=====
  
```

Signal 1: VWD1 A, Wavelength=254 nm

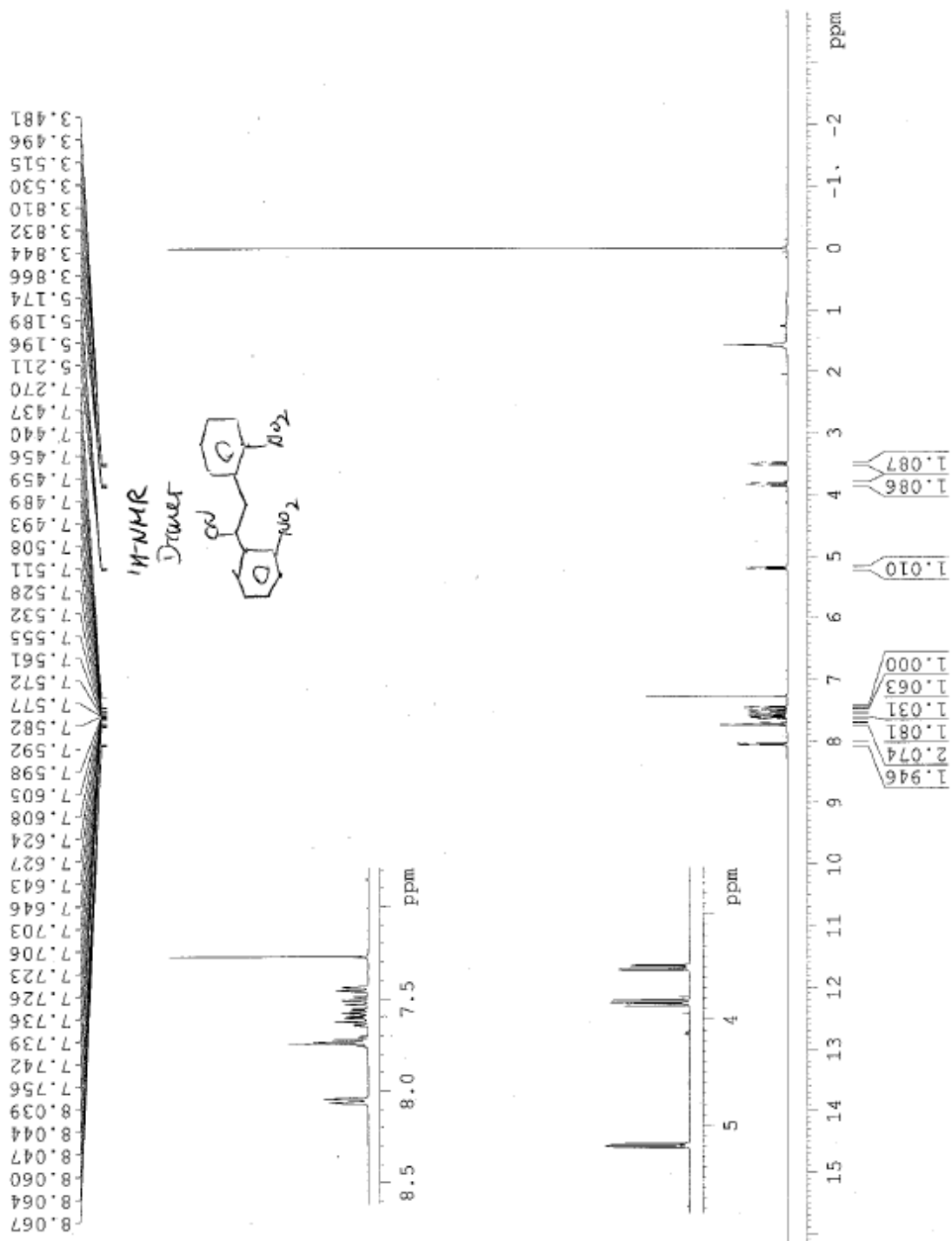
Peak #	RetTime [min]	Type	Width [min]	Area [mAU*s]	Height [mAU]	Area %
1	0.499	BV	0.0677	20.66085	4.65895	3.6081
2	0.569	VB	0.0590	16.04193	3.98427	2.8015
3	1.060	BV	0.1378	200.73991	22.12646	35.0564
4	1.234	VB	0.0832	23.51841	3.96463	4.1072
5	1.590	BB	0.0841	311.65836	55.83846	54.4268
Totals :				572.61946	90.57277	

Part 2. $^1\text{H}/^{13}\text{C}$ NMR spectroscopy and Mass spectrometry (ESI)

2.1. ^1H NMR of 2,3-bis(2-nitrophenyl)propanenitrile (dimer)

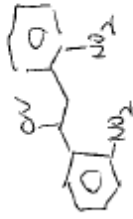
2.2. ^{13}C NMR of 2,3-bis(2-nitrophenyl)propanenitrile (dimer)

2.3. LR-MS (ESI) of 2,3-bis(2-nitrophenyl)propanenitrile (dimer)



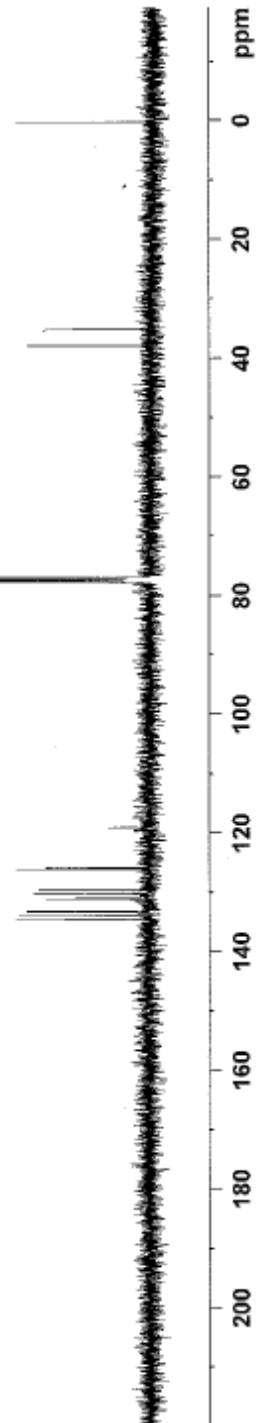
¹³C-NMR

Dimer



37.85
35.14

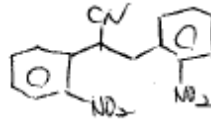
134.59
133.92
133.14
130.93
130.87
130.15
129.95
129.40
125.97
125.76
119.01



Print of window 80: MS Spectrum

Data File : D:\CHEM32\DATA\FOWLER\061215_DIMER.D

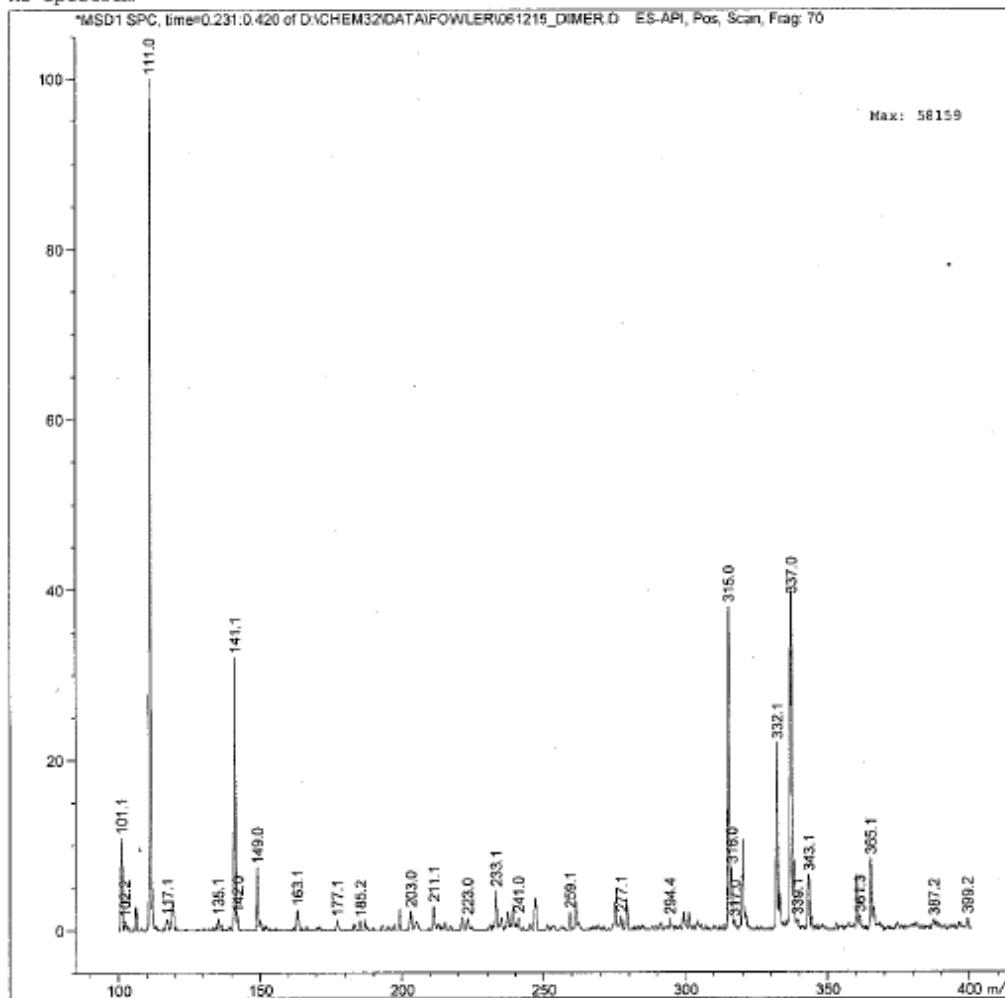
Sample Name : 061215_dimer.D



Acq. Operator : So Jeong
Acq. Instrument : Instrument 1 Location : Vial 1
Injection Date : 6/12/2015 6:49:57 PM Inj : 1
Inj Volume : 1.0 µl

Acq. Method : D:\CHEM32\METHODS\DIR-INJ-POS.M
Last changed : 6/12/2015 6:49:12 PM by So Jeong
(modified after Loading)
Analysis Method : D:\CHEM32\DATA\FOWLER\061215_DIMER.D\DA.M (DIR-INJ-POS.M, From Data File)
Last changed : 6/12/2015 6:51:34 PM by So Jeong
Method Info : Direct-inject (FIA) ESI positive
A1 (0.1%Ac): B1 (MeOH); 25:75(v:v); 0.25ml/min

MS Spectrum



Instrument 1 6/12/2015 6:51:59 PM rajesh

Page 1 of 1

CHAPTER 5.

Stereoselective Radiosynthesis of L-[4-¹¹C]-Asparagine from Cyclic Sulfamidate Precursor

1. Abstract

There is evidence that asparagine, similar to glutamine, plays an important role as a nitrogen source in plants. Our objective was to develop a stereospecific synthesis of ¹¹C-labeled L-asparagine, using a five-membered ring sulfamidate precursor and nucleophilic ring-opening with H¹¹CN. For that, efficient preparation of the cyclic sulfamidate and model reaction without radioisotope (cold chemistry) has been developed.

Preparation of (S)-di-tert-butyl 1,2,3-oxathiazolidine-3,4-dicarboxylate 2,2-dioxide (**4**) derived from commercially available Boc-*O*-benzyl-L-serine was accomplished in four steps: 1) tert-butyloxycarbonyl (Boc) protecting group synthesis; 2) cleavage of benzyl ether; 3) nucleophilic substitution with thionyl chloride to the activated β -position of L-serine; 4) further oxidation of sulfamidite to sulfamidate. Model reaction in cold chemistry to prepare radiosynthesis of L-[4-¹¹C] asparagine was performed via ring-opening nucleophilic cyanation followed by hydrolysis.

Anhydrous [¹¹C]HCN passed through a 50% H₂SO₄ followed by a P₂O₅ trap was collected in a reaction vessel containing base/18-Crown-6/DMF solution. Following the addition of sulfamidate in DMF, the reaction mixture was heated and then purified by solid phase extraction (SPE). The azeotropically dried [¹¹C]nitrile intermediate was then hydrolyzed via selective

deprotection with H₂SO₄ and TFA. L-[4-¹¹C]-asparagine was purified using Ag11-A8 resin and enantiomeric purity was determined by chiral radio-HPLC analysis of [¹¹C]aspartic acid, the hydrolyzed product of L- [4-¹¹C]-asparagine.

The overall yield of the cyclic sulfamidate (**4**) was 32 %. The radiochemical yield of [¹¹C]nitrile intermediate was 60 – 68 % (decay corrected, based on [¹¹C]HCN radioactivity). The overall radiochemical yield was 45 – 52 %, the radiochemical purity was > 96 % and the L/D ratio > 40/1 with a synthesis time of 50 min. The specific activity of desire product was 5.5 – 11.1 GBq/μmol at the end of bombardment.

Using a newly designed five-membered ring sulfamidate precursor, we have successfully synthesized L-[4-¹¹C]-asparagine through ring-opening nucleophilic [¹¹C]cyanation and selective acidic hydrolysis and deprotection reactions. Further biological studies via PET imaging are in progress.

2. Introduction

Amino acids are essential small organic molecules used in the synthesis of proteins and other biologically active compounds such as neurotransmitters and hormones that are present across the animals and plants as well¹. Due to the biological significance of many amino acids and their derivatives, the development of new methodology for the synthesis of labeled amino acids continues to attract the attention of many synthetic organic chemists²

Positron emission tomography (PET) is a powerful technique for the in vivo study of biochemical processes and has become a valuable tool for both basic biomedical research and

diagnostic imaging. This technique relies on the synthesis of tracer molecules, which are biologically important and labeling with short-lived positron emitting nuclides^{1,2b}.

α -Amino acids labeled with short-lived positron emitters carbon-11 ($t_{1/2} = 20$ min) and fluorine-18 ($t_{1/2} = 110$ min) are of particular interest and extensively used for the visualization of tumors³, measurements of protein synthesis rates⁴ and amino acid decarboxylation rates⁵ in humans using PET. Therefore, because of immense importance of amino acids in living systems as well as continuous development of positron imaging techniques such as small animal PET⁶ and beta microprobes⁷, the application of ¹¹C-labeled amino acids as the research tools has been developed in conjunction with PET for measurement of *in vivo* processes and expanded to other areas of life science.

This trend requires widely applicable, simple, inexpensive, robust and reliable synthetic methods to produce natural and non-natural amino acids labeled with short half-lived radioisotopes for nuclear medicine studies. During the last three decades many synthetic schemes for different amino acids labeled with C-11 have been developed and evaluated as potential PET imaging agents^{2b}.

For instance, the use of ¹¹C-labelled methionine for the detection and delineation of malignant brain tumors has increased markedly over the last few years⁸. Other ¹¹C-labelled amino acids such as [¹¹C]DOPA⁹, [¹¹C]tyrosine¹⁰ and [¹¹C]5-hydroxytryptophan¹¹ have been utilized in PET oncology studies in recent years. However, some of them either required harsh reaction conditions such as high pressure and high temperature in corrosive environments¹² or relatively complicated multistep syntheses with water-sensitive reagents involved¹³.

More recently, a preliminary investigation of the uptake of ¹¹C-labelled glutamate, glutamine and aspartate in tumor cell aggregates and *in vivo* in both rats and humans has been reported¹⁴.

Of these three amino acids, ^{11}C -aspartate appeared most promising, with a high uptake in neuroblastoma aggregates combined with relatively low organ uptake¹⁵.

There is a meaningful study for the synthesis of [4- ^{11}C]D,L-asparagine via the ring opening of aziridine-2-carboxylic acid with [^{11}C]cyanide to form β -[^{11}C]cyanoalanine which is hydrolyzed to [4- ^{11}C]D,L-asparagine which can be resolved by chiral HPLC to produce [4- ^{11}C]L-asparagine¹⁵. Although this nucleophilic ring opening of aziridine-2-carboxylate esters provided a useful route to amino acids, stereoselectivity was not considered in this approach.

Another synthesis suggested a more straightforward route to these important amino acids labeled with C-11 via [^{11}C]cyanation with protected chiral precursor¹⁶. Similarly our group recently reported efficient radiosynthesis of C-11 glutamine¹⁷ via nucleophilic [^{11}C]cyanation followed by [^{11}C]nitrile hydrolysis and deprotection with strong acid to improve radiochemical yield and reproducibility. These previous studies inspired us to consider nucleophilic [^{11}C]cyanation reactions using tracer levels of [^{11}C]cyanide-labeling precursor, especially when the radiosynthesis required the use of acid- or base- or moisture sensitive substrates. This careful consideration with respect to non-carrier added [^{11}C]cyanation also encouraged us forward to develop a stereoselective synthesis of L-[4- ^{11}C]asparagine, which has not been accomplished, via tracer level $\text{S}_{\text{N}}2$ [^{11}C]cyanation reaction.

For our new, efficient stereoselective route for the synthesis of L-[4- ^{11}C]asparagine, five-membered ring sulfamidate was considered as a precursor for [^{11}C]cyanation. A cyclic sulfamidate derived from serine might simultaneously activate the β -position to nucleophilic attack and partially protect the amino group, and thus provide a useful ' β -alanyl cation' synthon for the synthesis of α -amino acids¹⁸. Based on this hypothesis, constraining the leaving group in a five-membered ring would reduce the rate of elimination due to poor overlap between the

developing enolate and the leaving oxygen atom¹⁹. Accordingly, nucleophilic [¹¹C]cyanation would be more favorable than elimination which would result in epimerization.

Herein we describe newly designed synthesis for five-membered ring sulfamidate precursor. We have confirmed stereoselective strategy to obtain L-asparagine via cyanation followed by hydrolysis in a preliminary reaction without radioactivity. Based on the strategy tested without radioactivity, we also successfully synthesize L-[4-¹¹C]-asparagine through ring-opening nucleophilic [¹¹C]cyanation and selective acidic hydrolysis and deprotection reactions. Further biological studies via PET imaging are in progress.

3. Experimental details

3.1. General

All commercial chemical reagents, substrates and solvents for synthesis and analysis were purchased from Sigma-Aldrich Chemical Co. (St. Louis, MO, USA) with a minimum of ACS reagent grade and used without further purification. Solid phase extraction (SPE) cartridges (SepPak® C18 plus) manufactured by Waters (Waters® Association, MA, USA) were used. The reaction was carried out in a 10 cc microwave reaction vial sealed by a cap and septum to withstand high pressure (Biotage® INC., VA, USA). Thus, semi-reflux reaction system was maintained with a variety of alcoholic solvent/water solvents for hydrolysis and water was condensed on the cap.

Chemical reactions performed without radioisotope labeling were characterized by ultra-high performance liquid chromatography (UHPLC) using an Agilent model 1200 system (Agilent Technologies Inc., Santa Clara, CA). For the radiochemistry, high and low levels of

radioactivity were measured using a Capintec CRC-712MV and a Capintec CRC-ultra radioisotope dose calibrator (Capintec Inc. NJ, USA) respectively. Semi-preparative high performance liquid chromatography (HPLC) was performed using a Knauer HPLC system equipped with a model K-1001 pump, a model 87 variable wavelength monitor, a NaI detector and a SRI peak simple integration system. Analytical HPLC was performed using a Knauer model K-1001 pump, a Knauer model K2501 UV detector (254nm), a Geiger Muller ionization detector and a SRI Peak simple integration System. Radiochemical yields (decay-corrected back to end of cyclotron bombardment (EOB)) were obtained based on the total radioactivity trapped in the reaction vessel at the start of the reaction. Specific activities, decay corrected back to EOB and recorded in mCi/nmol, were determined from the C-11 activity in the product peak in the HPLC and the mass of compound. Total synthesis times were calculated from EOB to the end of radiotracer formulation.

3.2. Cold chemistry

Overall scheme for synthesis for five-membered ring sulfamidate precursor is shown on Figure 1. We also have confirmed stereoselective strategy to obtain L-asparagine via cyanation followed by hydrolysis in the model reaction without radioactivity (Figure 2).

Figure 1, Preparation of sulfamidate precursor for the synthesis of asparagin

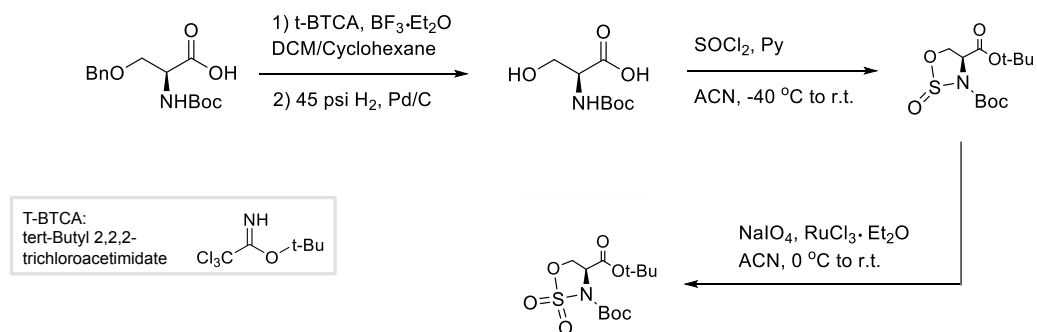
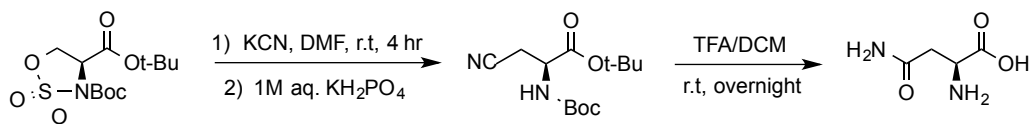
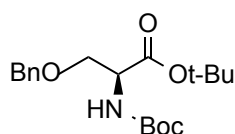


Figure 2. Cold reaction for asparagine via nucleophilic cyanation of sulfamidate followed by acidic hydrolysis



3.2.1. Synthesis of sulfamidate

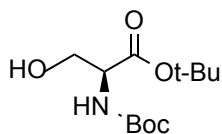
L-N-[(1,1-dimethylethoxy)carbonyl]-O-(phenylmethyl)-, 1,1-dimethylethyl ester (1)



Commercially available *N*-(*tert*-Butoxycarbonyl)-*O*-benzyl-L-serine (Boc-*O*-benzyl-L-serine) (1.475 g, 5 mmol, 1 equiv) was dissolved in dichloromethane (20 mL) in a 100 mL flask. To the 100 mL reaction flask, *tert*-Butyl 2,2,2-trichloroacetimidate (TBTA) (2.185 g, 10 mmol, 2 equiv) dissolved in cyclohexane (10 mL) was transferred then $\text{BF}_3 \cdot \text{Et}_2\text{O}$ (0.071 g, 0.5 mmol, 0.1 equiv) was used as a catalyst. The reaction was performed at r.t for 1 h until no starting material was left. NaHCO_3 (1.68 g, 20 mmol, 4 equiv) was added to the reaction mixture and stir for 5 min at the same temperature. The reaction crude was filtered through a plug of celite under suction and concentrated by rotary evaporator under vacuum. The crude product was purified by flash chromatography (silica gel, 300 g), eluting with 15 % ethyl acetate in hexane. Fractions containing the desire product **1** were identified by TLC (SiO_2 , 20/80 EtOAc/hexane, $R_f = 0.6$). The Boc protected **1** was obtained as a white powder (1.7 g, 97 %). ^1H NMR (400 Hz, CDCl_3): δ 7.26 – 7.27 (m, 5H), 5.38 (d, $J = 8.4$ Hz, 1H), 4.53 (dd, $J = 34, 12.4$ Hz, 2H), 4.32 (d, $J = 2$ Hz, 1H), 3.86 (dd, $J = 9.2, 6$ Hz, 1H), 3.66 (dd, $J = 9.2, 6$ Hz, 1H), 1.46 (s, 9H), 1.45 (s, 9H). ^{13}C

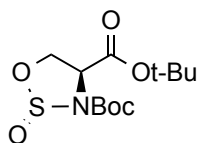
NMR (100 Hz, CDCl₃): δ 169.90, 128.57, 127.93, 127.81, 82.18, 79.90, 73.51, 70.72, 54.70, 28.55, 28.20. MS (ESI): m/z [M+H⁺] calcd for C₁₉H₂₉NO₅ 351.3 found 352.0.

L-N-[(1,1-dimethylethoxy)carbonyl]-, 1,1-dimethylethyl ester (2)



The selective cleavage of benzyl ether in **1** (1 g, 3 mmol, 1.0 equiv) using H₂ (45 psi) over Pd/C (10%) (32 mg, 0.3 mmol, 0.1 equiv) in EtOH (15 mL) was performed by Parr shaker at r.t for 4 h. The reaction crude was filtered through celite and rotary evaporated. The crude product was purified by flash chromatography (silica gel, 200 g), eluting with 15 % ethyl acetate in hexane. Fractions containing the desired product **2** were identified by TLC (SiO₂, 20/80 EtOAc/hexane, R_f = 0.2) with ninhydrin staining. The desired product **2** was obtained as a white powder (0.69 g, 88 %). ¹H NMR (400 Hz, CDCl₃): δ 5.43 (s, 1H), 4.25 (s, 1H), 3.89 (t, J = 4 Hz, 2H), 2.48 (s, 1H), 1.49 (s, 9H), 1.46 (s, 9H). ¹³C NMR (100 Hz, CDCl₃): δ 169.97, 156.10, 82.85, 80.34, 64.31, 56.56, 28.51, 28.21.

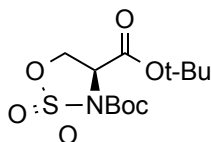
L-1,2,3-Oxathiazolidine-3,4-dicarboxylic acid, 3,4-bis(1,1-dimethylethyl) ester, 2-oxide (3)



Thionyl chloride (0.09 g, 0.75 mmol, 1.5 equiv) was prepared in the 15 mL-reaction flask and diluted with acetonitrile (2 mL) then cooled to -40 °C by EtOAc/dry ice bath. **2** (0.13 g, 0.5 mmol, 1.0 equiv) was dissolved in another 2 mL of acetonitrile and added dropwise to the 15 mL flask. The reaction mixture was stirred at the same temperature for 45 min then pyridine (0.2 g, 2.5 mmol, 5.0 equiv) was also added dropwise to the mixture. The reaction mixture was stirred

for 1h at -40 °C then gradually warmed up to r.t and kept stirring at the same temperature for additional 30 min. The reaction was quenched by poured into iced-water (10 mL). The crude mixture was partitioned between H₂O and EtOAc. The aqueous layer was extracted with ethyl acetate (10 mL × 3) and the combined organic extracts were washed with 1M aqueous HCl (5 mL × 2), ice-cold NaHCO₃ (5 mL), and brine (5 mL) then dried (Na₂SO₄), filtered and concentrated. The cyclic sulfamidate **3** identified by TLC (SiO₂, 20/80 EtOAc/hexane, *R_f* = 0.45) with ninhydrin staining was dried under vacuo and this crude **3** used for further oxidation without purification.

L-1,2,3-Oxathiazolidine-3,4-dicarboxylic acid, 3,4-bis(1,1-dimethylethyl) ester, 2,2-dioxide
(4)



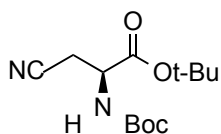
The crude **3** (0.154 g, 0.5 mmol, 1.0 equiv) stored in the 25 mL of reaction flask was dissolved in acetonitrile (3 mL) and the solution was cooled with ice-water bath. To the solution, RuCl₃•H₂O (3 mg, 0.015 mmol, 0.03 equiv) and NaIO₄ (0.16 g, 0.75 mmol, 1.5 equiv) was added and 3 mL of H₂O was also added, respectively. The reaction was performed at 0 °C for 2 h then poured into diethyl ether (10 mL). The crude mixture was partitioned between H₂O and Et₂O. The aqueous layer was extracted with Et₂O (10 mL × 2) and the combined organic layers were washed with ice-cold saturated aqueous NaHCO₃ (5 mL) and brine (5 mL). The organic phase was submitted to NaSO₄, filtered and concentrated. The crude product was purified by flash chromatography (silica gel, 100 g), eluting with 15 % ethyl acetate in hexane. Fractions containing the desire product **4** were identified by TLC (SiO₂, 20/80 EtOAc/hexane, *R_f* = 0.32) with ninhydrin staining. The product **4** was obtained as a white powder (0.16 g, 99 %). ¹H

NMR (400 Hz, CDCl₃): δ 4.76 – 4.71 (m, 1H), 4.64 – 4.62 (m, 2H), 1.57 (s, 9H), 1.52 (s, 9H).

¹³C NMR (100 Hz, CDCl₃): δ 166.35, 148.43, 86.21, 84.83, 68.09, 58.45, 28.22, 28.15.

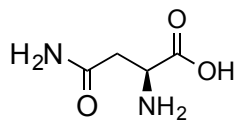
3.2.2. Synthesis of asparagine from prepared sulfamidate

3-Cyano-2-[[[(1,1-dimethylethoxy)carbonyl]amino]-, 1,1-dimethylethyl ester, (2S)- (5)



To the sulfamidate **4** (96 mg, 0.3 mmol, 1 equiv) in a reaction vial, KCN (39 mg, 0.6 mmol, 2 equiv) was added and dissolved in dry DMF (3 mL). The reaction mixture was stirred at r.t for 4 h. The reaction crude was poured into 1M aqueous KH₂PO₄ (20 mL) and the organic phase was extract with ethyl acetate (15 mL \times 3) and rinsed with brine (15 mL \times 2). The crude mixture was dried (NaSO₄), filtered and concentrated under vacuo. The crude **5** was identified by TLC (SiO₂, 20/80 EtOAc/hexane, R_f = 0.4) with ninhydrin staining. The crude product was purified by flash chromatography (silica gel, 100 g), eluting with 15 % ethyl acetate in hexane. However fractions containing the desire product **5** contained unknown impurity as well. This unknown impurity which is UV active but ninhydrin inactive was detected by TLC (SiO₂, 20/80 EtOAc/hexane, R_f = 0.38). The two spots of product **5** and the unknown impurity were too close to be separated. The presence of product **5** in the crude mixture was confirmed by MS spec and ¹H NMR. According to ¹H NMR spectrum (**Supporting information**), product **5**/unknown aromatic impurity = 2/1 was confirmed. The product **5** including unknown impurity was used for hydrolysis to obtain asparagine. ¹H NMR (400 Hz, CDCl₃): δ 5.44 (d, J = 5.6 Hz, 1H), 4.37 (d, J = 6 Hz, 1H), 2.92 (qd, J = 17.4, 5.2, 2H). MS (ESI): m/z [M+H⁺] calcd for C₁₄H₂₄N₂O₄ 284.17 found 285.

Asparagine (6)

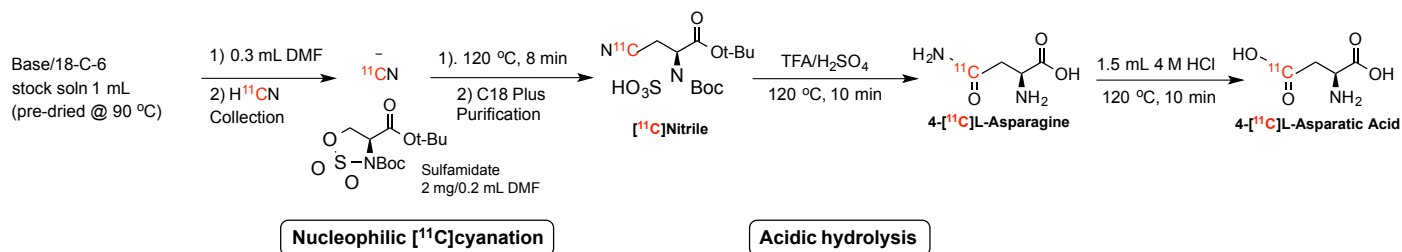


The product **5** including unknown aromatic impurity (27 mg of **5** in total 40 mg of crude, 0.1 mmol, 1 equiv) was dissolved in methylene chloride (2 mL) and treated with trifluoroacetic acid (10 % v/v, 0.2 mL, 2.6 mmol, 26 equiv) and DMSO (10 μ L) as a scavenger. The reaction mixture was stirred at r.t for 12 hr then the resulting crude was concentrate by rotary evaporator. The resulting crude was dissolved in H₂O (1mL) and neutralized by adding 5% aqueous NH₃ solution dropwise. A plug of Ag 50W-X8 resin (3.6 g) was prepared for the purification of the neutralized crude mixture. Fractions containing the desire asparagine (**6**) were identified by TLC (SiO₂, 20/80 EtOAc/hexane, *R_f*= 0.3) with ninhydrin staining. The product **6** was confirmed by mass spectroscopy. MS (ESI): *m/z* [M+H⁺] calcd for C₄H₈N₂O₃ 132.05 found 133.1.

3.3. Radiochemistry

Based on the strategy tested without radioactivity (**3.2. Cold chemistry**), we also carried out the synthesis of L-[4-¹¹C]-asparagine through ring-opening nucleophilic [¹¹C]cyanation and selective acidic hydrolysis and deprotection reactions (Figure 3).

Figure 3. Radiosynthesis of [¹¹C]asparagine via [¹¹C]cyanation followed by alkaline hydrolysis from sulfamidate precursor



3.3.1. Production of [^{11}C]CO $_2$ and [^{11}C]HCN

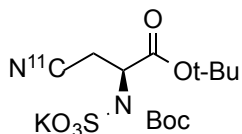
Carbon-11 was generated as [^{11}C]CO $_2$ using 17.4 MeV proton irradiation of N $_2$ gas target containing 100 ppm O $_2$ to induce the $^{14}\text{N}(\text{p}, \alpha)^{11}\text{C}$ nuclear reaction. Irradiations were carried out on the BNL EBCO TR-19 cyclotron. The [^{11}C]HCN was produced via automated gas phase synthesis by a homemade system²⁰. Briefly, [^{11}C]CO $_2$ produced from this process was collected over molecular sieves, catalytically reduced to [^{11}C]CH $_4$ with H $_2$ over Ni at 420°C. The [^{11}C]CH $_4$ was converted to the [^{11}C]HCN by adding gaseous ammonia and passage through a Pt furnace at 950°C at a flow rate of 350~400 mL/min. Radioactivity measurements were made in a Capintec CRC-712MV radioisotope dose calibrator (Capintec Inc., Ramsey, NJ).

3.3.2. Purification of [^{11}C]HCN

The purification procedure for delivering anhydrous [^{11}C]HCN was modified and optimized based on previously published method²¹. [^{11}C]HCN was transferred from the cyclotron vault in a gas stream in the presence of NH $_3$ and H $_2$ O. Before trapping of the [^{11}C]cyanide, it was passed through 5 mL of 50 % sulphuric acid heated to 65 °C followed by 1 – 2 g of phosphorous pentoxide. Anhydrous [^{11}C]cyanide was trapped in reaction vessel containing reaction solvent (0.3 mL), cation source (0.3 mmol) in presence of 18-C-6 (0.6 mmol) and stir bar.

3.3.3. Radiosynthesis of [^{11}C]aspragine

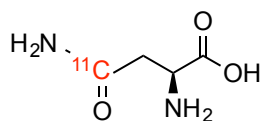
[^{11}C]Cyanation from sulfamidate precursor (4) to [^{11}C]nitrile intermediate ([^{11}C]5)



Stock solution of K $_2$ CO $_3$ /KHCO $_3$ /18-crown-6 (0.1 mmol/0.2 mmol/0.6 mmol) in H $_2$ O (3 mL)/acetonitrile (17 mL) was prepared in advance. 1 mL of the stock solution

(K₂CO₃/KHCO₃/18-crown-6 (5 μmol/10 μmol/30 μmol)) was transferred to a U-shape reaction vessel with a stirring bar and the reaction vessel was capped. The basic solution in the reaction vessel was azeotropically dried by Ar at room temperature then dissolved in 0.3 mL of dimethylacetamide (DMF). After trapping the anhydrous [¹¹C]HCN directly into the reaction vessel for 3 min at r.t, sulfamidate precursor (2 mg, 6.19 μmol) dissolved in 0.2 mL of DMF was added then the [¹¹C]cyanation reaction was performed at 120 °C for 8 min. To the crude reaction mixture, ice-cold aqueous formic acid solution (2 % v/v, 1 mL) was added for quenching the reaction. The resulting mixture was diluted with aqueous formic acid solution (2 % v/v, 9 mL) and loaded to a C18 plus SepPak® cartridge. The cartridge holding [¹¹C]nitrile intermediate was rinsed with 5 mL of deionized water and dried with air to minimize dead volume of residual water. The [¹¹C]nitrile intermediate was eluted with acetonitrile (1.5 mL) into the second reaction vessel. The intermediate [¹¹C]5 was not stable during analytical HPLC performance so [¹¹C]5 eluted from SepPak® cartridge was directly used for following hydrolysis without analysis by HPLC. Radiochemical yield of [¹¹C]5 (61%, decay-corrected) was calculated based on purified radioactivity via solid phase extraction with SepPak® measured by Capintec .

Acidic hydrolysis to [¹¹C]asparagine ([¹¹C]Asn) ([¹¹C]6)



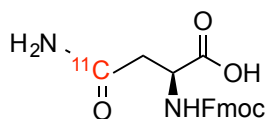
The crude [¹¹C]nitrile intermediate in the second reaction vessel was azeotropically dried under Ar flow by adding acetonitrile (1 mL × 2) at 120 °C. To the dried [¹¹C]nitrile intermediate trifluoroacetic acid/sulfuric acid (v/v = 2/1, 0.25 mL) was added and hydrolysis was performed at 120 °C for 10 min. The resulting crude was diluted with deionized water and loaded to the formulation column (D × H, 0.5'' × 2.65'', 4.5 g Ag11-A8 resin preconditioned with 0.5 M NaCl

aqueous solution (10 mL × 2) and deionized water (100 mL). After purification, three fractions (fraction 1: 2 mL, fraction 2: 4 mL and fraction 3: 2 mL) were collected separately. Radiochemical yield of [¹¹C]asparagine was obtained with the formulated [¹¹C]asparagine (fraction 2). pH of each fraction (pH ~ 7) was confirmed. The fraction 2 (4 mL) was split for 1) analysis of the quality of the [¹¹C]asparagine (**3.3.6. General procedure of [¹¹C]Asn quality control**); 2) specific activity (**3.3.7. General procedure for obtaining Fmoc-[¹¹C]Asn specific activity**); 3) further hydrolysis to [¹¹C]Asp to confirm stereoselectivity (**3.3.8. Further hydrolysis to [¹¹C]Asp and confirmation of L/D ratio**).

3.3.4. General procedure of [¹¹C]Asn quality control

A 10 – 20 µL of aliquot from the fraction 2 was injected to analytical HPLC using isocratic system with 2 mM Cu(AcO)₂ aqueous solution at flow rate 1.0 mL/min on a Chirax chiral column (Phenomenex, 250 × 4.6 mm, 5 µm). The combined L/D-[¹¹C]Asn was eluted at 12 min. Radiochemical yield of [¹¹C]Asn was 45 – 52 % and radiochemical purity was > 96 %.

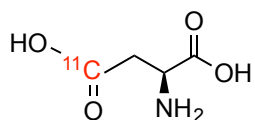
3.3.5. General procedure for obtaining Fmoc-[¹¹C]Asn specific activity



100 µL of [¹¹C]Asn from the fraction 2 was combined with 100 µL sodium borate buffer solution (pH 7.8) and vortexed. 200 µL of aliquot from the batch of Fmoc-Cl (15 mg, 0.058 µmol) dissolved in acetone (1 mL) was added to the vortexed [¹¹C]Asn mixture and vortexed every 5 min. After 15 min, reaction mixture (10 µL) was injected. The Fmoc-[¹¹C]Asn was eluted at 10 min. The UV-Fmoc-Asn peak was integrated to give nmoles. The radioactivity with injection syringe was counted in µCi before and after the injection to HPLC by Capintec and recored with clock times. The actual activity injected to HPLC was decay corrected from

Capintec to end-of-bombardment (EOB) and converted to mCi. According to this information, 5.5 – 11.1 GBq/ μmol of specific activity of [^{11}C]Asn were obtained. Determination of specific activity was carried out by Colleen Shea (**Supplementary information Part1.**)

3.3.6. Hydrolysis of [^{11}C]Asn to [^{11}C]Asp and confirmation of L/D ratio



An efficient method for the separation of L- and D-asparagine has not been developed. Further hydrolysis to [^{11}C]Asp was required to confirm the L/D ratio of [^{11}C]asparagine. 1 mL of the formulated [^{11}C]Asn from fraction 2 was transferred to a U-shape reaction vessel with stir bar. To the [^{11}C]Asn, 0.5 mL of 12M HCl was added and the reaction was performed at 130 °C for 10 min. The resulting crude mixture was diluted with deionized water and loaded over the formulation column. The formulation procedure for purifying [^{11}C]Asp is the same as shown above (**3.3.5. Acidic hydrolysis to [^{11}C]asparagine**). The pH of each fraction from the formulation (pH ~ 7) was confirmed. The fraction 2 (20 μL) was used for HPLC analysis to configure the L/D ratio of [^{11}C]Asp using isocratic system with IPA/2.0 mM CuSO₄ aqueous solution = 10/90 (v/v) at flow rate 0.8 mL/min on a Chirex chiral column (Phenominex, 150 \times 4.6 mm, 5 μm). The L-[^{11}C]Asp was eluted at 11 min and D-[^{11}C]Asps was eluted at 14 min. L/D ratio (> 40/1) was confirmed based on the analytical HPLC profile.

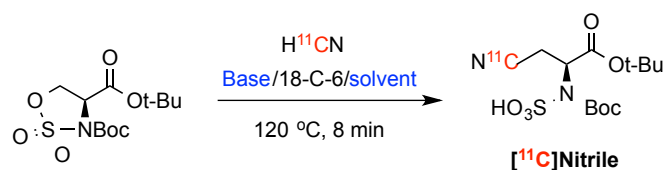
4. Result and discussion

Synthesis of the desired cyclic sulfamidate was achieved from commercially available Boc-O-benzyl-L-serine using essentially straightforward methodology shown on Scheme 1. The tert-

butyloxycarbonyl (Boc) group was chosen for protection of the ester group to limit nucleophilic and/or basic attack both on this functionality and at the α -position in the cyanation for preparation of nitrile intermediate for asparagine. The benzyl ether group cleavage was performed under hydrogenation with H₂ and Pd/C (10%) in quantitative yield. Formation of the cyclic sulfamidate (**4**) was achieved from the 1,2-amino alcohol by nucleophilic substitution with thionyl chloride to yield the sulfamidate using sodium periodate in presence of catalytic ruthenium (VIII).

We examined the nucleophilic ring opening of the cyclic sulfamidate (**4**) with cyanide nucleophile in the model reaction shown on Scheme 2. The sulfamidate (**4**) was shown to react efficiently with potassium cyanide under basic conditions to give the nitrile (**5**). The desired asparagine (**6**) was obtained via hydrolysis with strong acid (THF/H₂SO₄ = 2/1). This asparagine was identified by analytical HPLC and mass spectroscopy.

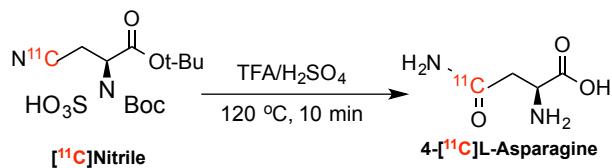
Table 1. Optimization of [¹¹C]cyanation reaction



Entry	[¹¹ C]HCN trapping salt	Reaction condition	[¹¹ C]nitrile RCY (%)	L/D ratio
1	CsHCO ₃ /18-C-6 (pH 8.5)	DMF, 120 °C, 8 min	57	33/1
2	KHCO ₃ /18-C-6 (pH 8.4)	DMSO, 120 °C, 8 min	38	15/1
3	KHCO ₃ /18-C-6 (pH 8.4)	DMA, 120 °C, 8 min	66	136/1
4	KHCO ₃ /K ₂ CO ₃ /18-C-6 (pH 9)	DMF, 120 °C, 8 min	68	306/1
5	KHCO ₃ /K ₂ CO ₃ /18-C-6 (pH 10)	DMF, 120 °C, 8 min	61	Only L

Radiosynthesis of L-[4-¹¹C]asparagine was designed via non-carrier added nucleophilic [¹¹C]cyanation followed by hydrolysis via selective deprotection with THF/H₂SO₄. Further hydrolysis with concentrate HCl to L-[4-¹¹C]aspartic acid to easily confirm its stereochemistry by known analytical HPLC method identifying L/D-isomer Scheme 3. The investigation of reaction parameters started with the nucleophilic [¹¹C]cyanation (Table 1). We first tested [¹¹C]cyanation with previously optimized reference condition¹⁷: CsHCO₃/18-C-6 (0.015 mmol/0.03 mmol, pH = 8.5) in DMF (0.5 mL) at 120 °C for 8 min (entry 1). The [¹¹C]cyanation (57 %) and stereoselectivity (L/D = 33/1) was promising at the first time with CsHCO₃ but the result was not reproducible. This may be due to instability of the cesium bicarbonate at high temperature. Although ore more stable base, KHCO₃, was used to result in corresponding pH (pH 8.4), [¹¹C]nitrile intermediate was rapidly decomposed in DMSO. The radiochemical yield (RCY) of [¹¹C]cyanation was low (38%) with poor stereoselectivity (entry 2). Indeed, RCY of [¹¹C]cyanation and stereoselectivity was recovered immediately (66% and L/D=136/1, respectively in entry 3) by using robust base KHCO₃ in DMA. By increasing basicity with K₂CO₃ in DMF, highly stereoselective [¹¹C]cyanation was carried out in high RCY (entry 4 and entry 5).

Table 2. Optimization of acidic hydrolysis and deprotection to L-[4-¹¹C]asparagine



Entry	Acidic hydrolysis conditions	[¹¹ C]Asn RCY
6	TFA/H ₂ SO ₄ , (4:1, 0.2 mL), 120 °C, 10 min	36
7	TFA/H ₂ SO ₄ , (2:1, 0.2 mL), 120 °C, 10 min	73
8	TFA/H ₂ SO ₄ , (2:1, 0.25 mL), 120 °C, 10 min	96

Optimization of following acidic hydrolysis and selective deprotection of [^{11}C]nitrile intermediate by modifying proportion and volume of trifluoroacetic acid/sulfuric acid is described in Table 2. This hydrolysis procedure and deprotection was successfully achieved (96 %) with 0.25 mL of TFA/ H_2SO_4 (2/1) at 120 °C for 10 min (entry 8).

In summary, the current best result from non-carrier added nucleophilic [^{11}C]cyanation (61%) was obtained with $\text{KHCO}_3/\text{K}_2\text{CO}_3/18\text{-C-6}$ (0.005 mmol/0.005 mmol/0.03 mmol, pH = 8.5) in DMF (0.5 mL) at 120 °C for 8 min. The overall yield of the desired [$4\text{-}^{11}\text{C}$]asparagine was obtained in 52% without D-isomer. This stereospecificity was determined by L/D ratio of [$4\text{-}^{11}\text{C}$]aspartic acid by further hydrolysis from [$4\text{-}^{11}\text{C}$]asparagine. The radiochemical purity of the final product was ≥ 96 %. The specific activity of the final product [$4\text{-}^{11}\text{C}$]asparagine, based upon our Fmoc-derivatization method, was 5.5 – 11.1 GBq/ μmol .

5. Conclusion

In summary, we have developed an improved method for synthesizing the biologically interesting PET radiotracer L-[$4\text{-}^{11}\text{C}$]asparagine, which features mild reaction conditions and increased yields. The synthesis process was based on successful preparation of cyclic sulfamidate precursor via synthesis in four steps in high yield.

Additionally, the conditions that we report here will become the cornerstones of further systematic investigation of reaction parameters for which included varied [^{11}C]cyanide trapping conditions, PTC, solvents, temperatures and reaction times, as well as investigating the impact of a trace amount of H_2O , etc. in order to understand the $\text{S}_{\text{N}}2$ [^{11}C]cyanation of a base- and moisture-sensitive substrate with non-carrier added conditions better. Reproducibility of this

method also must be proved by repeated experiments. Similar systematic investigations should be very beneficial for future [^{11}C]cyanide-based radiotracer development.

6. Reference

1. Ametamey, S. M.; Honer, M.; Schubiger, P. A., Molecular Imaging with PET. *Chem. Rev. (Washington, DC, U. S.)* **2008**, *108* (5), 1501-1516.
2. (a) Ermert, J.; Coenen, H. H., Methods for ¹¹C- and ¹⁸F-labeling of amino acids and derivatives for positron emission tomography imaging. *J. Labelled Compd. Radiopharm.* **2013**, *56* (3-4), 225-236; (b) Miller, P. W.; Long, N. J.; Vilar, R.; Gee, A. D., Synthesis of ¹¹C, ¹⁸F, ¹⁵O, and ¹³N radiolabels for positron emission tomography. *Angew. Chem., Int. Ed.* **2008**, *47* (47), 8998-9033.
3. Weber, W. A.; Wester, H.-J.; Grosu, A. L.; Herz, M.; Dzewas, B.; Feldmann, H.-J.; Molls, M.; Stocklin, G.; Schwaiger, M., O-(2-[¹⁸F]Fluoroethyl)-l-tyrosine and l-[methyl-¹¹C]methionine uptake in brain tumors: initial results of a comparative study. *Eur. J. Nucl. Med.* **2000**, *27* (5), 542-549.
4. Kole, A. C.; Pruijm, J.; Nieweg, O. E.; Van Ginkel, R. J.; Hoekstra, H. J.; Koops, H. S.; Vaalburg, W., PET with L-[¹¹C]tyrosine to visualize tumors and measure protein synthesis rates. *J. Nucl. Med.* **1997**, *38* (2), 191-195.
5. Sundin, A.; Eriksson, B.; Bergstrom, M.; Bjurling, P.; Lindner, K. J.; Oberg, K.; Langstrom, B., Demonstration of [¹¹C] 5-hydroxy-L-tryptophan uptake and decarboxylation in carcinoid tumors by specific positioning labeling in positron emission tomography. *Nucl. Med. Biol.* **2000**, *27* (1), 33-41.
6. Myers, R., The biological application of small animal PET imaging. *Nucl Med Biol* **2001**, *28* (5), 585-93.
7. Woody, C. L.; Stoll, S. P.; Schlyer, D. J.; Gerasimov, M.; Vaska, P.; Shokouhi, S.; Volkow, N.; Fowler, J. S.; Dewey, S. L., A study of scintillation beta microprobes. *IEEE Trans. Nucl. Sci.* **2002**, *49* (5, Pt. 1), 2208-2212.
8. Jager, P. L.; Vaalburg, W.; Pruijm, J.; De Vries, E. G. E.; Langen, K.-J.; Piers, D. A., Radiolabeled amino acids: basic aspects and clinical applications in oncology. *J. Nucl. Med.* **2001**, *42* (3), 432-445.
9. Lindstrom, L. H.; Gefvert, O.; Hagberg, G.; Lundberg, T.; Bergstrom, M.; Hartvig, P.; Langstrom, B., Increased dopamine synthesis rate in medial prefrontal cortex and striatum in schizophrenia indicated by L-(beta-¹¹C) DOPA and PET. *Biological psychiatry* **1999**, *46* (5), 681-8.
10. Studenov, A. R.; Szalda, D. E.; Ding, Y. S., Synthesis of no-carrier-added C-11 labeled D- and L-enantiomers of phenylalanine and tyrosine for comparative PET Studies. *Nucl Med Biol* **2003**, *30* (1), 39-44.
11. Sundin, A.; Eriksson, B.; Bergstrom, M.; Langstrom, B.; Oberg, K.; Orlefors, H., PET in the diagnosis of neuroendocrine tumors. *Annals of the New York Academy of Sciences* **2004**, *1014*, 246-57.
12. (a) Adam, M. J.; Grierson, J. R.; Ruth, T. J.; Pedersen, K.; Pate, B. D., Routine synthesis of carbon-11-carboxyl-labeled L-dopa. *Journal of nuclear medicine : official publication, Society of Nuclear Medicine* **1987**, *28* (10), 1599-603; (b) Halldin, C.; Schoeps, K. O.; Stone-Elander, S.; Wiesel, F. A., The Bucherer-Strecker synthesis of D- and L-(¹¹C)tyrosine and the in vivo study of L-(¹¹C)tyrosine in human brain using positron emission tomography. *European*

- journal of nuclear medicine* **1987**, *13* (6), 288-91; (c) Hayes, R. L.; Washburn, L. C.; Wieland, B. W.; Sun, T. T.; Turtle, R. R.; Butler, T. A., Carboxyl-labeled ¹¹C-1-aminocyclopentanecarboxylic acid, a potential agent for cancer detection. *Journal of nuclear medicine : official publication, Society of Nuclear Medicine* **1976**, *17* (8), 748-51.
13. (a) Fasth, K. J.; Antoni, G.; Langstrom, B., Asymmetric-Synthesis of L-[³-C-11] Alanine and L-[³-C-11] Phenylalanine by a Phase-Transfer Alkylation Reaction. *J Chem Soc Perk T I* **1988**, (12), 3081-3084; (b) Fasth, K. J.; Hornfeldt, K.; Langstrom, B., Asymmetric-Synthesis of C-11 Labeled L-Amino and D-Amino Acids by Alkylation of Imidazolidinone Derivatives. *Acta Chem Scand* **1995**, *49* (4), 301-304; (c) Mosevich, I. K.; Kuznetsova, O. F.; Vasil'ev, D. A.; Anichkov, A. A.; Korsakov, M. V., Automated synthesis of [³-C-11]-L-alanine involving asymmetric alkylation with (CH₃I)-C-11 of the nickel complex of the Schiff base derived from glycine and (S)-2-N-(N'-benzylpropyl)aminobenzophenone. *Radiochemistry+* **1999**, *41* (3), 273-280.
14. Venneti, S.; Dunphy, M. P.; Zhang, H.; Pitter, K. L.; Zanzonico, P.; Campos, C.; Carlin, S. D.; La Rocca, G.; Lyashchenko, S.; Ploessl, K.; Rohle, D.; Omuro, A. M.; Cross, J. R.; Brennan, C. W.; Weber, W. A.; Holland, E. C.; Mellinshoff, I. K.; Kung, H. F.; Lewis, J. S.; Thompson, C. B., Glutamine-based PET imaging facilitates enhanced metabolic evaluation of gliomas in vivo. *Science translational medicine* **2015**, *7* (274), 274ra17.
15. Gillings, N. M.; Gee, A. D., Synthesis of [4-¹¹C]amino acids via ring-opening of aziridine-2-carboxylates. *J. Labelled Compd. Radiopharm.* **2001**, *44* (13), 909-920.
16. Qu, W.; Oya, S.; Lieberman, B. P.; Ploessl, K.; Wang, L.; Wise, D. R.; Divgi, C. R.; Chodosh, L. A.; Thompson, C. B.; Kung, H. F., Preparation and characterization of L-[⁵-¹¹C]-glutamine for metabolic imaging of tumors. *Journal of nuclear medicine : official publication, Society of Nuclear Medicine* **2012**, *53* (1), 98-105.
17. Gleede, T.; Riehl, B.; Shea, C.; Kersting, L.; Cankaya, A. S.; Alexoff, D.; Schueller, M.; Fowler, J. S.; Qu, W., Investigation of SN₂ [¹¹C]cyanation for base-sensitive substrates: an improved radiosynthesis of L-[⁵-¹¹C]-glutamine. *Amino Acids* **2015**, *47* (3), 525-533.
18. Baldwin, J. E.; Spivey, A. C.; Schofield, C. J., Cyclic Sulphamidates - New Synthetic Precursors for Beta-Functionalized Alpha-Amino-Acids. *Tetrahedron-Asymmetr* **1990**, *1* (12), 881-884.
19. Baldwin, J. E.; Adlington, R. M.; Coates, J. B.; Crabbe, M. J.; Crouch, N. P.; Keeping, J. W.; Knight, G. C.; Schofield, C. J.; Ting, H. H.; Vallejo, C. A.; et al., Purification and initial characterization of an enzyme with deacetoxycephalosporin C synthetase and hydroxylase activities. *The Biochemical journal* **1987**, *245* (3), 831-41.
20. Kim, D.; Alexoff, D.; Kim, S. W.; Hooker, J.; Ferrieri, R. A. ¹¹C-Labeled cyanide production system. US20130045151A1, 2013.
21. Antoni, G.; Omura, H.; Bergstrom, M.; Furuya, Y.; Moulder, R.; Roberto, A.; Sundin, A.; Watanabe, Y.; Langstrom, B., Synthesis of L-2,4-diamino[4-¹¹C]butyric acid and its use in some in vitro and in vivo tumor models. *Nucl. Med. Biol.* **1997**, *24* (6), 595-601.

Supplementary Information for CHAPTER 5.

Part 1. HPLC analysis

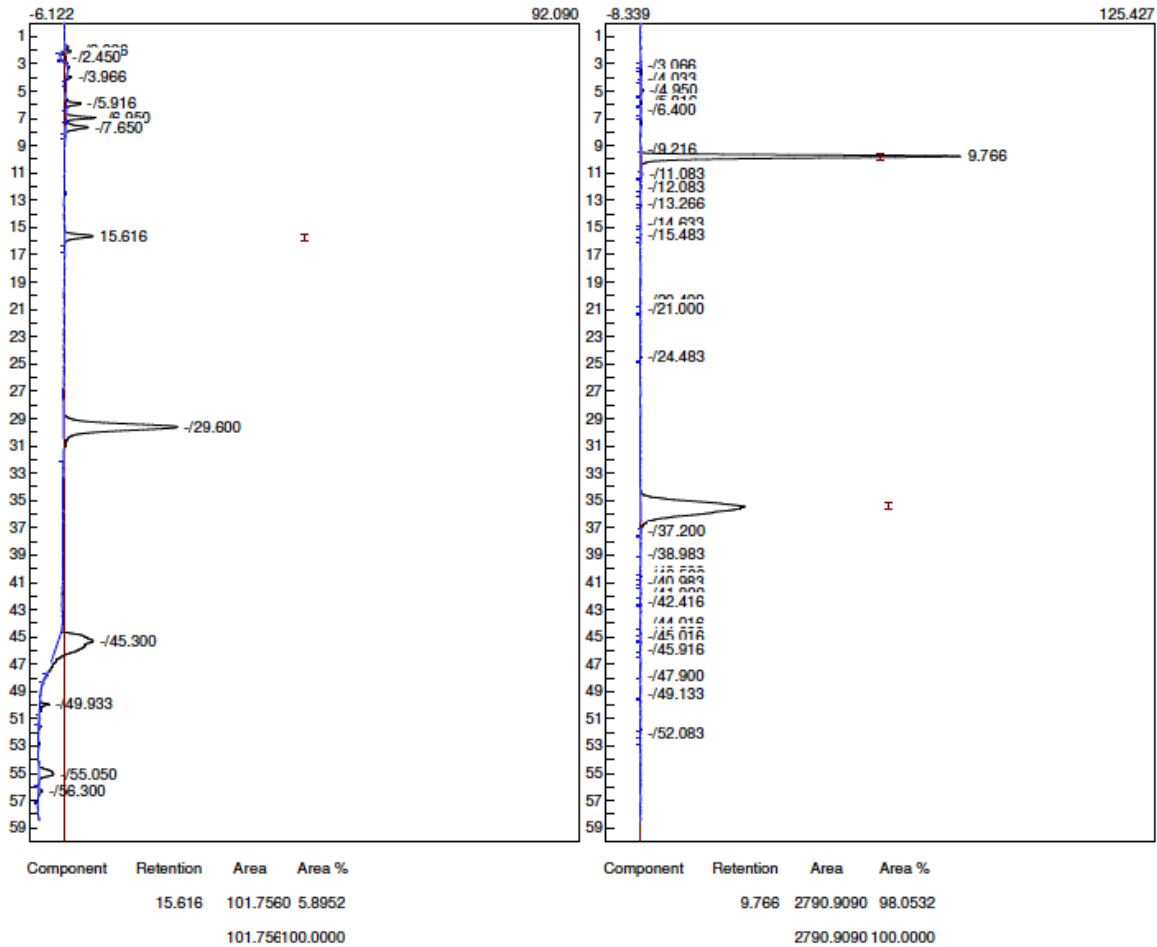
Part 2. $^1\text{H}/^{13}\text{C}$ NMR spectroscopy and Mass spectrometry (ESI)

Part 1. HPLC analysis

1.1. Quality control of [¹¹C]asparagine

Lab name: SRI Instruments
 Collected: 01-22-2015
 Analysis date: 02/04/2015 10:42:21
 Method: Syringe Injection
 Description: Analytical UV
 Column: Luna C18 250x4.6
 Carrier: 40:60 FA(0.1%) : ACN
 Sample: E056_QC#1
 Operator: Youwen/So Jeong
 Comments: flow: 1 mL/min 254 nm
 QC batch: 01-15-2015 QC#1

Lab name: SRI Instruments
 Collected: 01-22-2015
 Analysis date: 02/04/2015 10:42:21
 Method: Syringe Injection
 Description: Analytical Rad
 Column: Luna C18 250x4.6
 Carrier: 40:60 FA(0.1%) : ACN
 Sample: E056_QC#1
 Operator: Youwen/So Jeong
 Comments: flow: 1 mL/min 254 nm
 QC batch: 01-15-2015 QC#1



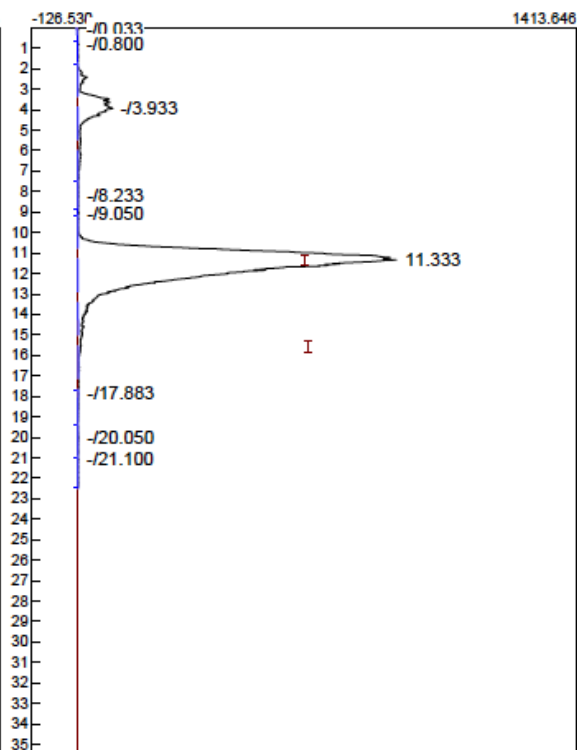
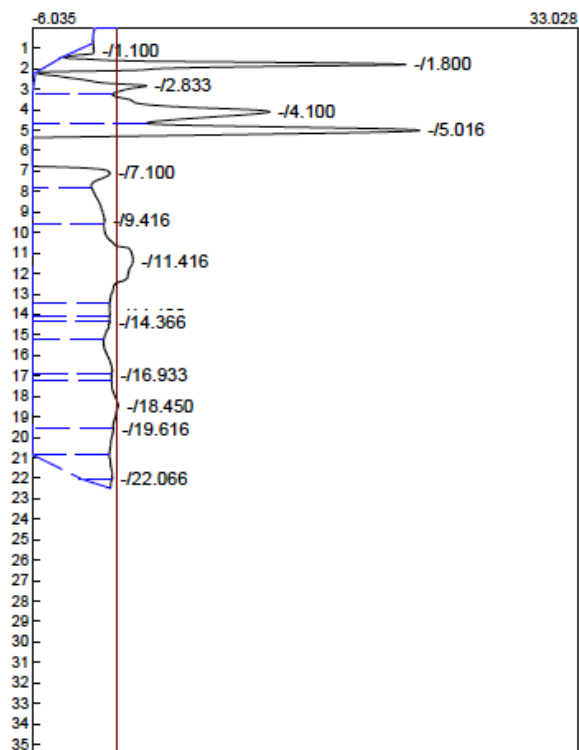
1.2. Quality control of [¹¹C]aspartic acid for L/D ratio determination

Lab name: BNL Cyclotron
 Client: Cyclotron Hot Lab
 Collected: 02/04/2015
 Analysis date: 02/04/2015 11:18:10
 Method: syringe injection
 Description: UV
 Column: Chirex3126 150 x 4.60
 Carrier: 5% IPA : 2 mM CuSO4
 Data file: E058-Asp QC_U01.CHR ()
 Sample: [¹¹C]Asp final QC
 Comments: 20 ul injection
 Temperature: RT
 Flow: 1.0 mL/min

Lab name: BNL Cyclotron
 Client: Cyclotron Hot Lab
 Collected: 02/04/2015
 Analysis date: 02/04/2015 11:18:10
 Method: syringe injection
 Description: Radio
 Column: Chirex3126 150 x 4.60
 Carrier: 5% IPA : 2 mM CuSO4
 Data file: E058-Asp QC_R01.CHR ()
 Sample: [¹¹C]Asp final QC
 Comments: 20 ul injection
 Temperature: RT
 Flow: 1.0 mL/min

QC batch: E058_Asp QC

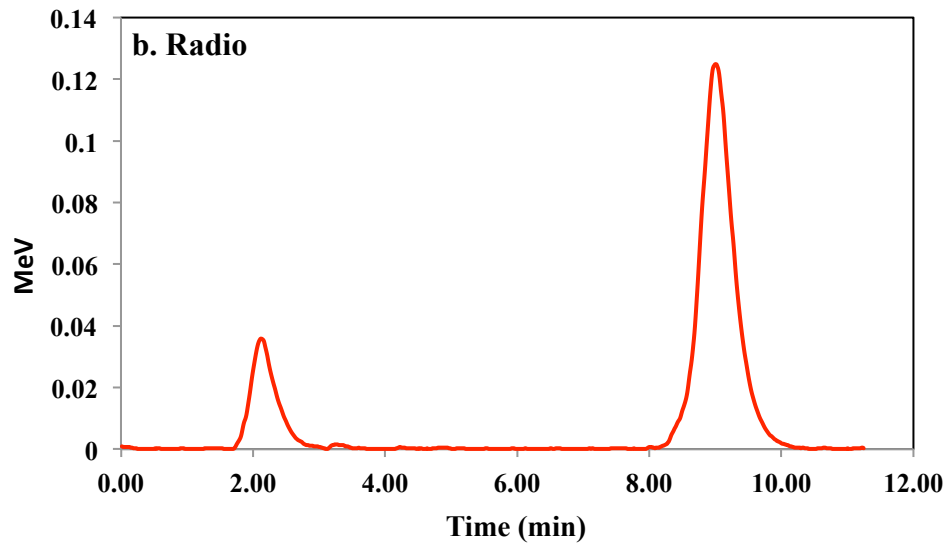
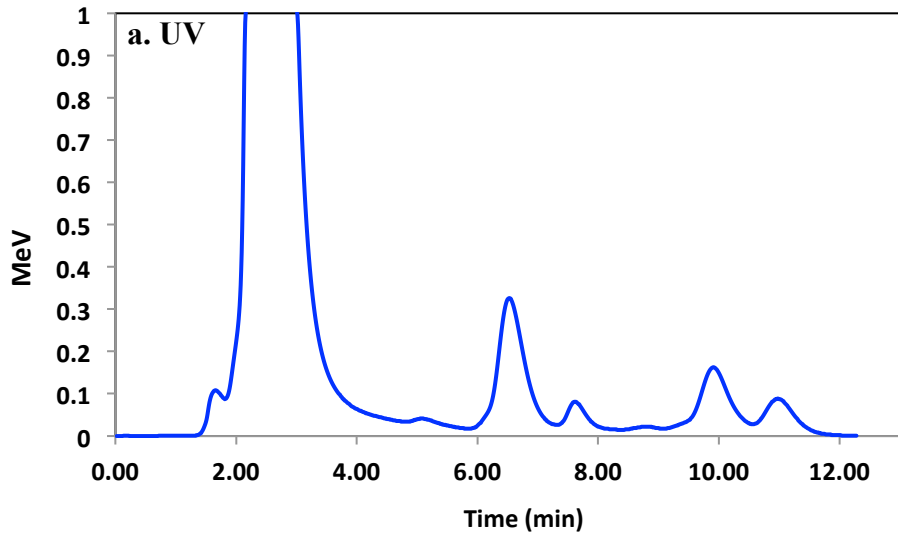
QC batch: E058_Asp QC



Component	Retention	Area	Area %
		0.000100.0000	

Component	Retention	Area	Area %
	11.333	68520.9900	90.0551
		68520.9900	100.0000

1.3. Specific activity determination (Fmoc- ^{11}C Asn)



Part 2. $^1\text{H}/^{13}\text{C}$ NMR spectroscopy and Mass spectrometry (ESI)

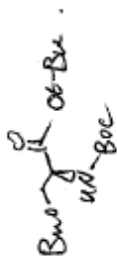
2.1. ^1H NMR

2.2. ^{13}C NMR

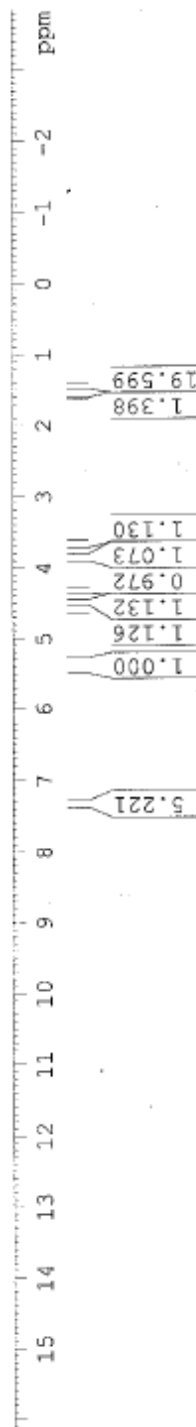
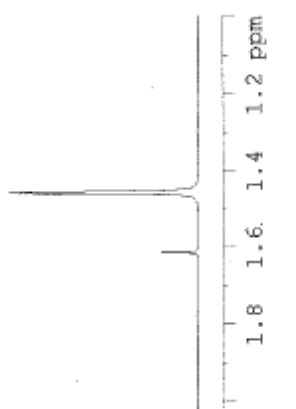
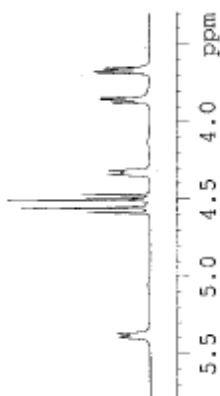
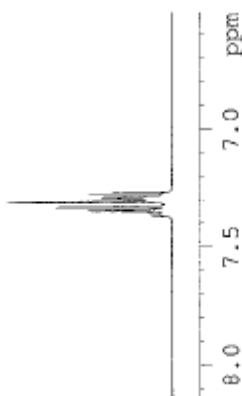
2.3. Mass spectrometry

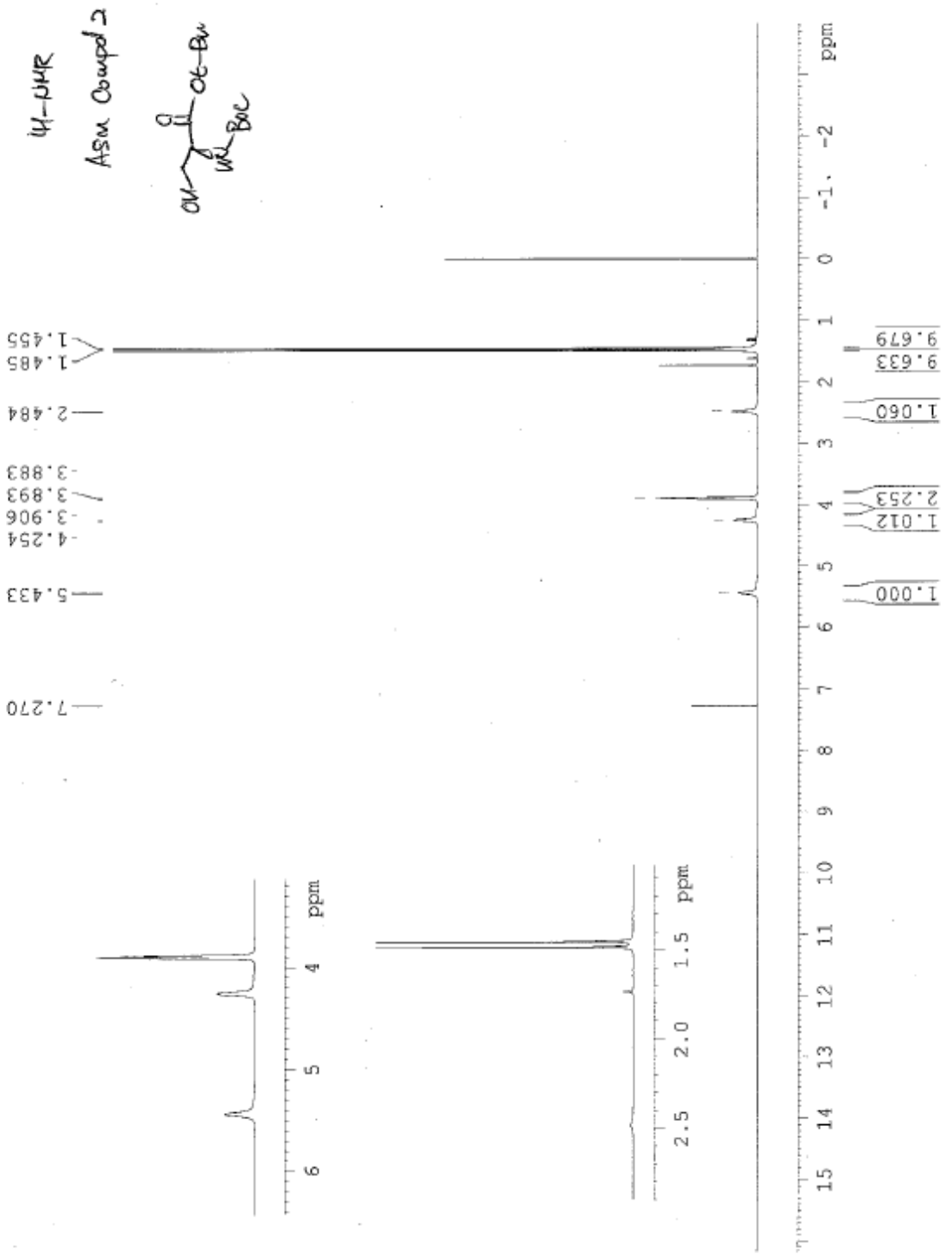
¹H-NMR

ASU Compd 1

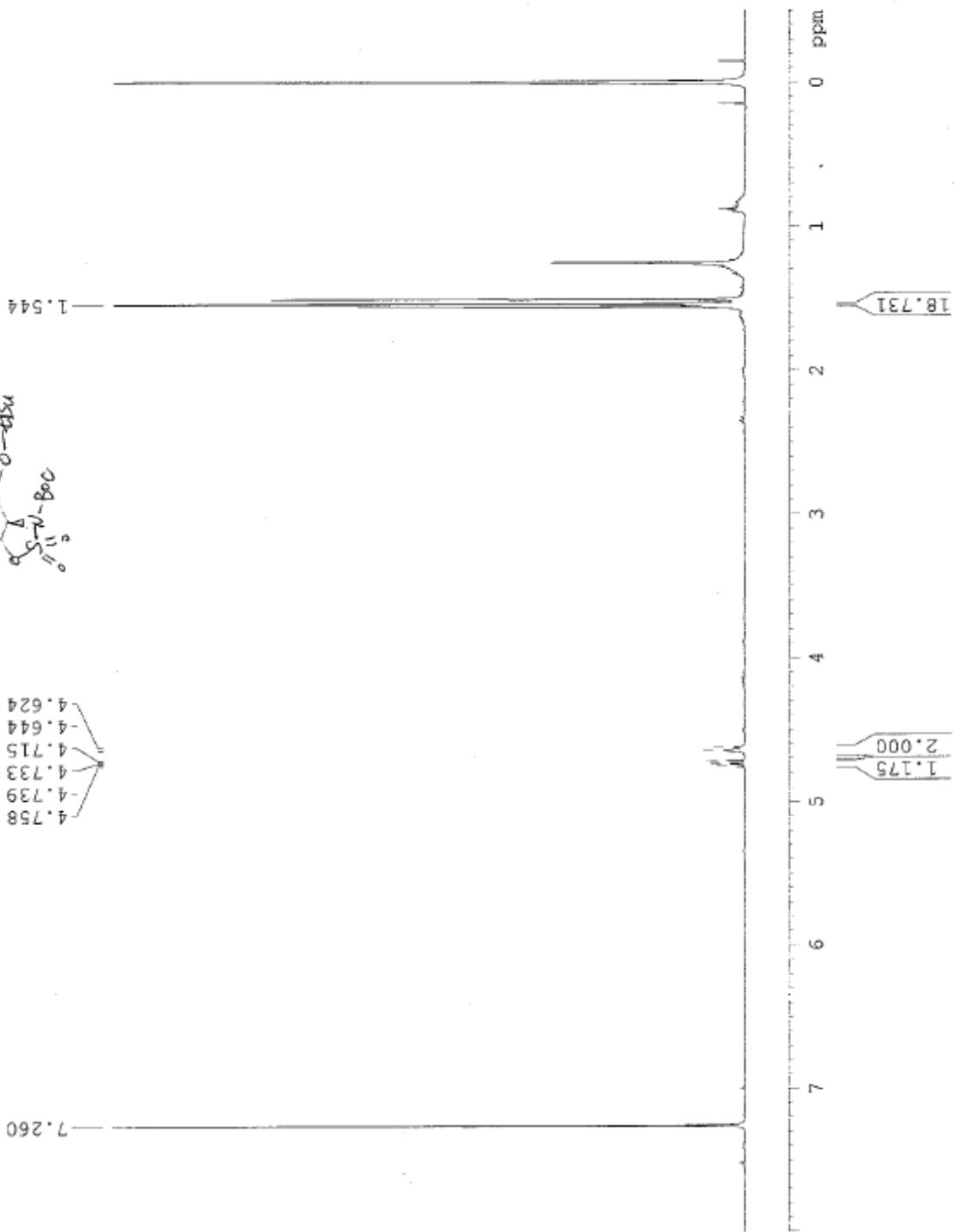


7.363
7.342
7.337
7.327
7.305
7.296
7.288
7.270
5.391
5.370
4.585
4.554
4.500
4.469
4.335
4.327
4.322
4.314
3.875
3.867
3.852
3.844
3.682
3.674
3.659
3.651
1.612
1.457
1.454

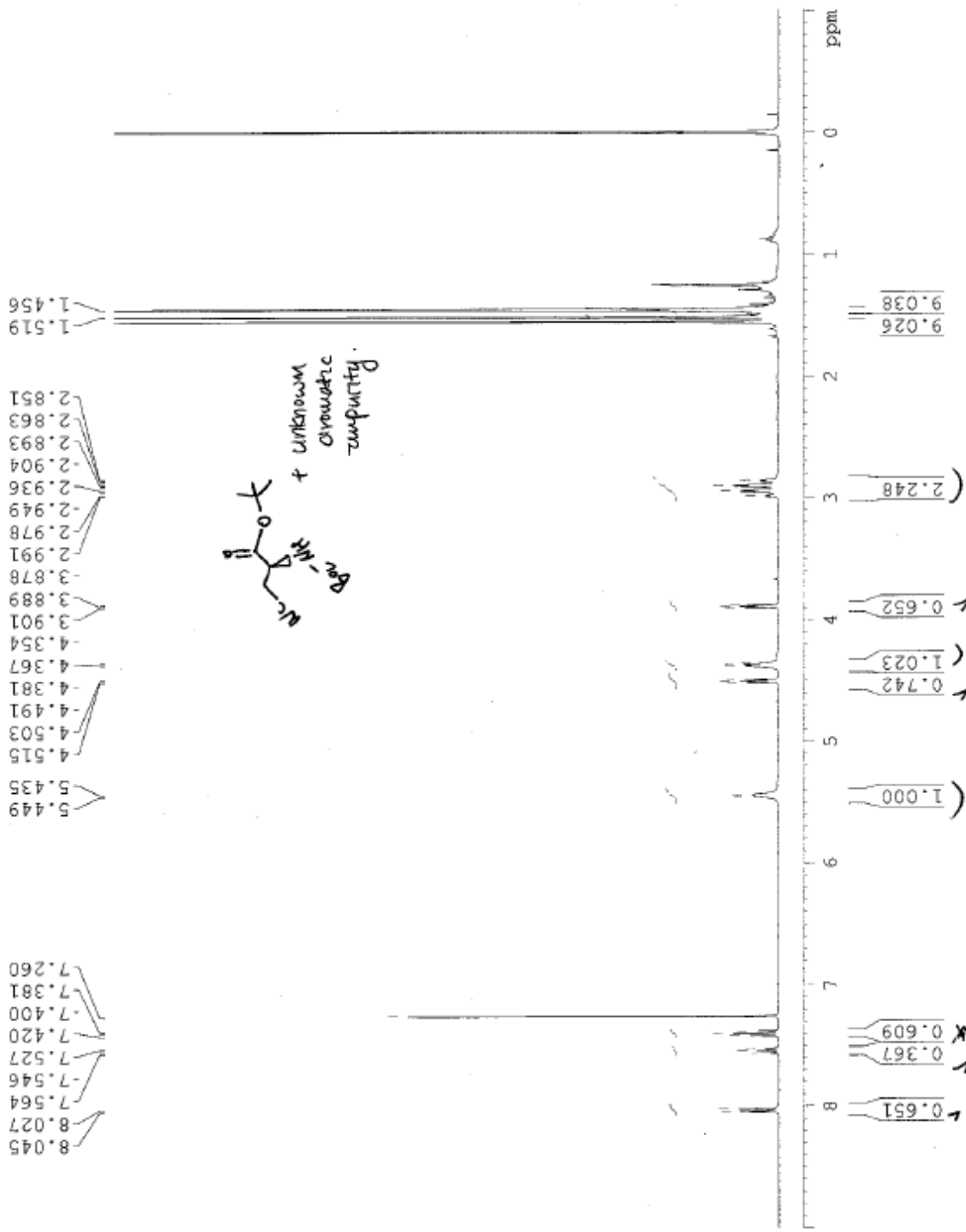


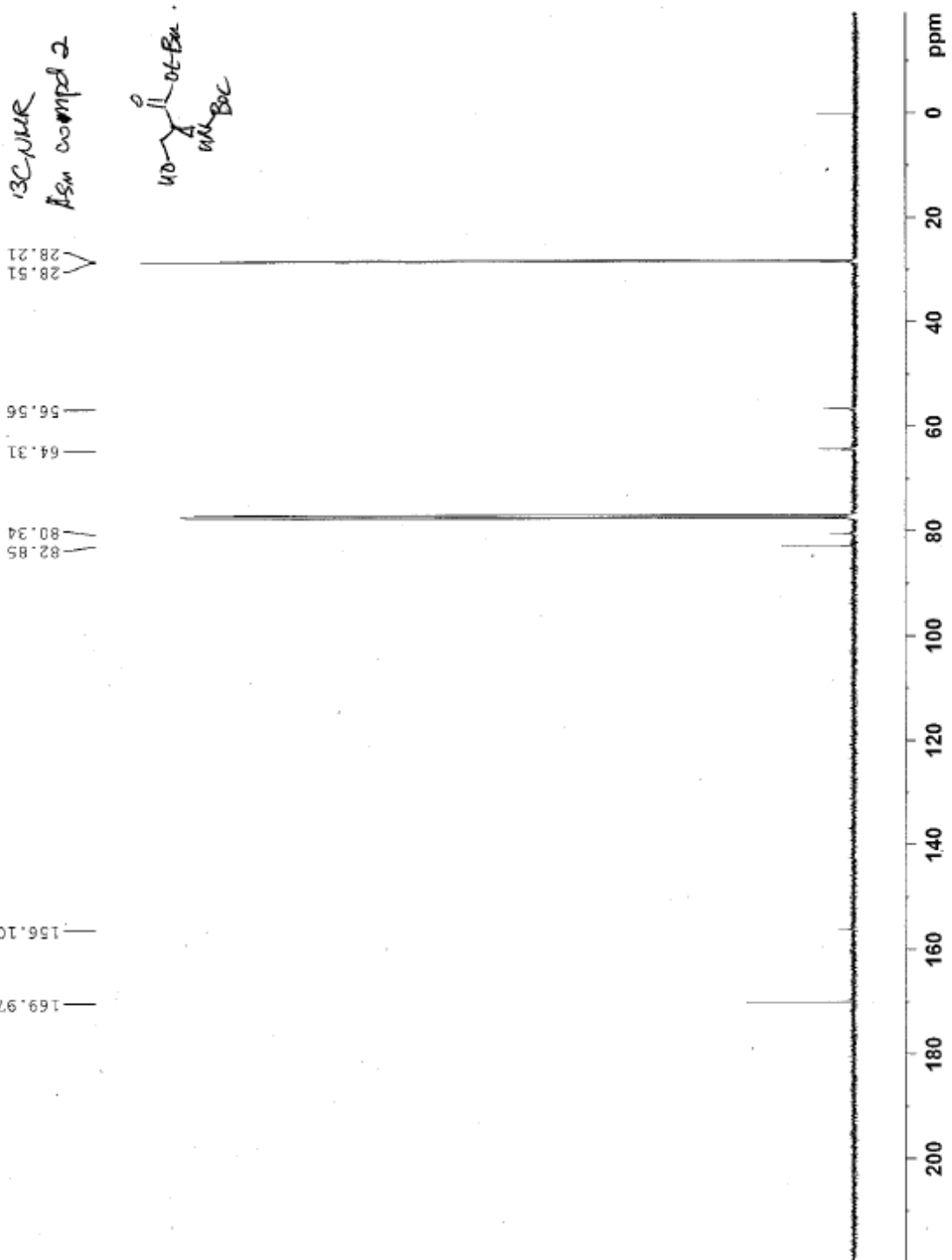


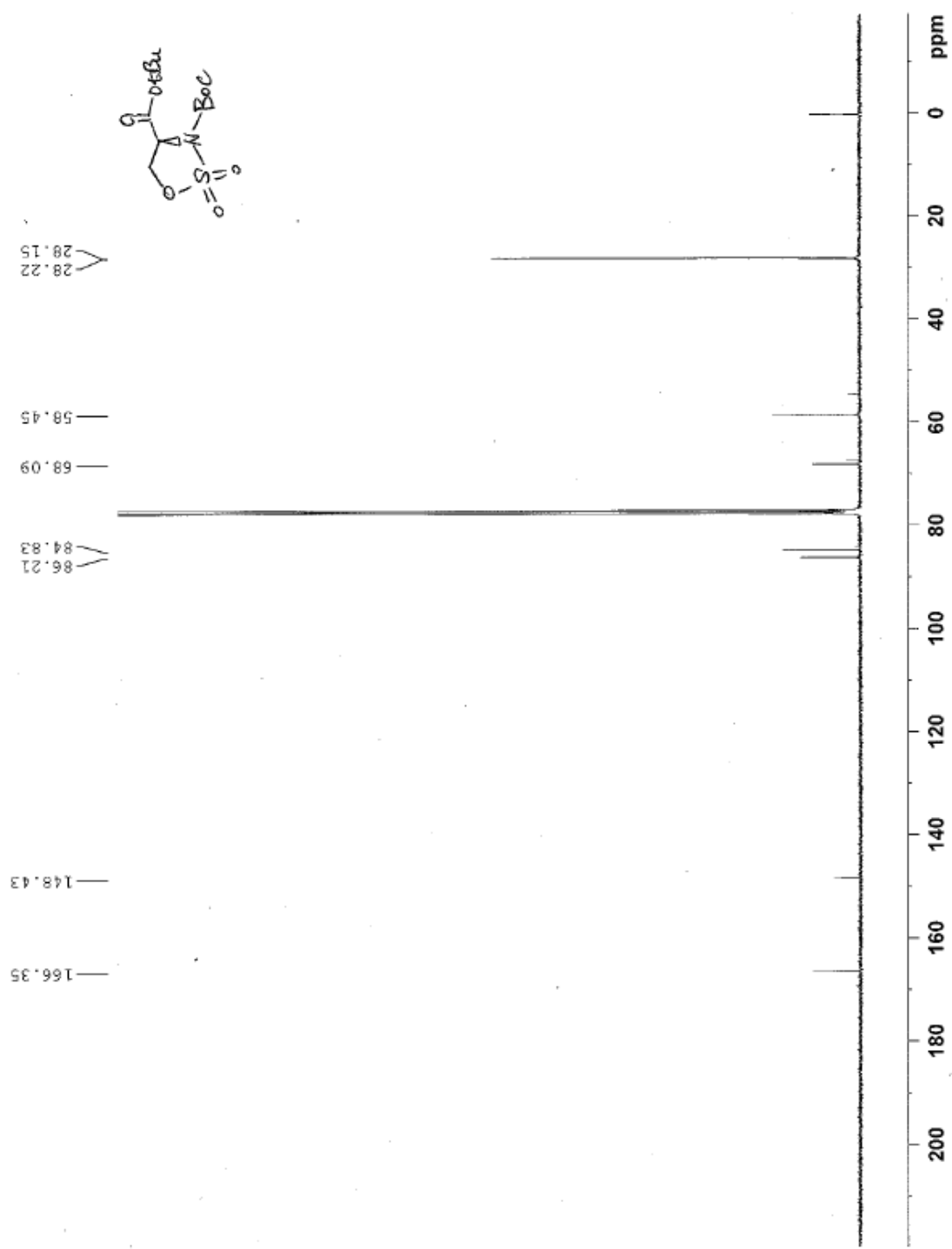
A 010815_final



A 011615 final







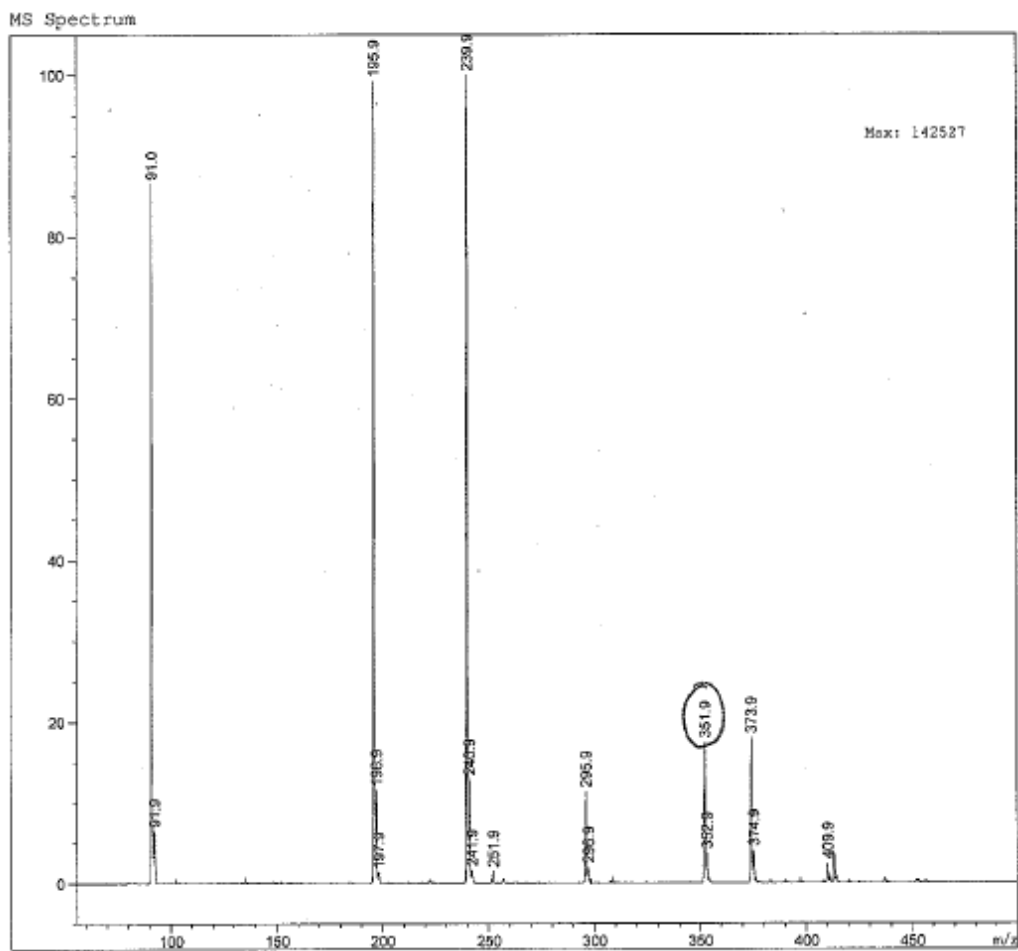
Print of window 80: MS Spectrum

Data File : D:\CHEM32\DATA\FOWLER\A123114_COMPD1.D

Sample Name : A123114_compdl

=====
Acq. Operator : Jee
Acq. Instrument : Instrument 1 Location : F1-F-01
Injection Date : 1/23/2015 4:36:18 PM Inj : 1
Inj Volume : 3.0 µl
Acq. Method : D:\CHEM32\METHODS\DIR-INJ-POS.M
Last changed : 1/23/2015 4:35:10 PM by Jee
(modified after loading)
Analysis Method : D:\CHEM32\DATA\HONDA\CWC-I-126-2.D\DA.M
Last changed : 1/8/2015 5:03:28 PM by Chih-Wei
Method Info : Direct-inject (FIA) ESI positive
A1 (0.1%Ac): B1 (MeOH); 25:75(v:v); 0.3ml/min

Sample Info : pos



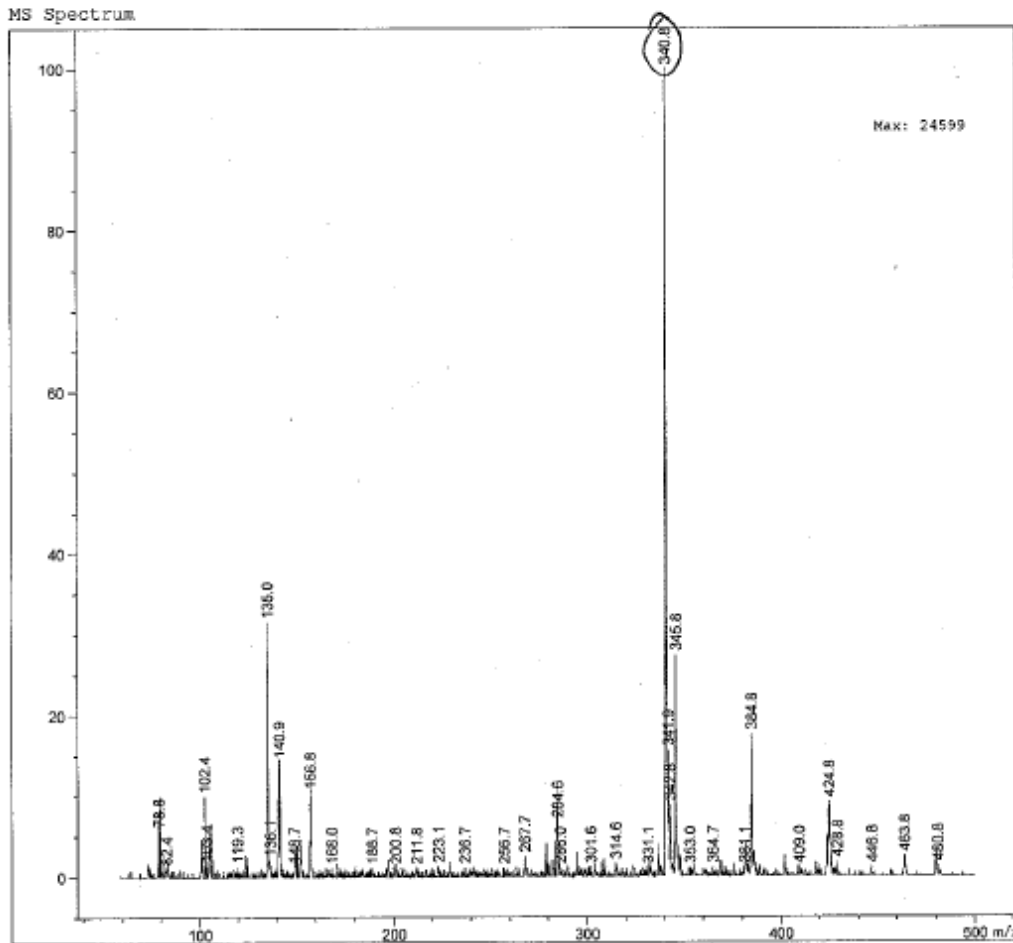
Print of window 80: MS Spectrum

Data File : D:\CHEM32\DATA\FOWLER\A011215_COMPD3.D *compd 4*

Sample Name : A011215_COMPD3.D

=====
Acq. Operator : Jee
Acq. Instrument : Instrument 1 Location : P1-F-03
Injection Date : 1/23/2015 4:43:58 PM Inj : 1
Inj Volume : 3.0 µl
Acq. Method : D:\CHEM32\METHODS\DIR-INJ-POS.M
Last changed : 1/23/2015 4:41:40 PM by Jee
(modified after loading)
Analysis Method : D:\CHEM32\DATA\HONDA\CWC-I-126-2.D\DA.M
Last changed : 1/8/2015 5:03:28 PM by Chih-Wei
Method Info : Direct-inject (FIA) ESI positive
Al (0.1%Ac): B1 (MeOH); 25:75(v:v); 0.3ml/min

Sample Info : pos



Instrument 1 1/23/2015 4:46:33 PM Chih-Wei

Page 1 of 1

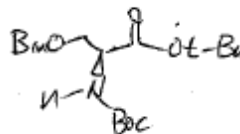
Print of window 80: MS Spectrum

Data File : D:\CHEM32\DATA\FOWLER\A123114_COMPD1.D

Sample Name : A123114_compdl

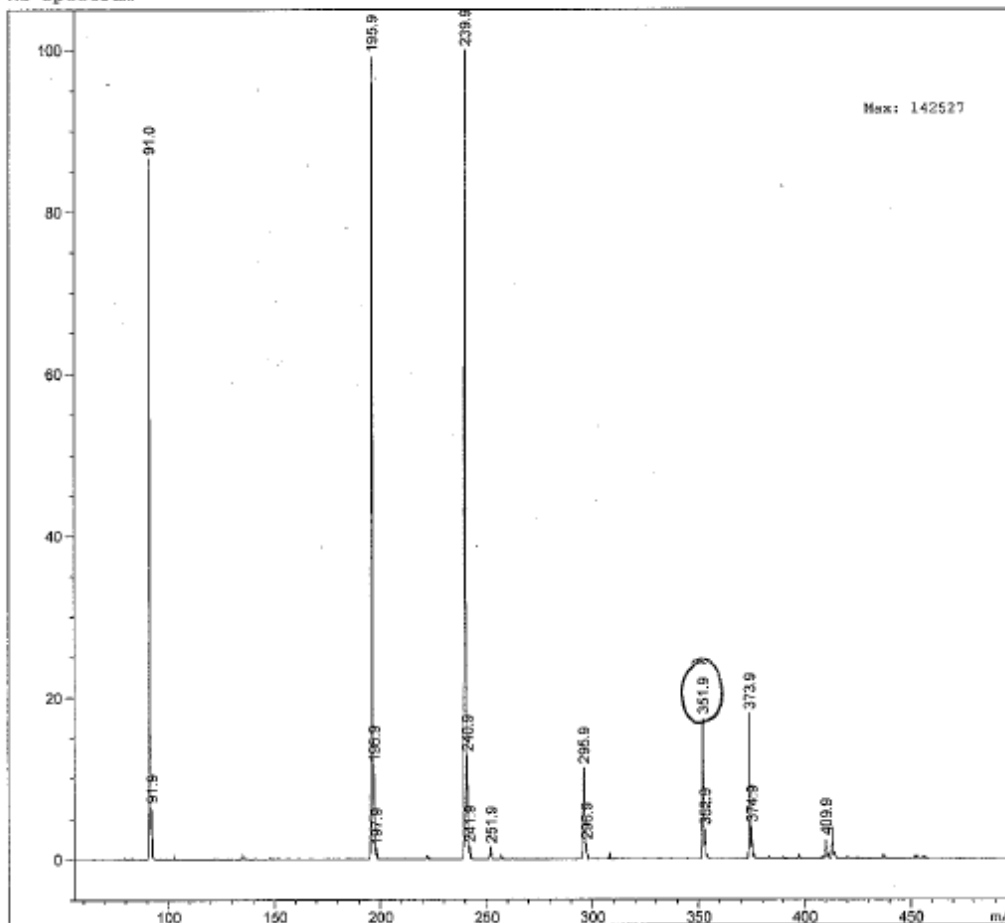
=====
Acq. Operator : Jee
Acq. Instrument : Instrument 1 Location : P1-F-01
Injection Date : 1/23/2015 4:36:18 PM Inj : 1
Inj Volume : 3.0 µl
Acq. Method : D:\CHEM32\METHODS\DIR-INJ-POS.M
Last changed : 1/23/2015 4:35:10 PM by Jee
(modified after loading)
Analysis Method : D:\CHEM32\DATA\HONDA\CWC-I-126-2.D\DA.M
Last changed : 1/8/2015 5:03:28 PM by Chih-Wei
Method Info : Direct-inject (FIA) ESI positive
Al (0.1%Ac): B1 (MeOH); 25:75(v:v); 0.3ml/min

Asm Comp 1



Sample Info : pos

MS Spectrum

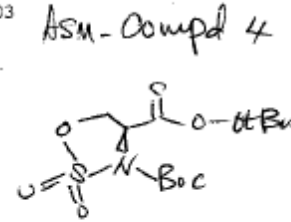


Instrument 1 1/23/2015 4:40:56 PM Chih-Wei

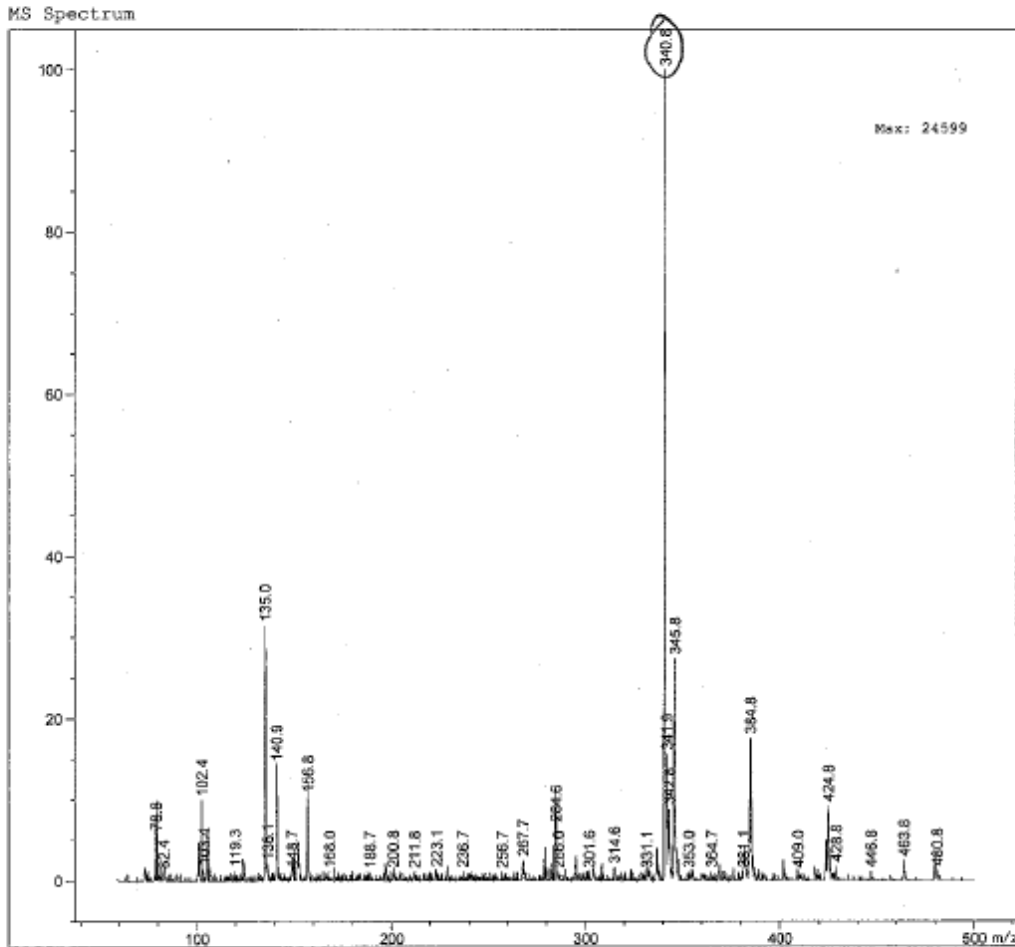
Page 1 of 1

Print of window 80: MS Spectrum
Data File : D:\CHEM32\DATA\FOWLER\A011215
Sample Name : A011215_COMPD3.D

=====
Acq. Operator : Jee
Acq. Instrument : Instrument 1 Location : P1-F-03
Injection Date : 1/23/2015 4:43:58 PM Inj : 1
Inj Volume : 3.0 µl
Acq. Method : D:\CHEM32\METHODS\DIR-INJ-POS.M
Last changed : 1/23/2015 4:41:40 PM by Jee
(modified after loading)
Analysis Method : D:\CHEM32\DATA\HONDA\CWC-I-126-2.D\DA.M
Last changed : 1/8/2015 5:03:28 PM by Chih-Wei
Method Info : Direct-inject (FIA) ESI positive
AL (0.1%Ac): BL (MeOH); 25:75(v:v); 0.3ml/min



Sample Info : pos



Instrument 1 1/23/2015 4:46:33 PM Chih-Wei

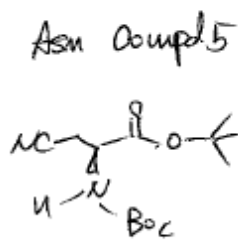
Page 1 of 1

Print of window 80: MS Spectrum

Data File : D:\CHEM32\DATA\FOWLER\A010115

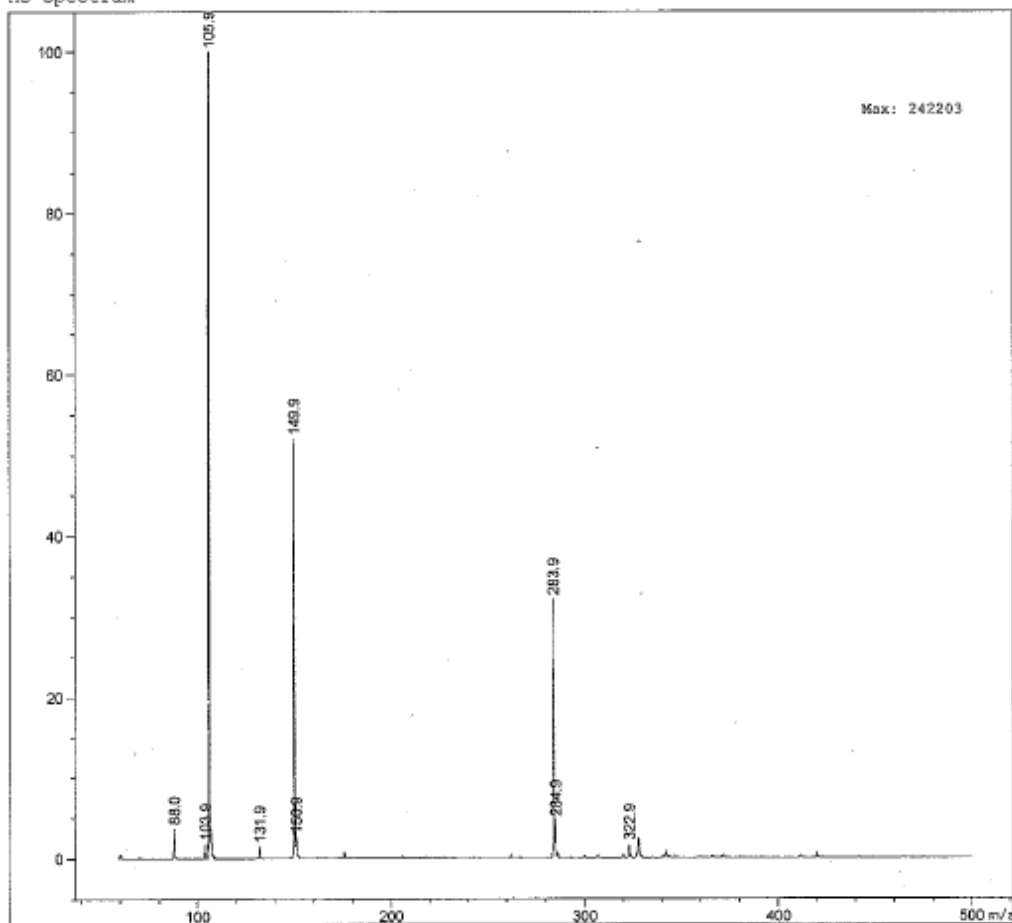
Sample Name : A010115_COMPD2.D

=====
Acq. Operator : Jee
Acq. Instrument : Instrument 1 Location : P1-F-02
Injection Date : 1/23/2015 4:40:26 PM Inj : 1
Inj Volume : 3.0 µl
Acq. Method : D:\CHEM32\METHODS\DIR-INJ-POS.M
Last changed : 1/23/2015 4:37:30 PM by Jee
(modified after loading)
Analysis Method : D:\CHEM32\DATA\HONDA\CWC-I-126-2.D\DA.M
Last changed : 1/8/2015 5:03:28 PM by Chih-Wei
Method Info : Direct-inject (FIA) ESI positive
A1 (0.1%Ac): B1 (MeOH); 25:75(v:v); 0.3ml/min



Sample Info : pos

MS Spectrum



Instrument 1 1/23/2015 4:44:35 PM Chih-Wei

Page 1 of 1

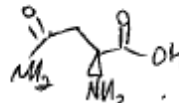
Print of window 80: MS Spectrum

Data File : D:\CHEM32\DATA\FOWLER\061215_ASN.D

Sample Name : 061215_Asn

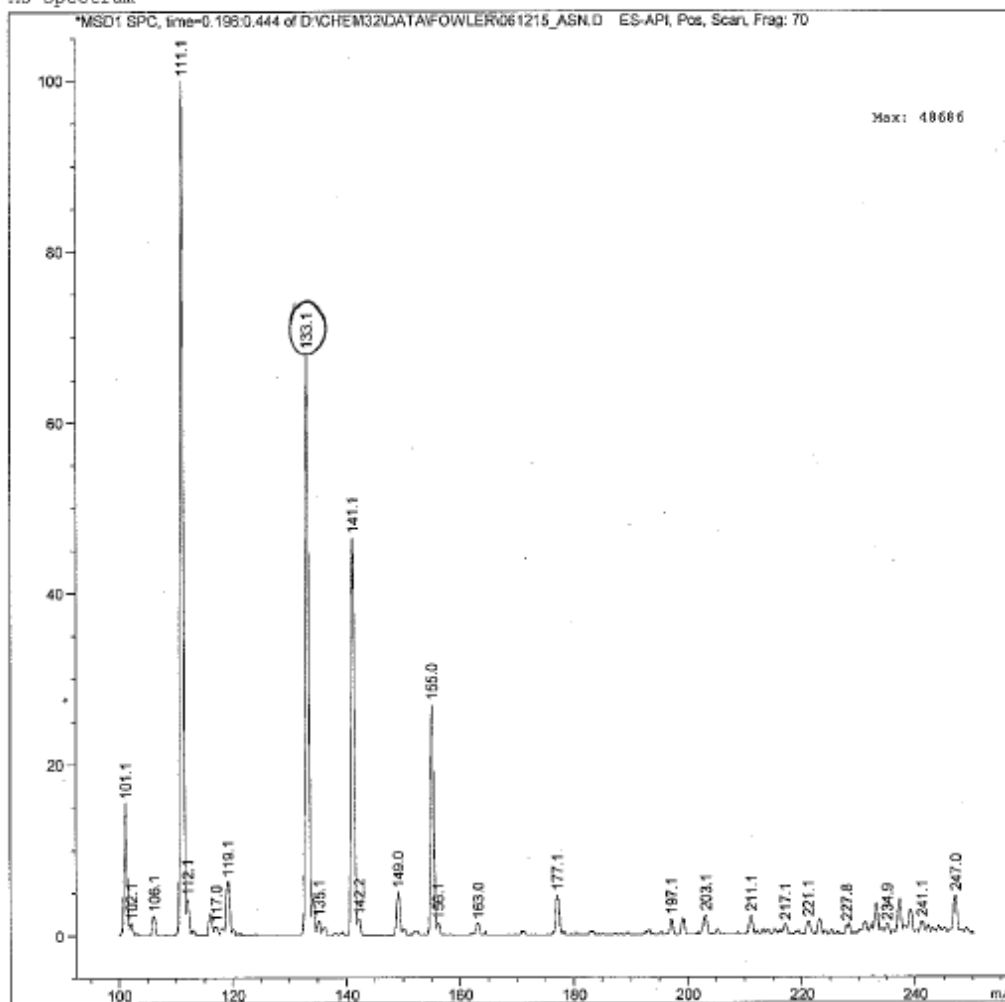
Asn Compd 6
(Asparagine)

Acq. Operator : So Jeong
Acq. Instrument : Instrument 1 Location : Vial 1
Injection Date : 6/12/2015 6:53:29 PM Inj : 1
Inj Volume : 1.0 µl



Acq. Method : D:\CHEM32\METHODS\DIR-INJ-POS.M
Last changed : 6/12/2015 6:52:51 PM by So Jeong
(modified after loading)
Analysis Method : D:\CHEM32\DATA\FOWLER\061215_ASN.D\DA.M (DIR-INJ-POS.M, From Data File)
Last changed : 6/12/2015 6:55:08 PM by So Jeong
Method Info : Direct-inject (FIA) ESI positive
A1 (0.1%Ac): B1 (MeOH); 25:75(v:v); 0.25ml/min

MS Spectrum



Instrument 1 6/12/2015 6:55:24 PM rejesh

Page 1 of 1